2008-06-10

Small RNA Sorting in Drosophila Produces Chemically Distinct Functional RNA-Protein Complexes: A Dissertation

Michael D. Horwich
University of Massachusetts Medical School

SMALL RNA SORTING IN *DROSOPHILA* PRODUCES CHEMICALLY DISTINCT FUNCTIONAL RNA-PROTEIN COMPLEXES

A Dissertation Presented

By

MICHAEL D. HORWICH

Submitted to the Faculty of the

University of Massachusetts Graduate School of Biomedical Sciences, Worcester

in partial fulfillment of the requirements for the degree of

DOCTOR OF PHILOSOPHY

JUNE 10, 2008

MD/PhD Program in Biomedical Sciences

A Dissertation Presented
By
Michael D. Horwich

The signature of the Dissertation Defense Committee signifies completion and approval as to style and content of the Dissertation

Phillip D. Zamore, Thesis Advisor

William Theurkauf, Committee Member

Marian Walhout, Committee Member

Gregory J. Hannon, Committee Member

The signature of the Chair of the Committee signifies that the written dissertation meets the requirements of the Dissertation Committee

Craig C. Mello, Chair of Committee

The signature of the Dean of the Graduate School of Biomedical Sciences signifies that the student has met all graduation requirements of the school

Anthony Carruthers, Ph.D., Dean of the Graduate School of Biochemical Sciences
Department of Biochemistry and Molecular Pharmacology

June 10, 2008

Acknowledgements

I am very fortunate to have found my way to the Zamore lab and to UMass. My wife hit the jackpot by landing a job at Amherst College; I got lucky too, because following her to Western Massachusetts led me to Phil's lab at UMass. Phil has assembled a fantastic group of people who are incredibly bright and incredibly nice to each other. I owe a lot to my fellow labmates: Klaus taught me that S2 cells are practically indestructible in culture, key to the success of the overcommitted (and/or lazy). Klaus was also a great teacher and technical resource. Vasia taught me fly genetics; Alla taught me how to dissect; Ben, Dianne, and Gyorgy welcomed me into the lab and were great first bay-mates. Gwen has bailed me out too many times and for that I am grateful. Tiffanie also has been incredibly helpful and always on top of things. Chris, Brad, Jen, Megha, Herve, Elif, and Tingting; Wee, Chengjian, Ira and Fabian - thank you all for tolerating my messiness and for making it fun to be in the lab. And of course, thank you Phil for being a fantastic mentor and creating an outstanding environment to do a PhD in. I am consistently amazed by your abilities, as a scientist, a teacher, and a parent (and a skier too!), and am grateful for all that you have taught me. I also want to thank Craig Mello, who has been supportive of me from when I first interviewed, letting me rotate in his lab and still agreeing to chair my committee. Thank you also Bill and Marian for your helpful guidance at my committee meetings. Without a doubt, I owe the most thanks to my wife, Hilary, who has unfailingly loved and supported me through long hours during the seemingly endless training program that I have embarked on. I could not do it without you.

Table of Contents

Figures

Tables

Copyright Information

The chapters of the dissertation have appeared in whole or part in publications below:

Horwich MD*, Li C*, Matranga C*, Vagin V, Farley G, Wang P, Zamore PD. The *Drosophila* RNA methyltransferase, DmHen1, modifies germline piRNAs and single-stranded siRNAs in RISC. Current Biology. 2007 Jul 17;17(14):1265-72.

Förstemann K*, Horwich MD*, Wee L, Tomari Y, Zamore PD. *Drosophila* microRNAs are sorted into functionally distinct argonaute complexes after production by dicer-1. Cell. 2007 Jul 27;130(2):287-97.

Ghildiyal M*, Seitz H*, Horwich MD, Li C, Du T, Lee S, Xu J, Kittler EL, Zapp ML, Weng Z, Zamore PD. Endogenous siRNAs derived from transposons and mRNAs in *Drosophila* somatic cells. Science. 2008 May 23;320(5879):1077-81.

Horwich MD and Zamore PD. Design and Delivery of Antisense Oligonucleotides to Block miRNA Function in Cultured *Drosophila* and Human Cells. Nature Protocols. *In press.*

* These authors contributed equally to this work

Abstract

Small interfering RNAs (siRNAs), microRNAs (miRNAs), and piRNAs (piRNA) are conserved classes of small single-stranded ~21-30 nucleotide (nt) RNA guides that repress eukaryotic gene expression using distinct RNA Induced Silencing Complexes (RISCs). At its core, RISC is composed of a single-stranded small RNA guide bound to a member of the Argonaute protein family, which together bind and repress complementary target RNA. miRNAs target protein coding mRNAs—a function essential for normal development and broadly involved in pathways of human disease; small interfering RNAs (siRNA) defend against viruses, but can also be engineered to direct experimental or therapeutic gene silencing; piwi associated RNAs (piRNAs) protect germline genomes from expansion of parasitic nucleic acids such as transposons. Using the fruit fly, *Drosophila melanogaster*, as a model organism we seek to understand how small silencing RNAs are made and how they function.

In *Drosophila*, miRNAs and siRNAs are proposed to have parallel, but separate biogenesis and effector machinery. miRNA duplexes are excised from imperfectly paired hairpin precursors by Dicer1 and loaded into Ago1; siRNA duplexes are hewn from perfectly paired long dsRNA by Dicer2 and loaded into Ago2. Contrary to this model we found one miRNA, miR-277, is made by Dicer1, but partitions between Ago1 and Ago2 RISCs. These two RISCs are functionally distinct—Ago2 could silence a perfectly paired target, but not a centrally bulged target; Ago1 could silence a bulged target, but not a perfect target. This was surprising since both Ago1 and Ago2 have endonucleolytic cleavage activity necessary for perfect target cleavage in vitro. Our detailed kinetic studies suggested why—Ago2 is a robust multiple turnover enzyme, but Ago1 is not.

Along with a complementary in vitro study our data supports a duplex sorting mechanism in which Diced duplexes are released, and rebind to Ago1 or Ago2 loading machinery, regardless of which Dicer produced them. This allows structural information embedded in small RNA duplexes to direct small RNA loading into Ago1 and/or Ago2, resulting in distinct regulatory outputs.

Small RNA sorting also has chemical consequences for the small RNA guide. Although siRNAs were presumed to have the signature 2′, 3′ hydroxyl ends left by Dicer, we found that small RNAs loaded into Ago2 or Piwi proteins, but not Ago1, are modified at their 3′ ends by the RNA 2′-*O*-methyltransferase DmHen1. In plants Hen1 modifies the 3′ ends all small RNAs duplexs, protecting and stabilizing them. Implying a similar function in flies, piRNAs are smaller, less abundant, and their function is perturbed in *hen1* mutants. But unlike plants, small RNAs are modified as single-strands in RISC rather than as duplexes. This nicely explains why the dsRNA binding domain in plant Hen1 was discarded in animals, and why both dsRNA derived siRNAs and ssRNA derived piRNAs are modified. The recent discovery that both piRNAs and siRNAs target transposons links terminal modification and transposon silencing, suggesting that it is specialized for this purpose.

Introduction:

In 1969 Britten and Davidson proposed a theory to explain how multicellular organisms achieve tissue specific gene expression (Britten and Davidson, 1969). They postulated the existence of regulatory RNAs that would control batteries of genes, defining the gene expression program for a given cell type. They reasoned that eukaryotic genomes - much larger and harboring far more repetitive sequences than prokaryotic genomes – may contain RNAs corresponding to these repetitive sequences that could base pair in *cis*- or *trans*- to homologous elements scattered throughout the genome to regulate sets of non-contiguous cell specific genes. "Activator" RNAs binding repetitive DNA proximal to a gene could displace repressive histones, allowing transcription to proceed. Employing occam's razor they considered, but dismissed the possibility that proteins might carry out such a function.

Because protein transcription factors had not been discovered yet, the idea of ribo-regulation seemed simpler. Moreover, it led directly to ideas about how genetic drift in repeteated sequences might alter gene expression and drive evolution. While the discovery of transcription factors filled the regulatory role proposed for Britten and Davidson's "activator" RNAs, a new class of RNAs, collectively known as small silecing RNAs, appears possess many of the properties they suggested—but they perform an equally important role in repressing gene expression instead. Small silencing RNAs are often cell type specific, some derive from repetitive sequences, they broadly regulate gene expression utilitzing basepairing interactions to elements dispersed throughout the genome, and alterations in their sequences appear to play an important role in evolution (Bartel, 2004; Zamore and Haley, 2005; Aravin et al., 2007). Importantly, the discovery

of small RNAs has forced us to reconsider gene expression paradigms; ribo-regulation by small RNAs is now recognized as a critical point of regulation in the conversion of genetic information from DNA to protein. Now, 15 years after the first small RNA was described, it appears that few biological processes in animals and plants function optimally in the absence of small RNA regulation. Here we discuss the evolution of the small RNA field in order to frame the research presented in chapters II, III and Apendices. Subsequent studies will be discussed in Chapter IV.

miRNAs, siRNAs, and RNAi

miRNA Discovery

Victor Ambros and colleagues identified the first small RNA, a microRNA (miRNA) named *lin-4* (Lee et al., 1993). Over 10 years of genetic studies by the Ruvkun and Ambros groups suggested an interaction between the *lin-4* gene and the 3′untranslated region (UTR) of another gene *lin-14*, which encoded a nuclear protein (Ambros and Horvitz, 1984; Ruvkun et al., 1989; Arasu et al., 1991; Wightman et al., 1991). Mutation in either gene gave a "heterochronic" phenotype - a defect in the timing of developmental transitions in the nematode, *C.elegans* (Ambros and Horvitz, 1984). Ambros' finding that *lin-4* was not a protein, but rather a small 22 nt non-coding RNA with a 61 nt precursor came as a shock - but it fit perfectly with the careful genetic analyses implicating an interaction with the *lin-14* 3′UTR (Wightman et al., 1993); *lin-4* small RNA had extensive complementarity to 7 sites in the *lin-14* 3′UTR. Moreover, the mutations in both *lin-4* and *lin-14* mapped precisely to the complementary regions and partial deletion of the sites gave a weaker phenotype than deletion of them all. *lin-14*

mRNA abundance was unaltered in all mutants, but disruption of the *lin-4:lin-14* mRNA duplex by mutations at the 5′ end of *lin-4* caused persistent production of Lin-14 protein, suggesting that *lin-4* binding inhibits translation of *lin-14* mRNA (Lee et al., 1993).

These studies were an amazing feat of forward genetics that revealed many of the fundmental principles of miRNA regulation. That is, miRNAs are encoded in the genome, commonly in introns. They contain characteristic hairpin precursors that are processed to yield 22 nt RNAs. These 22 nt guides basepair with partially complementary target mRNA sequences in 3′UTRs and inhibit translation.

Unfortunately, *lin-4* is only conserved in worms, leading the scientific community (and Ambros and Ruvkun) to wonder whether *lin-4* was an innovation unique to worms, or perhaps even unique in worms (hence the news and views title, "Deviants – or Emissaries?")(Wickens and Takayama, 1994). The former seemed likely when another miRNA, *let-7*, and its target *lin-41*, also heterochronic *C. elegans* genes, were discovered by Ruvkun's group 7 years later (Reinhart et al., 2000). The potenial for a more general role of small RNAs became clear when Pasquinelli and colleagues found that *let-7* was conserved in both its sequence and the timing of its expression at the transition to adulthood in bilaterian animals (Pasquinelli et al., 2000). At this point, parallel studies of the RNA interference pathway converged with the budding miRNA field and the line between the two pathways began to blur.

RNAi Discovery

RNA interference (RNAi) phenomena were first observed in plants by two groups in their efforts to make a purple petunia more purple. Paradoxically, transgenic

introduction of the pigment synthesis genes chalcone synthase or dihydroflavonol-4-reductase, often resulted in production of white or mottled white flowers instead (Napoli et al., 1990; van der Krol et al., 1990). This phenomenon of homologous transgenes triggering silencing of an endogenous gene was termed “Co-suppression”. Further studies by Baulcombe and colleagues suggested that this might be caused by transgene derived antisense RNA targeting the endogenous RNA; such a phenomenon might be related to a system to silence plant viruses (Baulcombe, 1996; Ratcliff et al., 1997; Voinnet and Baulcombe, 1997; Brigneti et al., 1998).

Antisense RNA regulation of endogenous genes had also been observed in *C. elegans*. Fire and colleagues disrupted myofilament genes *unc-22* and *unc-54* by injecting oocytes with vectors expressing corresponding antisense fragments. They observed high levels of antisense RNA with little change in sense mRNA levels and speculated that either transport to the cytoplasm or translation were affected (Fire et al., 1991). Extending this approach Guo and Kemphues injected worm oocytes with in vitro transcribed antisense RNA targeting, *par-1*, a kinase gene important for establishing embryo polarity. To their surprise, their sense RNA control phenocopied *par-1* with the same frequency as antisense RNA (Guo and Kemphues, 1995).

In their landmark study, Fire and Mello revealed that the effect seen by Guo and Kemphues (RNA interference or RNAi) was likely due to unintended formation of dsRNA (Fire et al., 1998). Injected dsRNA was over 100-fold more potent trigger for silencing of *unc-22* than either sense or antisense suggesting that even small amounts of contaminating sense or antisense RNA produced during in vitro transcription could produce a phenotype. Injected long dsRNAs (300-1000 nt) could silence genes

systemically, causing mRNA reduction even at a distance from the injection site; RNAi only worked if exons were targeted implying a post-transcriptional mechanism, and remarkably, silencing could be transmitted to progeny. This fact was especially intriguing—it suggested that the silencing mechanism involved amplification or a catalytic component, because dilution alone would not produce more than a few molecules per cell of dsRNA from the original injection. Fire and Mello's Nobel Prize winning characterization of RNAi in worms ignited the field. The tremendous potential of RNAi as a reverse genetic tool and as important biology drove the field forward at a furious pace.

Conservation of an RNAi response was rapidly demonstrated in a host of organisms, including plants, flies, trypanosomes, planaria, zebrafish embryos, hydra, and mouse oocytes or early embryos (Ngo et al., 1998; Kennerdell and Carthew, 1998; Waterhouse et al., 1998; Lohmann et al., 1999; Sánchez-Alvarado and Newmark, 1999; Wargelius et al., 1999; Wianny and Zernicka-Goetz, 2000; Svoboda et al., 2000). The finding that RNAi activity was present in *Drosophila* embryos led to the development of an important in vitro system that recapitulates RNAi – addition of long dsRNA to syncitial blastoderm extracts can induce specific degradation of a homologous mRNA (Tuschl et al., 1999). Further biochemical studies examining the fate of both the dsRNA and targeted mRNA showed that the dsRNA trigger is processed to 21-23 nt fragments, even in the absence of a target; target mRNA is also cleaved at intervals of the same size, suggesting that mRNA degradation in RNAi is directed by the dsRNA derived small RNA fragments (Zamore et al., 2000). Similarly, fly S2 cells treated with dsRNA produced ~25 nt RNAs that co-fractionated with an mRNA degradation activity

(Hammond et al., 2000). These studies along with an earlier study in plants showing that accumulation of 25 nt antisense RNAs correlated with transgene silencing (Hamilton and Baulcombe, 1999) and a later study in worms (Parrish et al., 2000) strongly suggested that RNAi is mediated by small RNAs 21-25 nt long that guide degradation of homologous mRNAs. The fractionation experiments also suggested that a small RNA guided nuclease resides in a high molecular weight ribonucleoprotein (RNP) complex, which they dubbed RNA Induced Silencing Complex (RISC).

Common Features of siRNA and miRNA Biogenesis in Animals

The discovery that RISC contains small RNA guides cleaved out of long dsRNA immediately suggested the action of an RNAse III enzyme, the only class of double-stranded RNA nuclease known to produce small RNA fragments (Bass, 2000). Experiments using RNAi in S2 cells and recombinant proteins showed that this was the case – the eukaryotic RNase III enzyme responsible for this was named "Dicer" (Bernstein et al., 2001). Bacterial RNAse III enzymes were already known to leave characteristic dsRNA ends containing 5′ phosphates, 2′, 3′ hydroxyl ends with 2 nt 3′ overhangs (Nicholson, 1999). Concurrent, studies by the Tuschl group found that the small RNAs produced from dsRNA in *Drosophila* extracts, small interfering RNAs (siRNA), were sensitive to calf intestine phosphatase (indicating the presence of a 5′ or 3′ phosphate) and periodate oxidation followed by β-elimination (indicating that the 3′ end contained both a 2′ and 3′ OH groups, rather than a 3′ cyclic phosphate) (Elbashir et al., 2001b). Although this was "data not shown" in the manuscript it was consistent with RNase III processing. Furthermore, synthetic small RNA duplexes with 5′ phosphates, 3′ hydroxyls and the characteristic RNase III-like 3′ overhangs could mediate target

cleavage in vitro. This allowed precise mapping of mRNA target cleavage sites, indicating that homologous mRNAs were cleaved in the middle of the antisense small RNA guides by an unidentified nuclease activity, later termed "Slicer" activity (Parker et al., 2004). Elucidation of siRNA's chemistry also formed the basis for Tuschl's major breakthough—that siRNAs can direct RNAi in mammalian cells, bypassing the Protein Kinase R (PKR) response (Elbashir et al., 2001a). The PKR response, a mammalian anti-viral response to long dsRNA that causes global translational arrest, was the main impediment to RNAi in mammalian cells. Overcoming this barrier opened up a new approach to reverse genetics in mammals. Armed only with a gene's mRNA sequence, now readily available with completed human and mouse genomes, researchers could perform loss of function experiments by introducing a gene specific siRNA. siRNA therapeutics were an obvious extension of this approach.

The surprisingly similar size of siRNAs to small temporal RNAs (miRNAs) and their double-stranded hairpin origin hinted that they might be related. Are small temporal RNAs also made by Dicer? The overwhelming repsonse - yes. Genetic studies in worms demonstrated that Dicer mutants and RNAi knockdown gave phenotypes reminiscent of *let-7* and *lin-4*, caused accumulation of precursor RNAs, and worms had defective RNAi responses (Grishok et al., 2001; Ketting et al., 2001). Just as siRNAs were excised from long dsRNA in fly extracts, *let-7* could be excised from an in vitro transcribed hairpin precursor. Endogenous *let-7* had the same 5′ phosphate and 3′ hydroxyl ends as siRNAs, and depletion of Dicer in human cells also caused accumulation of its precursor (Hutvágner et al., 2001).

Although Dicer was originally presumed to make both cuts in miRNA maturation from their longer precursors, Narry Kim's group found that a second nuclear RNAse III protein, Drosha, cuts long primary miRNA tanscripts (pri-miRNA) derived from independent pol II or III transcription units or introns (Lee et al., 2003; Han et al., 2006). The resulting 60-80 nt hairpin—a pre-miRNA—is then exported to the cytoplasm where Dicer makes a second cut to produce a small RNA duplex intermediate, consisting of the miR strand (which is stabilized accumulates), bound to the miR* strand (which is degraded). Thus a miR/miR* duplex has two RNAse III-like ends – one made in the nucleus by Drosha, the other made in the cytoplasm by Dicer.

Identical in their chemistry, miRNAs could in theory be cloned, just as Tuschl's lab had done for siRNAs. Indeed, cloning of endogenous small RNAs by the Ambros, Bartel, and Tuschl groups from *C. elegans* (Lau et al., 2001; Lee and Ambros, 2001), *Drosophila* embryo extracts, and human tissue culture cells (Lagos-Quintana et al., 2001) clearly demonstrated that, (1) miRNAs are a diverse and extensive class of genes, (2) that many are conserved in vertebrates and invertebrates, (3) that they are differentially expressed, and (4) that their signature feature in the genome is formation of hairpin precursor transripts. While this initial round of sequencing revealed ~90 miRNAs between these three species, increasing sophistication in sequencing technologies and bioinformatics has fueled a massive expansion of known miRNA genes; the human genome alone appears to contain over one thousand miRNA genes (Berezikov et al., 2006).

In addition to Dicer, the Mello lab identified another class of genes central to both the RNAi and miRNA pathways—Argonaute proteins. Argonautes are highly conserved,

containing two distinctive domains – Paz and Piwi. Dicer also has a Paz domain suggesting it may be specialized for small RNA pathways. A genetic screen in the Mello lab identified *rde-1* as a mutant unable to perform RNAi, but viable and fertile. Rde-1 was one of 27 Argonaute proteins in worms. Two more Argonaute mutants, *alg-1* and *alg-2* gave phenotypes similar to Dicer and the *lin-4* and *let-7* genes, lending additional support to the idea that similar mechanisms governed the RNAi and miRNA pathways (Grishok et al., 2001). Importantly, this was the first evidence indicating that Argonautes had specialized functions, dedicated to the similar but discrete RNAi and miRNA pathways. The importance of Argonautes in RNAi was reinforced by biochemical and functional studies in the Hannon lab; the fly protein Argonaute 2 co-purified with target degradation activity and RNAi knockdown studies in fly S2 cells crippled RNAi activity. Furthermore, Ago2 associated with Dicer. (Hammond et al., 2001). A human Argonaute protein eiF2C2 (later called Ago2) also copurified with miRNAs (Mourelatos et al., 2002) and siRNA target cleavage activity (Hutvágner and Zamore, 2002; Martinez et al., 2002). Remarkably, endogenous *let-7* associated with Ago2 could also cleave a perfectly paired target, but not one resembling its bulged native target, *lin-41*. Thus it appeared that siRNAs and miRNAs utilized the same RISC in human cells, spawning the idea that the mode of small RNA silencing - translational repression or target cleavage - may be solely determined by the structure of the guide:target duplex. Supporting this view, Doench and Sharp found that siRNAs can also direct miRNA-like translational repression in human cells (Doench et al., 2003). Conversely, an siRNA sequence engineered into a miRNA-like hairpin precursors might be used in place of synthetic siRNA for RNAi in

mammalian cells. Indeed, small hairpin RNAs are now routinely used for RNAi experiments (Paddison et al., 2002; McManus et al., 2002).

Initially, 22 nt miRNAs were known to be single-stranded (Lee et al., 1993), while their siRNA counterparts were duplexes (Elbashir et al., 2001b). The idea that mature siRNAs were duplexes in cleavage competent RISC diminished, as biochemical analyses of RISC formation in fly extracts suggested an ATP-dependent unwinding step in RISC assembly (Nykanen et al., 2001); single-stranded siRNAs could also cleave targets, albeit inefficiently (Schwarz et al., 2002; Martinez et al., 2002). Finally, two studies definitively showed that functional RISC contained only a single-stranded guide. Using biochemical and cellular assays, Schwarz and colleagues found that alterations in the thermodynamic stability of the siRNA ends governed which strand of the siRNA duplex entered RISC; the strand with the less stable 5′ end is loaded into RISC—the other stand is destroyed (Schwarz et al., 2003). An identical result was obtained by Khvorova and collegues using high-throughput screening of siRNA efficacy and *in silico* analysis (Khvorova et al., 2003). Not only did these studies guide experimentalists in future siRNA design—they implied the same principles might be used *in vivo* to make single-stranded miRNAs from a duplex intermediate consisting of a mature miRNA and its imperfectly paired complement, miRNA*. After production of a miRNA/miRNA* duplex by Dicer, the miRNA would be retained in RISC, while the miRNA* would be destroyed. The 5′U bias of miRNAs (Lau et al., 2001)and examination of known miRNAs supported this idea; the fact that miRNAs can be made from either arm of the pre-miRNA hairpin also suggested a duplex intermediate (Lau et al., 2001; Lagos-Quintana et al., 2001; Lee and Ambros, 2001).

Additional protein components are required for siRNA or miRNA/miRNA* duplexes to be loaded into RISC. dsRNA binding proteins and appear to have a conserved role directing assembly small RNAs into RISC. In worms *rde-4*, a protein with two dsRNA binding domains (dsRBD), associates with Dicer and the argonaute protein Rde-1, and is required for RNAi (Tabara et al., 2002). There are two Rde-4 homologues in flies—R2D2 and Loquacious (Loqs). R2D2 binds Dicer2 and is required for siRNAs to assemble into RISC (Liu et al., 2003), while Loqs binds Dicer1 and is required for efficient miRNA processing (Jiang et al., 2005; Saito et al., 2005; Förstemann et al., 2005). Similarly, miRNA and siRNA RISC assembly in human cells requires the dsRBD proteins TRBP and PACT, which interact with Dicer (Lee et al., 2006; Chendrimada et al., 2005). RNA helicases seem to play conserved roles in RNAi (Dalmay et al., 2001; Tabara et al., 2002; Tomari et al., 2004; Meister et al., 2005; Robb and Rana, 2007; Ishizuka et al., 2002; Ishizuka et al., 2002). While several studies indicate that helicases play facilitate assembly of active RISC their precise function remains unclear (Tomari et al., 2004; Meister et al., 2005; Robb and Rana, 2007). Other RISC associated proteins that impacted RNAi efficacy include RNA binding proteins Vasa Intronic Gene (Vig), Fragile-X mental retardation protein (dFXR), the helicase Dmp68, and a staphylococcal nuclease homologue, Tudor-SN (Caudy et al., 2002; Caudy et al., 2003).

Despite the growing catalogue of RISC associated proteins, the identity of RISC's "Slicer" remained elusive. From previous studies and increasingly rigorous biochemical purifications it became clear that human and fly Argonaute 2 were intimately associated with small RNA cleavage activity (Meister et al., 2004b; Rand et al., 2004). Definitive proof that Ago2 is Slicer was provided by two studies which showed that that the Piwi

domain of Argonautes had an RNase H-like fold (Song et al., 2004) and that mutation of the putative catalytic residues of a tagged version of human Ago2 protein abolished its nuclease activity (Liu et al., 2004). Notably, overexpressed tagged Ago1, 3, and 4, three close homologues that can also bind miRNAs and siRNAs, lack these catalytic residues and cannot cleave target mRNAs (Meister et al., 2004b; Liu et al., 2004). The crystal structure also revealed a groove ideally suited for small RNA guided target cleavage—large enough for a guide-target duplex and running close to the DDH catalytic site. Combined with earlier structural and biochemical studies showing that the Paz domain binds siRNA 3′ ends (Yan et al., 2003; Lingel et al., 2003; Song et al., 2003), a clear picture now emerged; an Argonaute protein bound to a small RNA guide forms the catalytic core of RISC.

Common Features of miRNA and siRNA Silencing

From Ambros and Ruvkun's original studies, miRNAs appeared to regulate their targets through imperfect base-pairing. The precise patterns of that basepairing have been rigorously scrutinized both computationally and experimentally. Because miRNAs and siRNAs appear to assemble into the same RISCs (at least in mammals), the rules governing target specificity suggest both putative targets of a miRNA, as well as potential unintended "off-targets" of an siRNA. A number of studies immediately suggested that the specificy of miRNAs was very small indeed. Eric Lai noticed that newly sequenced miRNAs paired perfectly to 8 base K-box motifs that had been identified genetically as sites of negative post-transcriptional regulation (Lai, 2002). Several groups used bioinfomatic approaches to look for miRNA targets in mammals, flies, and worms, considering both miRNA:target duplex thermodynamics and cross species conservation

of putative target sites that might basepair with miRNAs (Stark et al., 2003; Lewis et al., 2003; Enright et al., 2003; Lewis et al., 2005; Brennecke et al., 2005). The results of these studies agreed with Lai's observation; specificity is determined by basepairing of bases 2-7 at the 5′ end of a miRNA—the so-called "seed" sequence. This also agreed with mutational analysis of reporter target:miRNA pairing in tissue culture cells (Doench and Sharp, 2004). Kinetic analysis of in vitro target cleavage by *Drosophila* RISC also indicated that the "seed" region is critical for target binding, while pairing of the central bases of the small RNA guide are required for catalysis (Haley and Zamore, 2004). The tiny size of the "seed" sequence has big implications; each miRNA could regulate hundreds of target mRNAs - an estimated ~30% of mRNAs (Lewis et al., 2005). This may underestimate the true number, because only conserved sites in 3′UTRs are considered. As we and others have observed, miRNAs can also regulate target sites that reside in coding sequences (Appendix II) (Kloosterman et al., 2004; Easow et al., 2007; Duursma et al., 2008).

Because miRNAs were thought to repress translation (Lee et al., 1993; Olsen and Ambros, 1999) it was surprising that a transfected siRNA reduced mRNA levels of unintended target transcripts that contained only signatures of the siRNA seed (Jackson et al., 2003). This along with a study cataloguing the transcripts downregulated by miRNA-like siRNAs (Lim et al., 2005), suggested that small RNAs could induce cleavage independent degradation of targeted transcripts in mammalian cells. Studies in worms, mice, zebrafish, and fly cells also confirmed that miRNAs could cause degradation of targets in addition to or instead of translational repression (Bagga et al., 2005; Giraldez et al., 2006; Behm-Ansmant et al., 2006; Krutzfeldt et al., 2005). Although there is some

evidence that the specific pattern of pairing at the central bases can influence whether a reporter miRNA target is degraded or repressed (Aleman et al., 2007), the biochemical nature of these mechanistic options remains to be determined. Likely due to the comparative difficulty of proteomic approaches versus mRNA expression arrays, no studies to date have assessed the extent of siRNA off-target effects at the translational level.

In contrast to RNAi, lack of an in vitro system that recapitulates small RNA directed translational repression has hampered efforts to understand the mechanism of miRNA directed translational repression. Although the translational repression mechanism has been intensely scrutinized, a unified picture has not yet emerged. Early studies in worms suggested a post-initiation translational block (Olsen and Ambros, 1999), as did more recent studies in human tissue culture cells (Petersen et al., 2006; Maroney et al., 2006). By contrast, several recent studies suggest that translational initiation is blocked (Pillai et al., 2005; Thermann and Hentze, 2007; Mathonnet et al., 2007; Chendrimada et al., 2007; Kiriakidou et al., 2007). This includes two studies that finally recapitulate miRNA directed translational repression using fly and mouse in vitro systems (Thermann and Hentze, 2007; Mathonnet et al., 2007). Although the findings that RISC associates with eIF6, a ribosome anti-association factor (Chendrimada et al., 2007), and that Argonaute proteins contain a conserved 7meG cap binding motif in the "mid" domain (Kiriakidou et al., 2007), support a pre-initiation block, a recent study in *Drosophila* cells disputes these claims; eIF6 knockdown has no effect on miRNA silencing, and mutation of the cap binding motif of fly Argonaute prevents miRNA binding all together (Eulalio et al., 2008). Complicating matters further, one study even

suggests that miRNAs can stimulate translation in non-proliferating cells (Vasudevan et al., 2007).

Translational repression and target mRNA degradation likely occur in P-bodies, cytoplasmic organelles consisting of mRNP aggregates. Defined by the human auto-antigen GW182, these foci also contain miRNAs, Argonautes, mRNAs, decapping enzymes, deadenylating enzymes, translational repression factors, and a host of other RNA processing machinery (Parker and Sheth, 2007). Argonaute proteins can directly bind GW182 in humans, flies, and worms, likely inducing formation of P-bodies (Behm-Ansmant et al., 2006; Liu et al., 2005; Ding et al., 2005). The importance of this interaction is suggested by experiments showing that disruption of human GW182 relieves translational inhibition of a targeted miRNA (Liu et al., 2005), and that tethering of an mRNA to GW182 is sufficient for silencing in fly cells (Behm-Ansmant et al., 2006). Because silencing by small RNAs as well as other RNA decay processes can proceed in the absence of visible P-bodies (Eulalio et al., 2007), appearance of P-body aggregates is likely a result, not a cause of silencing.

miRNA and siRNA Functions in Animals

The dramatic developmental phenotypes seen in animals with defective small RNA biogenesis machinery indicate critical functions for small RNAs in development. Ablation of Alg-1 and 2 or Dicer in worms (Grishok et al., 2001), Ago2 or Dicer in mice (Bernstein et al., 2003), Dicer1, Loqs, or Ago1 in flies (Kataoka et al., 2001; Lee et al., 2004; Park et al., 2007), and Dicer in zebrafish (Giraldez et al., 2005), all result in embryonic lethality. More recent studies creating tissue specific loss of Dicer in mice, also suggest important roles for small RNAs in the mophogenesis and homeostasis of the

heart, brain, limbs, lung, muscle, pancreas, and skin (Chen et al., 2008; Kim et al., 2007; Andl et al., 2006; Cuellar et al., 2008; Davis et al., 2008; O'Rourke et al., 2007; Lynn et al., 2007; Zhao et al., 2007; Harris et al., 2006; Harfe et al., 2005). So why then did miRNAs evade genetic detection for so long? The explanation likely comes from (1) their small size, (2) their complex genomic organization in polycistrons and introns, and (3) extensive functional redundancy. The original *lin-4* heterochronic alleles were isolated at 1/10 the frequency of protein coding genes (Ambros and Horvitz, 1984). Furthermore, in a recent study in which deletions were reported for 83% of known miRNA genes in *C. elegans*, loss of most individual miRNA genes caused no obvious phenotype (Miska et al., 2007). Functional redundancy likely explains this result, as combining deletions of several *let-7* family members that alone had no phenotype, caused distinct phenotypes (Abbott et al., 2005). Similarly, another recent study in mice showed that deletion of two miRNA cluster paralogs miR-106a~363 or miR-106b~25 produced no obvious phenotype; yet combining these deletions with a third paralagous cluster, mir-17~92, results in embryonic lethality (Ventura et al., 2008).

Despite the functional redundancy of many miRNA genes, several cases do now exist in flies and mice where disruption of a single miRNA produces a visible phenotype. Two genetic screen based studies in *Drosophila* found that defects in individual miRNAs, bantam or miR-14, resulted in defects in apoptosis and cell proliferation (Brennecke et al., 2003; Xu et al., 2003). These early studies confirmed that miRNAs play important roles in animals besides worms; intriguingly, as negative regulators of apoptosis and cell proliferation they suggested that miRNAs might be tumor suppressors. More focused studies using targeted deletions of muscle specific miR-1 in mice and flies demonstrated

its requirement for myogenesis and cardiogenesis (Zhao et al., 2007; Sokol and Ambros, 2005; Kwon et al., 2005). Deletion of miR-9a in flies produces ectopic peripheral sensory neurons (Li et al., 2006), while deletion of miR-8 induces neuronal apoptosis (Karres et al., 2007). In both of these cases, the miRNAs and their targets appear to be conserved in mammals.

The rapidly expanding catalogue of miRNA genes coupled with the difficulty of obtaining genetic mutants prompted development of a new tool to study miRNA function—antisense oligonucleotide (ASO) inhibitors. ASOs are nuclease resistant oligonucleotides that bind cognate miRNAs in RISC (Hutvágner et al., 2004; Meister et al., 2004a). Our group developed 31 nt 2'-*O*-Me ASO inhibitors that block the function of siRNAs or miRNAs in vitro and in transfected human tissue culture cells, permitting miRNA loss of function studies to be conducted in human cells. ASOs can also inactivate miRNAs in worms—injected *let-7* ASO phenocopies *let-7* mutants (Hutvágner et al., 2004). ASOs have several advantages over genetic approaches. (1) studies are rapid and require only the miRNA's sequence, (2) they can simulataneously inactivate miRNA paralogues differing by one or two bases, and (3) they can be used in human cultured cells to inactivate miRNAs.

We found that addition of a 3′- cholesterol moiety enhances the potency and duration of action of our ASOs in *Drosophila* S2 cells, and facilitates delivery without the use of a lipid carrier (Appendix 2). Subsequent to our finding the Stoffel group reported that injection of 3′-cholesterol-modified ASOs, called "antagomirs", into mice not only inactivated, but directed degradation of targeted miRNAs (Krutzfeldt et al., 2005). Furthermore, miRNA degradation occurred in every tissue except brain. When

miR-122, a liver specific miRNA, was inactivated mRNAs containing miR-122 seeds in their 3′UTRs increased, and many mRNAs devoid of miR-122 seeds decreased—likely a secondary effect. These reduced mRNAs were enriched in cholesterol biosynthesis genes and a corresponding decrease in plasma cholesterol was observed. A similar study performed with 2'-Methoxy-ethyl ASOs, confirmed their result, but only showed partial reduction of detected miR-122 signal (Esau et al., 2006). Because our previous results indicated that ASOs were stoichiometric inhibitors, we were suspicious of the antagomir directed degradation. We found that (1) antagomirs do not direct degradation of miRNA in S2 cells, (2) incubation of a small RNA with excess antagomir can cause a northern blot artifact that prevents accurate detection of the small RNA, and (3) this artifact can be largely corrected by use of an LNA northern probe instead with high hybridization temperature, instead of a DNA probe. Our data indicates that the apparent degradation seen in antagomir treated mice could be caused by excess antagomir which might prevent detection of the targeted miRNA on Northern blot with a DNA probe (See Appendix 2).

Regardless of the mechanism, ASO studies in flies, mice, and cultured cells have been an important tool to dissect miRNA function (see Appendix 2 for review). Their use has led to findings that individual miRNAs are involved in insulin release, cholesterol metabolism, hepatitis C replication, cardiac arrhythmia, apoptosis, and cell cycle progression (Poy et al., 2004; Krutzfeldt et al., 2005; Yang et al., 2007; Bommer et al., 2007; Pedersen et al., 2007; Matsubara et al., 2007), just to name a few.

To understand the function of the highly conserved *let-7* family of miRNAs we used an ASO based approach to identify mRNA targets whose abundance is regulated by the human *let-7* gene family (Appendix 1). Because *let-7* has 8 paralogues, equivalent

genetic studies would be extremely demanding. We sought to identify genuine endogenous targets of *let-7* by comparing two set of mRNAs: those that are upregulated when endogenous *let-7* is inactivated by an ASO, and those that are down regulated when a *let-7* siRNA is introduced into cells that do not express *let-7*. Our study identified a set of genes that included the oncogenic architectural transcription factor HMGA2 and Dicer. HMGA2 is the top predicted target for *let-7* (Lewis et al., 2005), which contains seven conserved *let-7* seeds in its 3′UTR. Dicer also contains four conserved *let-7* sites, but these are in its coding sequence rather than its 3′UTR. Dicer regulation by *let-7* was confirmed in adult mice, and inappropriate introduction of *let-7* can lead to accumulation of pre-miRNAs in cultured cells. This suggests a novel function for *let-7* as part of a regulatory loop for miRNA biogenesis (Appendix II).

Our finding that HMGA2, an oncogene, is regulated by *let-7* lends further support to the idea that miRNAs can function as tumor suppressors. While our study was in revision Bartel and co-workers also showed that HMGA2 is targeted by *let-7*; they also noted that some oncogenic chromosomal translocations occur in its 3′UTR, removing *let-7* regulation (Mayr et al., 2007). *Let-7* has an additional tumor suppressor function through its regulation of the Ras oncogene (Johnson et al., 2005). This gene escaped our detection, likely because it is regulated by translational repression. miRNAs can also function as oncogenes (He et al., 2005), promote metastasis (Ma et al., 2007), or prevent metastasis (Tavazoie et al., 2008). Thus therapeutic modulation of miRNAs, by introduction or inhibition may offer a novel treatment.

Unique Aspects of Small RNA Silencing

The RNAi and miRNA pathways have evolved unique features in different organisms. Key differences are reviewed here.

Argonautes

Worms appear to have greatly elaborated their RNAi silencing pathways—by contrast to S. Pombe which contains one Argonaute protein, worms contain 27; Plants contain 10, Humans 8, and flies 5 (Tolia and Joshua-Tor, 2007). Argonaute proteins fall into two major clades—Ago and Piwi. To date all Ago subclade Argonautes interact with small RNAs processed by a Dicer enzyme; this includes all Argonautes in plants, Ago1-4 in humans, Ago1 and 2 in flies, Ago1 in *S.Pombe*, and Alg-1 and Alg-2 in worms. Not all Ago proteins retain their catalytic function. For instance human Ago1, 3, and 4 lack catalytic activity, suggesting their small RNA guides (miRNAs), do not require it to function. Piwi proteins however, all seem to have catalytic residues, but they bind small RNAs (piwi interacting RNAs or piRNAs) that don't require Dicer for their production (see piRNAs below). *C.elegans* also contains a third class of Argonautes that don't fit into either clade. This class includes Rde-1 which binds siRNA generated by Dicer, as well as the Argonautes Csr-1 and Sago-1 and -2, which do not.

RNA-dependent RNA Polymerases

The presence of an RNA-dependent RNA polymerase (RdRP) seems to be a major determinant of how RNAi works in different organisms. Worms, *S. pombe*, and plants require RdRPs for their RNAi response, but *Drosophila* and mammals do not—RdRP genes have not been detected biochemically or computationally in insect or mammalian genomes (Zamore and Haley, 2005).

RdRPs appear to function differently in plants and worms. In plants single-stranded transcripts are cleaved by miRNAs or other small RNA classes, a second strand is synthesized by RdRPs from the 3′ end of the cleavage site, and the resulting long dsRNA is Diced into phased siRNAs by one of 4 plant dicers (Ramachandran and Chen, 2008). This amplification step generates small RNAs upstream from the region originally targeted, a phenomenon termed "transitive RNAi". RdRPs mediate transitive RNAi in worms too, confirming Fire and Mello's prediction of an amplification step (Fire et al., 1998). But in worms Dicer is only required for production of primary siRNAs from the double-stranded trigger. As expected, sense and antisense primary siRNAs have 5′ phosphates and 3′ hydroxyl groups and are loaded into Rde-1 (Sijen et al., 2007). Secondary siRNAs, however, are only antisense, they have 5′ di- or tri-phosphates generated by RdRPs, and are loaded into "secondary" argaonautes, Csr-1, Sago-1, and Sago-2 (Yigit et al., 2006; Aoki et al., 2007; Pak and Fire, 2007; Sijen et al., 2007). Csr-1 has in vitro target cleavage activity, suggesting its silencing mechanism (Aoki et al., 2007). Thus plant secondary siRNAs require both dicer and RdRPs for initiation and production, while worm secondary siRNAs require dicer for initiation targeting by primary siRNAs, but not production (Aoki et al., 2007). *S. pombe* also has a single RdRP, which seems to act most similarly to those in plants; it mediates second strand synthesis after targeting by an Ago1 bound siRNA, elongates a nascent transcript, producing a long dsRNA which is then Diced, producing new siRNAs (Colmenares et al., 2007). Perhaps this pathway accounts for the robust chromatin silencing roles mediated by the RNAi machinery in these organisms (Buhler and Moazed, 2007).

Plant miRNAs

Like animal miRNAs, plant miRNAs are derived from hairpin precursors and they silence endogenous mRNAs. Unlike animal miRNAs that bind mRNA 3′UTR sequences with partial complementarity to induce translational repression or slicer independent decay, plant miRNAs slice their targets; conserved sites to plant miRNAs with near perfect complementarity are easily identified in coding and 3′UTR sequences of mRNAs (Jones-Rhoades et al., 2006). Also, unlike animal miRNAs, plant miRNAs are produced by the action of a single RNAse III enzyme in the nucleus, Dicer-like-1(DCL-1) (Kurihara and Watanabe, 2004). miRNAs are also loaded into Ago1 in the nucleus, but exported to the cytoplasm where they are believed to act on their targets (Park et al., 2005; Jones-Rhoades et al., 2006).

Plants miRNAs also appear to be chemically distinct from miRNAs in animals; plant miRNAs and indeed all plant small RNAs are methylated at their 3′ ends by the Hen1 methyltransferase. Hen1 (Hua Enhancer 1) was discovered by Xuemei Chen in her characterization of a plant mutant that enhanced the reproductive organ identity defects seen in *HUA* mutants (Chen et al., 2002). Because *hen1* mutants had phenotypes similar to *carpel factory* (DCL-1), a plant Dicer orthologue, they checked miRNA levels and found that they were greatly reduced in both mutants (Park et al., 2002). *hen1* mutants also have impaired transgene silencing with reduced transgene siRNA accumulation and impaired resistance to cucumber mosaic virus (Boutet et al., 2003). A specific role was suggested for Hen1 when an N-terminal dsRNA binding domain and a C-terminal methyltransferase domain were recognized; biochemical studies showed that all plant small RNAs have a terminal 2’-*O*-Methyl modification which protects them from both an exonuclease and a 3′ Uridylation activity that might trigger their degradation (Yu et al.,

2005; Li et al., 2005). 3′ end uridylation of cleaved miRNA targets is a conserved activity in plants and animals; it appears to trigger decapping and 5′ exonuclease activity (Shen and Goodman, 2004). This same activity might mediate degradation of small RNAs in *hen1* mutants. Recombinant plant Hen1 specifically methylates small RNA duplexes with 3′ overhangs, suggesting that in plants, both strands of a small RNA duplex get modified after production by Dicer (Yang et al., 2006).

Although the methyltransferase domain of Hen1 has homologues in all species with an RNAi pathway (including mammals, flies, worms, and *S.pombe*, but not *S. cerevisiae*), no small RNA species were known to have modified 3′ ends. Chapter III details our studies that contradict early findings demonstrating that fly siRNAs and miRNAs have unmodified 3′ ends. Indeed the *Drosophila* Hen1 homologue (DmHen1) modifies the 3′ ends of siRNAs, some miRNAs, and piRNAs, by a mechanism distinct from that in plants. Explaining why the dsRNA binding domain is dispensible in animal Hen1, we found that only single-stranded small RNAs are modified after loading into Ago2 or Piwi in flies.

Separate miRNA and RNAi Pathways in Drosophila

Genetic and biochemical studies in *Drosophila Melanogaster* have provided much of the mechanistic detail about general principles of small RNA silencing. In fact, flies have proved to be an valuable model system for understanding RNAi and miRNA silencing in mammals. Because both organisms lack RdRP activity, small RNA silencing involves multiple turnover catalytic activities of RISC (Hutvágner and Zamore, 2002; Haley and Zamore, 2004), rather than the combinatorial amplification and catalysis seen in worms and plants.

While most animals have one Dicer gene, flies have two—Dicer1 and Dicer2. Early studies showed that recombinant Dicer1 could process long dsRNA, but to impair RNAi in S2 cell knockdown experiments both Dicers were knocked down simultaneously (Bernstein et al., 2001). Purification of the dicing activity from S2 cell extracts revealed that Dicer2 and its dsRNA binding domain partner, R2D2, process long dsRNA, and load that siRNA to Ago2 RISC (Liu et al., 2003). Elegant genetic and biochemical studies by the Carthew and Sontheimer groups confirmed that Dicer2 is required in vivo for RNAi, and that dicing of dsRNA and siRNA loading into RISC are genetically separable activities—mutations in Dicer2's helicase domain ($dcr2^{G31R}$) or several in its RNAseIII domain block RNAi triggered by dsRNA, but not siRNA. Furthermore, they assign a function for Dicer1 in processing of pre-miRNAs. Consistent with this, Dicer1 flies have eye patterning defects, while Dicer2 mutants have no obvious developmental defects. This along with a study by Tomari and colleagues suggest that fly Dicers assemble into their respective RISCs, rather than simply transferring small RNAs into a separate RISC (Pham et al., 2004; Lee et al., 2004; Tomari et al., 2004). The Dicer2:R2D2 complex also plays a critical role in directing asymmetric RISC assembly—R2D2 binds the more thermodynamically stable end of an siRNA duplex, defining the 3′ end of the guide strand (Tomari et al., 2004). The human R2D2 orthologue, TRBP, along with Dicer and Ago2 can mediate asymmetric small RNA loading from recombinant proteins but it is unknown whether the mechanism of asymmetry detection is conserved (MacRae et al., 2008).

Further supporting the idea that the fly miRNA and RNAi pathways are separated, the Siomi group found miRNA functions associated with Ago1 and confirmed Ago2's

role in the RNAi pathway. Using lysates from an Ago2 deletion mutant (*ago2*^{414}), they showed that Ago2 is required for accumulation of single-stranded siRNA and that Ago2 is required for cleavage of targets by siRNAs, but dispensible for target cleavage by miRNAs. Conversely, an Ago1 mutation impaired target cleavage by miRNAs, but not by siRNAs. Furthermore, the miRNA bantam was reduced in Ago1, but not Ago2 mutants and RNAi knockdown S2 cells. Similarly, Dicer1, but not Dicer2 knockdown increased pre-bantam levels and a physical interaction between Ago1 and Dicer1 from immunoprecipitations suggested coupling of pre-miRNA processing by Dicer1 to Ago1 RISC loading, like that observed in the RNAi pathway (Okamura et al., 2004). This showed that miRNA loaded Ago1 RISC had catalytic activity, just like human RISC in human cells. The finding that Dicer1 also had its own double-stranded binding partner, Loquacious, also suggested the parallel nature of the RNAi and miRNA pathways in Drosophila (Förstemann et al., 2005; Saito et al., 2005; Jiang et al., 2005). Further studies demonstrated that indeed, recombinant Ago1 and Ago2 can slice perfect targets (Miyoshi et al., 2005). Thus each pathway has a separate Dicer, dsRNA binding protein, and slicer equipped Argonaute protein, ready to make their respective miRNA or siRNA guided RISC (Figure 1).

Given all the evidence suggesting separation of these pathways, we were surprised to find that our model somatic miRNA, miR-277, did not behave as expected. The existence of a sole Argonaute protein for miRNAs in flies prompted us to isolate Ago1 loaded miRNAs and their targets biochemically to identify fly miRNA targets. But when we immunodepleted S2 cell extract of Ago1, most miR-277 remained in the supernatant. This combined with functional data from reporter S2 cells and a parallel

Figure I-1. A Model For *Drosophila* Small RNA Silencing Pathways, circa 2006.

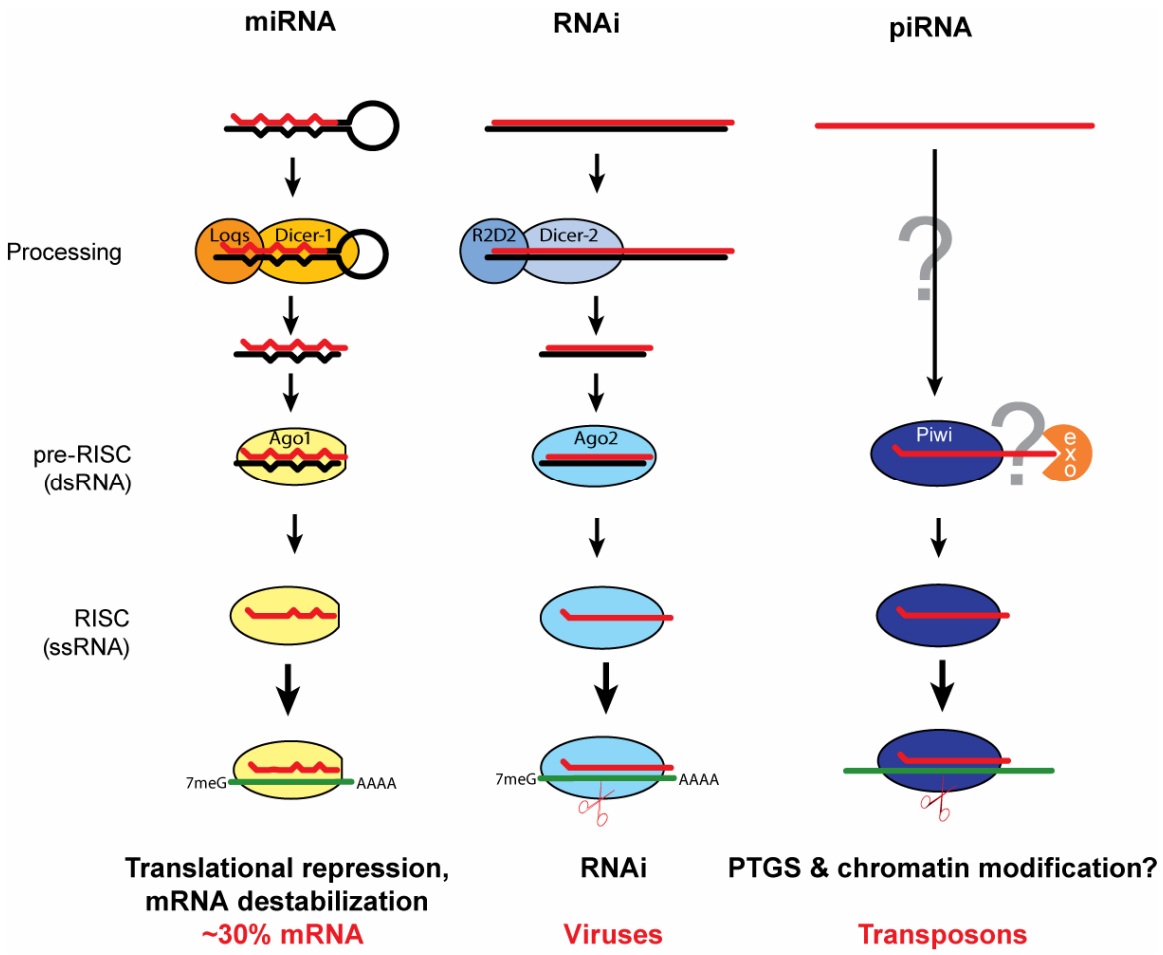

study done by Yuki Tomari demonstrating that small RNA duplexes partition between Ago1 and Ago2 based on duplex structure, proved that in flies small RNA assembly into RISC is not strictly coupled to the Dicer that produced them. Additionally, we found that loading into Ago1 or Ago2 RISC impacts target specificity—Ago1 is required to silence a miRNA-like bulged target and Ago2 is required to silence a perfectly paired target. These studies appear in Chapter II.

Innate Immune Response to dsRNA in Vertebrates

While RNAi in *Drosophila* constitutes innate anti-viral response to dsRNA (Zambon et al. 2006, Wang et al. 2006), vertebrates appear to have additional innate anti-viral pathways. The existence of such pathways, as well as a more sophisticated cellular and humoral immune system, may patially explain why vertebrates lack dedicated the dedicated RNAi machinery seen in flies. The vertebrate response to viral dsRNA is modulated by two classes of dsRNA sensors, 1) cell surface/endosomal receptors from the toll-like receptor family (TLR3) and 2) cytoplasmic sensors, including Protien Kinase R (PKR), or the helicase Retinoic acid inducible-1 (RIG-I) and its homologue Melanoma differentiation associated-5 (MDA5) (Akira et al. 2006). These sensors bind dsRNA in their respective cellular compartments and activate distinct signaling cascades that ultimately converge to activate transcription of pro-inflamatory cytokines via the transcription factor NF-κB or IRF3 and/or type I interferon via IRF7 (Akira et al. 2006). Activation of PKR also induces a general translational inhibition to combat viral replication; dsRNA induces dimerization of PKR, autophosphorylation and activation, followed by phosphorylation of the translation initiation factor eIF-2α, which blocks translation (Garcia et al. 2006). PKR is activated by dsRNA > 30 nt and RIG-I is

activated by blunt ended dsRNA, but not RNA with 2 base 3′ overhangs (Marques et al. 2006). Thus endogenous miRNAs or exogenous siRNAs evade the cytoplasmic dsRNA sensors. However, recent evidence suggests that TLR3 can respond to exogenous siRNAs. Although type I interferons do not seem to be induced by exogenous siRNAs, a TLR3 dependent non-sequence-specific anti-angiogenic effect was seen when siRNA were injected into mouse eyes (Kleinman et al. 2008). Thus siRNAs may trigger a distinct anti-angiongenic signaling cascade through TLR3. While endogenous miRNAs appear to have anti-viral functions in mammals (Lecellier et al. 2004, Pedersen et al. 2007), it is unclear if processing of viral RNA by the vertebrate RNAi/miRNA pathway is important in viral defense as seen in flies. Innate immune responses mediated by dsRNA sensors may be sufficiently robust to defend against RNA viruses in vertebrates. Yet to be discovered connections between dsRNA sensors and the RNAi/miRNA pathway may also contribute to innate viral immunity.

piRNAs

Transposons are "selfish" virus-like elements present in eukaryotic genomes, capable of replicating and re-inserting. Their expansion has clearly had a major impact on genome evolution; ~22% of fly, ~40% of human and 80% of maize genomes consist of transposon derived sequence (Kapitonov and Jurka, 2003; Lander et al., 2001; Flavell et al., 1974). While the bulk of this genomic scaffolding contains benign transposon relics, genomic defense systems to silence active mutagenic transposons are required to maintain genomic integrity in eukaryotes.

The first implication that RNAi phenomenae might keep transposons in place came from two studies in worms: the Mello group found that some RNAi deficient (Rde) mutants mobilized transposons in the germline(Tabara et al., 1999); conversely, the Plaskerk group found that some mutants with germline transposon mobilization were RNAi deficient(Ketting et al., 1999). The fact that *rde-1* and *rde-4*, were otherwise normal suggested that there might not be a simple connection. Although the Argonaute protein *rde-1* had no overt phenotype besides its RNAi deficiency, a *Drosophila* homologue, *sting* (now known as Aubergine, a piwi protein) failed to silence Stellate, a protein that forms crystals in testes if homologous repetitive loci on the Y chromosome are absent(Schmidt et al., 1999). Corresponding small RNAs were later detected, but differed in size—they were 25-27 nt long instead of the 21-23 nt Dicer products previously described. Intriguingly, a mutant in the helicase *Spindle-E* that affected Stellate silencing also affected long terminal reapeat (LTR) retrotransposon silencing(Aravin et al., 2001). Small RNAs cloned from *Drosophila* embryos revealed hundreds of larger 23-27 nt RNAs corresponding to transposons and repetitive elements in heterochromatin, termed repeat associated siRNAs (rasiRNAs). rasiRNA are enriched in germline tissues and early embryos, correlating with expression of the Drosophila piwi proteins, Piwi, Aubergine, and Ago3(Aravin et al., 2003; Williams and Rubin, 2002).

The conundrum posed by rasiRNAs' large size was explained when Vagin and colleagues found that rasiRNAs constitute a distinct germline specific silencing pathway to silence transposons and repetitive sequences, that does not require Dicer(Vagin et al., 2006). Along with other groups studying mammalian piwi proteins, they confirmed that rasiRNAs are piwi associated RNAs (piRNAs), they are derived from discrete loci,

predominantly from long single-stranded transcripts rather than double-stranded precursors, transposons are de-silenced in piwi mutants, but not miRNA or RNAi pathway mutants, and piRNAs have modified 3′ ends—further supporting their independence from Dicer(Vagin et al., 2006; Girard et al., 2006; Aravin et al., 2006; Lau et al., 2006). The piRNA pathway is likely required for maintenance of genomic integrity in the germline; piRNA pathway mutants are generally sterile with embryonic axis specification defects, but these defects can be suppressed by mutations in the ATR/Chk2 DNA damage signal transduction pathway. Whether the DNA damage that occurs in the absence of a functional piRNA pathway is a direct consequence of transposon mobilization has yet to be determined(Klattenhoff et al., 2007). Although several studies indicate that piwi proteins contain slicer activity, it is unclear whether they generally act at the level of transcription or post-transcriptionally(Lau et al., 2006; Saito et al., 2006). Transcriptional silencing at the level of chromatin or DNA modification may be the mechanism, as studies now indicate piRNA-dependent DNA methylation of some mouse transposons(Aravin et al., 2007) and both histone methylation and heterochromatin protein HP1 deposition on the telomeric HeT-A transposon in fly ovaries, but not somatic tissues (Klenov et al., 2007). However, this contradicts an earlier study that reported mislocalization of HP1 on fly salivary gland polytene chromosomes in Piwi, Aubergine, and Spindle-E mutants (Pal-Bhadra et al., 2004).

How are piRNAs made? Two studies that cloned fly piRNAs from immunoprecipitates of Piwi, Aubergine, and Ago3 suggest that piRNAs make piRNAs—at least their 5′ ends(Brennecke et al., 2007; Gunawardane et al., 2007). Piwi and Aubergine bound small RNAs tend to be antisense to transposons, and have a U bias at

Figure I-2. The "Ping-Pong" Model for piRNA Biogenesis.

* Indicates 3′ terminal modification

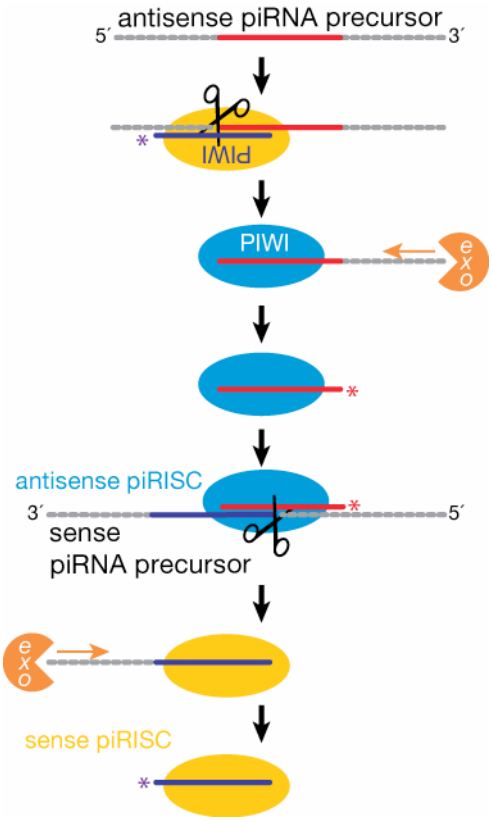

their 5′ end. Ago3 bound piRNAs generally correspond to sense transposon sequences, and have an A bias at position 10, the nucleotide adjacent to the cleavage site. Alignment of the piRNA sequences revealed that almost 50% of Ago3 piRNAs had 10 nt complementarity to the first 10 nt of Aubergine bound piRNAs, suggesting that piwi proteins' slicer activity generates the 5′ end of both sense and antisense piRNAs. This predicts the existence of an elegant amplification loop (the "ping-pong" model) in which sense transcription of transposable elements in the presence of antisense piRNAs produces sense piRNAs, which will in turn slice antisense transcript to produce more antisense piRNAs (Figure 2). The result of this model is the prediction that antisense transcription of a piRNA locus containing transposons could silence distant genomic copies in *trans*. Remarkably, uniquely mapping antisense piRNAs clustered in a transposon rich locus called *flamenco* that had already been shown to be critical to repress the transposon *gypsy*(Prud'homme et al., 1995; Pelisson et al., 1994). This suggests that antisense transcription of a piRNA locus can regulate many homologous genes throughout the genome, providing an adaptable innate immunity locus for transposon silencing. To date, this mode of piRNA silencing is conserved in flies, mice, zebrafish, platypus, and planaria(Vagin et al., 2006; Aravin et al., 2007; Houwing et al., 2007; Tam et al., 2008; Murchison 2008; Palakodeti 2008).

While "ping pong"-ing explains how the 5′ end of some piRNAs are made, many piRNAs, such as those associated with *Drosophila* Piwi, lack detectable pairing partners, suggesting additional biogenesis mechanisms for 5′ ends. Some details of 3′ end biogenesis are beginning to emerge. First, piRNA length appears to be largely determined by which piwi protein they bind. In flies piRNAs are on average 23, 24, or 26 nt

depending on whether they are bound to Ago3, Aubergine, or Piwi respectively. Mammals have longer piRNAs, 27 nt on average in Mili and 30 nt in Miwi. Second, modification of piRNA 3′ ends is conserved in flies, mammals, and zebrafish. Like small RNAs in plants, piRNAs are 2'-*O*-Methylated at their 3′ terminal base(Vagin et al., 2006; Houwing et al., 2007; Kirino and Mourelatos, 2007a; Ohara et al., 2007). Our group and the Siomi group found that the fly orthologue of Hen1 is the piRNA methyltransferase(Horwich et al., 2007; Saito et al., 2007). Recombinant mouse Hen1 can also methylate small RNA in vitro (Kirino and Mourelatos, 2007b). We hypothesize that piRNA length is determined by the geometry of individual piwi protein:Hen1 complexes. We predict that after the 5′ end of a nascent piRNA is bound to a piwi protein, that an unidentified 3′ exonuclease trims the single-stranded precursor until it is small enough to contact the Hen1 catalytic domain. Mutations in the putative nucleases, Zucchini and Squash, reduce piRNA production, but their precise role is not known(Pane et al., 2007).

Although it is clear that piRNAs have a conserved role in defence against transposons, the abundance of non-transposon derived piRNAs suggests additional functions. Many of the principles that direct piRNA biogenesis and function remain to be determined.

Chapter II:

Drosophila microRNAs Are Sorted into Functionally Distinct Argonaute Complexes after Production by Dicer-1

Contributions: The work presented in this chapter was a collaborative effort. I performed experiments shown in Figures 4, S1, S3, and S4. Klaus Förstemann conducted experiments in Figures 2, 3, and 5. Liang-Meng Wee and Yuki Tomari did experiments shown in Figures 6 and S5, and Table 1. Klaus Förstemann and Phillip Zamore wrote the paper.

Summary

Small interfering RNAs (siRNAs) and microRNAs (miRNAs) guide distinct classes of RNA-induced silencing complexes (RISCs) to repress mRNA expression in biological processes ranging from development to antiviral defense. In *Drosophila*, separate but conceptually similar endonucleolytic pathways produce siRNAs and miRNAs. Here, we show that despite their distinct biogenesis, double-stranded miRNAs and siRNAs participate in a common sorting step that partitions them into Ago1- or Ago2-containing effector complexes. These distinct complexes silence their target RNAs by different mechanisms. miRNA-loaded Ago2-RISC mediates RNAi, but only Ago1 is able to repress an mRNA with central mismatches in its miRNA-binding sites. Conversely, Ago1 cannot mediate RNAi, because it is an inefficient nuclease whose

catalytic rate is limited by the dissociation of its reaction products. Thus, the two members of the *Drosophila* Ago subclade of Argonaute proteins are functionally specialized, but specific small RNA classes are not restricted to associate with Ago1 or Ago2.

Introduction

microRNAs (miRNAs) are 22 nt RNA guides that control gene expression in both plants and animals (Bartel, 2004; Du and Zamore, 2005). miRNAs regulate genes required for a wide range of cellular functions such as differentiation and development (Lee et al., 1993; Reinhart et al., 2000; Grishok et al., 2001; Ketting et al., 2001; Bernstein et al., 2003; Lee et al., 2004; Li and Carthew, 2005; Harfe et al., 2005; Kanellopoulou et al., 2005), metabolic homeostasis (Poy et al., 2004; Teleman et al., 2006), and memory (Ashraf et al., 2006; Schratt et al., 2006). In animals, miRNAs typically reduce the stability or repress translation of the mRNAs they regulate. miRNAs can regulate mRNAs with which they are only partially complementary, because they bind their target RNAs largely through a small region at the 5′ end of the miRNA (positions 2–7 or 8), the "seed" (Lai, 2002; Lewis et al., 2003; Brennecke et al., 2005). Consequently, half or more of the protein-coding genes in *Drosophila* and humans are predicted to be regulated by miRNAs (Stark et al., 2003; Lewis et al., 2003; Rajewsky and Socci, 2004; Lewis et al., 2005; Krek et al., 2005).

Animal miRNAs are produced by the sequential action of two distinct RNase III endonucleases. Drosha converts primary miRNAs, most of which are full-length RNA polymerase II transcripts, into pre-miRNAs, 70 nt RNAs that fold into a stem-loop or

hairpin structure. Dicer then excises the mature miRNA, bound to its miRNA* strand, from the pre-miRNA (Hutvágner et al., 2001; Grishok et al., 2001; Ketting et al., 2001; Lee et al., 2003). In *Drosophila*, distinct Dicer enzymes produce siRNA and miRNA. Dicer-1 (Dcr-1) acts with a double-stranded RNA (dsRNA)-binding protein partner, Loquacious (Loqs), to convert pre-miRNA to a miRNA/miRNA* duplex, whereas Dicer-2 (Dcr-2) produces siRNA duplexes by cleaving long dsRNA (Bernstein et al., 2001; Lee et al., 2004; Förstemann et al., 2005; Saito et al., 2005; Jiang et al., 2005). Dcr-2 also acts with its dsRNA-binding partner protein, R2D2, to load an siRNA duplex into Ago2 (Liu et al., 2003; Tomari et al., 2004; Tomari et al., 2004; Matranga et al., 2005; Liu et al., 2006), a function that is separable from its role in siRNA production (Pham et al., 2004; Lee et al., 2004).

Both siRNAs and miRNAs act as components of RNA-induced silencing complexes (RISCs); the core protein component of all RISCs is a member of the Argonaute family of small RNA-guided RNA-binding proteins (Tabara et al., 1999; Hammond et al., 2001; Song et al., 2003; Liu et al., 2004; Meister et al., 2004b; Rand et al., 2004; Song et al., 2004; Qi et al., 2005; Rivas et al., 2005; Baumberger and Baulcombe, 2005). The *Drosophila* genome encodes five Argonaute proteins, which form two subclades. The Ago subclade comprises Ago1 and Ago2, which have been reported to bind miRNAs and siRNAs, respectively (Hammond et al., 2001; Okamura et al., 2004). Piwi, Aub, and Ago3 form the Piwi subclade of Argonaute proteins and bind repeat-associated siRNAs (rasiRNAs; also called piRNAs), which direct silencing of selfish genetic elements such as transposons (Saito et al., 2006; Vagin et al., 2006; Gunawardane et al., 2007; Brennecke et al., 2007).

Argonaute proteins are readily identified by their characteristic single-stranded RNA-binding PAZ domain (Song et al., 2003; Lingel et al., 2003; Yan et al., 2003) and their Piwi domain, a structural homolog of the DNA-directed RNA endonuclease, RNase H (Song et al., 2004). The Piwi domain is thought to bind a small RNA guide both by coordinating its 5′ phosphate and through contacts with the phosphate backbone, arraying the small RNA so as to create the seed sequence (Ma et al., 2004; Ma et al., 2005; Parker et al., 2004; Parker et al., 2005; Yuan et al., 2005). Only a subset of Argonaute proteins contain Piwi domains that retain their RNA-directed RNA endonuclease activity: e.g., Ago1 in plants, Ago2 in mammals, and both Ago1 and Ago2 in flies. *Drosophila* Ago1 and Ago2 have been proposed to be restricted to the miRNA and siRNA pathways respectively (Okamura et al., 2004; Saito et al., 2005). Such restriction of each class of small RNA to a distinct Argonaute complex could occur because miRNAs and siRNAs are produced by different Dicer pathways in flies (Figure 1A).

In this manuscript, we show that the specific pathway that produces a miRNA or siRNA does not predestine that small RNA to associate with a particular Argonaute protein (Figure 1B). Rather, we find that a miRNA produced by Dcr-1 and Loqs can nonetheless be loaded by Dcr-2 and R2D2 into an Ago2-containing RISC. Our data from both cultured *Drosophila* cells and adult flies suggest that small RNA production and small RNA loading into Argonaute protein complexes are separate steps in vivo. In the accompanying paper (Tomari et al., 2007), we describe the molecular basis for sorting small RNA duplexes, explaining why some miRNAs associate predominantly with Ago1 while others associate mainly with Ago2. Here, we show that the sorting of miRNAs into Ago1- and Ago2-RISCs has unexpected consequences for the mechanism of target

mRNA regulation: Ago1, but not Ago2, can repress an mRNA containing multiple, partially complementary miRNA-binding sites in its 3′ untranslated region (UTR), whereas Ago2, but not Ago1, can silence an mRNA containing fully complementary miRNA-binding sites. The different regulatory capacities of Ago1 and Ago2 can be explained, in part, by our finding that while Ago2 is a robust, multiple-turnover RNA-directed RNA endonuclease, Ago1 is not.

Results

miR-277 Is Produced by Dcr-1, But Loaded into Ago2

Like all known *Drosophila* miRNAs, miR-277 is produced by cleavage of its precursor by Dcr-1 acting with Loqs, rather than Dcr-2, which generates siRNAs (Lee et al., 2004; Saito et al., 2005; Förstemann et al., 2005; Jiang et al., 2005). Both siRNAs and miRNAs are proposed to be loaded into Argonaute-containing effector complexes from double-stranded intermediates: guide/passenger strand duplexes for siRNAs and miRNA/miRNA* duplexes for miRNAs (Hutvágner and Zamore, 2002; Rand et al., 2005; Miyoshi et al., 2005; Matranga et al., 2005; Leuschner et al., 2006). The miR-277/miR-277* duplex is predicted to have more double-stranded character than typical miRNA/miRNA* duplexes, which are interrupted by mismatches and internal loops (Khvorova et al., 2003; Han et al., 2006). Thus, miR-277 has a miRNA/miRNA* duplex that resembles an siRNA. We asked if the resemblance of the miR-277/miR-277* duplex to an siRNA led to its being loaded into Ago2, rather than Ago1, in *Drosophila* cells. That is, is the biogenesis of a miRNA tightly coupled to its loading into Ago1? Or are

miRNAs, and perhaps siRNAs, sorted into distinct Ago proteins by a step unlinked to the Dicer that produced them?

To this end, we established stable lines of S2 cells expressing green fluorescent protein (GFP) mRNA alone, with a 3′ UTR containing one or two sites fully complementary to miR-277 or with four 3′ UTR sites complementary to miR-277 but bearing mismatches with miR-277 nucleotides 9, 10, and 11 (Figures S1–S3). Surprisingly, repression of the reporter bearing two fully complementary miR-277-binding sites required Ago2 but not Ago1 (Figure 1). Treating the S2 cells with dsRNA to deplete Ago2 by RNAi increased GFP expression 6-fold (Figures 2A and 2B). This agrees well with the extent of derepression observed with a miR-277-specific antisense oligonucleotide (ASO; Figure S1), suggesting that without Ago2, the reporter is no longer repressed. Moreover, *ago1*(*RNAi*) increased repression of this reporter. Essentially identical data were obtained for a reporter containing a single miR-277-binding site (Figure S3).

Expression of the miR-277-regulated reporter also increased when the cells were treated with dsRNA to deplete Drosha, the enzyme that excises pre-miRNAs from their primary transcripts or with dsRNA to deplete Dcr-1 or Loqs, which together convert pre-miRNA to miRNA/miRNA* duplexes (Figure 2A). RNAi directed against *ago1*, *ago2*, or *drosha* had no detectable effect on the expression of the GFP reporter lacking miR-277-binding sites.

We note that a control dsRNA was not inert with respect to Ago2-dependent silencing (i.e., RNAi), likely because it can compete with miR-277 for Ago2 loading. The idea that nonspecific dsRNA can compete for Ago2 and other components of the Ago2-loading machinery is consistent with earlier reports that RNAi is a saturable (Haley and

Zamore, 2004). Thus, the most straightforward method to assess the significance of the effect of different dsRNAs on miR-277-directed repression of the perfect reporter in this

Figure II-1. Two Models for the miRNA and siRNA Pathways in *Drosophila*

(A) Small RNA biogenesis and RISC assembly are tightly coupled. miRNAs are exclusively loaded into Ago1 and siRNAs into Ago2. (B) Small RNA biogenesis and RISC assembly are independent. After their production, small RNA duplexes are proposed to be actively sorted into distinct Ago proteins solely according to their structures.

Figure II-1

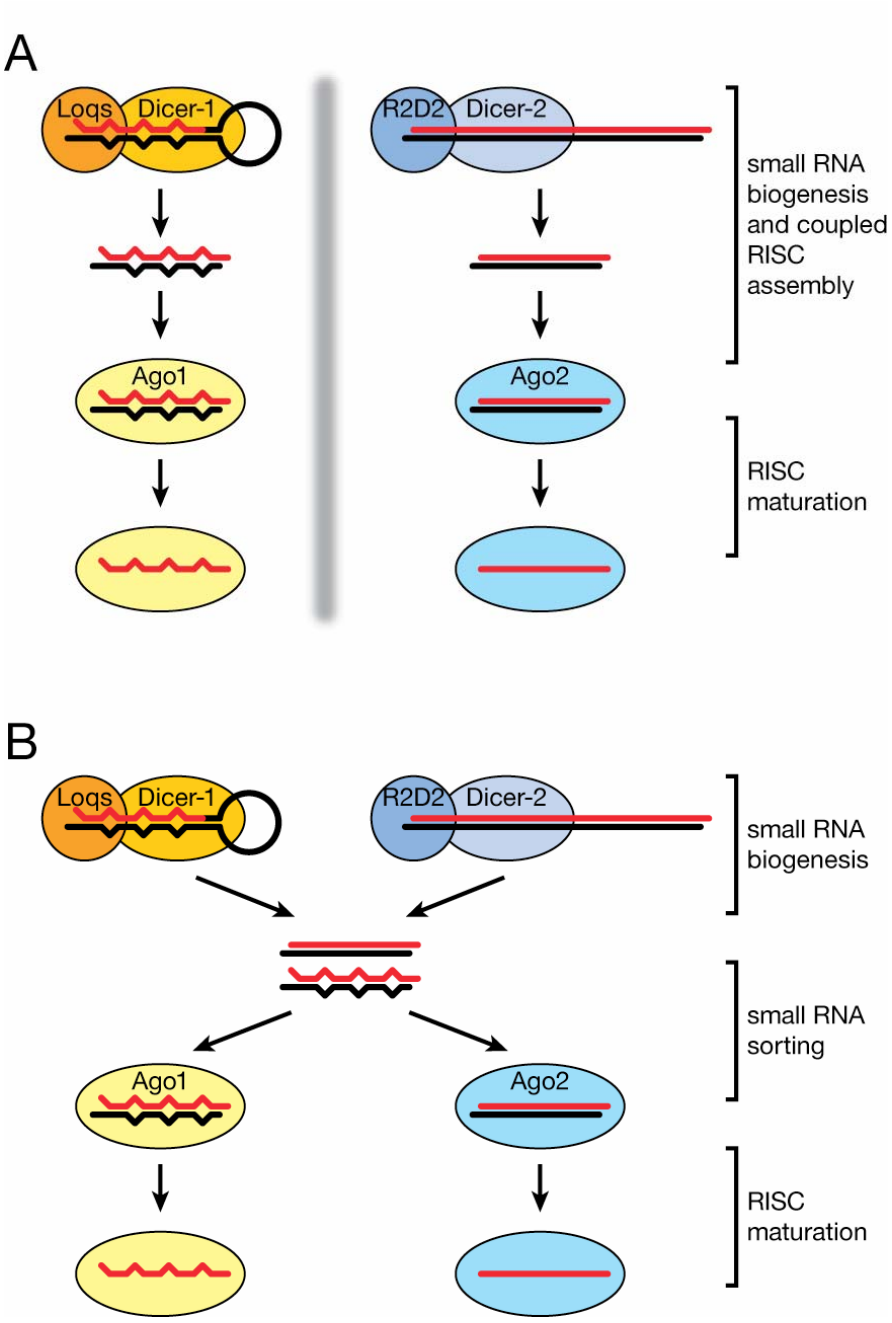
A
Loqs
Dicer-1
R2D2
Dicer-2
small RNA biogenesis and coupled RISC assembly
Ago1
Ago2
RISC maturation
B
Loqs
Dicer-1
R2D2
Dicer-2
small RNA biogenesis
small RNA sorting
Ago1
Ago2
RISC maturation

Figure II-2. Components of Both the miRNA and the RNAi Pathways Are Required to Silence a Reporter with Perfect Matches to miR-277

(A) Mean GFP fluorescence (average ± standard deviation for three or four trials). DsRNA-triggered RNAi was used to deplete the cells of the indicated protein.

(B) Western blotting confirmed the extent and specificity of the RNAi-mediated depletion for each protein. *dcr-2*(*RNAi*) reduced the abundance of both Dcr-2 and R2D2, as previously reported (Liu et al., 2003), but r2d2(RNAi) had no detectable effect on Dcr-2 abundance. The three isoforms of Loqs are indicated at the right of the Loqs panel. The bands above and below Ago2 correspond to crossreacting proteins characteristically detected with this antibody.

Figure II-2

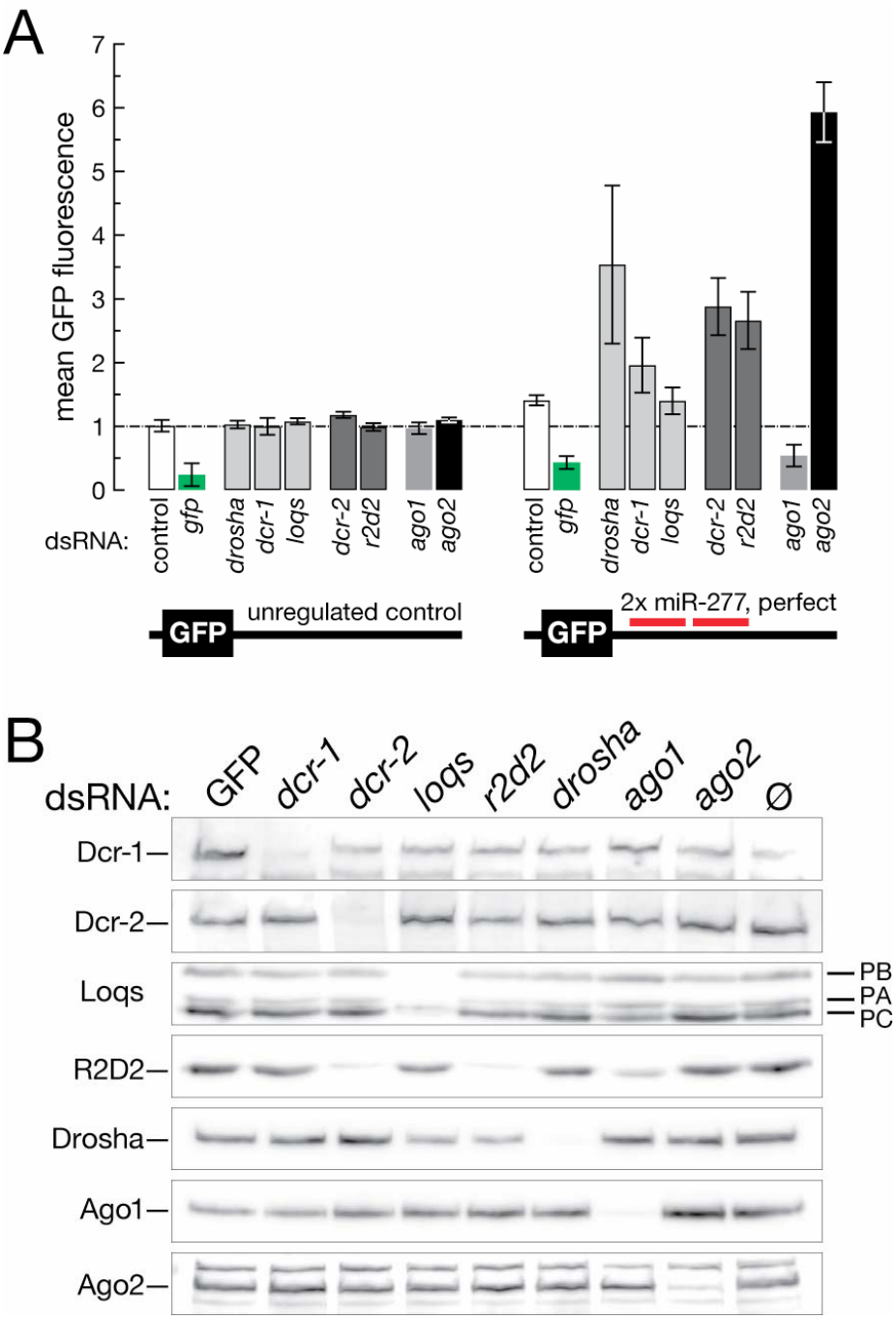
A
mean GFP fluorescence
0
1
2
3
4
5
6
7
dsRNA:
control
gfp
drosha
dcr-1
loqs
dcr-2
r2d2
ago1
ago2
control
gfp
drosha
dcr-1
loqs
dcr-2
r2d2
ago1
ago2
GFP
unregulated control
GFP
2x miR-277, perfect
B
dsRNA:
GFP
dcr-1
dcr-2
loqs
r2d2
drosha
ago1
ago2
Ø
Dcr-1
Dcr-2
Loqs
PB
PA
PC
R2D2
Drosha
Ago1
Ago2

experiment is not to compare the individual specific knockdown experiments to the control dsRNA, but rather to compare the change in GFP expression for the unregulated reporter to that observed for the perfect reporter for each RNAi knockdown. Analyzed this way, depletion of components of the miRNA biogenesis pathway clearly has a significant effect on miR-277-directed repression of the reporter: *dcr-1*(*RNAi*), $p < 0.005$; *drosha*(*RNAi*), $p < 0.007$; *loqs*(*RNAi*), $p < 0.028$.

Together with previously published results (Förstemann et al., 2005), our data therefore suggest that miR-277 is produced by the standard miRNA pathway, but directs repression of a perfectly matched GFP reporter through Ago2.

Ago1 But Not Ago2 Mediates Repression of mRNAs Bearing Bulged miR-277-Binding Sites

mRNAs containing miRNA-binding sites with perfect complementarity to specific miRNAs occur in animals, but are rare (Yekta et al., 2004; Mansfield et al., 2004; Davis et al., 2005). Instead, most miRNAs are incompletely complementary to the mRNAs they repress. Typically, these miRNAs bind to multiple sites in the 3′ UTR of their targets. This mode of miRNA-directed repression can be recapitulated by engineering into the 3′ UTR of the reporter mRNA four, partially mismatched, miRNA-binding sites, each of which forms a central bulge when paired to its cognate miRNA (Zeng et al., 2002; Doench et al., 2003).

We established stable lines of S2 cells expressing a GFP mRNA bearing four such sites (Figure S1A). Repression of the reporter was modest, but required miR-277:

transfection of a miR-277-specific, but not a control, ASO caused a small but statistically significant ($p < 0.003$) increase in GFP fluorescence (Figure S1B). miR-277 is relatively abundant in S2 cells, which contain 2200 miR-277 molecules per cell (M.H. and P.D.Z., unpublished data). Nonetheless, we wondered if the free pool of endogenous Ago1-loaded miR-277 was insufficient to repress expression of the bulged reporter.

We increased the expression of miR-277 by engineering stable S2 lines expressing both the GFP reporter and a "mini" pri-miR-277 driven by the ubiquitin promoter. The resulting doubling of miR-277 expression caused a dramatic increase in the repression of the bulged GFP reporter, as evidenced by the more than 3-fold increase in GFP fluorescence observed when a miR-277-specific ASO was transfected into the cells (Figure 3A). Compared to the repression of this reporter by endogenous miR-277, the exogenous miR-277 increased repression of the bulged reporter by 230% (Figures S1A and 3A). Repression was also enhanced, but to a smaller extent, for the reporter bearing two perfectly complementary miR-277-binding sites.

For both the reporter bearing perfectly complementary miR-277-binding sites and the reporter with four bulged miR-277-binding sites, miR-277 reduced GFP expression by reducing the stability of the reporter mRNA, rather than by repressing GFP translation. We used qRT-PCR to measure the steady-state reporter mRNA abundance (Figure S4A) and fluorescence-activated cell sorting (FACS) to measure GFP protein abundance (Figure S4B). For each stable cell line, we measured reporter mRNA and protein expression after transfection with a control ASO or a miR-277-specific ASO. Even when miR-277 was overexpressed, nearly all of the increased GFP-protein expression observed when miR-277 was blocked could be accounted for by a

corresponding increase in GFP-mRNA expression. Figure S4C reports the relative GFP-protein expression normalized to the relative GFP-mRNA expression. In all cases, when

Figure II-3. Only Components of the miRNA Pathway Are Required to Silence a Reporter Bearing Four Imperfectly Matched miR-277 Target Sites

(A) Overexpression of miR-277 from a mini-pri-miRNA transgene increased repression of the miR-277-regulated perfectly matched and bulged reporters.

(B) Mean GFP fluorescence (average ± standard deviation for three or four trials). DsRNA-triggered RNAi was used to deplete the cells of the indicated protein.

Figure II-3

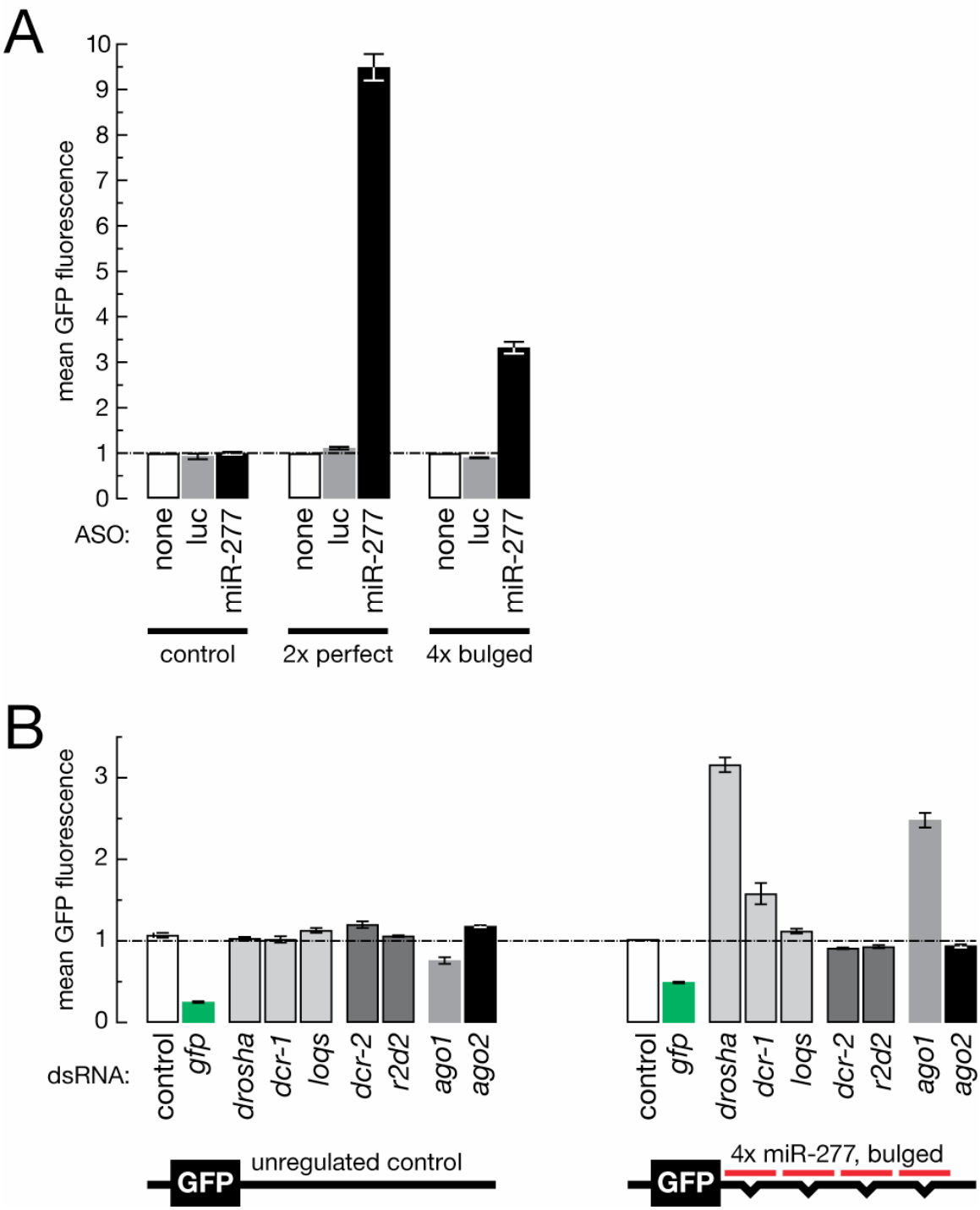
A
mean GFP fluorescence
10
9
8
7
6
5
4
3
2
1
0
ASO:
none
luc
miR-277
none
luc
miR-277
none
luc
miR-277
control
2x perfect
4x bulged
B
mean GFP fluorescence
3
2
1
0
dsRNA:
control
gfp
drosha
dcr-1
loqs
dcr-2
r2d2
ago1
ago2
control
gfp
drosha
dcr-1
loqs
dcr-2
r2d2
ago1
ago2
GFP
unregulated control
GFP
4x miR-277, bulged

miR-277 was inhibited, the ratio of relative protein expression to relative mRNA expression was close to one, indicating that most of the miR-277-directed reporter repression reflected mRNA destabilization rather than translational repression. However, for the bulged reporter, mRNA degradation might be tightly coupled to translational repression and therefore be a consequence, rather than a cause, of the decrease in protein production.

Silencing of the bulged reporter required Ago1 but not Ago2: *ago1*(*RNAi*) increased reporter expression, whereas *ago2*(*RNAi*) (Figure 2B) caused a small but statistically significant decrease in reporter expression ($p < 0.008$) (Figure 3B). While RNAi directed against *drosha*, *dcr-1*, or *loqs*—all genes required for biogenesis—increased expression of the bulged reporter, *dcr-2*(*RNAi*) and *r2d2*(*RNAi*)—both genes required to load small RNAs into Ago2 but not Ago1—caused a small but statistically significant ($p < 0.001$ and $p < 0.003$, respectively) increase in reporter silencing. These data suggest that (1) the Ago1 and Ago2 pathways compete for miR-277, and (2) Ago1 and Ago2 are functionally distinct and nonredundant, with Ago2 alone mediating small RNA-directed silencing of perfectly complementary target mRNAs (RNAi) and Ago1 mediating silencing of mRNAs with central mismatches in the target sites.

miR-277 Accumulation Requires Ago2

Our experiments in stable S2 reporter cell lines suggest that miR-277 is loaded predominantly into an Ago2-containing RISC and that Ago1 and Ago2 compete for miR-277 in cultured *Drosophila* cells. Moreover, they suggest that miR-277 repressed the

reporter to which it was fully complementary as a component of an Ago2-RISC, but repressed the bulged reporter as a component of an Ago1-RISC. Supporting this view, the

Figure II-4. Most Endogenous miR-277 Is Not Associated with Ago1 in S2 Cells

(A) Northern analysis revealed that *ago2*(*RNAi*) reduced the steady-state abundance of miR-277, but not *bantam*, whereas *ago1*(*RNAi*) decreased the abundance of *bantam*, but not pre-*bantam* or miR-277. (B) Western blotting showed that immunoprecipitation of Ago1 depleted nearly all Ago1, but little or no Ago2, from S2 cell cytoplasmic extract. (C) The majority of *bantam*, but not pre-*bantam* coimmunoprecipitated with Ago1 (northern analysis). In contrast, the majority of endogenous and of overexpressed miR-277 remained in the supernatant, unbound by Ago1. The asterisk marks nonspecific hybridization of the probe with 5S rRNA.

Figure II-4

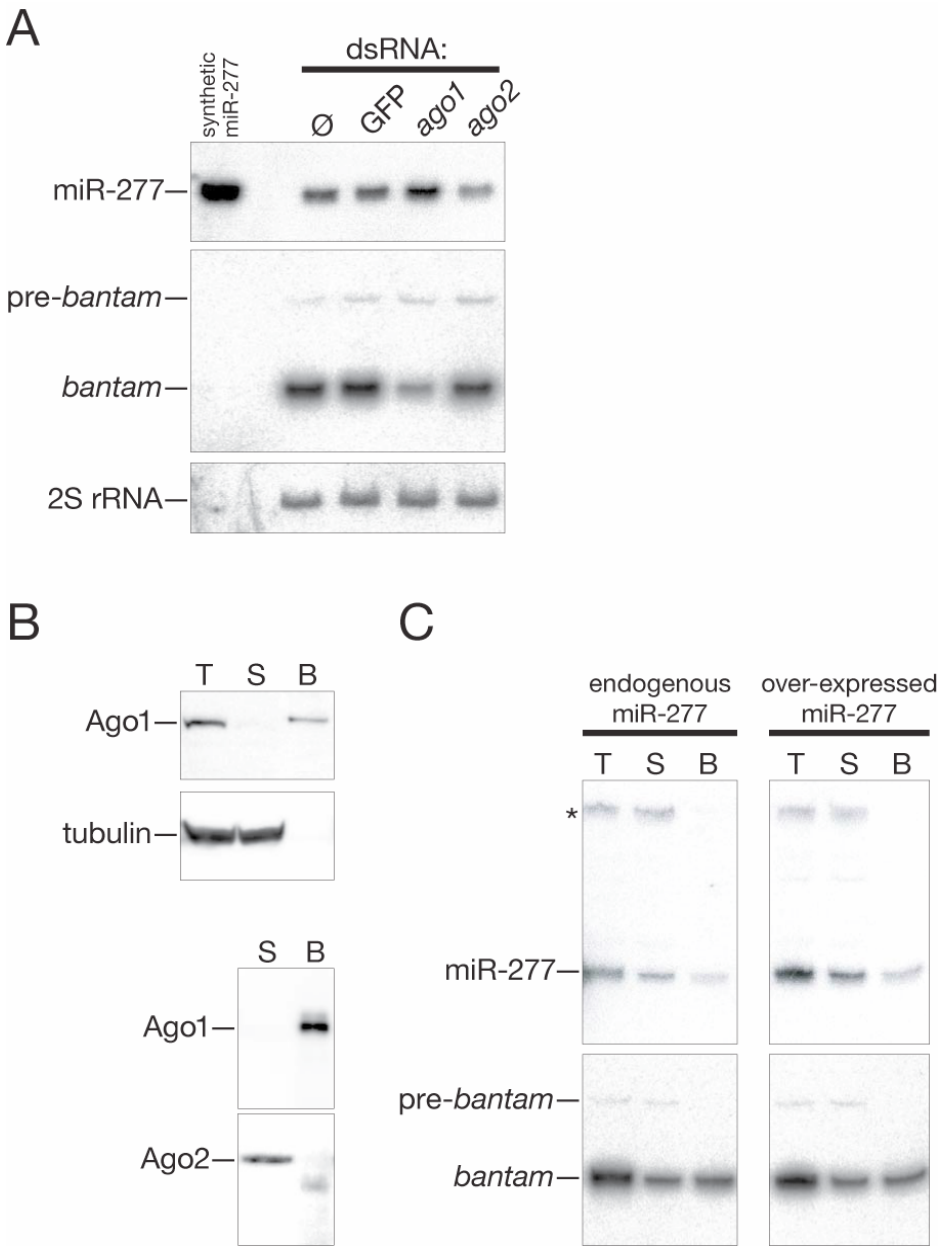
A
dsRNA:
synthetic miR-277
Ø
GFP
ago1
ago2
miR-277—
pre-bantam—
bantam—
2S rRNA—
B
T S B
Ago1—
tubulin—
S B
Ago1—
Ago2—
C
endogenous miR-277
over-expressed miR-277
T S B
T S B
*
miR-277—
pre-bantam—
bantam—

cellular concentration of miR-277 decreased when Ago2 was depleted by RNAi but not when Ago1 was depleted (Figure 4A). The concentration of *bantam*, a miRNA shown previously to associate with Ago1 (Okamura et al., 2004), was reduced by *ago1*(*RNAi*), but unaffected by *ago2*(*RNAi*). Pre-*bantam* RNA was unaltered by either treatment (Figure 4A), supporting the idea that the loss of *bantam* in *ago1*(*RNAi*) S2 cells reflects a failure to load the miRNA into its Ago1-RISC, rather than a defect in pre-miRNA processing, which would cause pre-*bantam* to accumulate. Moreover, most *bantam* but only a minority of miR-277 is physically associated with Ago1 (Figures 4B and 4C). We immunoprecipitated Ago1 using a monoclonal antibody bound to agarose beads. Western blotting with the same antibody demonstrated that the overwhelming majority of Ago1, but little or no Ago2, was depleted from the supernatant and recovered with the beads (Figure 4B). By northern blotting, more than half of *bantam*, but less than a third of miR-277, was recovered with the beads (Figure 4C).

In Vivo, miR-277 Is Produced by Dcr-1, Then Loaded by Dcr-2 into Ago2

Both *dcr-1*(*RNAi*) and *dcr-2*(*RNAi*) increased GFP expression for the reporter mRNA bearing two fully complementary miR-277-binding sites (Figure 2A). While the effect of *dcr-1* dsRNA was anticipated, current models for the miRNA pathway in *Drosophila* do not predict a role for Dcr-2 in miRNA function. Moreover, *dcr-2*(*RNAi*) did not detectably alter the expression of components of the miRNA pathway, Dcr-1, Loqs, Drosha, or Ago1 (Figure 2B). We can imagine two explanations for the reduction in miR-277 function when Dcr-2 was depleted. Dcr-1 and Dcr-2 might both act in the

production of miR-277, with each contributing to the conversion of pre-miR-277 to miR-277/miR-277* duplex. Alternatively, Dcr-1 alone might excise miR-277 from pre-miR-277, remanding the resulting miR-277/miR-277* duplex to the RISC-loading complex (RLC), whose core constituent is the Dcr-2/R2D2 heterodimer and which is required to load siRNA duplexes into Ago2.

To distinguish between these two explanations, we examined in adult flies the expression of the same GFP reporter bearing two fully complementary miR-277-binding sites that we used in our S2 cell experiments. The *dcr-2*^{G31R} allele (Lee et al., 2004)separates siRNA production from Ago2 loading because it selectively inactivates the nuclease function of Dcr-2. The GFP miR-277-reporters were expressed in transgenic flies heterozygous and homozygous for the *dcr-2*^{G31R} mutation. We also examined GFP reporter expression in *dcr-2*^{L811fsX} mutant flies, which produce no Dcr-2 protein and can neither produce siRNA duplexes nor load them into Ago2. We prepared protein extracts from adult flies and measured GFP expression by western blotting and fluorescence (Figure 5 and data not shown).

By both measures, expression of the reporter bearing two perfectly complementary miR-277-binding sites increased significantly in homozygous *dcr-2*^{L811fsX} mutant flies, relative to that measured in extracts from their heterozygous siblings (Figure 5), corroborating our observation that expression of this reporter was increased in S2 cells treated with *dcr-2* dsRNA (Figure 3A). However, reporter expression was unaltered in homozygous *dcr-2*^{G31R} mutant flies, relative to their heterozygous siblings (Figure 5). Reporter expression similarly increased in flies lacking R2D2 (Figure 5); R2D2 acts together with Dcr-2 to load Ago2 but is not required for siRNA production

(Liu et al., 2003). We conclude that the requirement for Dcr-2 in miR-277-directed silencing of the GFP reporter bearing two fully complementary miR-277-binding sites

Figure II-5. In Adult Flies, Repression of the miR-277 Reporter via Perfectly Complementary Sites Requires the Loading Activity of Dcr-2 and R2D2, But Repression via Bulged Sites Does Not

(A) Representative western blotting data for -tubulin and GFP in total lysates from adult flies of the indicated heterozygous (+/–) and homozygous (–/–) mutant genotypes. (B) The average (± standard deviation) GFP expression in homozygous mutant flies, relative to heterozygotes, for three (*r2d2*) or four trials of the experiment in (A). The *dcr-2*^{L811fsX} mutant lacks detectable Dcr-2 protein, whereas the *dcr-2*^{G31R} point mutant produces a Dcr-2 protein that cannot dice long dsRNA, but can nonetheless load siRNA and miRNA/miRNA* duplexes into Ago2.

Figure II-5

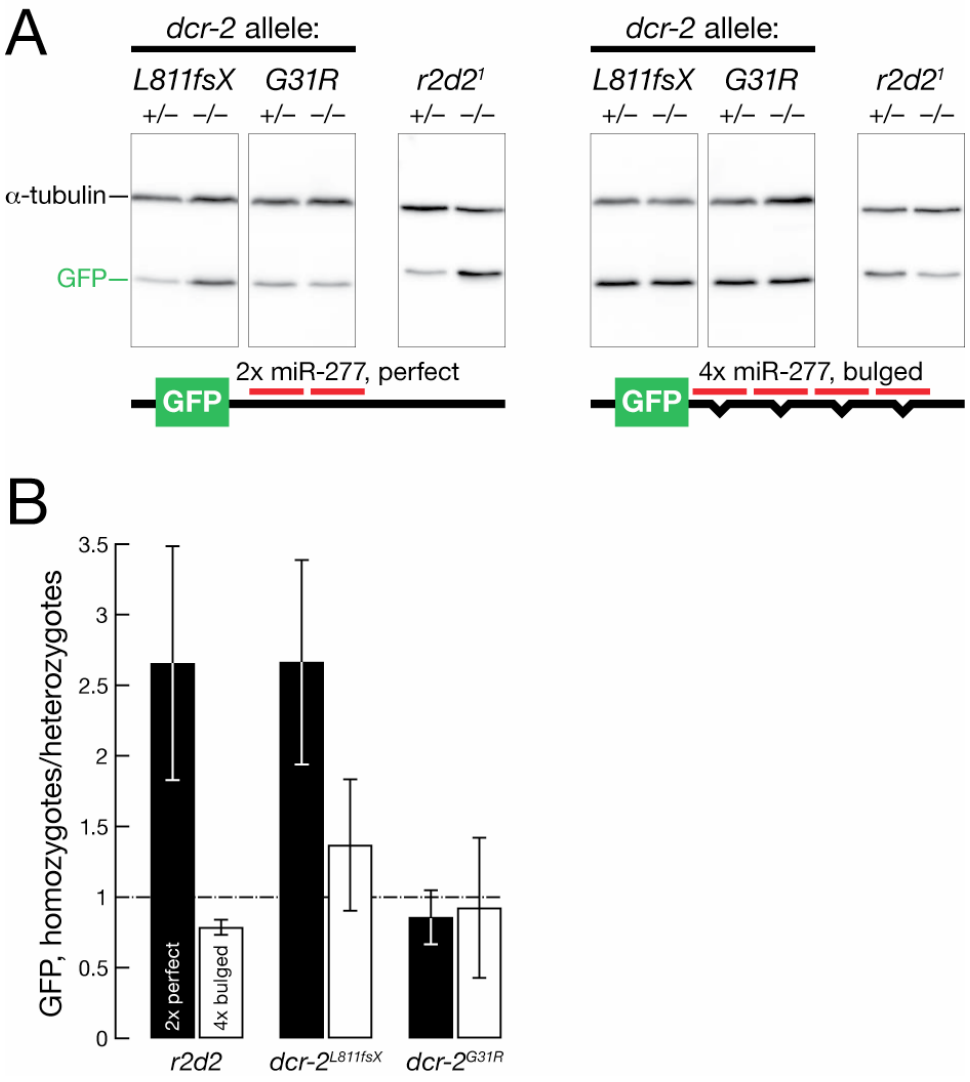
A
dcr-2 allele:
L811fsX
G31R
r2d2¹
+/– –/–
α-tubulin
GFP
2x miR-277, perfect
GFP
dcr-2 allele:
L811fsX
G31R
r2d2¹
+/– –/–
4x miR-277, bulged
GFP
B
GFP, homozygotes/heterozygotes
3.5
3
2.5
2
1.5
1
0.5
0
2x perfect
4x bulged
r2d2
dcr-2L811fsX
dcr-2G31R

reflects a role for Dcr-2 in loading miR-277 into Ago2, rather than in the conversion of pre-miR-277 into mature miR-277.

In contrast to the perfectly matched reporter, the GFP reporter bearing four bulged miR-277-binding sites was unaltered in flies homozygous for either the *dcr-2*^{L811fsX} null allele or the *dcr-2*^{G31R} separation-of-function allele. Thus, repression of this reporter in vivo does not require Ago2 loading, strong support for our conclusion that the bulged reporter is regulated by miR-277-programmed Ago1-RISC. In fact, we observed a small but statistically significant increase in the repression of the bulged reporter in flies homozygous for the *r2d2*^{1} allele (Figure 5B). These data suggest that as in vitro (Tomari et al., 2007) and in cultured cells (see above), Ago1 and Ago2 compete in vivo for loading with miR-277 and that in the absence of the Ago2-loading machinery, more miR-277-programmed Ago1-RISC is produced.

Ago1 Cleaves Target RNAs with Low Efficiency

Drosophila Ago1 retains the ability to catalyze endonucleolytic cleavage of a perfectly matched target RNA (Okamura et al., 2004; Miyoshi et al., 2005). Thus, it is surprising that for the reporter bearing two perfectly complementary miR-277-binding sites, the subpopulation of miR-277 associated with Ago1 did not detectably rescue the loss of silencing caused by depletion from S2 cells of Ago2 or the loss in adult flies of Dcr-2—a core component of the Ago2-loading machinery. To assess the molecular basis for the distinct functional capacities of Ago1 and Ago2, we analyzed in vitro the kinetics of target cleavage by each protein (Figure 6).

In *Drosophila*, the structure of a small RNA duplex governs into which Argonaute protein—Ago1 versus Ago2—it is loaded (Tomari et al., 2007). For the *let-7*

Figure II-6. Ago1 Is a Poor Endonuclease

(A) Distinct cleavage kinetics distinguish Ago1- and Ago2-RISC. At approximately equal enzyme concentrations, the initial velocity for Ago2-RISC was 12-fold greater than that of Ago1-RISC. Cleavage by Ago2-RISC was linear throughout the reaction, as long as the substrate remained in vast excess, whereas cleavage by Ago1-RISC was biphasic, suggesting that product release is the rate-determining step. The RISC concentration estimated by burst analysis (3.2 nM; red arrow) correlated well with that measured by 2′-*O*-methyl ASO affinity capture (4.6 nM). (B and C) Pseudo-Michaelis-Menten (B) and Michaelis-Menten (C) analyses of Ago1- and Ago2-RISC, respectively. Michaelis-Menten parameters are summarized in Table 1.

Figure II-6

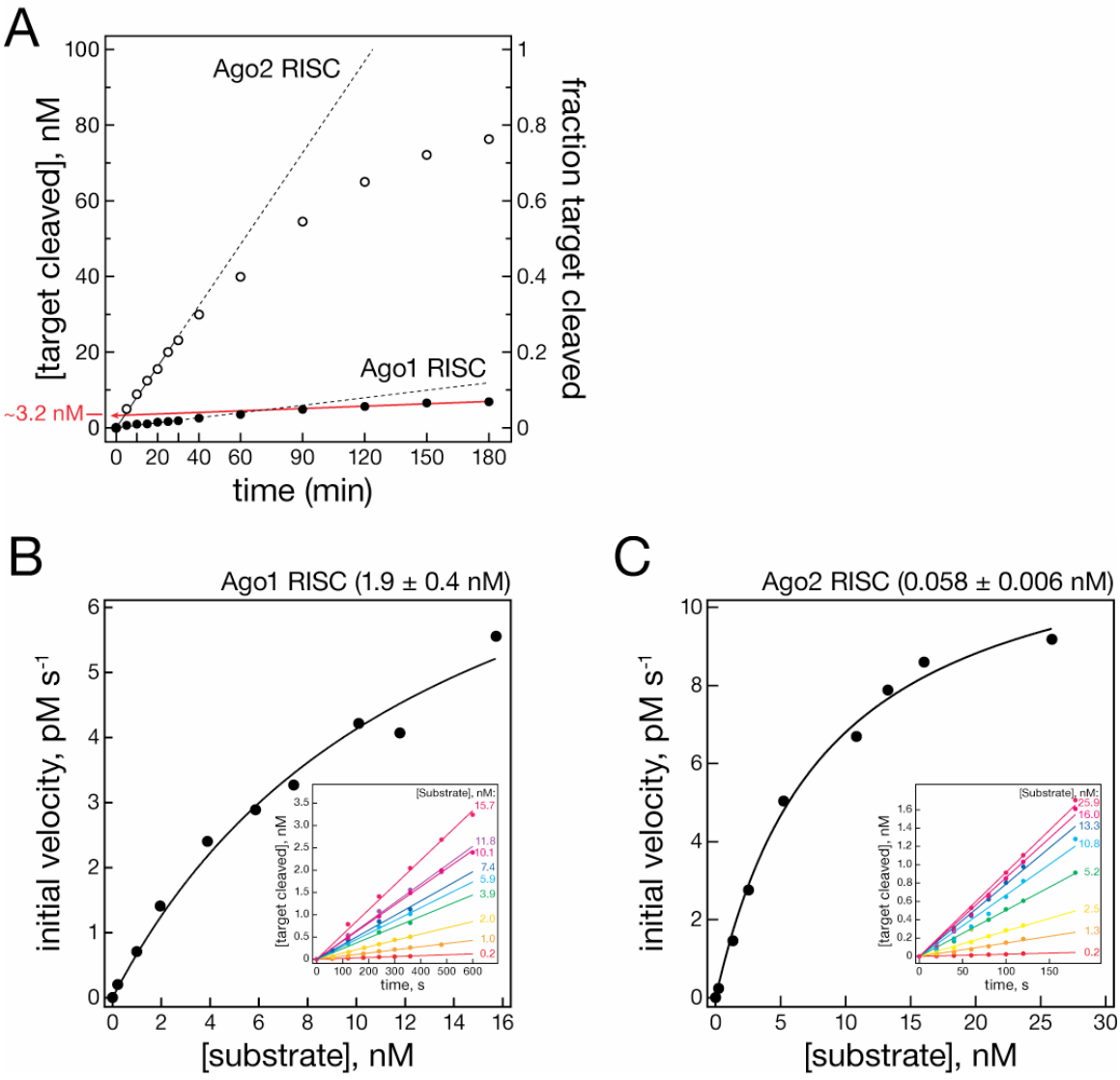
A
Ago2 RISC
Ago1 RISC
~3.2 nM
[target cleaved], nM
fraction target cleaved
time (min)
B
Ago1 RISC (1.9 ± 0.4 nM)
initial velocity, pM s-1
[substrate], nM
[Substrate], nM:
15.7
11.8
10.1
7.4
5.9
3.9
2.0
1.0
0.2
time, s
C
Ago2 RISC (0.058 ± 0.006 nM)
initial velocity, pM s-1
[substrate], nM
[Substrate], nM:
25.5
16.0
13.3
10.8
5.2
2.5
1.3
0.2
time, s

miRNA sequence, an siRNA duplex containing *let-7* as its guide strand loads Ago2 almost exclusively, whereas the *let-7*/*let-7** duplex loads only Ago1. By adjusting the time allowed for RISC assembly, we generated approximately equal concentrations (4.6–4.7 nM) of Ago1- and Ago2-associated *let-7*. For each *let-7*-programmed RISC, we measured the rate of cleavage of a 5′ ^{32}P-radiolabled RNA target containing a single site with complete complementarity to *let-7* (Figure 6A).

Our data reveal two differences between *Drosophila* Ago1 and Ago2. First, Ago2 is a faster enzyme than Ago1: the initial rate of target cleavage for Ago2 was at least 12-fold greater than that of Ago1 (Figure 6A). Second, Ago1, unlike Ago2, failed to efficiently catalyze multiple rounds of target cleavage in vitro, even in the presence of ATP. That is, for Ago2-RISC, the rate of target cleavage was the same throughout the steady-state phase of the reaction, while the rate of target cleavage for Ago1-RISC was biphasic (Figures 6A). Such biphasic behavior was reported previously for both *Drosophila* and human Ago2-mediated target cleavage in the absence of ATP and suggests that product release is rate determining for Ago2 under these conditions (Haley and Zamore, 2004; Rivas et al., 2005). The first phase of the Ago1 reaction in the presence of ATP likely corresponds to a presteady state period in which most Ago1 proteins have not yet released the product of their first target cleavage event. The second phase may correspond to a steady-state period in which the products of target cleavage are slowly released from Ago1. Supporting this view, the second phase fit well to a line whose *y* intercept, 3.2 nM, was similar to the amount of Ago1-RISC, 4.7 nM, measured

by affinity purification using an immobilized 2′-*O*-methyl *let-7* ASO.

The difference in efficiency between Ago1- and Ago2-catalyzed target cleavage might reflect a difference in the rate of catalysis or in the affinity for the target RNA. To distinguish between these two explanations, we performed a kinetic analysis of Ago1- and Ago2-RISC programmed with *let-7* in *Drosophila* embryo lysate. We estimated the amount of active *let-7*-programmed RNAi enzyme complex from the size of the burst for Ago1-RISC in the presence of ATP and for Ago2-RISC by depleting ATP after RISC assembly. In the presence of ATP, Ago2-RISC conforms to a simple Michaelis-Menten scheme (Haley and Zamore, 2004):

Ago2-*let-7* + target RNA <—> [Ago2-*let-7*•target RNA] —> Ago2-*let-7* + cleaved target RNA

In contrast, Ago1-RISC appears to follow a more complex kinetic scheme, even in the presence of ATP:

Ago1-*let-7* + target RNA <—> [Ago1-*let-7*•target RNA] —>
[Ago1-*let-7*•cleaved target RNA] <—> Ago1-*let-7* + cleaved target RNA

Because Michaelis-Menten parameters are determined from the initial velocity of the enzyme observed at different concentrations of substrate (target RNA), we analyzed Ago1 as if it followed the same kinetic scheme as Ago2. This pseudo-Michaelis-Menten analysis allows the Ago1 K_M to retain the same meaning—an approximation of the affinity of the enzyme for its substrate—as that determined for Ago2. Our data (Figure 6B and Table 1) suggest that *let-7*-programmed Ago1 and Ago2 bind the *let-7* complementary sequence in the target RNA with nearly the same affinity. In vitro, Ago1 binds its target RNAs as well as Ago2 but cleaves them much more slowly than Ago2.

This suggests that in vivo, Ago1 is too inefficient to silence a perfectly matched target by endonucleolytic cleavage.

II-Table 1. Kinetic analysis of *Drosophila* Ago1- and Ago2-RISC.

	K_M (nM)	V_{max} (nM s^{-1})	[RISC] (nM)	k_{cat} (s^{-1})	**k_{cat} (relative)**	k_{cat}/K_M (nM^{-1} s^{-1})	**k_{cat}/K_M (relative)**
Ago 1	13.3 ± 3.2	0.0096 ± 0.0013	1.9 ± 0.4	0.005 ± 0.0013	**1**	0.4 ± 0.1	**1**
Ago 2	8.4 ± 1.0	0.0125 ± 0.006	0.058 ± 0.006	0.215 ± 0.025	**43**	25.5 ± 4.3	**64**

Discussion

In lysates from *Drosophila* embryos, in cultured *Drosophila* S2 cells, and in adult flies, miRNA can be loaded into both Ago1 and Ago2. Our data suggest that sorting miRNAs into Ago1- and Ago2-RISC generates silencing complexes with distinct functional capacities: Ago1-RISC represses expression of targets with which its guide miRNA matches only partially, whereas Ago2 silences fully matched target RNAs. These differences result, in part, from the surprisingly different catalytic efficiencies of Ago1 and Ago2: only Ago2 catalyzes robust, multiple-turnover target cleavage.

Why Does Drosophila Ago1 Retain Its Endonuclease Activity?

In mammals, only Ago2 retains the ability to catalyze guide RNA-directed endonucleolytic cleavage of RNA; the three other mammalian Argonaute proteins, Ago1, Ago3, and Ago4, lack a functional active site that is presumed to have been present in the evolutionarily ancestral Argonaute protein. Why then has *Drosophila* Ago1 retained any endonuclease activity at all, if it is so inefficient at target cleavage that it cannot measurably contribute to small RNA-directed RNAi? One potential explanation is that the primary role of the Ago1 endonuclease activity is to facilitate loading of Ago1-RISC. That is, the predominant substrate for the Ago1 endonuclease is not target RNA but, rather, miRNA* strands and perhaps the occasional siRNA passenger strand. Because miRNA* strand cleavage would occur only in *cis* and only once per loaded Ago1-RISC, efficient, multiple-turnover cleavage of target RNA would not be required.

Our data reveal an important biochemical difference between Ago2 and Ago1, but they do not explain the molecular basis for the inefficiency of Ago1-directed cleavage of target RNA. We can envision two explanations for the more than 40-fold lower k_{cat} of Ago1 compared to Ago2. First, the active site of Ago1 might be less well suited to catalyzing phosphodiester bond cleavage. Alternatively, Ago1 might be slow to assume a catalytically active conformation. In this second model, the rate of a conformational rearrangement would limit the speed of target RNA cleavage by Ago1. Such a conformational rearrangement of the siRNA guide has been proposed previously for Ago2 (Filipowicz, 2005; Tomari and Zamore, 2005).

Implications for the Mechanism of Guide Strand Choice

Neither the current genome sequence of *Drosophila melanogaster* nor GenBank in its entirety contains a *Drosophila* mRNA with complete complementarity to miR-277. Why then do flies load miR-277 into Ago2-RISC? Perhaps there are—yet unknown—viral RNAs targeted by Ago2-loaded miR-277. Such an innate immune response function has previously been proposed for miRNAs in mammals (Lecellier et al., 2005). Regardless of the biological purpose for loading miR-277 into Ago2, miR-277 provides an important in vivo test of the controversial proposal that the production of small RNA duplexes by Dicer is uncoupled from the loading of Argonaute proteins (Khvorova et al., 2003; Schwarz et al., 2003; Aza-Blanc et al., 2003). That Dcr-2 and R2D2 act in vivo to load Ago2 with miR-277, a miRNA produced by Dcr-1 and Loqs, confirms previous in vitro data suggesting that both ends of a small RNA duplex are available for examination by the Ago2 loading machinery (Schwarz et al., 2003; Tomari et al., 2004; Preall et al., 2006). Our results suggest that the miR-277/miR-277* duplex dissociates from Dcr-1

after the dicing of pre-miR-277 and is then bound by the Dcr-2/R2D2 heterodimer, which loads it into Ago2; Sontheimer and colleagues reached similar conclusions about small RNA loading from in vitro experiments that asked if Dicer processing and Ago2 loading were coupled (Preall et al., 2006).

We reason that Ago1 loading is also uncoupled from dicing. In all animals, some miRNAs are found on the 5′ and others on the 3′ arm of their pre-miRNA stem loops. In contrast, the geometry of Dcr-1 with respect to the two arms of the pre-miRNA stem is essentially the same for all miRNAs: Dcr-1 always makes staggered cuts that separate the pre-miRNA loop from the miRNA/miRNA* duplex. If Dcr-1 were to load miRNAs directly into Ago1, without first releasing the miRNA/miRNA* duplex, we would expect that all miRNAs would reside on the same arm of the pre-miRNA stem. The simplest explanation, and one most consistent with the partitioning of miR-277 into both Ago1- and Ago2-RISCs, is that miRNA/miRNA* duplexes are released from Dicer immediately after their production, then rebound by the Ago1- and Ago2-loading machineries. Such a model allows both the terminal thermodynamics of the miRNA/miRNA* duplex to determine the mature miRNA strand (rather than its position within the pre-miRNA) and the pattern of mismatches within the duplex to determine how the miRNA partitions between Ago1 and Ago2.

Why Are Ago1 and Ago2 Functionally Specialized?

In mammals, siRNAs produce off-target effects largely by acting like miRNAs (Jackson et al., 2003; Lim et al., 2005; Jackson et al., 2006). In flies, siRNAs loaded into Ago2 are believed to defend against viral infection (Wang et al., 2006; Galiana-Arnoux et al., 2006). Virus-derived siRNAs might therefore trigger widespread, off-target silencing

of host genes as flies mount an antiviral RNAi response. The partitioning of siRNAs into Ago2-RISC appears to circumvent this problem, because silencing by *Drosophila* Ago2 requires greater complementarity between the siRNA and its target than silencing by Ago1. It is tempting to speculate that a similar functional specialization among Argonaute proteins has gone undetected in mammals.

Experimental Procedures

Construction of reporter plasmids and RNAi trigger dsRNAs

To create an expression vector for both cultured cells and transgenic flies, we PCR amplified the 3′ UTR and SV40 poly-A signal from plasmid pEGFP-N1 (Clontech, Mountain View, CA, USA) with oligonucleotides 5′-ATC ACT CTC GGC ATG GAC GAG-3′ and 5′-GTG AAT TCA TAC ATT GAT GAG TTT GGA C-3′ and inserted the resulting PCR product into pUbi-Casper2 (a kind gift of Dr. Siu Ing The) using the *Not*I and *Eco*RI restriction sites, creating vector pKF60. For the GFP-insert, we transferred a *Bam*HI-*Not*I fragment from pEGFP-N1 (Clontech) into pBluescript (Stratagene, La Jolla, CA, USA) cut with *Bam*HI/*Not*I, creating pKF20. Subsequently, we annealed the oligos 5′-CAT GGA ACA AAA ACT TAT TTC TGA AGA AGA CTT GGG-3′ and 5′-CAT GCC CAA GTC TTC TTC AGA AAT AAG TTT TTG TTC -3′, encoding a myc-tag, and ligated this DNA-fragment into *Nco*I-cut pKF20. After sequencing, one clone was selected that contained a triple insertion in the correct orientation (pKF30). From this plasmid, the myc_3-GFP-sequence was transferred as a *Bam*HI-*Not*I-fragment into pKF60, resulting in plasmid pKF62. To remove an *Xba*I-site from the pCASPER2 polylinker, pKF62 was cut with *Xba*I, the ends treated with Klenow polymerase (New England

Biolabs, Ipswitch, MA, USA), and the vector was re-ligated, creating pKF63. This plasmid was transformed into *dam/dcm* negative bacteria (strain GM2163, New England Biolabs), which rendered a second *Xba*I-site in the 3′-UTR, adjacent to the *Not*I-site, cleavable. To insert the miR-277 target sites, we annealed oligos 5′-GGC CTG TCG TAC CAG ATA GTG CAT TTA CAG TGT CGT ACC AGA TAG TGC ATT TA-3′ and 5′-CTA GTA AAT GCA CTA TCT GGT ACG ACA CTG TAA ATG CAC TAT CTG GTA CAG CA-3′ for the two perfectly matched sites, and oligos 5′-GGC CTG TCG TAC CAG AGG ATG CAT TTA CAG TGT CGT ACC AGA GGA TGC ATT TAT GTC GTA CCA GAG GAT GCA TTT ACA GTG TCG TAC CAG AGG ATG CAT TTA -3′ and 5′-CTA GTA AAT GCA TCC TCT GGT ACG ACA CTG TAA ATG CAT CCT CTG GTA CGA CAT AAA TGC ATC CTC TGG TAC GAC ACT GTA AAT GCA TCC TCT GGT ACG ACA-3′ for the four bulged sites, then ligated the DNA fragments into *Not*I-*Xba*I-cut pKF63, creating pKF67 and pKF68, respectively.

These pCASPER2-derived expression plasmids were used both for the generation of stable S2-cell lines and for the P-element-mediated genetic transformation *Drosophila melanogaster* (Rubin and Spradling, 1982).

Constructs to make dsRNA directed against GFP, *dcr-1*, *dcr-2*, *loqs* and *drosha* were described previously (Förstemann et al., 2005). Templates for the synthesis of dsRNA directed against *ago1* and *ago2* were generated by T/A-cloning PCR products generated using the oligonucleotides 5′-CGC ACC ATT GTG CAT CCT AAC GAG-3′and 5′-GGG GAC AAT CGT TCG CTT TGC GTA-3′ for *ago2* and 5′-ATT TGA TTT CTA TCT ATG CAG CCA-3′ and 5′-GCC CTG GCC ATG GCA CCT GGC GTA-3′ for *ago1* into the modified Litmus28i vector described previously (Förstemann et al.,

2005). The template for producing dsRNA targeting *r2d2* was generated by PCR using oligonucleotides 5′-CGT AAT ACG ACT CAC TAT AGG CAT ACA CGG CTT GAT GAA GGA TTC-3′ and 5′-CGT AAT ACG ACT CAC TAT AGG TTG CTT GTG CTC GCT ACT TGC-3′. Templates for in vitro transcription were generated by PCR-amplification of each plasmid construct using a single primer corresponding to the T7 promotor (5′-CGT AAT ACG ACT CAC TAT AGG-3′) and dsRNA for knock-down was generated as described in (Haley et al., 2003)

Construction of Cell Lines with Increased miR-277 Expression

A 270 nt fragment of genomic DNA encompassing the miR-277 sequence was PCR amplified from S2-cell genomic DNA using the oligonucleotides 5′-GCG GAT CCG GTA CCT ATA CAT ATA TAA CGA GGC CTA ACG-3′ and 5′-ATG CGG CCG CAA AAC AGT GTC TTA CAA ACA AGT GG-3′ and cloned BamHI to *Not*I into pKF62, yielding a mini-pri-miR-277 transgene under the control of the ubiquitin promotor.

Cell Culture and Flow Cytometry

Drosophila Schneider 2 (S2) cells were cultured at 28°C in Schneider's medium (Invitrogen; Carlsbad, CA) supplemented with 10% (v/v) fetal bovine serum (Invitrogen). GFP expression plasmids were transfected with siLentfect (see below) at 1 μg of plasmid per well of a 24-well plate. For selection of stable transformants, 20 ng of phsNeo (Steller and Pirrotta, 1985) was cotransfected with 1 μg each GFP reporter plasmid. Five days after transfection, cells were split 1:5 into medium supplemented with 1.2 mg/ml G418 (Invitrogen) and diluted 1:5 every 7 days into G418-containing medium for 3 weeks; then, serial dilutions were plated in a 96-well plate in growth medium supplemented with 1% (v/v) sterile-filtered conditioned medium. After 2 weeks, wells with a single colony

of cells were expanded and analyzed by flow cytometry. Cell clones that produced a single peak in the flow cytometer were retained as reporter lines.

For dsRNA transfection, cells were seeded at a density of 1×10^6 cells/ml in 24-well plates (500 µl/well) using Schneider's medium without G418. One hundred microliters of liposome/nucleic acid complexes (prepared by incubating at room temperature for 45 min 1.5 µl siLentfect (BioRAD; Hercules/CA) or Dharmafect 4 (Darmacon; Lafayette, CO) and either 1 µg of dsRNA or 10 pmol of 3′ cholesterol-conjugated, 2′-*O*-methyl modified antisense-oligonucleotide (see Figure S1B) in 100 µl Schneider's medium without serum) were added per well of a 24-well plate. After 6 days, cells were analyzed by FACS (BD FACScan flow cytometer; Becton Dickinson; Franklin Lakes, NJ). GFP expression was quantified as the arithmetic mean of fluorescence (CellQuest; Becton Dickinson).

Anti-Dcr-1 and Ago2 Antibodies

Keyhole limpet hemocyanin-conjugated peptides (Dcr-1: CQGLIAKKD; R2D2: CSDEYESSKDKAMD) or the Ago2 PAZ domain fused to glutathione-S-transferase (Lingel et al., 2003) were used to immunize rabbits (Covance Research Products; Denver, PA, or ProSci, Poway; CA) or chickens (Gallus Immunotech; Cary, NC) and the antiserum affinity purified using immobilized peptide (Sulfolink, Pierce; Rockford, IL) or NusA-Ago2-PAZ fusion protein (Aminolink Plus, Pierce).

Western Blotting

Proteins from cultured S2 cells or from hand-dissected adult fly heads and thoraces were extracted in PBS containing 1% Triton X-100 (Sigma; St. Louis, MO) and protease inhibitors (Complete without EDTA, Roche Molecular Biochemicals; Basel,

Switzerland). To quantify myc_3-GFP expression in transgenic flies, 20 μg of total protein was resolved by electrophoresis through a 12% polyacrylamide/SDS gel and transferred to PVDF membrane (Immobilon-P, Millipore; Billerica, MA) by semidry transfer (BioRAD; Hercules, CA) at 20 V for 120 min in 25 mM Tris (pH 8.3), 250 mM glycine, 10% (v/v) methanol as anode buffer, and 20 mM CAPS (pH 11.0) as cathode buffer. The blot was incubated for 90 min at room temperature with purified monoclonal anti-myc 9E10 (Sigma #M4439) diluted 1:1000 in 25 mM Tris, 137.5 mM NaCl, 2.5 mM KCl, and 0.02% (v/v) Tween-20 (Sigma) for 90 min at room temperature and then horseradish peroxidase (HRP)-conjugated goat anti-rabbit secondary antibody diluted 1:1000, then developed with Pierce SuperSignal West Dura kit (Pierce). HRP-conjugated rabbit anti-chicken secondary antibody (Gallus Immunotech), diluted 1:15,000, was used to detect the affinity purified anti-R2D2 chicken IgY. Western blot images were acquired using a Fuji LAS-3000 (Fujifilm Life Sciences; Stamford, CT) and quantified using ImageGauge (Fujifilm Life Sciences). -tubulin was detected with DM1A antibody (Sigma #T6199) diluted 1:1000. myc_3-GFP western blot signals were corrected using a standard curve for created by diluting extract from pKF63-transgenic flies into extract from yw flies.

For S2 cell proteins, 50 μg total protein was resolved by electrophoresis through an 8% polyacrylamide/SDS gel, transferred to PVDF, incubated with primary antibodies (1:2000) overnight at 4°C, and secondary antibodies for 120 min at room temperature. Anti-Dcr-2 antibody was the kind gift of Qinghua Liu (Liu et al., 2003).

Ago1 and Ago2 Target Cleavage Kinetics

Target cleavage reactions were performed essentially as described (Haley et al., 2003; Haley and Zamore, 2004). In Figure 6A, 50 nM *let-7* siRNA or *let-7*/*let-7** duplex was

incubated with Drosophila 0–2 h embryo lysate for 2 min to program Ago2-RISC (4.7 nM) or 5 min to program Ago1-RISC (4.6 nM). In Figure 6B, 20 nM *let-7* siRNA or *let-7/let-7** duplex was incubated with lysate for 3 min or 8 min to program Ago2- or Ago1-RISC. For Ago2 cleavage in Figure 6B, RISC was diluted 10-fold in *N*-ethyl maleimide (NEM)-treated embryo lysate (Nykanen et al., 2001; Haley and Zamore, 2004). *let-7* siRNA assembled little or no active RISC in *ago2*^{414} lysate, whereas *let-7/let-7** was as active in *ago2*^{414} as in wild-type lysate, indicating that the *let-7* siRNA and *let-7/let-7** duplex are almost exclusively loaded into Ago2- and Ago1-RISC, respectively.

RISC assembly was stopped by treatment with NEM followed by DTT to quench unreacted NEM for both Ago1- (Figure S4A) and Ago2-RISC (Nykanen et al., 2001). Control experiments (Figure S4B) established that the biphasic kinetics of Ago1-RISC in the presence of ATP were not a consequence of treatment with NEM. RISC concentration was estimated by 2′-*O*-methyl ASO affinity purification in Figure 6A and by the size of the presteady-state burst in Figure 6B (Schwarz et al., 2002; Haley and Zamore, 2004). The concentration of RNA target was 100 nM in Figure 6A and 0.5–100 nM in Figure 6B. Data were analyzed using IGOR 5 (WaveMetrics) and *Visual*Enzymics 2005 (Softzymics) software.

Figure II-S1. Regulation of GFP reporter expression in cultured Drosophila S2 cells by endogenous miR-277

Clonally derived stable cell lines were generated that expressed control GFP unregulated by miR-277, GFP bearing two miR-277-complementary sites in its 3′ untranslated region (UTR), and GFP bearing in its 3′ UTR four miR-277-complementary sites, each containing three mismatches to miR-277 at nucleotides 9, 10 and 11, producing a 'bulge.' Each cell line was transfected with a cholesterolconjugated, 2′-*O*-methyl modified, antisense oligonucleotide (ASO) complementary to miR-277 or to an unrelated luciferase sequence. In cultured cells and in vivo, ASOs inhibit the function of miRNAs to which they are complementary, relieving repression of their mRNA targets (Hutvágner et al., 2004; Meister et al., 2004a; Krutzfeldt et al., 2005; Berger et al., 2005). As a control, the unregulated GFP reporter cell line was transfected with GFP dsRNA. GFP expression was quantified by flow cytometry. (A) Representative FACS profiles from a single experiment. (B) The average ± standard deviation for the mean fluorescence recorded in three trials. *P*-values were calculated using a two-sample T-test assuming equal variances.

Figure II-S1

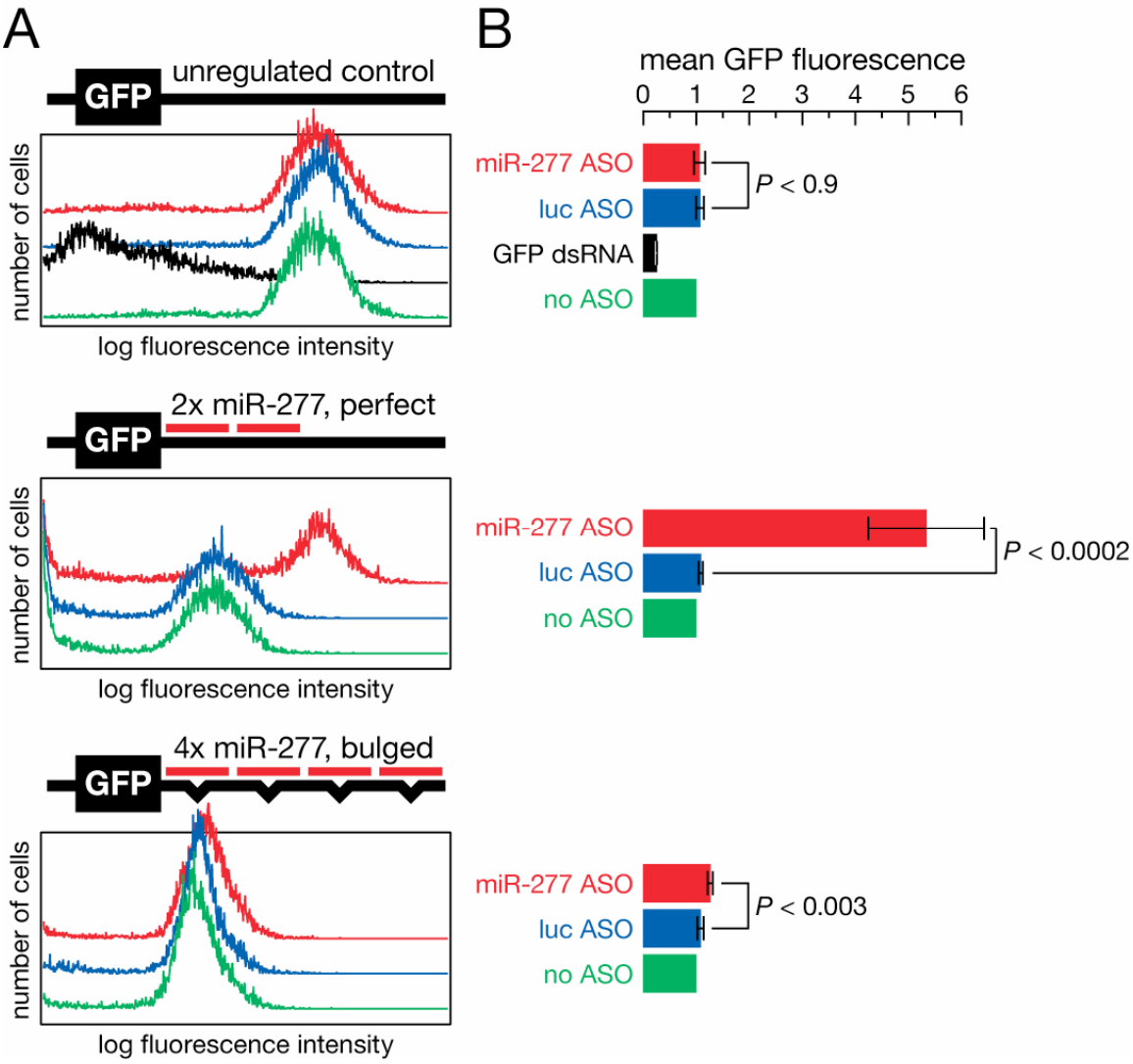
A
unregulated control
GFP
number of cells
log fluorescence intensity
2x miR-277, perfect
GFP
number of cells
log fluorescence intensity
4x miR-277, bulged
GFP
number of cells
log fluorescence intensity
B
mean GFP fluorescence
0 1 2 3 4 5 6
miR-277 ASO
luc ASO
GFP dsRNA
no ASO
P < 0.9
miR-277 ASO
luc ASO
no ASO
P < 0.0002
miR-277 ASO
luc ASO
no ASO
P < 0.003

Figure II-S2. siRNA, siRNA-binding-site, and antisense oligonucleotide (ASO) structures

(A) Structure of the miR-277-binding sites in 3′ UTR of the perfectly complementary or the partially complementary GFP reporter mRNAs. (B) Structure of the 3′-cholesterol conjugated, 2′-*O*-methyl modified, antisense oligonucleotides (ASOs) used as a control (luciferase-specific) or used to inhibit miR-277 expression in cultured S2 cells. Every ribose 2′ hydroxyl in each ASO was replaced with a methoxy group.

Figure II-S2

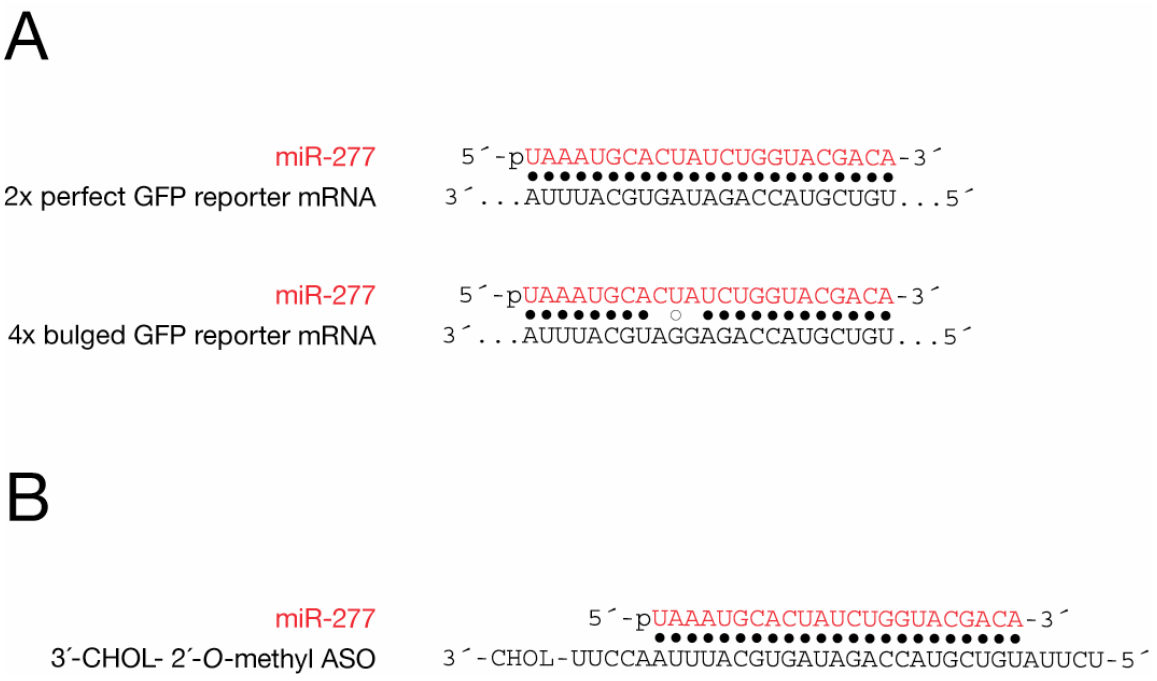
A
miR-277
5´-pUAAAUGCACUAUCUGGUACGACA-3´
2x perfect GFP reporter mRNA
3´...AUUUACGUGAUAGACCAUGCUGU...5´
miR-277
5´-pUAAAUGCACUAUCUGGUACGACA-3´
4x bulged GFP reporter mRNA
3´...AUUUACGUAGGAGACCAUGCUGU...5´
B
miR-277
5´-pUAAAUGCACUAUCUGGUACGACA-3´
3´-CHOL- 2´-O-methyl ASO
3´-CHOL-UUCCAAUUUACGUGAUAGACCAUGCUGUAUUCU-5´

Figure II-S3. Endogenous miR-277-programmed Ago2, not Ago1, represses a GFP reporter containing a single, perfectly complementary site in its 3′ UTR

At left, clonally derived S2 cells bearing the GFP reporter were transfected with the indicated antisense oligonucleotide (ASO), including an ASO complementary to miR-277. At right, the cells were transfected with dsRNA corresponding to the indicated gene. Each bar represents the average ± standard deviation for three independent experiments.

Figure II-S3

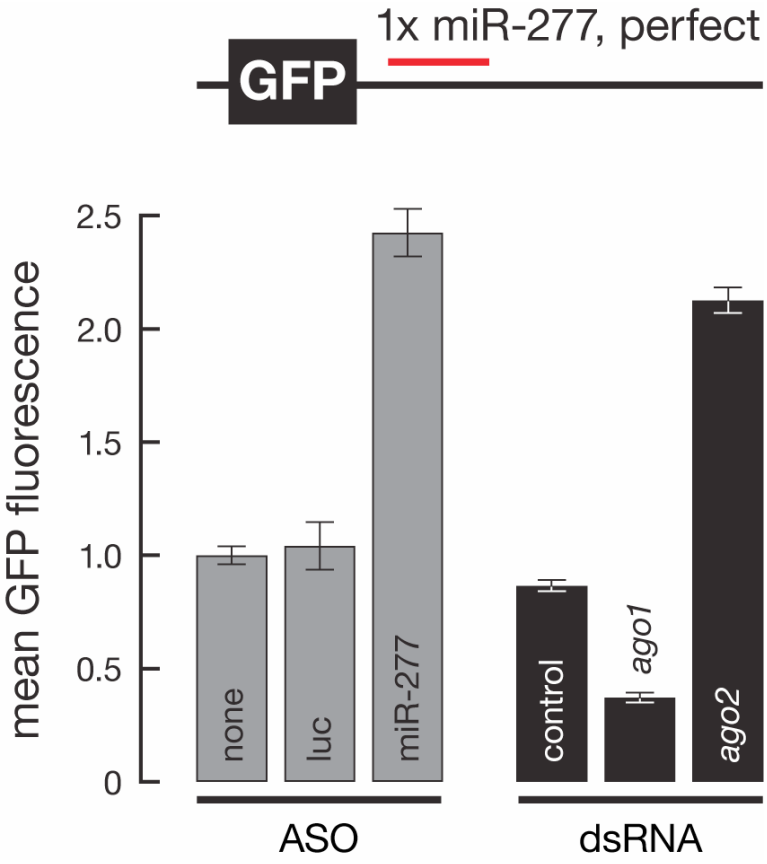
1x miR-277, perfect
GFP
mean GFP fluorescence
2.5
2.0
1.5
1.0
0.5
0
none
luc
miR-277
control
ago1
ago2
ASO
dsRNA

Figure II-S4. miR-277 regulates reporter mRNA steady state abundance

Inhibition of miR-277 by a specific ASO increased both the mRNA abundance (A) and the production of GFP protein (B) for the perfect and bulged GFP reporters, but not the unregulated control, even when additional miR-277 ("+miR-277") was expressed from a transgene. After 72 hrs, mRNA abundance was measured by qRT-PCR and GFP protein expression measured by FACS analysis. Three replicate transfections were performed for the cell line containing the 4x bulged reporter and expressing additional miR-277; single transfections were performed for all other cell lines. For qRT-PCR, total RNA was extracted from ~107 cells with Trizol (Invitrogen, Carlsbad, CA). Reverse transcription was performed with Superscript II (Invitrogen) according to the manufacturer's instructions, using gene specific primers (forward primer and RT/reverse primer) for the GFP and RP49 coding regions: 5′-CCG CTT CAA GGG ACA GTA TCT G-3′ and 5′-ATC TCG CCG CAG TAA ACG C-3′ for RP49; 5′-TGT CGG GCA GCA GCA C-3′ and 5′-AAC GGC ATC AAG GTG AAC TTC-3′ for GFP. Relative GFP mRNA abundance was calculated using the 2-ΔΔCt method. Values were normalized to the no treatment control. Error bars represent the standard deviation of three PCR replicates. For the 4x bulge+miR277 sample, error bars represent standard deviation of the means of three independent transfection experiments. (C) miR-277 does not affect the ratio of reporter GFP protein to RNA. For each cell line tested, the ratio of the mean GFP fluorescence to the relative GFP mRNA abundance is shown, normalized to the no treatment control.

Figure II-S4

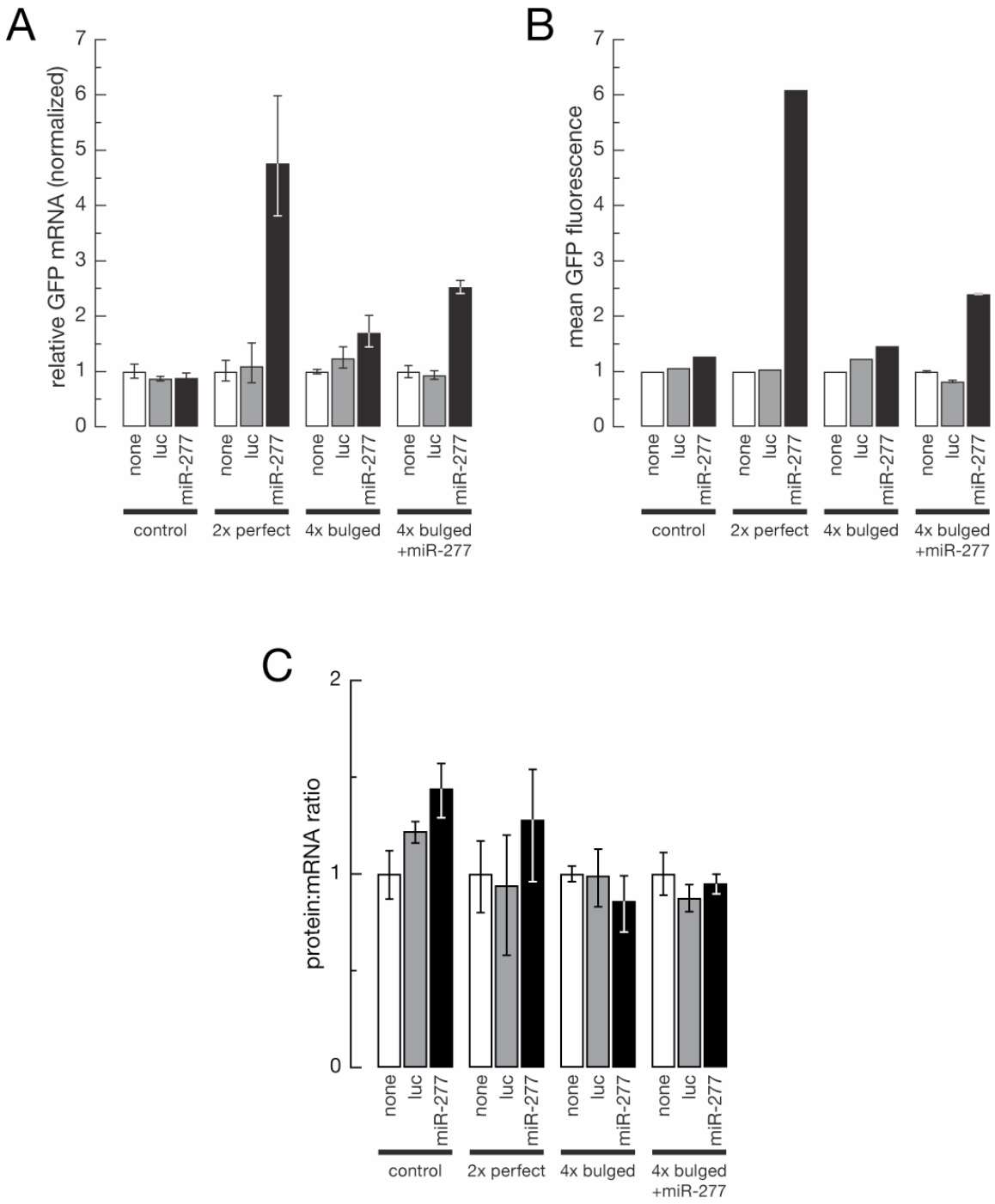
A
relative GFP mRNA (normalized)
0
1
2
3
4
5
6
7
none
luc
miR-277
control
2x perfect
4x bulged
4x bulged +miR-277
B
mean GFP fluorescence
C
protein:mRNA ratio
0
1
2

Figure II-S5. *N*-ethyl maleimide (NEM) inactivates assembly of Ago1-RISC, but does not alter the kinetics of Ago1-mediated target cleavage

(A) Ago1 was programmed with the kinetics of Ago1-mediated target cleavage. *let-7* in vitro using 50 nM *let-7/let-7** duplex, then the reaction treated NEM at the indicated time. Unreacted NEM was quenched with DTT. The relative amount of Ago1-RISC assembled was then determined by measuring the rate of cleavage of 50 nM target RNA containing a single *let-7*-complementary site. (B) 50 nM *let-7/let-7** duplex was incubated with embryo lysate for 60 min to program Ago1-RISC, then the reaction treated with NEM, followed by DTT. As a control, DTT was added before the NEM. The cleavage of 200 nM target RNA by *let-7* programmed Ago1-RISC was then assayed. Both reactions displayed the burst kinetics characteristic of Ago1-mediated target cleavage.

Figure II-S5

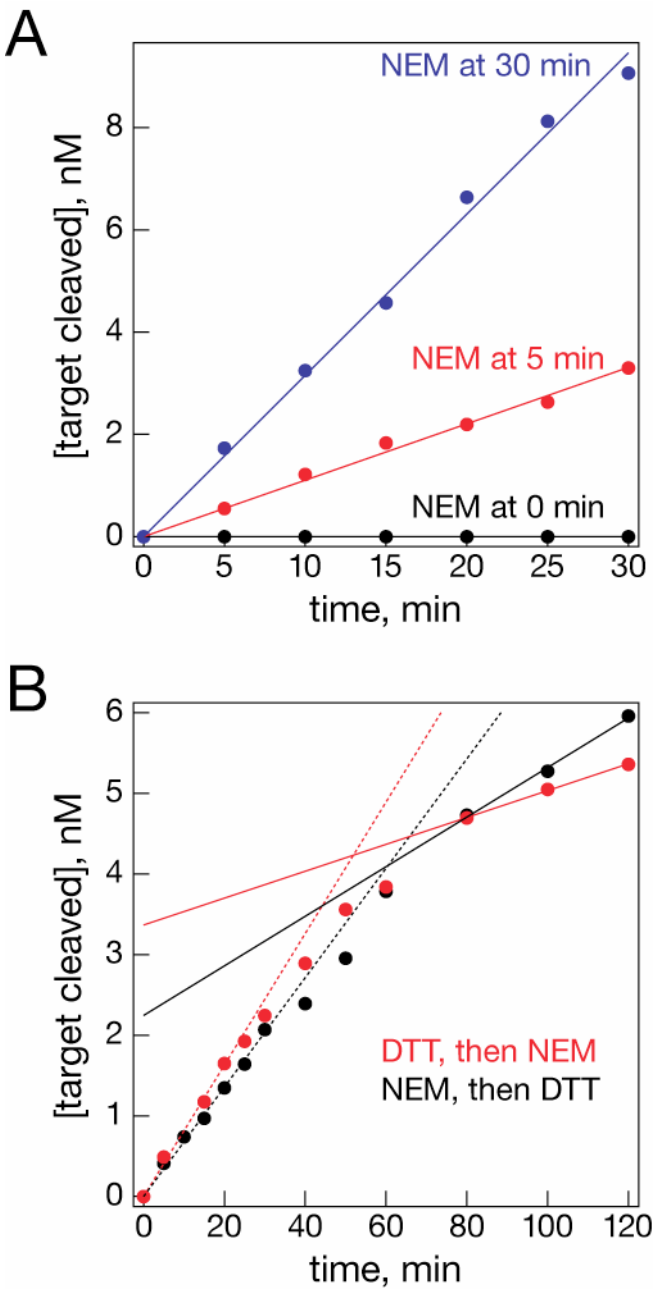
A
NEM at 30 min
NEM at 5 min
NEM at 0 min
[target cleaved], nM
time, min
B
DTT, then NEM
NEM, then DTT
[target cleaved], nM
time, min

Chapter III:

The *Drosophila* RNA methyltransferase, DmHen1, modifies germ line piRNAs and single-stranded siRNAs in RISC

Contributions: The work presented in this chapter was a collaborative effort. The author performed experiments shown in Figures 2A, 2D, 3A, 3B, 3C (repeated for publication by CM), S3, S4 with Peng Wang, and S6. Chengjian Li performed experiments in figures 1A, 2B, 2C, S1, and S2. Christian Matranga performed experiments in figure 3C, 4A, 4B, and S7. Gwen Farley purified the protein in figure S5. Vasia Vagin and Peng Wang tested the in vitro siRNA modification assay. Phillip Zamore wrote the paper.

Summary

In plants and animals, small silencing RNAs guide Argonaute proteins to repress gene expression by a set of related mechanisms collectively called RNA silencing pathways (Zamore and Haley, 2005; Meister and Tuschl, 2004). In the RNA interference (RNAi) pathway (Fire et al., 1998), small interfering RNAs (siRNAs) defend cells from invasion by foreign nucleic acids, such as those produced by viruses. In contrast, microRNAs (miRNAs) sculpt expression of endogenous mRNAs (Bartel and Chen, 2004). In animals, a third class of small RNAs, Piwi-interacting RNAs (piRNAs), defends the genome from molecular parasites such as transposons (Aravin et al., 2003; Aravin et al., 2007; Aravin et al., 2001; Vagin et al., 2006; Brennecke et al., 2007). Here, we report that piRNAs in

flies contain a 2′-*O*-methyl group on their 3′ termini, a modification previously reported for miRNAs and siRNAs in plants (Yang et al., 2006) and piRNAs in mice (Kirino and Mourelatos, 2007a; Ohara et al., 2007) and rats (Houwing et al., 2007). In plants, small RNA methylation is catalyzed by the HEN1 protein and serves to protect miRNAs and siRNAs from degradation (Li et al., 2005; Yang et al., 2006; Yu et al., 2005). We find that the *Drosophila* homolog of HEN1, DmHen1, methylates the termini of both siRNAs and piRNAs. In the absence of DmHen1, both the length and abundance of piRNAs are decreased, and piRNA function is perturbed. Unlike plant HEN1, the *Drosophila* enzyme acts on single-stranded rather than duplex small RNAs, explaining how it can use as substrates both siRNAs—which derive from double-stranded precursors—and piRNAs—which do not (Houwing et al., 2007; Vagin et al., 2006). 2′-*O*-methylation of siRNAs may be the final step in assembly of the RNAi-enzyme complex, RISC, occurring after an Argonaute-bound siRNA duplex is converted to single-stranded RNA.

Results and Discussion

Drosophila piRNAs are 2′-O-methylated at their 3′ termini

In flies, both piRNAs (also known as repeat-associated siRNAs, rasiRNAs) and siRNAs, but not miRNAs, are modified at their 3′ termini (Pelisson et al., 2007; Vagin et al., 2006). We selectively labeled (Figure S1) the terminal nucleotide of *Drosophila melanogaster* 0–2 h embryo and mouse and bull testicular piRNAs. The resulting ^{32}P-radiolabeled nucleoside 2′ or 3′-monophosphates were resolved by two-dimensional thin-layer chromatography (2D TLC) using a solvent system that can resolve nucleoside 2′ monophosphates, nucleoside 3′ monophosphates, and 2′-*O*-methyl nucleoside 3′

monophosphates (Figure S2). Modified nucleoside monophosphates derived from the 3′ termini of piRNAs were identified by comparison to modified and unmodified nucleoside

Figure III-1. 2′-*O*-methylation of piRNAs in *Drosophila*

(A) *Drosophila* piRNAs are 2′-*O*-methylated at their 3′ termini. The modified nucleotides on the 3′ termini of piRNAs from 0–2 h fly embryos, and mouse and bull testes were selectively ^{32}P radiolabeled. The radiolabeled modified mononucleotides from each species were resolved by 2D-TLC individually (piRNA), with ^{32}P-radiolabeled 3′ mononucleotide standards (piRNA+3′NMPs), and with ^{32}P-radiolabeled 2'-*O*-methyl, 3′ phosphate mononucleotide standards (piRNA+2'mNMPs). The modified nucleotides from the piRNA from all three animals co-migrated with 2'mNMPs standards, but not with 3′NMPs standards. Ap, 3′AMP; Gp, 3′GMP; Cp, 3′CMP; Up, 3′UMP; 2′mAp, 2'-*O*-methyl AMP; 2′mGp, 2'-*O*-methyl GMP; 2′mCp, 2'-*O*-methyl CMP; 2′mUp, 2'-*O*-methyl UMP; and P_i, phosphate. The asterisk marks a contaminant, likely 3′ AMP, present in the [5′ ^{32}P] cytidine 5′,3′ bis-phosphate used to radiolabel the piRNA. † marks a contaminant present in the 2'-*O*-methyl, 3′ phosphate mononucleotide standards. (B) *Drosophila hen1* gene (CG12367), mRNA, and protein. The piggyBac transposon, PBac(WH)CG12367[f00810], is inserted 207 bp upstream of the second exon. The open arrow indicates the predicted start of transcription. The closed arrows denote the position of the qRT-PCR primers used in Figure 2A. The first intron of *hen1* contains another gene, CG8878, transcribed in the opposite direction, whose expression is unaltered by the piggyBac insertion (Figure S3).

Figure III-1

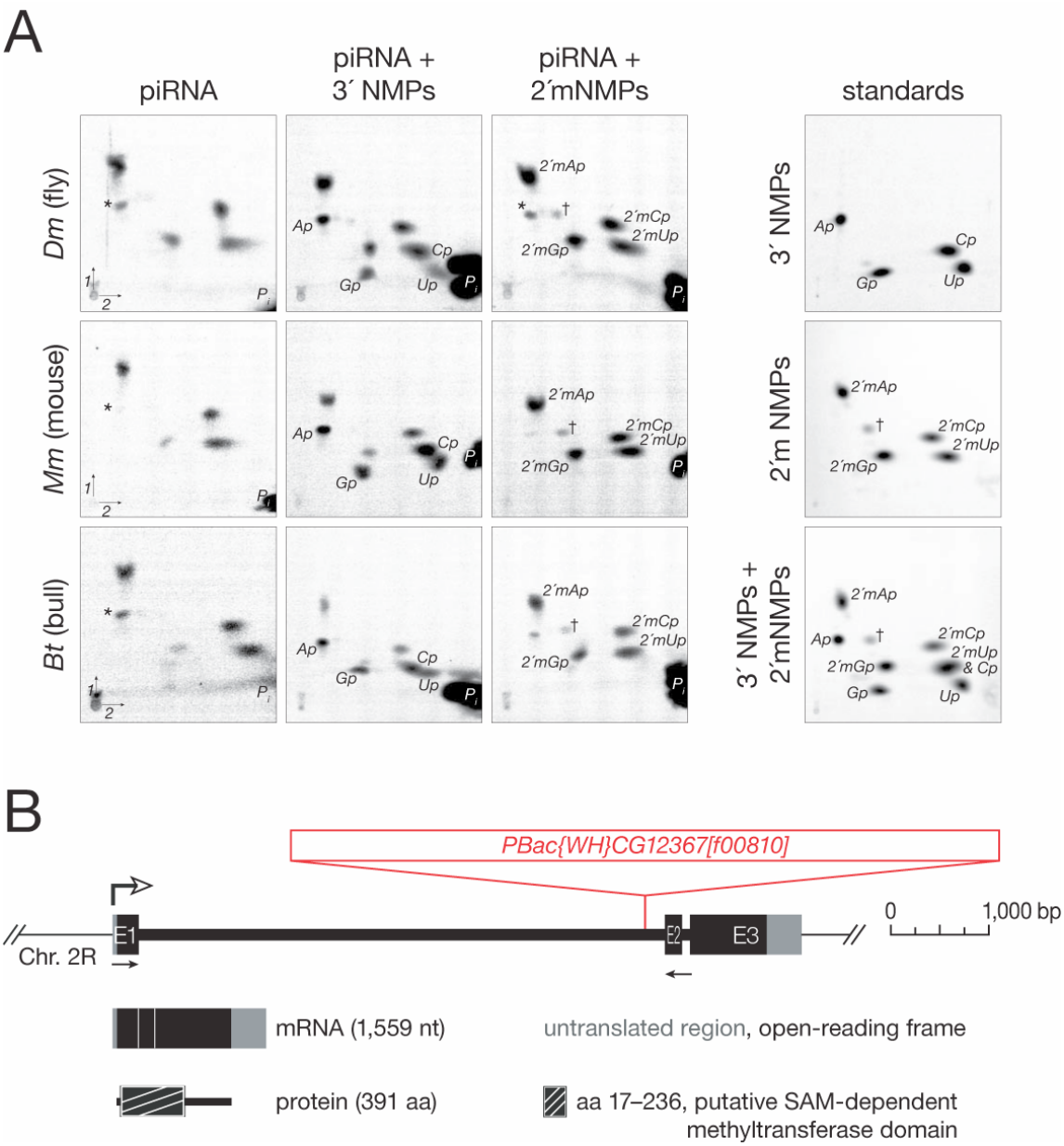
A
piRNA
piRNA + 3´ NMPs
piRNA + 2´mNMPs
standards
Dm (fly)
Mm (mouse)
Bt (bull)
3´ NMPs
2´m NMPs
3´ NMPs + 2´mNMPs
Ap
Cp
Gp
Up
2´mAp
2´mCp
2´mUp
2´mGp
& Cp
B
PBac{WH}CG12367[f00810]
Chr. 2R
E1
E2
E3
0
1,000 bp
mRNA (1,559 nt)
untranslated region, open-reading frame
protein (391 aa)
aa 17–236, putative SAM-dependent methyltransferase domain

2′ and 3′ monophosphate standards (Figure 1A). The terminal nucleotide of the piRNAs of all three animals co-migrated with 2′-*O*-methyl nucleoside 3′ monophosphate standards, but not with any unmodified nucleoside monophosphate standard. Since mouse piRNAs were previously shown to contain 2′-*O*-methyl modified 3′ termini using both mass spectrometry (Ohara et al., 2007) and a 2D TLC system (Kirino and Mourelatos, 2007a) distinct from ours, we conclude that *Drosophila* and bull piRNAs also contain a 2′-*O*-methyl group at their 3′ termini.

DmHen1 is required for piRNA modification in vivo

In *Arabidopsis*, the RNA methyltransferase, HEN1, modifies the terminal 2′ hydroxyl group of small silencing RNAs. In *Drosophila*, predicted gene CG12367, whose 1559 nucleotide mRNA encodes a 391 amino acid protein with a 220 amino acid evolutionarily conserved methyltransferase domain (Tkaczuk et al., 2006), most closely resembles *Arabidopsis* HEN1 (Figure 1B)(Park et al., 2002). For simplicity, we call this gene *Drosophila melanogaster* (Dm) *hen1*. When homozygous, a piggyBac transposon insertion (PBac(WH)CG12367[f00810]) within the first intron of the fly *hen1* gene reduces the accumulation of *hen1* mRNA by 1,000-fold in testes and by more than 40,000-fold in ovaries (Figures 2A) and can therefore be considered a null mutation, which we refer to as $hen1^{f00810}$.

We examined the 3′ termini of two types of highly abundant piRNAs in the germ line of flies heterozygous or homozygous for $hen1^{f00810}$. In testes, the *Suppressor of Stellate* (*Su(Ste)*) locus produces 24–27 nt rasiRNAs, a subclass of piRNAs that directs

silencing of the selfish genetic element *Stellate*. *Su(Ste)* rasiRNAs, like other *Drosophila* piRNAs, are modified at their 3´ termini and therefore do not react with $NaIO_4$

Figure III-2. DmHen1 is required for normal piRNA biogenesis and complete silencing of the *HeT-A* Transposon

(A) Quantitative RT-PCR of *hen1* mRNA in testes and ovaries from wild-type or $hen1^{f00810}$ flies, relative to *rp49*. Bars report the average ± standard deviation for at least four independent experiments. (B, C) Northern hybridization to detect modification of small RNAs in wild-type and $hen1^{f00810}$ testes (B) or ovaries (C). The same blot was probed sequentially to detect the most abundant *Su(Ste)* rasiRNA (B) or the three most abundant *roo* rasiRNAs (C), miR-8, and 2S ribosomal RNA. (D) Quantitative RT-PCR of *HeT-A* transposon mRNA in ovaries. *HeT-A* mRNA levels were measured relative to *rp49* using total RNA prepared from wild-type, $hen1^{f00810}$ heterozygous or homozygous ovaries. Bars report the average ± standard deviation for at least four independently prepared samples.

Figure III-2

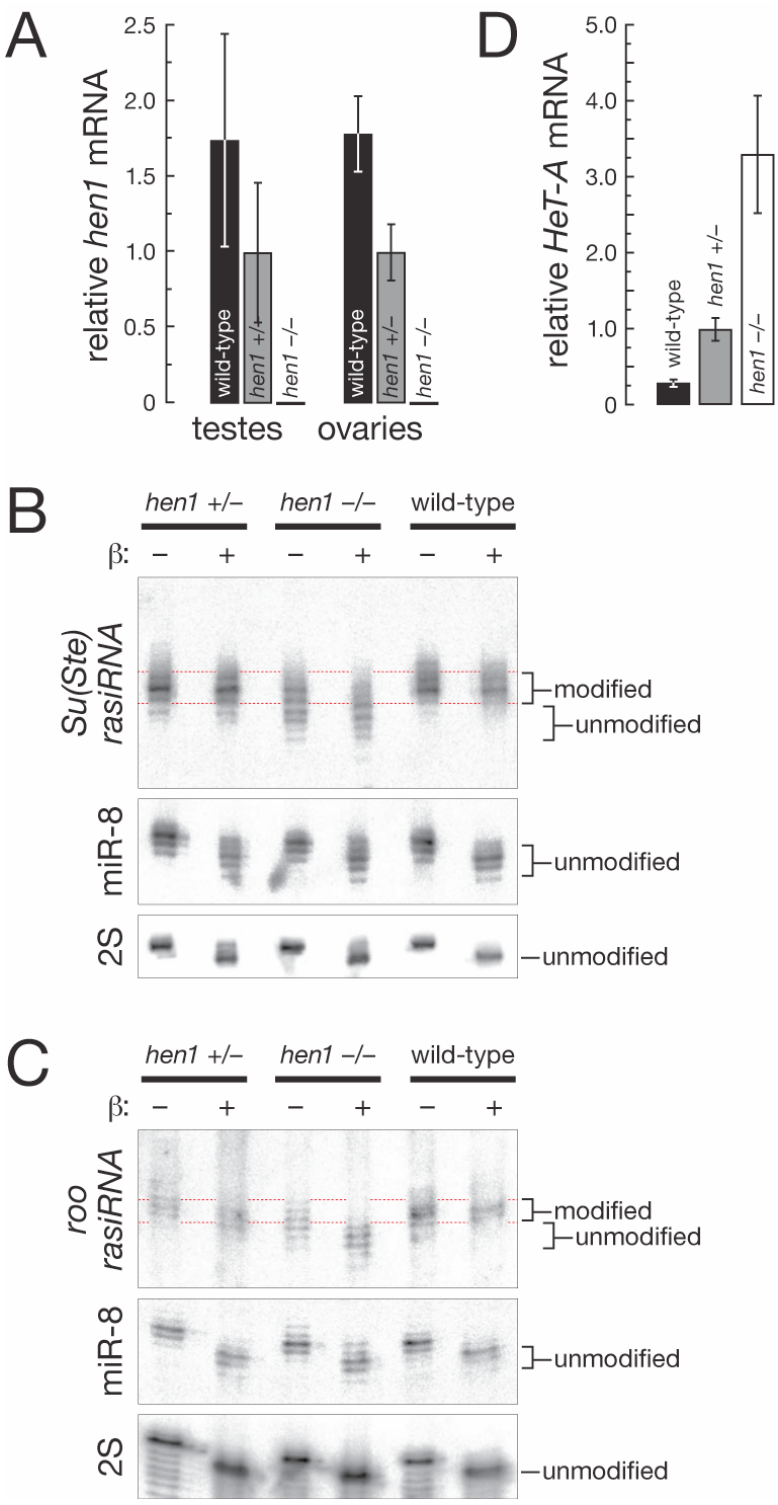

(Vagin et al., 2006). In contrast, *Su(Ste)* rasiRNAs from *hen1*^{f00810}/*hen1*^{f00810} mutant testes reacted with $NaIO_4$ and could therefore be β-eliminated to remove the last nucleotide of the RNA, increasing their gel mobility (Figure 2B) and indicating that in the absence of

DmHen1 protein, they are not modified. Similarly, rasiRNAs that guide silencing of *roo*, the most abundant retrotransposon in *Drosophila melanogaster*, were not modified in *hen1*^{f00810} homozygous ovaries (Figure 2C). The *Su(Ste)* and *roo* rasiRNAs were also shorter in the *hen1*^{f00810} homozygotes. In contrast, the length and amount of miR-8, which is expressed in both the male and female germ line, was unaltered in *hen1*^{f00810} homozygotes. For both *Su(Ste)* and *roo*, rasiRNAs were on average shorter and less modified even in *hen1*^{f00810} heterozygotes, compared to wild-type, suggesting that the abundance of DmHen1 protein limits the stability or production of piRNAs in flies.

DmHen1 is required for piRNA function in vivo

Modification of the termini of *Drosophila* piRNAs plays a role in their function: mRNA expression from *HeT*-A, the element whose expression is most sensitive to mutations that disrupt piRNA-directed silencing in the female germ line (Vagin et al., 2006; Vagin et al., 2004; Savitsky et al., 2006), quadrupled in *hen1*^{f00810} heterozygotes and was increased more than 11-fold in homozygotes, relative to wild-type tissue (Figure 2D). We conclude that Hen1 protein is required for piRNA-directed silencing in the *Drosophila* germ line.

DmHen1 is required for siRNA modification

To test if DmHen1 is required for modification of the 3′ termini of siRNAs, we depleted Hen1 by RNAi in cultured *Drosophila* S2 cells. We transfected the cells with

Figure III-3. DmHen1 modifies Ago2-associated small RNAs

(A) Modification of siRNAs and miRNAs in *Drosophila* S2 Cells. A stable S2 cell line expressing GFP was treated with the indicated dsRNA alone (day 1 and 5), then together

with GFP dsRNA (day 8). Two non-overlapping dsRNAs were used to target *hen1*. Total RNA was collected on day 9, treated with $NaIO_4$/β elimination, then dsGFP-derived siRNA, miR-277 and *bantam* detected by sequential Northern hybridization of the same blot. (B) In vitro siRNA modification in dsRNA-treated S2 cell lysates. (C) In vitro siRNA modification in *Drosophila* mutant ovary lysates.

Figure III-3

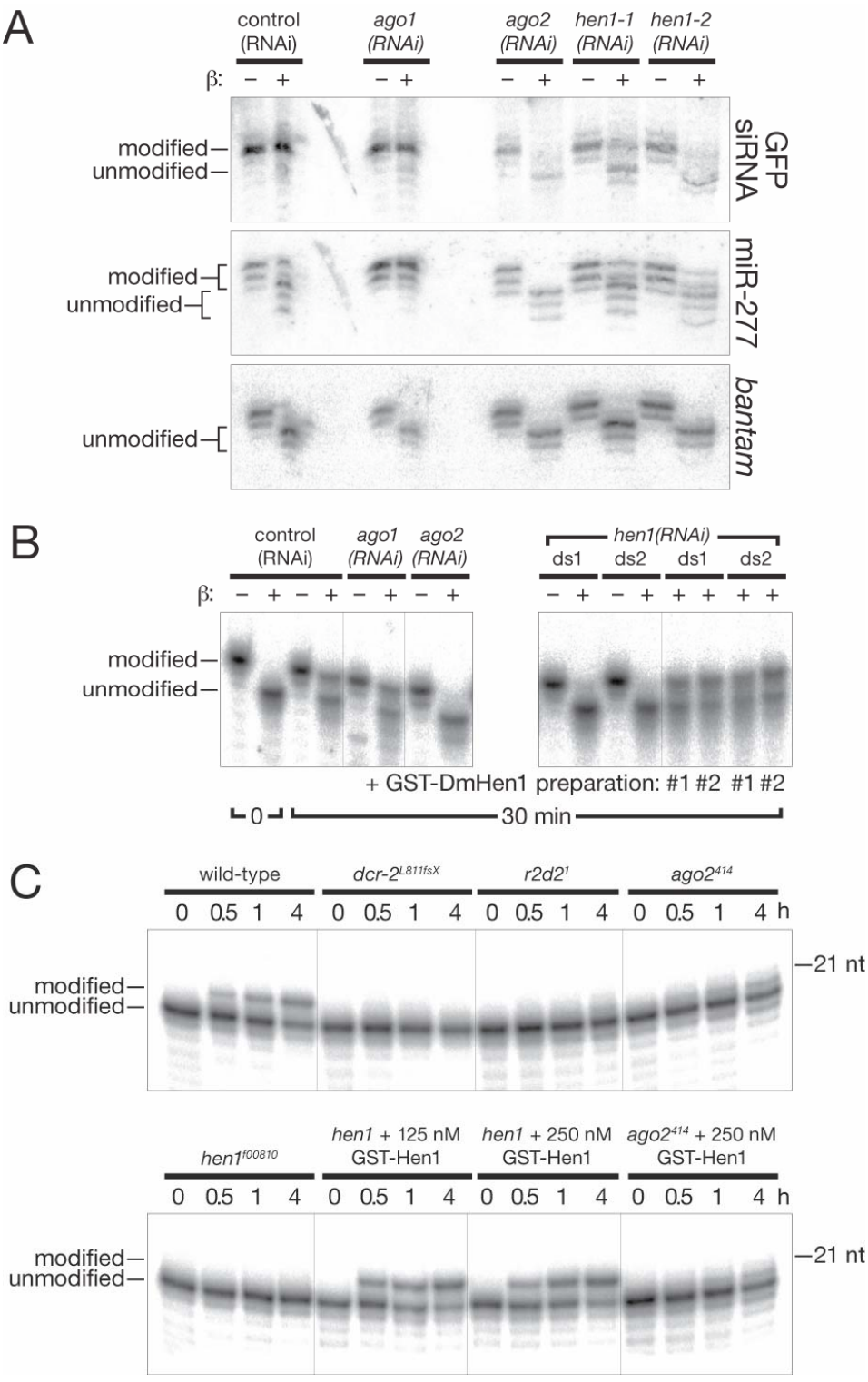

long double-stranded RNA (dsRNA) targeting *hen1* on day 1 and day 5, then co-transfected them with both GFP dsRNA and *hen1* dsRNA on day 8. Total RNA was

harvested on day 9, probed for modification with $NaIO_4$/β-elimination, and analyzed by Northern hybridization using a 5′ ^{32}P-radiolabeled DNA probe complementary to the most abundant GFP-derived siRNA (MDH, Megha Ghildiyal, and PDZ, unpublished data). DsRNAs targeting two different regions of the fly *hen1* mRNA both reduced the amount of GFP siRNA modified at its 3′ terminus, whereas all the GFP siRNA remainedmodified when a control dsRNA was used (Figure 3A).

Surprisingly, RNAi-mediated depletion of Ago2, but not Ago1, prevented the GFP siRNA from being modified. This result suggests that Ago2, but not Ago1, plays a role in the modification of siRNAs by DmHen1. To test this idea, we examined the modification status of the 3′ terminus of miR-277, an siRNA that partitions into both Ago1 and Ago2 complexes in vivo(Förstemann et al., 2007). *Drosophila* miRNAs associate predominantly or exclusively with Ago1 (Okamura et al., 2004) and have unmodified 3′ termini (Hutvágner et al., 2001; Pelisson et al., 2007; Vagin et al., 2006). In contrast, about half the miR-277 in cultured S2 cells failed to react with $NaIO_4$ (Figure 3A), suggesting that about half of miR-277 is modified at its 3′ terminus. The fraction of miR-277 that was modified was reduced when two different dsRNAs were used to deplete DmHen1 by RNAi. When the cells were treated with dsRNA targeting *ago1*, all detectable miR-277 was modified, whereas all miR-277 became unmodified when dsRNA targeting *ago2* was used. In contrast, *bantam*, a miRNA that associates nearly exclusively with Ago1 (Okamura et al., 2004), was unmodified under all conditions (Figure 3A).

siRNA modification correlates with Ago2-RISC assembly in vitro

siRNA modification can be recapitulated in lysates of embryos, ovaries, or cultured S2 cells. Modification of siRNA in vitro was inhibited by *S*-adenosyl homocysteine, but not by *S*-adenosyl methionine, consistent with DmHen1 transferring a methyl group from *S*-adenosyl methionine to the terminal 2′ hydroxyl group of the RNA, thereby generating *S*-adenosyl homocysteine as a product (Figure S4).

Our data from cultured S2 cells suggested that DmHen1 modifies that portion of miR-277 that enters the Ago2-RISC assembly pathway, but not the population of miR-277 that assembles into Ago1-RISC. To further test the idea that small RNA modification requires both Hen1 and the Ago2-RISC assembly pathway, we prepared cytoplasmic lysates from dsRNA-treated cultured S2 cells. Lysate from control-treated cells modified the 3′ terminus of a 5′ ^{32}P-radiolabeled synthetic siRNA duplex, but not lysate from *hen1*-depleted cells (Figure 3B). The addition of either of two different preparations of purified, recombinant DmHen1, expressed in *E. coli* as a ~74 kDa glutathione S-transferase fusion protein (GST-DmHen1; Figure S5), restored the ability of the lysates to modify the siRNA, indicating that loss of DmHen1 caused the loss of siRNA modification. Moreover, lysates depleted for Ago2, but not Ago1, could not modify the ^{32}P-siRNA in vitro (Figure 3B). These in vitro data, together with our S2 cell experiments, suggest that modification of the 3′ terminus of siRNAs and miRNAs is coupled to assembly into Ago2-RISC.

Dcr-2 and R2D2 act to load double-stranded siRNAs into Ago2. We prepared lysates from ovaries homozygous mutant for *hen1*, *dcr-2*, *r2d2*, and *ago2* using alleles unable to produce the corresponding protein (Lee et al., 2004; Liu et al., 2003; Okamura et al., 2004). A 5′ ^{32}P-radiolabeled siRNA duplex was incubated in each lysate to

assemble RISC. At each time point, we determined if the siRNA was 3′ terminally modified by assessing its reactivity with $NaIO_4$ (Figure 3C). No modified siRNA accumulated when the duplex was incubated in *hen1*^{f00810}, *dcr-2*^{L811fsX}, *r2d2*^{1}, or *ago2*^{414} mutant lysate. Adding 250 nM purified, recombinant GST-DmHen1 restored siRNA modification to the *hen1*^{f00810} but not the *ago2*^{414} lysate. We conclude that the defect in *ago2*^{414} reflects a requirement for Ago2 in small RNA modification by DmHen1, rather than an indirect effect, such as destabilization of DmHen1 in the absence of Ago2. GST-DmHen1 similarly rescued lysate from *hen1(RNAi)* but not *ago2(RNAi)* treated S2 cells (Figure S6). Together, the results of our experiments using cultured S2 cells—a somatic cell line—and ovaries, which comprise mainly germ line tissue, suggest that a functional Ago2-RISC assembly pathway is required for siRNA modification in *Drosophila*.

siRNAs are modified only after Ago2-RISC maturation

To test at which step in the Ago2-RISC assembly pathway siRNAs become modified, we determined if siRNAs are 2′-*O*-methylated by DmHen1 as single-strands or as duplexes. In vitro, assembly of siRNAs into Ago2-RISC follows an ordered pathway in which the siRNA duplex first binds the Dicer-2/R2D2 heterodimer to form the RISC-loading complex (RLC). The RLC determines which of the two siRNA strands will become the guide for Ago2 and which will be destroyed (the passenger strand). The siRNA is then loaded into Ago2 as a duplex, with the passenger strand occupying the same position as future target RNAs, generating pre-RISC (Kim et al., 2006). Cleavage of the passenger strand by the Ago2 endonuclease domain converts pre-RISC to mature RISC (Leuschner et al., 2006; Matranga et al., 2005; Rand et al., 2005; Miyoshi et al., 2005). No single-stranded guide or passenger RNA is produced prior to this maturation step. Thus, all

single-stranded siRNA produced in vitro or in vivo (Kim et al., 2006) corresponds to mature RISC.

We assembled Ago2-RISC in vitro using an siRNA designed to load only one of its two strands into Ago2 (Schwarz et al., 2003). We then sampled the reaction over time, isolating the 5′ ^{32}P-radiolabeled siRNA under conditions previously demonstrated to preserve its structure (Nykanen et al., 2001), and separated single- from double-stranded siRNA by native gel electrophoresis (Figure S7). (Full-length siRNA duplexes and siRNA heteroduplexes comprising a full-length guide paired to a cleaved passenger strand co-migrate as double-stranded siRNA in these gel conditions (Matranga et al., 2005).) The RNAs were then isolated from the gel and tested for reactivity with $NaIO_4$ to determine the presence of modification at their 3′ termini (Figure 4, A and B). At each time, total siRNA was analyzed in parallel. 3′ terminal modification increased over the course of RISC assembly and, at all times, was restricted to single-stranded siRNA: within our limits of detection, all double-stranded siRNA was unmodified, even after 3 h. We conclude that siRNA modification is coupled to RISC assembly and occurs only after the conversion of pre-RISC to mature RISC.

Recombinant DmHen1 modifies single-stranded small RNA

While *Arabidopsis* HEN1 contains an N-terminal double-stranded RNA-binding motif (Yu et al., 2005), DmHen1 does not. To test if DmHen1 modifies double-stranded small RNAs, we incubated purified, recombinant, GST-DmHen1 with either single-stranded or double-stranded siRNAs. We detected modification, evidenced by loss of reactivity with $NaIO_4$, only for the single-stranded RNA, suggesting that DmHen1 modifies single-

Figure III-4. siRNAs are modified after the conversion of pre-RISC—which

contains double-stranded siRNA—into mature RISC, which contains only single-stranded siRNA

siRNA duplexes with a 5′ ^{32}P-radiolabeled guide strand were incubated in *Drosophila* embryo lysate, and then tested for the presence of a 3′ terminal modification. (A) Total RNA from each time point in RISC assembly, without (–) and with (+) reaction with $NaIO_4$ and β-elimination. (B) At each times in (A), single- and double-stranded siRNA were resolved and purified by first native gel electrophoresis (Figure S7), then analyzed by denaturing electrophoresis separately for the presence of a 3′ terminal modification on the siRNA guide strand. (A) and (B) are the left and right halves of a single gel. (C) Recombinant, purified GST-DmHen1, but not GST alone, can modify single-stranded 21 nt RNA, but not double-stranded siRNAs or blunt 21 nt RNA duplexes. However, in contrast to GST-DmHen1 incubated with *hen1*^{f00810} mutant ovary lysate (Figure 3C), the enzyme alone is inefficient. All samples were oxidized with $NaIO_4$, then β-eliminated. (D) A model for 2′-*O*-methylation of siRNAs. (E) A proposed role for 2′-*O*-methylation in piRNA biogenesis.

Figure III-4

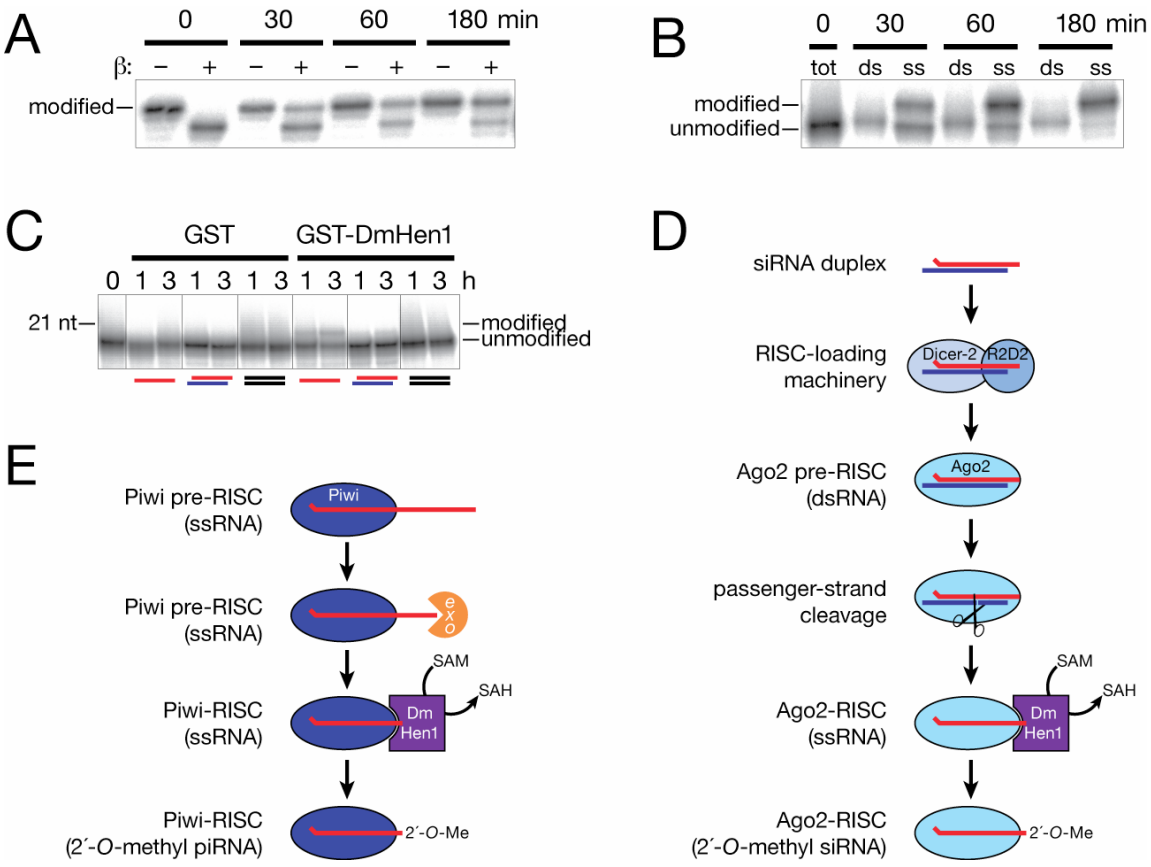
A
0
30
60
180 min
β: − + − + − + − +
modified
B
0
30
60
180 min
tot ds ss ds ss ds ss
modified
unmodified
C
GST
GST-DmHen1
0 1 3 1 3 1 3 1 3 1 3 1 3 h
21 nt
modified
unmodified
D
siRNA duplex
RISC-loading machinery
Dicer-2
R2D2
Ago2 pre-RISC (dsRNA)
Ago2
passenger-strand cleavage
Ago2-RISC (ssRNA)
SAM
SAH
Dm Hen1
Ago2-RISC (2′-O-methyl siRNA)
2′-O-Me
E
Piwi pre-RISC (ssRNA)
Piwi
Piwi pre-RISC (ssRNA)
exo
Piwi-RISC (ssRNA)
SAM
SAH
Dm Hen1
Piwi-RISC (2′-O-methyl piRNA)
2′-O-Me

stranded substrates, but not siRNAs or blunt RNA duplexes (Figure 4C). A preference for single-stranded RNA would explain how DmHen1 could act on both siRNAs, which are born double-stranded, and piRNAs, which are not. We note that the purified, recombinant GST-DmHen1 protein was more than 50-fold less active on its own than when supplemented with ovary lysate from *hen1*^{f00810} homozygous flies. We speculate that the Ago2-RISC machinery is required for Hen1 function in flies, although we cannot yet exclude the possibility that the lysate contains a factor (e.g. a kinase) required to activate Hen1.

Modification of single-stranded siRNAs—that is, those loaded in fully mature Ago2-RISC, but not double-stranded siRNAs (Figure 4D) might allow cells to distinguish siRNAs loaded successfully into functional complexes from those that fail to assemble. For example, if a 3′-to-5′ nuclease acts to degrade single-stranded siRNAs, 2′-*O*-methylation of single-stranded siRNAs in Ago2-RISC may protect them from destruction. Moreover, such a nuclease might trim the 3′ end of piRNAs. 2′-*O*-methylation of the piRNA 3′ terminus may occur only when the length of RNA extending beyond the Piwi family protein is short enough to permit the simultaneous binding of the final ribose sugar to the active site of DmHen1 and the interaction of DmHen1 with the Piwi protein itself (Figure 4E). Modification of the terminus of the trimmed piRNA would then block further 3′-to-5′ trimming of the small RNA, generating its Piwi-, Aubergine-, or Ago3-specific length. Our observation that piRNAs are shorter in *hen1*^{f00810} mutants supports this model.

We note that all 2′-*O*-methyl modified small RNAs identified thus far are associated with RISC complexes that efficiently cleave their RNA targets—i.e., Ago1-

associated plant miRNAs (Baumberger and Baulcombe, 2005; Qi et al., 2005), animal piRNAs (Lau et al., 2006), and Ago2-associated siRNAs in flies (Hammond et al., 2001)—whereas *Drosophila* miRNAs are typically both unmodified and associated with Ago1-RISC, which does not catalyze mRNA target cleavage in vivo(Förstemann et al., 2007). We speculate that DmHen1 is recruited to RISC complexes containing single-stranded small silencing RNAs according to the identity of their Argonaute protein. This model predicts that DmHen1 will bind only to complexes containing fly Ago2 or the three fly Piwi proteins, Piwi, Aubergine, and Ago3, but not Ago1. Clearly, future experiments will need to test this hypothesis.

Experimental Procedures

General Methods

Preparation of 0–2 h embryo, ovary, and S2 cell lysates and in vitro RISC assembly and RNAi reactions, and Northern hybridization were as described (Haley et al., 2003; Förstemann et al., 2005; Vagin et al., 2006). Sequences of synthetic RNA and DNA oligonucleotides are available online (Table S1).

^{32}P-radiolabeled 3′ mononucleotide standards

Synthetic RNA oligonucleotides (Table S1) were radiolabeled in a 20 µl reaction containing 50 mM Tris-HCl (pH 7.8), 10 mM $MgCl_2$, 1 mM ATP, 10 mM dithiothreitol, 10% (v/v) DMSO, 10 µg/ml BSA, 2 units/µl RNasin (Promega, Madison, WI), 1.5 µCi/µl [5′ ^{32}P] cytidine 5′,3′ bis-phosphate ([5′ ^{32}P]-pCp; Perkin-Elmer, Waltham, MA), 1 unit/µl T4 RNA Ligase 1 (New England Biolabs, Ipswich, MA) at 4°C, overnight. The radiolabeled small RNAs were purified from a 15% denaturing urea-polyacrylamide

sequencing gel, and then digested with 1.5 U/µl micrococcal nuclease (Takara Mirus Bio, Madison, WI) in a 40µl reaction containing 20 mM Tris-HCl pH 8.0, 5 mM NaCl, 2.5 mM $CaCl_2$. 3′ ^{32}P-mononucleotides were further purified from a 22.5% denaturing urea-polyacrylamide sequencing gel.

2D-TLC

Small RNAs (21-29 nt, containing both modified piRNAs and unmodified small RNAs) from 0–2 h wild-type (Oregon R) fly embryos and small RNAs (26-31 nt, containing mostly modified piRNAs) from mouse and bull testes were purified from a 10% denaturing urea-polyacrylamide gel stained with SYBR® Gold (Invitrogen). About 100 pmol purified small RNAs were radiolabeled as described above, except in a 40 µl reaction using 3µCi/µl [5′ ^{32}P]-pCp and 1 unit/µl T4 RNA Ligase 1, and then gel purified. The purified, ^{32}P-radiolabeled RNA was hydrolyzed in 200mM Na_2CO_3 at 100°C for 1h, then neutralized with an equal volume of 200 mM HCl, dephosphorylated with 0.5 units/µl calf intestinal alkaline phosphatase (New England Biolabs) in a 200 µl reaction containing 50 mM Tris-HCl pH 7.9, 100 mM NaCl, 10 mM $MgCl_2$, 1 mM dithiothreitol. Alkaline phosphatase was inactivated by extraction with phenol /chloroform, RNA in the aqueous phase was oxidized with 80 mM $NaIO_4$ in borax/boric acid buffer (60 mM borax, 60 mM boric acid, pH 8.6) at room temperature for 30 min, and then β-eliminated with 200 mM NaOH at 45°C for 90 min. 5 µl of this reaction was mixed with an equal volume of formamide loading buffer (98% deionized formamide, 10 mM EDTA (pH 8.0), 0.025% (w/v) xylene cyanol, 0.025% (w/v) bromophenol blue), and resolved on a 22.5% denaturing urea-polyacrylamide sequencing gel. Equal intensities of modified mononucleotides and standards were spotted on 20 x 20 cm PEI-cellulose F

glass TLC plates (EMD Chemicals, Gibbstown, NJ) and separated first with isobutyric acid/25%ammonia/water (66:1:33, v:v:v) and then 0.1 M sodium phosphate pH6.8/ammonium sulfate/1-propanol (100:60:2, v:w:v).

Analysis of RNA 3´ termini

RNA was incubated for 30 min at room temperature with 25 mM $NaIO_4$ in borax/boric acid buffer (60 mM borax, 60 mM boric acid, pH 8.6), then 45.2 mM (f.c.) NaOH added, and incubation continued for 90 min at 45°C (β-elimination). The reaction was stopped by the addition of 300 mM (f.c.) NaCl, 1 μg glycogen, and three volumes absolute ethanol. After 30 min on ice, the precipitated RNA was collected by centrifugation.

Recombinant *Drosophila* Hen1 Protein

DmHen1 coding sequence was amplified from *Drosophila* ovary cDNA and inserted into pEnt-D-Topo (Invitrogen, Carlsbad, CA). The entire *hen1* sequence was confirmed by sequencing. The entry plasmid was recombined with the N-terminal GST expression vector, pDest-15, using LR Clonase (Invitrogen). GST-Hen1 was expressed in BL21 Star DE3 cells (Invitrogen) grown at 37°C in LB broth containing 100 ug/ml ampicillin until to OD_{600} reached 0.50. The culture was then cooled to 25°C and 0.4 mM IPTG added to induce protein production. The culture was incubated at 25°C with vigorous shaking for three hours. The cells were harvested by centrifugation at 7,300 x g for 20 min, washed with PBS, centrifuged again, and then the cell paste frozen in liquid nitrogen and stored at -80°C.

Hen1 fusion protein was purified using the GST Purification Kit (Clontech, Mountainview, CA). Cells were resuspended in 40 ml of Extraction/Loading buffer and

lysed by sonication (duty 30% for 6 minutes; Branson Sonificator II, Danbury, CT), with cooling in an ice bath. Two ml of clarified lysate was added to the column resin, and the column inverted several times to disperse the resin. The resin was then allowed to pack, and the remaining 38 ml passed through the column by gravity flow. Subsequent steps were according to the manufacturer's directions.

Analysis of double- and single-stranded siRNA

Double and single-stranded, 5′ ^{32}P-radiolabeled siRNA guide strands (10 nM; Figure S7 and 4) were separated as described (Nykanen et al., 2001). Briefly, RISC assembly reactions were stopped with 2x Proteinase K buffer, 2 mg/ml Proteinase K, 1 μg glycogen, and 250 nM unlabeled siRNA guide strand to prevent reannealing. After incubation for 30 min at 25˚C, 3 volumes absolute ethanol were added, and the RNA precipitated for 30 min on ice. The precipitates were collected by centrifugation, washed with 80% (v/v) ethanol, then dissolved in 2 mM Tris-Cl (pH 7.5), 3% (w/v) Ficoll-400, 0.04% (w/v) bromophenol blue, 100 mM KOAc, 30 mM HEPES-KOH, 2 mM $Mg(CH_3CO_2)_2$, and resolved by electrophoresis through a 15% native polyacrylamide gel (19:1 acrylamide:bis; 89 mM Tris-Borate, pH 8.3, 2 mM Na-EDTA, 2.5 mM $Mg(CH_3CO_2)_2$). The region of the native gel corresponding to double-or single-stranded siRNA was excised, and the RNA eluted overnight in 1 M NaCl. 1 μg glycogen and ethanol (60% final volume) was added to the eluate, the RNA collected using MegaClear filter cartridges (Ambion), eluted with H_2O, and then precipitated for 30 min on ice by adding 500 mM (f.c.) $NH_4CH_3CO_2$ and 2.5 volumes absolute ethanol. The precipitate was collected by centrifugation, washed with 80% (v/v) ethanol, and the samples reacted with $NaIO_4$ and subsequent β-elimination (see above). The precipitated RNA was dissolved in

98% deionized formamide, 10 mM EDTA (pH 8.0), 0.025% (w/v) xylene cyanol, 0.025% (w/v) bromophenol blue, and then resolved on a 15% denaturing urea-polyacrylamide sequencing gel.

Figure III-S1. Scheme for selectively labeling the 3′ terminal nucleotide of modified small RNAs

Because Rnl1 will use either a 2′ or a 3′ hydroxyl as a ligation donor, the scheme will also label 3′ modified RNAs. Only phosphodiester linkages flanked by a 2′ hydroxyl are subject to base hydrolysis and only adjacent 2′ and 3′ hydroxyls react with $NaIO_4$, a prerequisite for b-elimination. X, 2′ or 3′ modification; *p, ^{32}P-radiolabeled phosphate group.

Figure III-S1

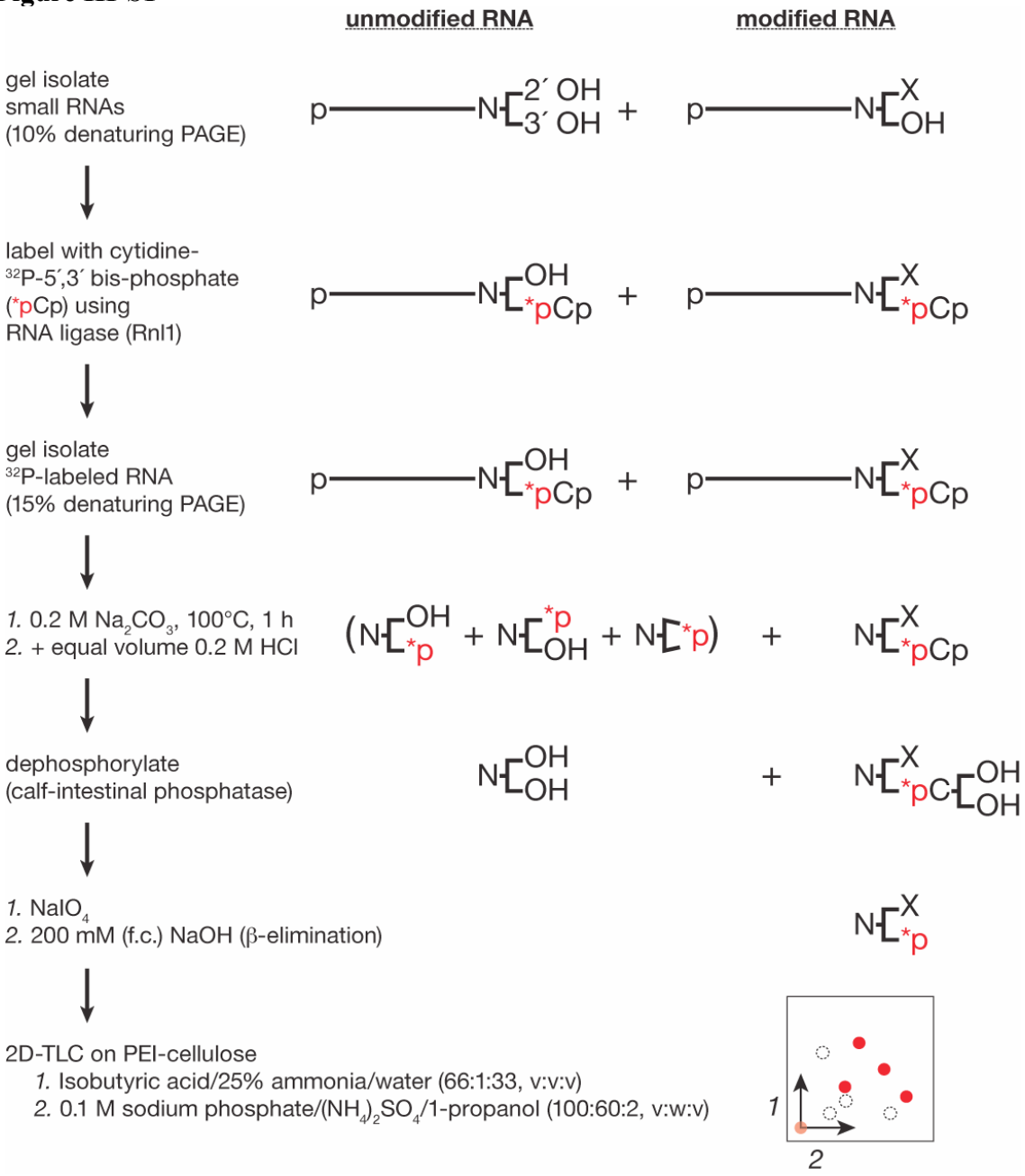

Figure III-S2. Comparison of 2D TLC systems

For both, the first dimension was Isobutyric acid/25% ammonia/water (66:1:33, v:v:v). Neutral second dimension (0.1 M sodium phosphate/(NH4)2SO4/1-propanol [100:60:2, v:w:v]) this paper; acidic second dimension (2-propanol/HCl/H2O [70:15:15, v:v:v]), Kirino Y., and Mourelatos Z. (2007). Mouse Piwi-interacting RNAs are 2′-*O*-methylated at their 3′ termini, *Nat Struct Mol Biol.* 14, 347-348. 2′ and 3′ NMPs were prepared by base hydrolysis, and 3′ NMP spots identified by their comigration with 3′ NMPs generated by complete digestion of RNA with micrococcal nuclease.

Figure III-S2

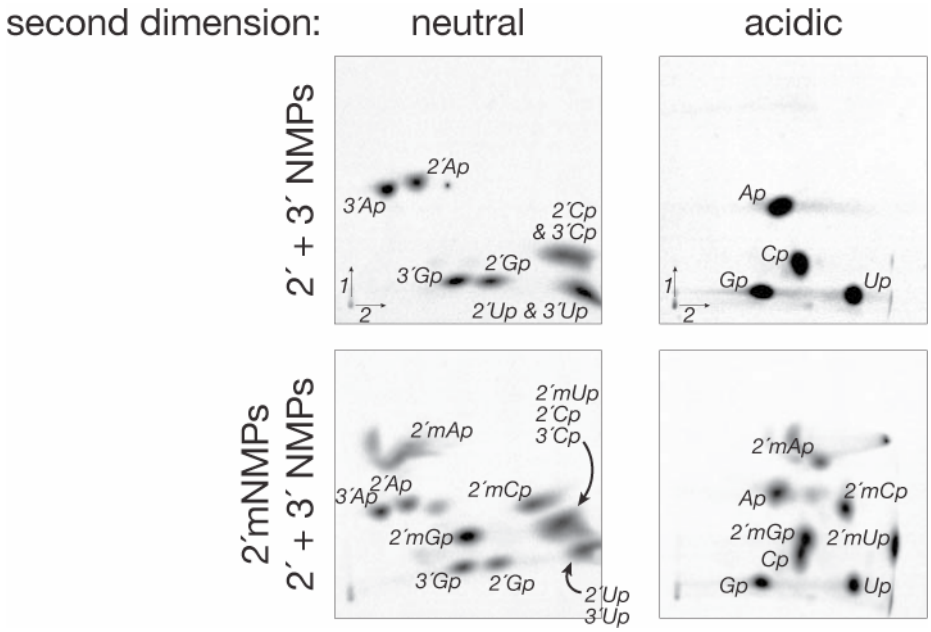

Figure III-S3. PBAC(WH)CG12367[f00810] disrupts *hen1* but not CG8878

(A) The gene CG8878 resides in the first intron of Drosophila *hen1* and is transcribed in the opposite orientation. The location of the qRT-PCR primers are shown as closed arrows. (B) We performed qRT-PCR to determine the effect on CG8878 expression of the PBAC(WH)CG12367[f00810] transposon insertion, which disrupts *hen1* (Figure 2A). In both testes and ovaries, we can detect no statistically meaningful effect of this piggyBac transposon insertion on the expression of CG8878. We conclude that the PBAC(WH)CG12367[f00810] insertion disrupts only *hen1*. We therefore rename this insertion $hen1^{f00810}$. Bars show average ± standard deviation for four or five independent trials.

Figure III-S3

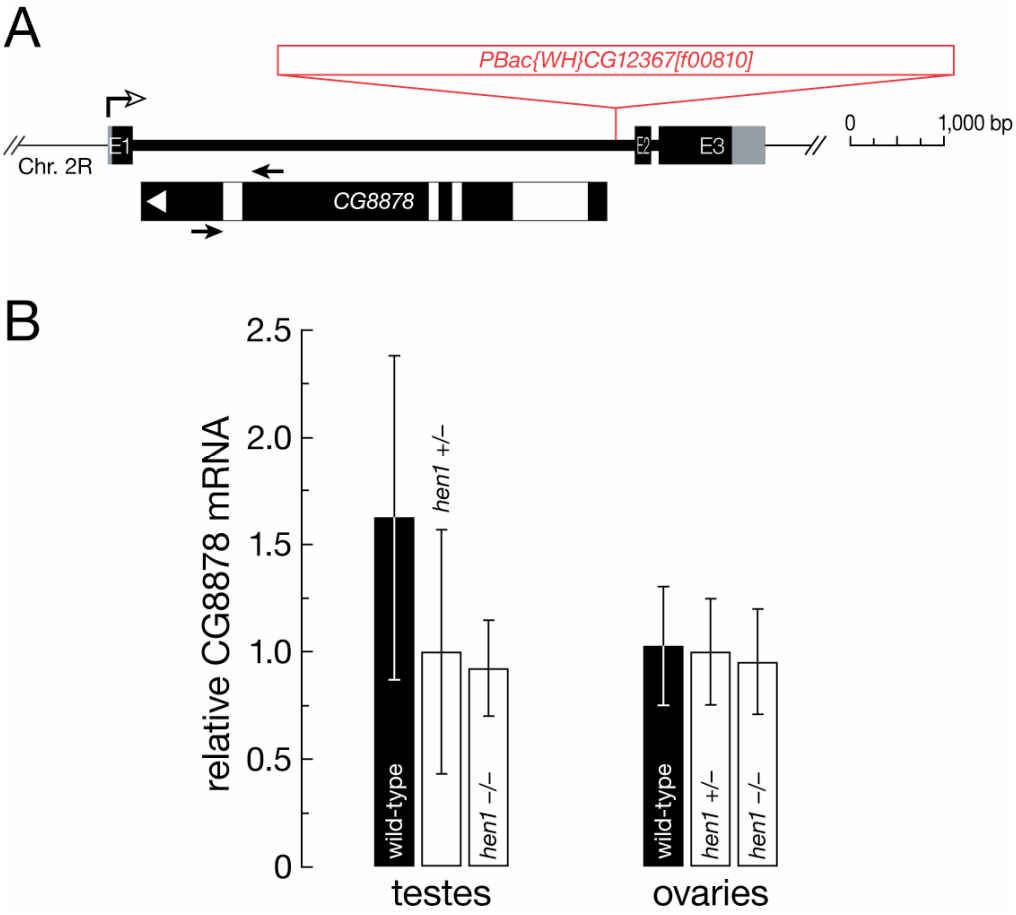

Figure III-S4. *S*-adenosyl homocysteine (SAH), an inhibitor of *S*-adenosyl methionine (SAM) dependent methyltransferases, inhibits modification of single-stranded siRNA in lysate prepared from either 0–2 h embryos or cultured S2 cells

RNA was purified from the reactions at the indicated times and then tested for modification by reaction with $NaIO_4$ followed by b-elimination. The RNA was resolved by denaturing electrophoresis.

Figure III-S4

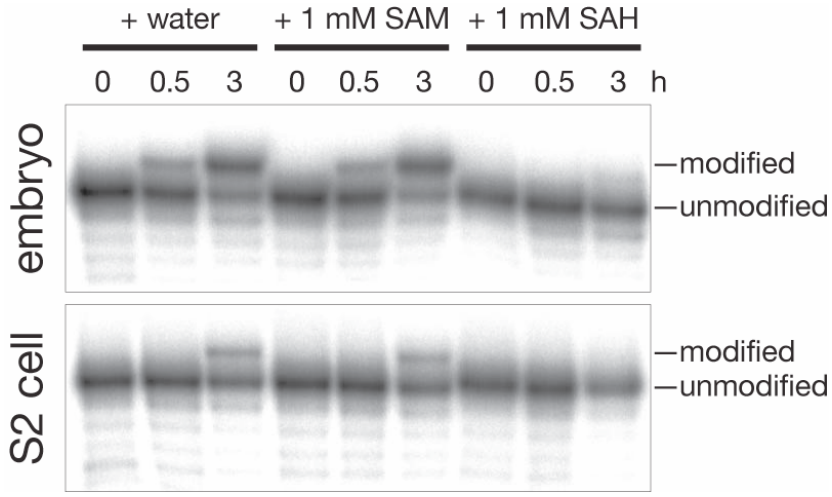

Figure III-S5. GST-DmHen1

(A) Schematic of the 74,254 Da fusion protein, comprising the 220 amino acid glutathione S-transferase (GST) module, a 30 amino acid linker, and the entire 391 amino acid DmHen1 protein, terminated at its native stop codon. (B) Purified, recombinant GST-DmHen1 protein (3 μg) was resolved by electrophoresis through a 4–20% polyacrylamide gradient SDS-gel, then stained with colloidal Coomassie G-250. The apparent masses of molecular weight markers (M) are indicated.

Figure III-S5

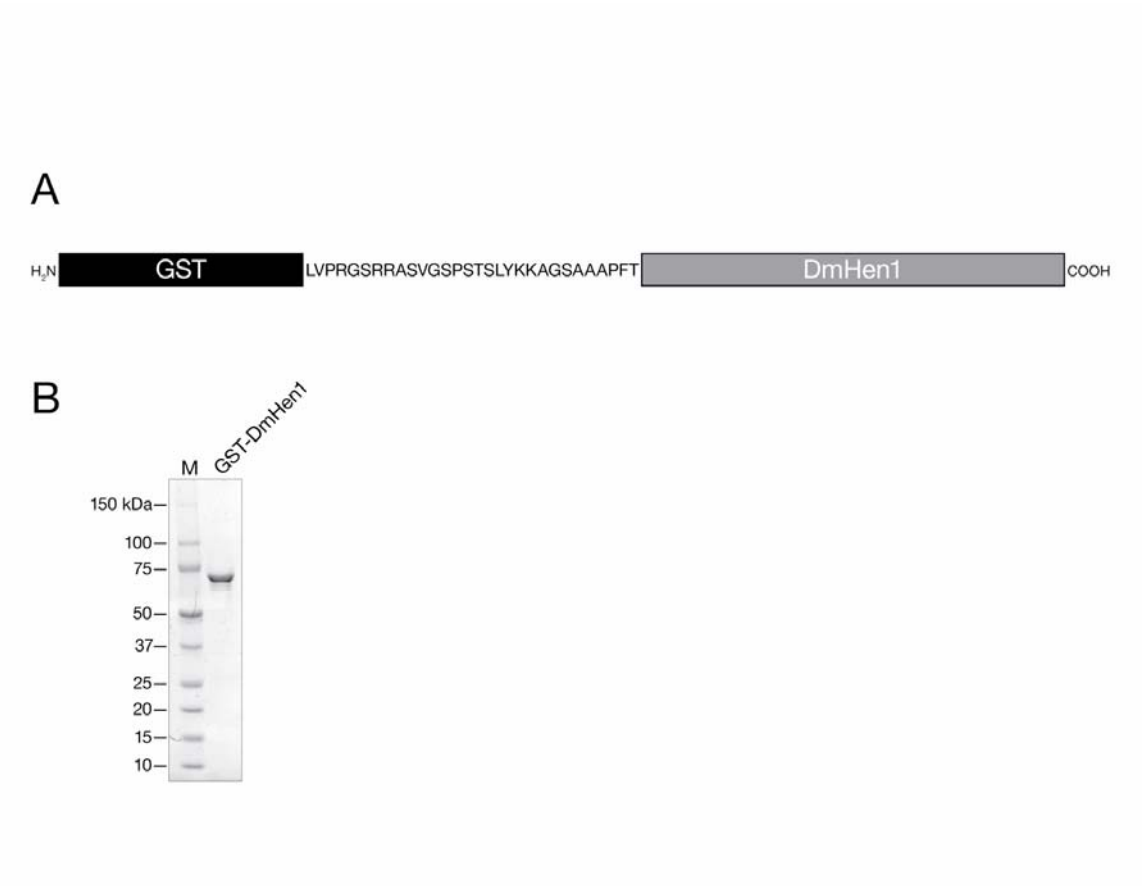

Figure III-S6. Purified, recombinant GST-DmHen1 protein rescues S2 cells depleted by RNAi of Hen1, but not Ago2

S2 cells were transfected as described with dsRNA targeting *ago2*, *hen1*, or a control sequence, then lysate prepared. siRNA was incubated in the S2 cell lysate to allow RISC assembly, then siRNA guide strand modification was assayed by reaction with $NaIO_4$ followed by b-elimination (b). Without the addition of GST-DmHen1 protein, *hen1(RNAi)* and *ago2(RNAi)* lysates are deficient in Hen1 activity, relative to the control dsRNA treated cells (Figure 3B). M, 5′-phosphorylated synthetic RNA size markers.

Figure III-S6

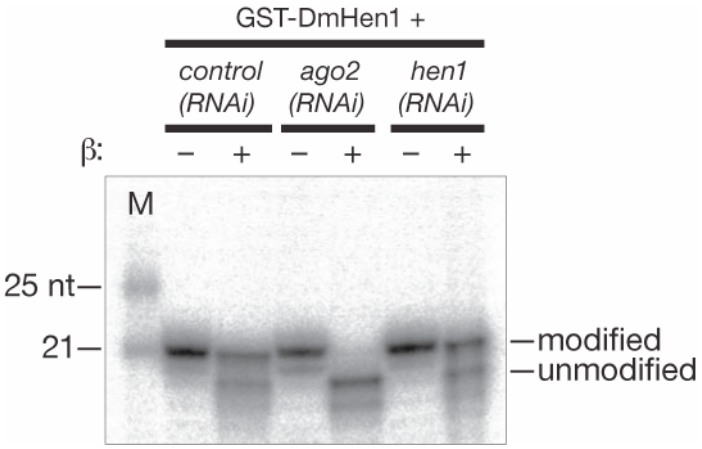

Figure III-S7. Strategy for testing when during RISC assembly siRNAs are modified at their 3´ termini

Double-stranded siRNA was incubated in embryo lysate to assemble RISC, then the siRNA purified away from protein using a procedure that preserves the single- or double-stranded structure of the siRNA at the time assembly was stopped. The siRNAs were then resolved on a native gel, and the single- and double-stranded siRNA was isolated from the gel, reacted with $NaIO_4$ followed by b-elimination and analyzed by denaturing gel electrophoresis (shown in Figure 4B).

Figure III-S7

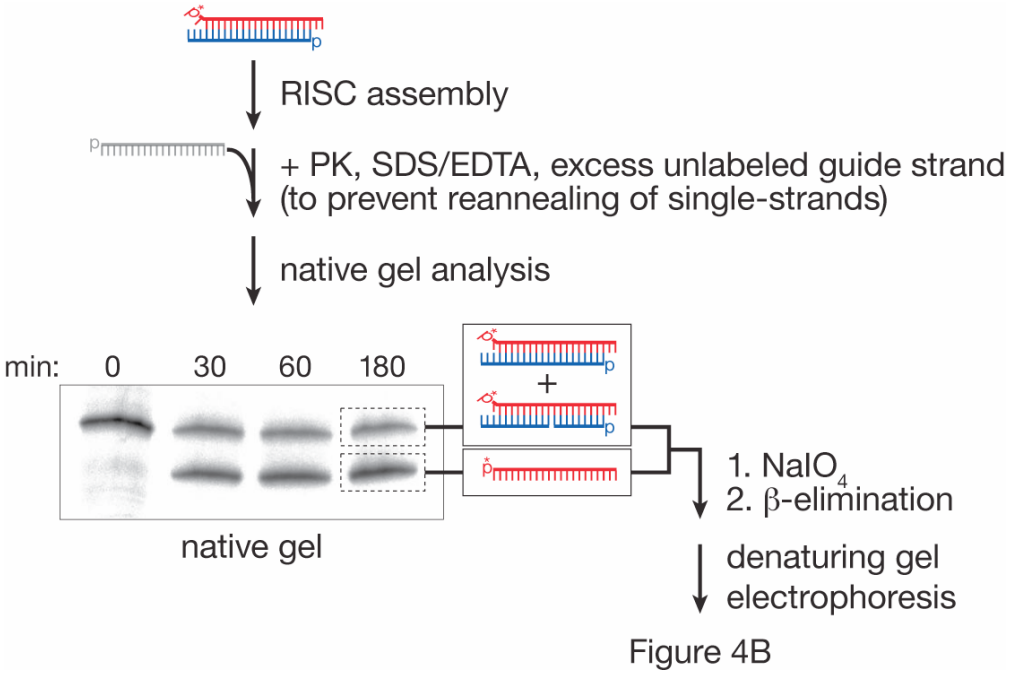

Figure 4B

Table S1. Synthetic oligonucleotides used in this study

RNA oligonucleotides

siRNAs derived from firefly luciferase

```
  5´-UGUACGCGGAAUACUUCGAAA-3´ (guide)
     °••••••••••••••••••
3´-GUGCAUGCGCCUUAUGAAGCU-5´(pasenger)
```

```
  5´-CGUACGCGGAAUACUUCGAAA-3´ (pasenger)
     ••••••••••••••••••
3´-GUGCAUGCGCCUUAUGAAGCU-3´(guide)
```

siRNA corresponding to the sequence of *let-7* microRNA

```
  5´-UGAGGUAGUAGGUUGUAUAGU-3´ (guide)
     -••••••••••••••••••
3´-UUCCUCCAUCAUCCAACAUAU-5´ (passenger)
```

RNA oligonucleotides used to generate mononucleotide standards for 2D-TLC

5´-CCUUAUCAUUCUCUCGCCCCG-3´

5´-CCUUAUCAUUCUCUCGCCCCC-3´

5´-CCUUAUCAUUCUCUCGCCCCU-3´

5´-CCUUAUCAUUCUCUCGCCCCA-3´

5´-UUACAUAAGAUAUGAACGGAGCCC-A-2´-*O*-Me,3´-OH

5´-UUACAUAAGAUAUGAACGGAGCCC-C-2´-*O*-Me,3´-OH

5´-UUACAUAAGAUAUGAACGGAGCCC-U-2´-*O*-Me,3´-OH

5´-UUACAUAAGAUAUGAACGGAGCCC-G-2´-*O*-Me,3´-OH´

5´-GCGUGGGCA-G-2´-OH,3´-*O*-Me

5´-UAUACAACCUACUACCUCCU-A-,2´-OH,3´-*O*-Me

Table III-S1 Cont'd.

RNA oligonucleotides used as markers

5′-GCGUGGGCAG-3′

5′-UGU ACG CGG AAU ACU UCG AAA-3′

5′-UUA UUU UAU AUG CAG GUA UAU GCA AG-3′

5′-AAGGUUGAGGUAGUAGGUUGUAUAGUUAAGA-3′

5′-UUACAUAAGAUAUGAACGGAGCCCA-3′

DNA oligonucleotides (F, forward; R, reverse)

DmHen1 PCR Primers used to create T7 RNA polymerase transcription templates to generate two different dsRNAs for *hen1(RNAi)*

#1 F GCGTAATACGACTCACTATAGGGTTCGGAAGAATTGAGGGACAC

#1 R GCGTAATACGACTCACTATAGGGGGTGCGCGTATCCACATAAA

#2 F GCGTAATACGACTCACTATAGGGAAATAGAGCTTCAGCGTTTCA

#2 R GCGTAATACGACTCACTATAGGGCGATCTTCGGTTTGTCTGG

DmHen1 Primers for Cloning

F CACCATGTTTTCGCACAAGTTTATTTGC

R TTATGATTCGGGGCCTTGATC

Table III-S1 Cont'd.

DmHen1 Primers for qPCR

F GCGTCGCATTGAGACCATAG

R GCGATTACAGCGTCAGTGTCC

CG8878 qPCR Primers

F TTG TCC AGG AGC ATA TTG AGG

R TGC CCT CCA TTG ATC TAT CC

RP49 qPCR Primers

F CCGCTTCAAGGGACAGTATCTG

R ATCTCGCCGCAGTAAACGC

Northern hybridization probes

#4 Su(Ste) antisense rasiRNA	5′-TCGGGCTTGTTCTACGACGATGAGA-3′
#1 roo antisense rasiRNA	5′-TGGGCTCCGTTCATATCTTATG-3′
#3 roo antisense rasiRNA	5′-TGAGAGTTCGCTATTCGAAGAA-3′
#7 roo antisense rasiRNA	5′-TCTGAGGCATCCGTTTGGTAAA-3′
miR-8	5′-GACATCTTTACCTGACAGTATTA-3′
bantam	5′-CAGCTTTCAAAATGATCTCACT-3′
2S rRNA	5′-TACAACCCTCAACCATATGTAGTCCAAGCA-3′
miR-277	5′-TCGTACCAGATAGTGCATTTA-3′
siGFP	5′-GGCCGCGACTCTAGATCATAAT-3′

Chapter IV:

Summary and General Discussion

Our studies give new mechanistic insight into *Drosophila* small RNA silencing. Our data suggest that, (1) small RNA duplexes are sorted into different RISCs in vivo. (2) Duplex structure, not Dicer identity or precursor structure, appears to determine how small RNAs partition between the Ago1 and Ago2 RISC; perfectly paired siRNAs assemble into Ago2, well paired miR-277/miR-277* duplexs partition between Ago1 and Ago2, bulged bantam/bantam* duplexes assemble into Ago1. (3) Sorting impacts target identity because Argonaute proteins have distinct target specificity and silencing capacity. Although both Ago1 and Ago2 can cleave targets in vitro, Ago1 cannot silence a perfect target efficiently in vivo, likely because it lacks the robust multiple turnover activity of Ago2. (4) DmHen1 is a single standed RNA 3′ terminal methyltransferase that modifies small RNAs bound to Ago2 or Piwi proteins, but not Ago1. (5) piRNAs in *hen1* mutants are smaller. (6) Hen1 is required for normal silencing of at least one retrotransposon, Het-A, in the female germline. Figure 1 depicts an updated model that incorporates our findings.

Small RNA Sorting

Our studies suggest that processing of dsRNA or pre-miRNA is uncoupled from RISC loading. This is in contrast to previous studies that suggest fly small RNA biogenesis and RISC loading consists of two parallel pathways, Dicer1/Loqs/Ago1 for

Figure IV-1: Model for Drosophila Small RNA Silencing Pathways

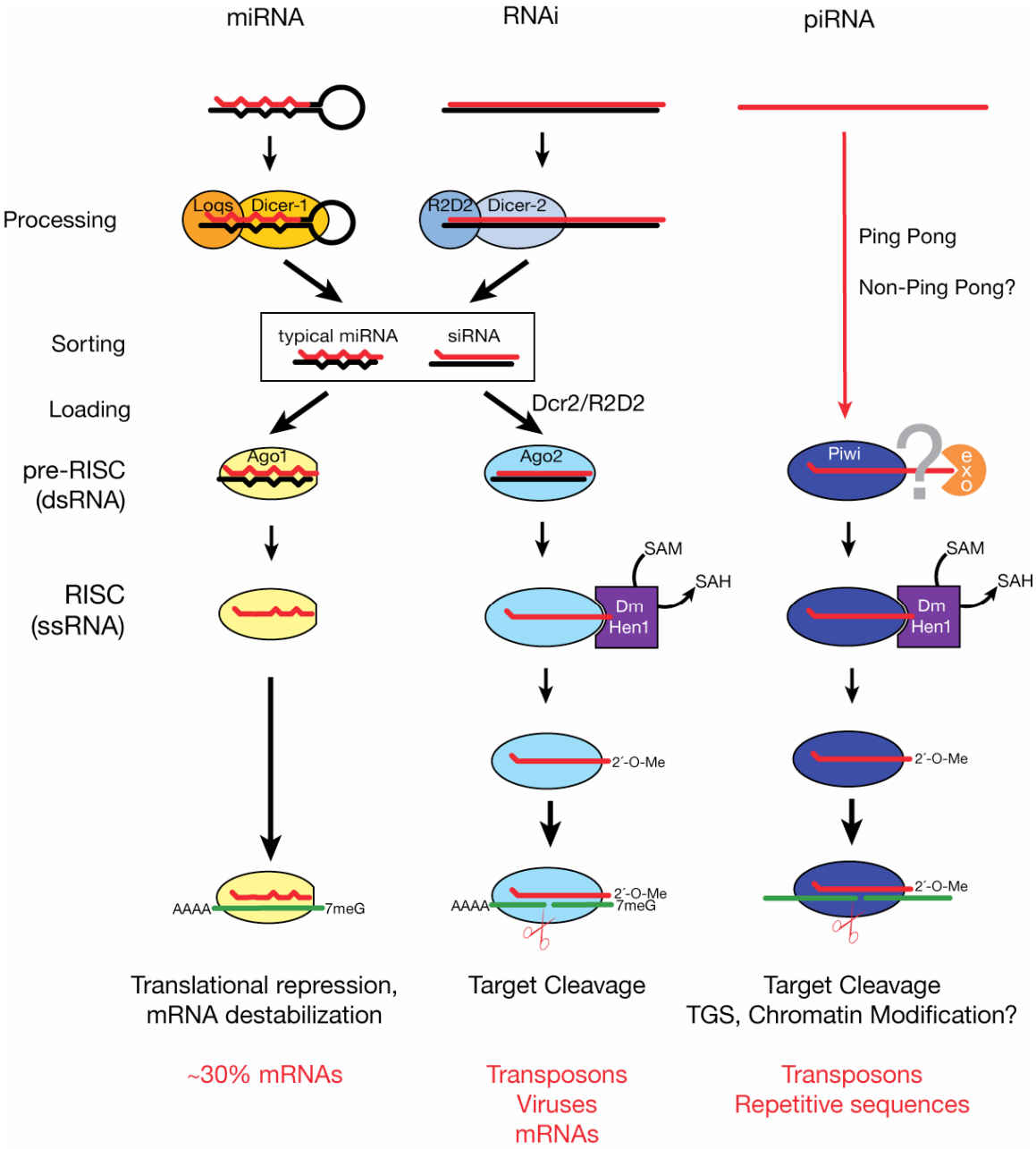

miRNAs and Dicer2/R2D2/Ago2 for dsRNA or siRNAs (Okamura et al., 2004; Miyoshi et al., 2005; Saito et al., 2005). Several observations predicted that siRNA and miRNA duplexes are released from Dicer after processing, and re-bind during RISC assembly. (1) Although Dicer binds the Drosha generated 3′ ends of pre-miRNAs using its Paz domain, positioning the loop near its RNAseIII domain (MacRae et al., 2007), miRNAs can be derived from either arm of the hairpin pre-miRNA and they generally follow the asymmetry rules (Schwarz et al., 2003). In the flies siRNA asymmetry is sensed by the RISC loading complex (RLC), where the more stable end binds R2D2. This orients the duplex and allows the correct guide to assemble into RISC (Tomari et al., 2004). It is unlikely that thermodynamic asymmetry can be sensed by R2D2 while the duplex is restricted in its orientation, bound to the Dicer Paz domain—release and re-binding of a miRNA duplex in the correct orientation is a more likely scenario. (2) Supporting this idea Preall and colleagues found that in fly extracts and eggs, siRNAs mediate RNAi better than short Dicer substrate equivalents. Furthermore, asymmetry rules are maintained, even when the end that gets diced is switched (Preall et al., 2006). While these studies suggested that siRNAs or miRNAs are released to rebind the same Dicer, it was undexpected that released small RNA duplexes could actually assemble into distinct loading complexes. Because pre-miR-277 is processed by the Dicer1/Loqs heterodimer (Förstemann et al., 2005), but enters the RNAi pathway via the RLC, even in non-dicing Dicer2 mutants, it must be released Dicer1/Loquacious as miR/miR* duplex, and sorted into the Ago2 loading pathway.

Is small RNA sorting a fly-specific phenomenon? Recent data suggest it is not. Steiner and colleagues came to remarkably similar conclusions in their studies of a

hairpin *let-7* precursors in worms. They found that the extent of pairing in a *let-7* hairpin trigger determined whether *let-7* entered either the RNAi or miRNA pathway. *Let-7* from perfectly paired hairpins assembled into Rde-1, while centrally bulged hairpins assembled into Alg-1. Their data also suggest that Dicing and RISC loading are uncoupled—in the absence of Rde-4 or Rde-1, perfectly paired *let-7* duplex is made, but its accumulation as *let-7*/*let-7** suggests that it cannot be loaded (Steiner et al., 2007). Sorting also occurs in plants, but it appears to be mainly defined by the identity of the terminal nucleotide, not duplex structure (Mi et al., 2008; Montgomery et al., 2008). With 10 specialized Argonautes, but only 4 terminal nucleotides it is anticipated that more sorting principles are at play in plants, such as cellular compartmentalization of biogenesis.

Do small RNA duplexes get sorted in vertebrates? Initial studies suggest they do not. Two groups reported that all four affinity tagged human Argonaute proteins associate indiscriminately with miRNAs and siRNAs when overexpressed in tissue culture cells (Liu et al., 2004; Meister et al., 2004b). Given that sorting phenomena have now been observed in plants, worms, and flies, this is surprising and should be revisited. It remains possible that sorting phenomenae went undetected due to an artifact of over expression; because Argonautes compete for small RNAs (Tomari et al., 2007) excess of one Argonaute may artificially favor its loading. It also remains possible that miRNAs or siRNAs bound to some Argonaute complexes do not correspond to mature single-stranded RISC, but rather consist of pre-RISC, complexes that contain small RNA duplexes. Ago1 pre-RISC was observed by Tomari and coworkers' who found that although fly Ago1 associates with siRNAs in vitro, it mostly corresponds to siRNA

duplex, not mature single-stranded RISC (Tomari et al., 2007). Similarly, an allele of fly Ago2 with a mutation in its catalytic residues fails to produce mature RISC efficiently, with accumulation of pre-RISC (Kim et al., 2006). These findings support the idea that efficient loading of human and fly Ago2 involves passenger strand cleavage (Matranga et al., 2005; Rand et al., 2005; Miyoshi et al., 2005). It would be interesting to test if siRNAs associated with human Ago1, 3, and 4, the non-cleaving Argonautes, are associated with siRNA duplexes rather than mature single-stranded guides. Perhaps well paired miRNA duplexes also associate with non-cleaving Argonautes to form pre-RISC, but not mature RISC. A recent study that identified putative miRNA targets by immunoprecipitating endogenous human Ago1 and Ago2 also suggests that miRNAs may be sorted preferentially into human Ago1 or Ago2; co-immunoprecipitating mRNAs had minimal overlap, despite similar total numbers of predicted miRNA targets (Beitzinger et al., 2007).

How mammals load their Argonaute proteins and how flies load Ago1 is currently unknown. Although a functional human RISC loading complex has been reconstituted containing Dicer, TRBP, and Ago2 (MacRae et al., 2008), it is unclear whether its mechanics mirror those of fly Dicer2/R2D2/Ago2, with respect to asymmetry sensing and the essential loading function of fly Dicer2. Although two reports that use RNAi to deplete Dicer suggest Dicer is required for siRNA mediated RNAi (Doi et al., 2003; Chendrimada et al., 2005), two studies using Dicer knockout ES cells suggest that siRNA mediated RNAi is Dicer independent (Murchison et al., 2005; Kanellopoulou et al., 2005). Further studies using reconstituted RISC should help determine how analogous mammalian RISC loading its Drosophila counterpart. Because *Drosophila* Ago1 is more

closely related to mammalian Ago proteins (Tolia and Joshua-Tor, 2007), studying mammalian RISC loading may give insight into how it is loaded.

Target Specificity of Slicing Argonautes and its Implications

The remarkable result of small RNA sorting is that information contained in a small RNA duplex's structure can be converted into distinct silencing outputs—highly bulged duplexes can silence bulged targets via Ago1 while highly paired duplexes can silence near perfect targets via Ago2. The inability of Ago1 to efficiently silence a perfect target was unanticipated, since in vitro target cleavage was observed previously (Okamura et al., 2004; Miyoshi et al., 2005). This suggests that the ability of an Argonaute protein to cleave targets does not mean it can do so efficiently—robust multiple turnover activity is needed. An interesting area of enquiry will be distinguishing what endows Ago2 with this ability, distinguishing it from Ago1. Conversely, it is unclear what prevents Ago2 from silencing bulged targets. Potential differences include: (1) Ago2's unique N-terminal domain that is rich in poly-glutamine repeats. Mutations in this domain were previously reported to interact genetically with Ago1, perhaps allowing Ago2 to interfere with Ago1 function (Meyer et al., 2006). (2) Only Ago1 contains a conserved phenylalanine motif in its Mid domain proposed to bind mRNA cap structures to repress translation (Kiriakidou et al., 2007). However recent studies by the Izaurralde group suggest that mutation of these residues prevents binding of GW182, a component essential for miRNA mediated translational repression and mRNA decay (Eulalio et al., 2008). Lacking these residues, Ago2 may not interact with GW182. This is supported by data showing a high correlation between Ago1 and GW182 regulated mRNAs, but not Ago2 regulated mRNAs in S2 cells (Behm-Ansmant et al., 2006). Given that GW182

association and consequent P-body formation appears to be conserved for miRNA associated Argonautes in flies, worms, and humans, the importance of this interaction for bulged target silencing seems plausible (Behm-Ansmant et al., 2006; Ding et al., 2005; Liu et al., 2005). (3) Another difference (discussed below) is that Ago2 bound small RNA guides have 2-*O*-Me modified 3′ ends. Although this modification does not appear to be required for perfect target silencing in vivo (MDH and C. Li unpublished), it may affect target specificity. Domain swapping experiments might shed light on the essential features of each protein required for perfect or bulged target silencing, as well as guide modification.

Because we could not immunoprecipitate Ago2, it was satisfying to see our results confirmed in the Hannon group's recent study cloning small RNAs from tagged Ago2 in S2 cells (Czech et al., 2008). In this study miR-277 was present in both Ago1 and Ago2 immunoprecipitates at about equal amounts relative to each total library sizes. This agrees with our data, showing that ~50% of miR-277 has a 3′ terminal modification (because it is loaded in Ago2). By contrast the Siomi group did not clone miR-277 in their S2 cell Ago2 immunoprecipitations using a monoclonal antibody (Kawamura et al., 2008). These two studies differed substantially in the number of miRNAs that were cloned in Ago2—while miRNAs accounted for 7.7% of Ago2 associated small RNAs from S2 cells (and 20% from fly ovaries) for Czech et al., Kawamura found only 1.4% of reads. We are not certain what accounts for this difference. One possibility is that the Ago2 loading pathway is activated and more accessible to miRNAs under certain cellular conditions, such as viral infection, high transposon activity, or active transgene silencing. Upon cloning small RNAs Czech et al. noticed that their S2 cells were concurrently

fighting a case of Flock house virus. Our experiments were done in cells stably expressing a GFP transgene. Notably, we cloned many small RNAs derived from the *white* gene, a marker on the integrated plasmid. We also noted that our cells expressed high levels of the Mdg1 retrotransposon mRNA, which was actually became more abundant than a ribosomal protein mRNA after Dicer2 depletion. Perhaps dsRNA abundance in these cells is high and RISC loading is enhanced as a response. Increasing the concentration of the RLC improves Ago2 loading (Tomari et al., 2007). To test this RLC concentration could be compared in these three cell lines by western blotting for Dicr2 and R2D2. miRNAs associated with Ago2 could also be examined in the presence and absence of a virus in Kawamura et al.'s S2 cell line to see if this alters the repertoire of Ago2 associated miRNAs.

Regardless of the exact nature of miR-277 partitioning in our S2 cells, it allowed us to show that Argonaute identity affects target specificity. An important implication of this is that siRNA directed knockdowns using the *Drosophila* Ago2 pathway should produce minimal off target effects. Because off-target effects are a major problem for experimentalists and for therapeutic applications (Jackson et al., 2003; Jackson et al., 2006), understanding the strategies animals already use to limit them may suggest better approaches for RNAi. We are currently testing the hypothesis that Ago2 bound small RNAs have reduced off target effects using mRNA expression arrays and transfected Ago1 or Ago2 directed duplexes in S2 cells.

What is the purpose of small RNA sorting? The likely answer is that Argonaute activities have evolved to best silence their respective targets. Ago1 associated miRNAs (97.6% of its associated small RNAs in S2 cells (Czech et al., 2008)) regulate

endogenous mRNAs and while Ago2 bound small RNAs defend against endogenous and exogenous parasitic nucleic acids. Because animal miRNAs have evolved to primarily use seed sequences as a minimal targeting determinant (Grimson et al., 2007; Lewis et al., 2005; Lewis et al., 2003), Ago1 loaded small RNAs should be capable of engaging and repressing mRNAs appropriately. Ago2 however appears to play an important role in defense against exogenous viral infection, as well as endogenous transposon and repetitive element silencing. Several recent studies, including one by our group (Appendix III), catalogue the small RNAs associated with Ago2. While those studies mentioned above cloned small RNAs from Ago2 immunoprecipitates (Czech et al., 2008; Kawamura et al., 2008), we selectively cloned small RNAs with 3′ terminal modifications from dsRNA treated S2 cells and fly heads expressing an inverted repeat RNAi trigger(Ghildiyal et al., 2008). Collectively, these studies show that Ago2's natural partner small RNAs consist of a diverse array of transposon and repeat derived siRNAs. Analysis of *ago2* and *dcr2* mutant flies and S2 cell knockdowns suggest that Ago2 and Dicer2 direct somatic and germline transposon silencing. Because Czech et al.'s cells fortuitously had flockhouse virus, they also showed that Ago2 and Dicer2 limit flockhouse virus expression, consistent with previous reports demonstrating anti-viral roles for Ago2 and Dicer2 (Zambon et al., 2006; van Rij et al., 2006). With such a diverse array of sequences bound to Ago2, staying "on-target" might be important to avoid unintended silencing of critical mRNA upon viral infection or transposon activation. miRNAs that are sorted into Ago2 may also have roles in anti-viral or transposon responses. In human cells, endogenous miRNAs have been shown to prevent infection by Primate foamy virus and limit replication of Hepatitis C virus (Lecellier et al., 2005;

Pedersen et al., 2007). Perhaps Ago2 associated miRNAs can play a similar role. Because few fly viruses have been characterized, testing the generality of this mechanism may be difficult.

Alternatively, loading miRNAs into Ago2 may be a posttranscriptional negative regulation mechanism for miRNAs. miR-277 has no annotated perfect or near perfect targets in the *Drosophila* genome, thus it should be relatively inert when loaded into Ago2. Because miR-277 appears to be ubiquitously expressed in adults, shunting it into Ago2 might prevent productive seed:target interactions that would take place if it were in Ago1. Thus Ago2 loading could act as an off-switch, or at least a rheostat, in the absence of transcriptional downregulation. Notably, miRNA specific regulation of biogenesis has been observed in mammals at the level of pri-miRNA processing (Thomson et al., 2006; Viswanathan et al., 2008). Perhaps miRNA sorting offers another level of posttranscriptional regulation of miRNAs via production of inert or less functional RISCs. Perhaps such RISCs could even bind and stabilize targets under some circumstances, blocking target sites from more potent RISCs. Our finding that bulged target silencing is modestly enhanced in *r2d2* flies is consistent with this idea.

2'-O-Methylation and Transposon Silencing

In data not shown, Ebashir and colleagues reported that incubation of dsRNA in *Drosophila* embryo lysate produced periodate sensitive siRNAs with 2′, 3′ hydroxyl ends, consistent with their production by an RNAseIII enzyme (Elbashir et al., 2001b). However, six years later, Pellison and colleagues unexpectedly found that like piRNAs, siRNAs in flies also have modified 3′ ends (Pelisson et al., 2007). We had already begun building reagents to test if the piRNA modification was a 2′-*O*-Methyl modification, like

in plants, and if the plant methyltransferase orthologue, DmHen1, is the small RNA methylase in flies (Yu et al., 2005). Our studies quickly suggested that DmHen1 modifies both classes of small RNAs in flies.

Our studies suggest several differences in the nature of small RNA modification in animals versus plants. In plants Hen1 has a dsRNA binding domain that is absent in animals. In vivo and in vitro plant Hen1 can modify both strands of 21-24 nt duplexes, whether they are perfectly paired siRNA or imperfectly paired miR/miR* duplexes (Yang et al., 2006; Yu et al., 2005). In animals this does not appear to be the case—rather single-stranded siRNAs appear to be modified while bound to Ago2. This was suggested by our experiments that showed, (1) in vitro siRNA modification in ovary extracts requires RLC and Ago2, (2) in vivo modification of siRNAs and miRNAs in S2 cells requires Hen1 and Ago2, but not Ago1, (3) only single-stranded siRNAs are detected during RISC assembly, and (4) recombinant Hen1 can modify single-stranded siRNAs, but not siRNA duplexes in vitro. Because single-stranded siRNAs are only stable when bound to Argonaute proteins a direct interaction between Ago2 and DmHen1 is suggested. This also leads to the prediction that DmHen1 might directly interacts with Piwi proteins to modify piRNAs derived from single-stranded precursors. Indeed, a parallel study by Saito and colleagues confirmed a direct interaction of DmHen1 with the piwi protein Aubergine using in vitro translated Aubergine and GST-Hen1 (Saito et al., 2007). We plan to confirm the Ago2:DmHen1 interaction by coimmunoprecipitation once we have unambiguously confirmed the specificity of our polyclonal anti-DmHen1 antibodies.

In contrast to the plieotropic effects of *hen1* in plants, flies carrying the intronic PiggyBac insertion allele *hen1*^{f00810}, a transcript null, are fertile with no visible defects, despite loss of all detectable piRNA and siRNA modification activity. In contrast to Saito and colleagues who found no changes in germline transposon expression, we found that ovaries from *hen1*^{f00810} flies had modest ~3 fold elevation of Het-A mRNA versus heterozygotes (*spindle-E*, *armitage*, *piwi*, and *aubergine* by contrast cause 25-200 fold increases in Het-A mRNA (Vagin et al., 2006)). Consistent with this modest effect, we saw a reduction in both average size and abundance of Roo and Suppressor of Stellate piRNAs in ovaries and testes respectively, by northern blot. Saito and colleagues reported no change in piRNA size or abundance, but unlike our northern blot, which detects piRNAs in vivo, they examined 5′ end labeled piRNAs that co-immunoprecipitated with piwi proteins. Their approach might not capture all piRNAs, especially those in nucleic, such as those bound to Piwi. It is also possible that shorter piRNAs are degraded during lysis or immunoprecipitation, preventing their detection. A modest reduction of small RNA size and abundance in *hen1*^{f00810} mutants was also reported in a recent study of Ago2 bound endogenous siRNAs (endo-siRNAs) derived from long hairpin transcripts (Okamura et al., 2008); northern blots showed a 2-6 fold reduction of Ago2 bound small RNAs. Supporting our previous findings, they observed that Ago2 associated endo-siRNAs regulate perfect targets, but not bulged targets. However, the functional impact Hen1 loss was not assessed.

All 2-*O*-methylated small RNA species reported to date (plant small RNAs, Ago2 associated siRNAs and miRNAs, and piRNAs) appear to use a target cleavage mechanism to silence perfect targets. This striking correlation suggests that terminal

methylation may play a conserved role in target cleavage. Moreover, the recent discoveries that *Drosophila* Ago2 binds endo-siRNAs corresponding to transposons suggests that 2′-*O*-Methylation endows small RNA guides, both siRNAs and piRNAs with properties uniquely suited for transposon silencing (Czech et al., 2008; Ghildiyal et al., 2008; Kawamura et al., 2008). It is tempting to speculate that the primary difference in the ability of Ago1 and Ago2 to cleave perfect targets derives from the different 3′ end chemistry of their guides. Studies of the human Paz domain, suggest that 2′-*O*-Me ends have roughly 15 fold lower affinity (Ma et al., 2004). Perhaps 3′ end release by the Paz domain is part of Argonautes' catalytic cycle, and lack of modification limits target release, as we observed for Ago1.

However, our preliminary data suggest that loss of Hen1 function has little affect on RNAi in our fly assays—target cleavage occurs in *hen1*^{f00810} ovary lysates, inverted repeat silencing in fly eyes does not appear to be affected in *hen1*^{f00810} (C. Li unpublished), and knocking down Hen1 in S2 cells has little if any affect on perfect reporter expression or RNAi (MDH unpublished). In vitro studies from plants also suggest that terminal methylation does not affect target cleavage in vitro (Qi et al., 2005). We are currently conducting experiments to determine if unmodified siRNAs in *hen1*^{f00810} are multiple turnover enzymes. We are also performing experiments to confirm that *hen1*^{f00810} is truely a null allele. Some of our data hints that it may not be; supporting this possibility, quantitative RT-PCR using primers contained in either the first or last exon, rather than primers that span the Piggybac insertion, imply that the transcript is in fact made and polyadenylated (MDH unpublished). Additionally, an affinity purified N-terminal polyclonal antibody reacts on western blot with recombinant Hen1 protein, an

epitope tagged Hen1 transgene expressed in flies or S2 cells, and a ~45 kD band in ovaries (the correct size for Hen1), but this band is not consistently reduced in *hen1*^{f00810} ovaries. We currently cannot rule out the possibility that this is a cross-reacting band of the same size, but it could also be a non-catalytic Hen1 protein that is similar in size, and retains some key aspect of Hen1 function—for instance, Ago2 or Piwi binding. We are testing if a weaker allele containing a P-element insertion in its 5′UTR (*hen1*^{ey22392}) gives reduced signal on western when transheterozygous with a chromosomal deletion. *hen1*^{ey22392} is also being used to generate a P-element excision allele. The fact that siRNA modification in *hen1*^{f00810} ovary lysate is fully rescued with recombinant protein however, suggests it is a null allele.

So what is the function of Hen1 and terminal methylation? Assuming our allele is in fact a null, the results from plants and flies suggest its role is to protect the 3′ end of small RNA guides from exo-nucleases or poly-uridylation machinery. In plants northern blots show poly-uridylation and degradation clearly—many small RNAs show reduced gel mobility and reduced abundance (Li et al., 2005). Cloning of small RNAs from plant *hen1* mutants revealed that small RNAs are both degraded from their 3′ ends by exonucleases and poly-uridylated. However, the extent of both varied depending on the particular RNA examined. Some miRNAs were uridylated, but not reduced in abundance. Interestingly, miR* strands were remarkably unaltered relative to their miR counterparts. Although there is no evidence suggesting that fly small RNAs get polyuridylated in *hen1*, our results and those of Okamura and colleagues (Okamura et al., 2008) suggest that modification by DmHen1 does protect 3′ ends from nucleases to some extent, both for

piRNAs and endo-siRNAs. Both species are reduced in mobility and abundance. However, these appear to be modest affects.

One possibility consistent with our data is that terminal modification does not enhance target cleavage directly, but perhaps it potentiates small RNA silencing by protecting guides in multiple turnover cleaving RISCs. Tomari and Zamore proposed a two-state model for target cleavage (Tomari and Zamore, 2005). In their model of target cleavage by RISC the 3′ end of the guide is bound to the Paz domain, but released during the target cleavage cycle to create an A form helix that can position the target in the Argonaute's catalytic site. Cleaved target is then released and the 3′ end re-binds the Paz domain. If this is correct, the 3′ end of a small RNA that silences its targets by multiple turnover catalysis would spend less time protected in the Paz binding pocket than that of animal miRNAs for instance, that are predicted to silence targets stoichiometrically using only seed sequences. This may make 2′, 3′ hydroxyl ends of cleaving Argonautes more vulnerable to nuclease activities that normally act to degrade cleaved targets, which also bear 2′,3′ hydroxyl ends. It is reasonable to suspect that RISCs are in close contact with other nucleases; for instance, Tudor-SN is a conserved nuclease found in fly Ago2 RISC that facilitates target degradation (Caudy et al., 2003). RISC may also be in close contact with the exosome, a collection of 3′ to 5′ exonucleases that were shown to mediate target degradation after cleavage (Orban and Izaurralde, 2005) or an unidentified conserved uridylation activity that acts on 3′ target ends after target cleavage (Shen and Goodman, 2004); indeed, non-templated 3′ U's have been detected on miRNAs in flies (Seitz et al., 2008). The prediction of such a model is that degradation in *hen1* mutants ought to be proportional to the number of rounds of target cleavage. This could be one explanation

for the heterogeneity of plant miRNA degradation in *hen1* mutants—maybe miRNAs whose abundance is most reduced are those that have the largest pool of targets to silence, relative to their levels of expression. Perhaps this also explains why plant miR* strands are not affected by *hen1* (because they do not have targets to cleave). This might also explain why we only see modest effects on piRNA silencing and minimal effects on RNAi—relative to target levels, small RNAs that are abundant would be less affected than those that are not. Perhaps our RNAi assays used to date (dsRNA treatment of S2 cells, inverted repeat silencing in eyes, mRNA cleavage in enzyme excess) produce excess small RNAs relative to the target. Consistent with this, mRNA levels from Het-A a retrotransposon maintained in multicopy arrays at fly telomeres (Danilevskaya et al., 1994), are most greatly affected in *hen1*^{f00810}, but we have been unable to detect Het-A piRNAs by northern blot. mRNA from Roo, the most abundant retrotransposon in flies, however is not affected in *hen1*^{f00810}, yet a modest decrease in its piRNAs is observed. Perhaps the ratio of piRNAs to target mRNA explains this difference. More extensive analysis of cloned small RNAs in *hen1*^{f00810} mutants, coupled with global analyses of mRNA expression using oligonucleotide arrays may give more insight into which piRNAs and targets are most affected. The hypothesis that target cleavage induces degradation of an unmodified small RNA guide is also easily testable in vitro; using ^{32}P-labeled siRNA in wt or *hen1*^{f00810} mutant ovary extracts we can determine if addition of excess perfect target or a bulged target causes degradation of the guide RNA.

Small RNA Methylation Complexes

To better understand how piRNAs and siRNAs are made and to confirm our model that predicts direct interactions of Hen1 with piwi proteins and Ago2, we are

conducting fractionation/proteomics experiments using a UASp epitope tagged DmHen1 rescue transgene expressed in germline cells (Nanos-Gal4 driver) or ubiquitously (Tubulin-Gal4 driver). It will be especially interesting to see if we can identify putative 3′ exonucleases in germline cells that might be involved in piRNA biogenesis.

Structure and Function of DmHen1

Our in vitro studies indicated two important features of DmHen1 catalysis. (1) DmHen1selectively modifies single-stranded RNA, and (2) the rate of catalysis is greatly enhanced in the presence of Drosophila lysate. We predict that this rate enhancement is due to DmHen1 binding of Ago2. We have begun studies to test this hypothesis and to understand small RNA modification structurally. We produced soluble pure DmHen1 by Tev mediated cleavage of a GST-DmHen1 fusion protein expressed in *E.coli*, but failed to obtain crystals in an initial screen. We are now collaborating with Tracy Hall's group on this project and intend on studying both DmHen1 alone and in complex with Ago2.

In sum these studies have shed light on several principles of small RNA silencing in *Drosophila*. They show the existence of a small RNA sorting step that gives small RNA duplexes from differing origins equal access to RISC loading pathways. Ultimately, duplex structure rather than origin determines function. Function is also correlated with guide chemistry—2′-*O*-methylation of guides in target cleaving RISC by DmHen1 affects transposon directed silencing by piRNAs and perhaps endo-siRNAs. This common modification also highlights the emerging functional connection between piRNA and endo-siRNA pathways, which offer distinct defenses in the ongoing struggle of eukaryotic genomes and their selfish repetitive elements.

Appendix I:Design and Delivery of Antisense Oligonucleotides to Block microRNAFunction in Cultured *Drosophila* and Human Cells

Note: This is a revised manuscript currently under review at Nature Protocols. The author conducted all experiments and wrote the paper with Phillip Zamore.

Abstract

MicroRNAs (miRNAs), ~21 nt RNAs that mediate post-transcriptional regulation of mRNAs in animals and plants, are a diverse class of regulatory genes whose specific biological functions are largely unknown. Here, we detail a protocol to design and introduce into cultured *Drosophila* and human cells sequence-specific antisense oligonucleotides (ASOs) that block the function of individual miRNAs. Coupled with recent studies that catalog the miRNAs expressed in diverse cultured cells, our method offers a rapid (< 1 week) approach to validate miRNA targets and to study the cellular functions of individual human and *Drosophila* miRNAs. ASO-based inactivation of miRNAs is faster and simpler than comparable genetic or "sponge" based approaches, for which extensive recombinant DNA manipulation is required. We present our ASO design principles and an optimized transfection protocol in which transfection efficiency of *Drosophila* Schneider 2 cells can approach 100%. Our 3′-cholesterol modified ASOs have enhanced potency, allowing miRNA inhibition for at least 7 days from a single transfection.

Introduction

MicroRNAs (miRNAs) are an ancient class of ~21 nt small silencing RNAs that mediate post-transcriptional regulation of mRNAs in animals and plants . When bound to partially complementary sequences in their target mRNAs, animal miRNAs tune gene expression by repressing translation or accelerating mRNA decay(Bagga et al., 2005; Lee et al., 1993; Lim et al., 2005; Wightman et al., 1993; Olsen and Ambros, 1999). This regulation is critical for diverse biological processes, including stem cell maintenance; musculoskeletal, circulatory, and nervous system development; insulin secretion; and oncogenic transformation(Förstemann et al., 2005; Hatfield et al., 2005; Sokol and Ambros, 2005; Zhao et al., 2007; Giraldez et al., 2005; Poy et al., 2004; He et al., 2005). More than 1000 miRNA genes have now been identified in animals, of which a large fraction are conserved between vertebrates and invertebrates. However, few specific functions have been described for individual miRNAs.

To accelerate the study of miRNA function and mechanism, we developed a method to disrupt individual miRNAs using antisense oligonucleotides (ASOs) in human tissue culture cells(Hutvágner et al., 2004) and adapted it for use in *Drosophila* S2 cells(Förstemann et al., 2007). ASOs bind complementary miRNAs and selectively block silencing in cell extracts, in cultured cells, and *in vivo* in worms, flies, mice, and primates(Boutla et al., 2003; Hutvágner et al., 2004; Krutzfeldt et al., 2005; Leaman et al., 2005; Meister et al., 2004a; Davis et al., 2006; Esau et al., 2006; Esau et al., 2004; Elmen et al., 2008a). Studying miRNA function using classical genetic approaches is challenging, as miRNAs often form multi-gene families with common mRNAs targets, reside in introns of protein coding genes, or derive from polycistronic non-coding transcripts(Lau et al., 2001; Lagos-Quintana et al., 2001; Abbott et al., 2005; Baskerville and Bartel, 2005; Kim and Kim, 2007; Okamura et al., 2007; Ruby et al., 2007). ASOs can be designed to inactivate a specific miRNA and its paralogs knowing only the

sequences of the mature miRNAs. Recent studies cataloguing miRNA sequences and expression profiles in flies, worms, mice, humans, and cultured cells provide a road map for the use of ASOs to study miRNA targets and the biological pathways they regulate(Aravin et al., 2003; Ruby et al., 2006; Berezikov et al., 2006; Gaur et al., 2007; Blower et al., 2007; Landgraf et al., 2007). Here, we describe the principles used in our laboratory to design ASO miRNA inhibitors and provide protocols for the efficient delivery of ASO inhibitors into cultured *Drosophila* Schneider 2 (S2) and human cells.

miRNAs and Their Targets

miRNAs are transcribed as hairpin precursors, then sequentially processed by the RNase III enzymes, Drosha and Dicer, to yield double-stranded intermediates bearing 2 nt, 3′ overhanging ends(Lee et al., 2003; Hutvágner et al., 2001; Grishok et al., 2001; Ketting et al., 2001). These imperfectly paired duplexes are then assembled into long-lived, cytoplasmic protein-RNA complexes called RISCs (*R*NA-*I*nduced *S*ilencing *C*omplexes) that mediate RNA silencing. Every RISC contains a single-stranded small RNA guide bound to a member of the Argonaute family of proteins(Bernstein et al., 2001; Hutvágner and Zamore, 2002). The miRNA and Argonaute protein act together to bind and silence target mRNAs (Fig. 1). Perfectly complementary targets are efficiently silenced by the endonucleolytic cleavage activity of some Argonaute proteins(Hutvágner and Zamore, 2002; Yekta et al., 2004; Davis et al., 2005), but the vast majority of predicted targets in animals are only partially paired(Grun et al., 2005; Krek et al., 2005; Rajewsky and Socci, 2004; Ruby et al., 2006; Lewis et al., 2005; Lewis et al., 2003; Brennecke et al., 2005) and likely cannot be cleaved(Haley and Zamore, 2004). Instead, they bind RISC using the "seed" of the miRNA, nucleotides 2-7, and are translationally repressed and/or degraded by a pathway distinct from the endonucleolytic activity of RISC(Doench and Sharp, 2004; Lewis et al., 2003; Aleman et al., 2007).

Figure AI-1

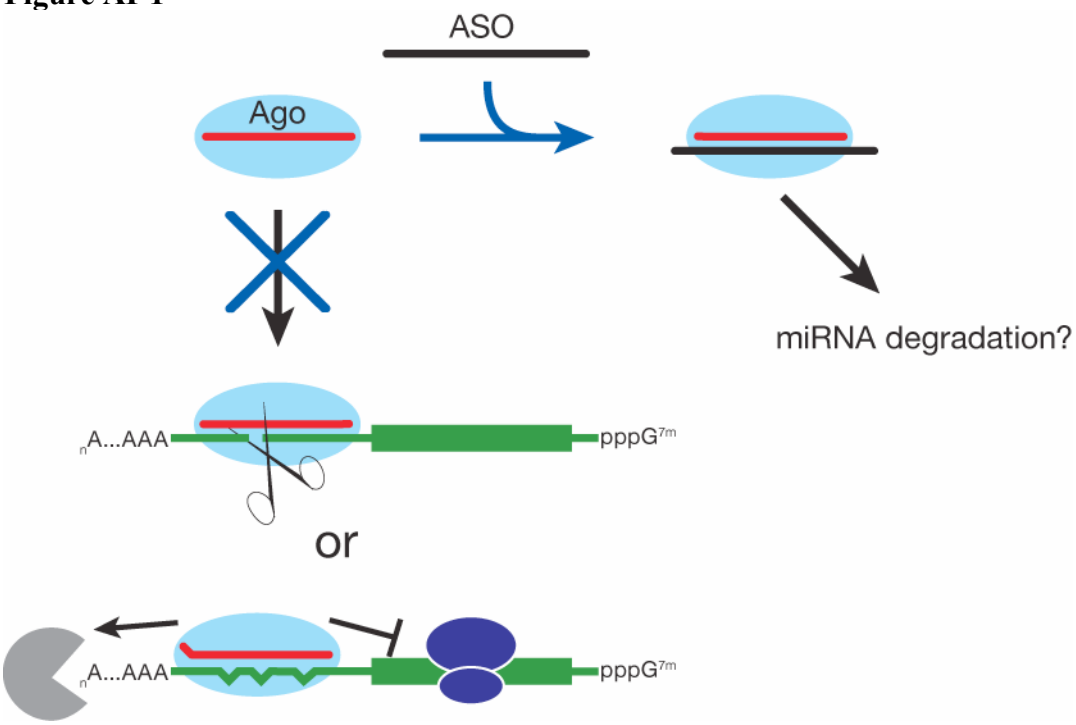

Figure AI-1. Model for Antisense Oligonucleotide Disruption of miRNA Silencing. Single-stranded, mature miRNAs bound to an Argonaute protein can cleave perfectly complementary mRNA targets. Imperfectly paired mRNAs are translationally repressed or degraded. ASOs bind miRNAs in RISC, thereby preventing miRNA from binding its target mRNA. In some cases, ASOs may secondarily promote miRNA degradation by an unknown mechanism.

The remarkably small number of nucleotides required for miRNA-directed target repression suggests that each miRNA may regulate hundreds of mRNA species(Grun et al., 2005; Krek et al., 2005; Rajewsky and Socci, 2004; Ruby et al., 2006; Lewis et al., 2005; Lewis et al., 2003; Brennecke et al., 2005). Experimentally validating computationally predicted miRNA targets and proving the biological significance of each mRNA candidate remains a daunting challenge. Selective inactivation of miRNAs with ASOs has already helped accelerate this task.

Selection of Antisense Oligonucleotide Chemistry

miRNA activity has been blocked effectively using ASOs containing several distinct nucleic acid modifications. In general, an effective ASO is (1) resistant to non-specific cellular ribonucleases, (2) resistant to miRNA-directed cleavage by RISC, and (3) binds miRNAs in RISC with high affinity, effectively out-competing binding to target mRNAs. We designed ASO inhibitors containing exclusively 2′-*O*-methyl (2′-*O*-Me) ribose sugars (Fig. 2). 2'-*O*-Me oligonucleotides are resistant to cleavage by both RISC and other cellular ribonucleases(Inoue et al., 1987; Hutvágner et al., 2004; Meister et al., 2004a). Moreover, 2′-*O*-methyl-modified RNA:RNA hybrids are more thermodynamically stable than either RNA:RNA or DNA:RNA duplexes(Inoue et al., 1987; Tsourkas et al., 2002). Other base modifications with enhanced hybridization stability have also been used successfully to inhibit miRNA function, including ASOs combining 2′-deoxy and Locked Nucleic Acid (LNA) nucleotides(Chan et al., 2005; Lecellier et al., 2005; Orom et al., 2006; Elmen et al., 2008b), 2′-*O*-methyl and LNA(Fabani and Gait, 2008), all 2′-*O*-methoxyethyl (2′-*O*-MOE) ASOs, and ASOs incorporating pyrimidines bearing 2′-*O*-fluoro modifications(Davis et al., 2006; Esau et al., 2006) (2′-*O*-MOE-modified oligonucleotides are not available commercially.)

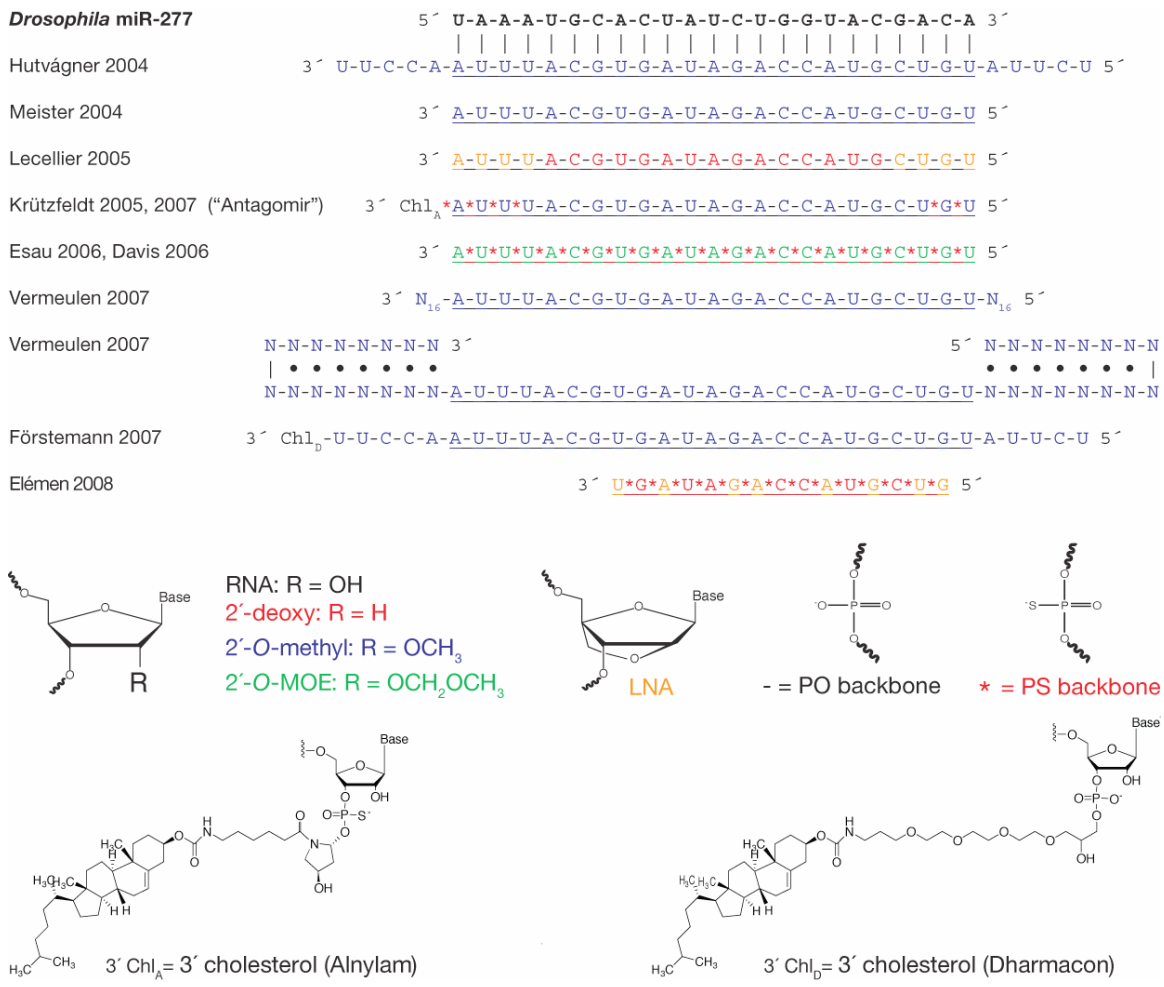

Figure AI-2. Chemical Structures of Antisense Oligonucleotides Used to Block miRNA Function. Anti-miR-277 is represented to illustrate the design principles used in different studies. All ASOs contain core sequences that are perfectly complementary to mature miR-277. A number of flanking sequence, backbone, base, and terminal modifications have been incorporated in the indicated studies. Chemical structures correspond to color coded sugar, backbone, and terminal modifications. The linkers used for 3´-cholesterol conjugation by Dharmacon and Alnylam (not commercially available) are also illustrated.

Nuclease-resistant phosphorothioate backbone linkages, in combination with ribose modifications, have also been employed in cultured cells, *in vivo* in mice and non-human primates (Davis et al., 2006; Esau et al., 2006; Krutzfeldt et al., 2007; Krutzfeldt et al., 2005; Elmen et al., 2008a)(Fig. 2). miRNA inhibition by peptide nucleic acid oligonucleotides has been reported for cultured cells(Fabani and Gait, 2008).

A 3′ terminal cholesterol group appears to aid delivery of ASOs to cells. Originally used to enhance delivery of ASOs targeting mRNAs(Desjardins et al., 1995; Krieg et al., 1993; Letsinger et al., 1989), cholesterol modification has been adapted to deliver both small interfering RNAs and miRNA-blocking ASOs to the liver and other tissues in mice(Soutschek et al., 2004; Krutzfeldt et al., 2005). We find that 3′ conjugation of cholesterol to ASOs makes them ~8-fold more potent when transfected into S2 cells (Fig. S2)(Förstemann et al., 2007). While cholesterol conjugation likely aids ASO delivery into cells, it may have properties that further enhance ASO activity, such as improved intracellular escape from liposomes, relocalization of the targeted miRNAs, or enhancement of ASO stability. Recent studies in mice support such ideas(Krutzfeldt et al., 2007).

Does Length Really Matter?

To make the ASO more "target-like," we added 5 extra nucleotides to its ends, for a total of 31 nucleotides(Hutvágner et al., 2004). 21 nt 2′-*O*-Me ASOs have also been used in cultured human and *Drosophila* cells and in fly embryos(Meister et al., 2004a; Leaman et al., 2005; Esau et al., 2006). Esau and coworkers reported no significant difference between 21 nt and longer ASOs in HeLa cells, but Hutvágner et al. found that 21-mer ASOs were measurably less potent. Similarly, Berger and co-workers observed only partial inhibition of miR-2 in *Drosophila* S2 cell reporter assays using a 21-mer

ASO(Berger et al., 2005). Vermeulen and coworkers found that increasing ASO length by adding as many as 16 nt to each side of the miRNA-complementary core increased ASO potency as much as 10-fold(Vermeulen et al., 2007).

Consistent with these observations, Ameres and colleagues recently described a sequence-independent, single-stranded RNA-binding activity associated with human RISC(Ameres et al., 2007). Non-sequence-specific binding by RISC of ASO sequence flanking the miRNA-complementary core may account for the enhanced potency of ASOs longer than 21 nt. These additional ASO sequences might also protect the core from cellular exonucleases. Krutzfeldt suggests this possibility to explain a "tendency" toward improved disruption of miR-122 *in vivo* when they extend the ASO by only 1 base on each end(Krutzfeldt et al., 2007). Interestingly, Vermeulen observed that addition of double-stranded, 8 base-pair hairpins to the ends of the ASO increased its potency more than the addition of 16 single-stranded nucleotides(Vermeulen et al., 2007). Double-stranded ends may protect the ASO from exonucleolytic destruction or the terminal hairpins may participate in coaxial stacking interactions with the ASO:miRNA duplex, increasing its thermodynamic stability(Walter et al., 1994). Supporting the idea that ASOs must have high thermodynamic stability, Elmen and colleagues recently showed that full complementarity of an ASO is not required if a very high affinity 16-mer LNA targeting the 5′ end of the miRNA is used(Elmen et al., 2008a; Elmen et al., 2008b). In our experience, 21 nt LNA-substituted ASOs and 31-mer 2′-*O*-Me ASOs performed similarly in S2 cells (PDZ and MDH, unpublished). While the higher affinity of LNAs may permit design of shorter effective ASO inhibitors, we believe that the bulk of published data suggest that the addition of single- or double-stranded sequences flanking the 21 ASO nucleotides complementary to the targeted miRNA potentiates miRNA inhibition by 2′-*O*-Me ASOs.

The Mechanism of miRNA Inhibition

The mechanism by which ASOs block miRNA function remains controversial. Initial studies suggested that ASOs block miRNA function by binding mature miRNAs in RISC. 31-mer 2′-*O*-Me ASOs act as stoichiometric inhibitors *in vitro* and in HeLa cells and bind miRNAs in RISC *in vivo* in *C. elegans*(Hutvágner et al., 2004). Unexpectedly, ASO-targeted miRNAs could not be detected by northern hybridization in mice that were injected with "antagomirs", cholesterol modified, 2′-*O*-Me ASOs with terminal phosphorothioate modifications, (Fig. 2)(Krutzfeldt et al., 2007; Krutzfeldt et al., 2005). Similarly, Esau and coworkers found that fully modified 2'-*O*-methoxyethyl phosphorothioate ASOs targeting the same miRNA, miR-122, induced the apparent destruction of the miRNA. Potentially, the phosphorothioate modification used in these studies triggered miRNA degradation. Chan and colleagues also report that 2'-*O*-methyl or LNA/DNA ASOs bearing phosphodiester backbones reduced apparent miRNA levels, but these authors suggest that standard northern hybridization probes may be unable to disrupt the high affinity of miRNA:ASO duplexes, even under denaturing conditions(Chan et al., 2005).

Consistent with this possibility, we find that when synthetic *let-7* was incubated with ~1000-fold excess of 2'-*O*-methyl ASO *in vitro*, only ~38% of the input *let-7* was detectable by northern hybridization using a DNA probe. However, when an LNA probe was used in conjunction with a higher hybridization temperature, virtually all the *let-7* was detectable (Fig. 3a). We see similar interference with Northern detection in S2 cells treated a miR-277 LNA ASO. Mature and pre-miR-277 was undetectable by northern blot with a DNA probe in total RNA samples from miR-277 LNA-transfected S2 cells (Fig. 3b). However, when an LNA northern probe was used ~ 30% of the miR-277 and pre-miR-277 signal becomes detectable. Interestingly, we observed two distinct types of Northern signal interference depending on the amount of LNA transfected. At 100 nM LNA, both the mature miRNA and pre-miRNA have reduced mobility. This suggests that even in a denaturing gel, the highly stable LNA:miRNA or LNA:pre-miRNA duplex is

Figure AI-3. Improved Detection of Synthetic *let-7* and Endogenous miR-277 in the Presence of High Levels of Antagomir ASO using an LNA Northern Probe. (A) 1 nM synthetic 21 nt *let-7* RNA was incubated with 1 nM, 10 nM, 100 nM, or 1 μM *let-7* antagomir (21 nt 2′-*O*-Me with partial pS backbone and 3′-Chl as in Fig. 2(Krutzfeldt et al., 2007)) in 30 mM HEPES-KOAc, pH 7.4, 100 mM KOAc, 2 mM $MgSO_4$ for 1 min at 95°C, then 20 min at 37°C. Samples were mixed with an equal volume of formamide loading dye, heated to 95°C for 2 min and then electrophoresed through a denaturing 15% acrylamide gel containing 7.5 M urea. RNA was transferred to a Hybond N+ membrane (Amersham) and probed with a 5′ ^{32}P-radiolabeled DNA oligo at 37°C. The membrane was stripped in 0.1% (w/v) SDS and reprobed with an LNA probe at 69°C. Percent detection values are normalized to the no antagomir lane for each probe. (B) and (C) *Drosophila* S2 cells containing two copies of the perfect miR-277 reporter were transfected with miR-277 ASOs with the indicated chemistry at very high concentration (100 nM) or at a concentration that gave 80-90% derepression of the GFP reporter (1–10 nM depending on chemistry) in three replicate wells of a 6 well plate. An ASO targeting firefly luciferase (100 nM) was used as a control. Three days after transfection, cells were split and analyzed for Northern Blot or FACS. (B) For Northern analysis, cells from replicate transfections were pooled and RNA was extracted using Trizol with 20 μg glycogen as a carrier. Ten μg total RNA was loaded per well and Northern hybridization was performed using either a miR-277 DNA or LNA probe as in (A). Percent detected corresponds to the miR-277 ASO signal normalized to the control signal. Transfected LNA ASO was identical to the LNA probe, which incorporated an LNA base at every third nucleotide(Valoczi et al., 2004). (C) Fold derepression represents the mean +/- standard deviation of the GFP FACS values for three replicate transfections, normalized to the control.

Figure AI-3

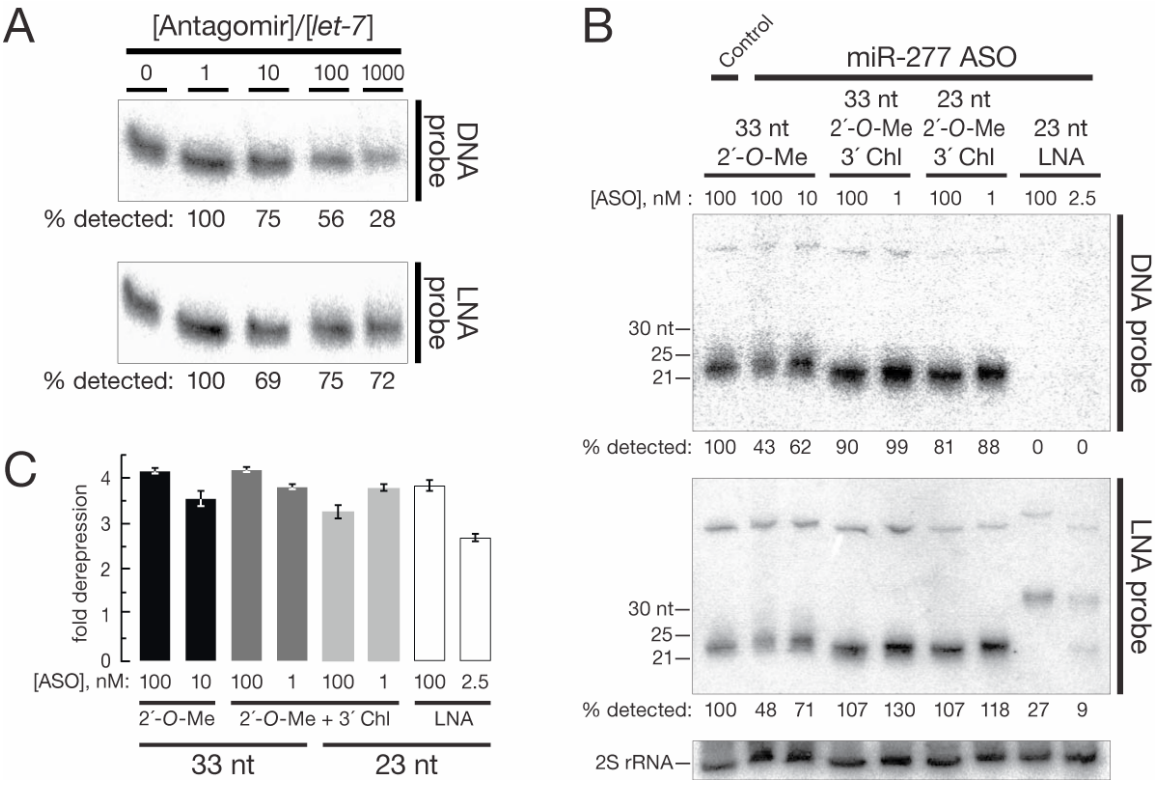
A
[Antagomir]/[let-7]
0 1 10 100 1000
DNA probe
% detected: 100 75 56 28
LNA probe
% detected: 100 69 75 72
B
Control
miR-277 ASO
33 nt 2′-O-Me
33 nt 2′-O-Me 3′ Chl
23 nt 2′-O-Me 3′ Chl
23 nt LNA
[ASO], nM : 100 100 10 100 1 100 1 100 2.5
30 nt
25
21
DNA probe
% detected: 100 43 62 90 99 81 88 0 0
LNA probe
% detected: 100 48 71 107 130 107 118 27 9
2S rRNA
C
fold derepression
0 1 2 3 4
[ASO], nM: 100 10 100 1 100 1 100 2.5
2′-O-Me
2′-O-Me + 3′ Chl
LNA
33 nt
23 nt

maintained, blocking access of lower affinity DNA northern probe. However, at lower ASO transfection concentration (2.5 nM LNA), there is a partial mobility shift for mature miRNA, but none for pre-miRNA. Nonetheless, miRNA and pre-miRNA were not detected with a DNA probe, but were detected with an LNA probe.

A likely explanation for this effect is that the LNA and miRNA are both denatured and migrate as single-stranded 23 nt oligonucleotides during electrophoresis, but hybridize to each other during transfer to the positively charged nylon membrane, blocking subsequent access of the lower affinity DNA probe to the miRNA. At high hybridization temperature, the LNA probe can compete with the ASO, giving a partial signal on Northern. Surprisingly, treating S2 cells with 2'-*O*-methyl ASOs did not substantially reduce mature miR-277 levels measured by Northern blotting, using an LNA or DNA probe. Nor did addition of 3′ cholesterol or phosphorothioate linkages alter miR-277 levels. In each case, whether miR-277 was >80% inhibited (1-10 nM ASO) or 100% inhibited (100 nM ASO), we did not observe a corresponding change in miR-277 level by northern blot (Fig. 3b and 3c). These data suggest that ASOs act as inhibitors, rather than directing degradation of miRNAs in S2 cells. Whether ASOs act as competitive inhibitors or target miRNAs for destruction in mammalian cells will clearly require further study.

Alternatives to ASOs for Studying miRNA Function

A number of alternative approaches are available to study the loss of function of specific miRNA genes.

Gene targeting using homologous recombination is possible in mice and flies(Thomas and Capecchi, 1986; Rong and Golic, 2000), and has elucidated roles for individual miRNAs in the mouse immune system(Rodriguez et al., 2007) and heart(Zhao et al., 2007) and in the development of fly muscle(Sokol and Ambros, 2005) and sensory organs(Li et al., 2006). While roles for miRNAs in development had been suggested by

the analysis of fly embryos injected with 2'OMe ASOs(Leaman et al., 2005) or developing zebrafish injected with pre-miRNA-complementary "morpholinos" (~25 nt oligonucleotides containing 6-carbon morpholine rings and a phophoramadite backbone instead of ribose sugars and a phosphodiester backbone)(Kloosterman et al., 2007), ASOs have yet to be utilized in developing mice. Thus, targeted deletion is currently the only way to study loss of miRNA function in mouse development.

Gene targeting is also possible in human and mouse tissue culture cells(Mortensen et al., 1992). Only a single study to date has used this approach(Bommer et al., 2007), likely because gene targeting in somatic cells is technically challenging and laborious, requiring construction of a targeting vector, recombination selection schemes that can vary widely in efficiency depending on the gene to be targeted, and screening to verify genotype. Moreover, the results obtained by Bommer and colleagues closely mirrored those obtained in parallel using ASOs (see Anticipated Results for more discussion).

A "knock-out" phenotype in an intact animal is, of course, the most convincing proof of the biological function of a miRNA. Often, however, no observable phenotype results from miRNA loss of function. In a recent study in which deletions were reported for 83% of known miRNA genes in *C. elegans*, loss of most individual miRNA genes caused no obvious phenotype(Miska et al., 2007). Functional redundancy likely explains this result, as combining deletions of several *let-7* family members that alone had no phenotype caused distinct phenotypes(Abbott et al., 2005). In mice, deletion of the miR-17~92 cluster produced dramatic defects in heart, lung, and B-cell development, accompanied by inappropriate apoptosis, but deletion of two other paralogs (miR-106a~363 or miR-106b~25) produced no obvious phenotype(Ventura et al., 2008). Still, it is unclear if one or all of the 6 miRNAs in the cluster contribute to the observed phenotype. Highlighting the utility of ASOs as an adjunct for rapid functional studies of individual miRNAs, Matsubara and colleagues had already found that lung cancer cell

lines expressing the miR-17~92 cluster undergo apoptosis when miR-17 or miR-20a are inhibited with ASOs(Matsubara et al., 2007). Thus, while gene deletion remains the biological gold standard, its technical difficulty paired with the complex organization of miRNA genes makes it a high risk, time consuming approach.

"miRNA sponges" offer a new alternative approach to inhibit miRNA function that may be superior for inhibiting whole miRNA families. Sponges are highly expressed transgenes bearing multiple, bulged (i.e., non-cleavable) miRNA-binding sites complementary to a miRNA of interest. These abundant RNAs compete with endogenous targets, and thus "soak up" RISC(Ebert et al., 2007). miRNA sponges have been transfected into tissue culture cells and appear to function as well as ASOs. Ebert and colleagues observed that sponges can inhibit miRNAs whose only shared sequence is their seed. This should be considered when targeting a single miRNA that is part of a family—sponges may not distinguish among family members, while ASOs appear to selectively silence family members that differ by more than two bases(Esau, 2008). In theory miRNA sponges could be used to make transgenic animals, but to date they have only been tested in cultured cells. Limitations of sponges, compared to ASOs, include 1) the time needed to design, build, and test the recombinant sponge vectors, 2) the reliance on plasmid DNA transfection, which is less efficient than oligonucleotide transfection, and 3) their limited selectivity for a single member of a miRNA family.

Transfected siRNAs directed against pre-miRNA loop regions have been reported to decrease miRNA abundance in human tissue culture cells(Lee et al., 2005; Vasudevan et al., 2007). This method should be used with caution as it appears to be comparatively inefficient, reducing the level of a mature miRNA ~80% at best, with the remaining 20% free to interact with targets. A number of issues likely account for the relative inefficiency of siRNA-directed depletion of miRNAs, including the secondary structure of pre-miRNAs which likely limits access to RISC. Secondary structure surrounding target sites is a well documented anti-determinant for RNAi(Ameres et al.,

2007; Kertesz et al., 2007). An siRNA targeting a pre-miRNA must also be able to cleave the pre-miRNA before Dicer converts it to a mature miRNA. To date, no evidence suggests that RISC has a kinetic advantage over Dicer. Additionally, miRNA depletion by pre-miRNA-directed siRNAs is limited by mature miRNA turnover. In contrast, ASOs directly inhibit mature miRNAs in RISC. Because RISC-bound miRNAs may be quite stable, this is an important consideration.

Advantages and Limitations of miRNA inhibition by ASOs

In principle, transfected ASOs can be used to study the loss-of-function phenotype for any miRNA expressed in cultured cells by measuring growth rate, induction of apoptosis, or changes in mRNA or protein abundance. Derepression of miRNA-regulated genes in the presence of an ASO is especially convincing evidence for a proposed miRNA:target interaction. In contrast to target validation approaches that use cloned 3′ UTR reporters and over-express miRNAs, ASO approaches can demonstrate that an endogenous miRNA interacts with an endogenous target mRNA.

To study miRNA function in human somatic cells, where genetic knockouts are difficult at best, ASO transfection is an essential tool. Studies using cell lines are, of course, limited by the repertoire of miRNAs expressed and by the cellular processes that can be recapitulated in immortalized or transformed cells. To study the role of miRNAs in complex developmental or physiological processes involving the interaction of multiple cell types, the use of model organisms in which miRNAs can be inactivated *in vivo* with ASOs or by targeted deletions (see above) may be preferable. However, even when studying miRNA function *in vivo*, validation of miRNA:target regulation in cell lines has the advantage that all the cells studied are essentially identical.

The main technical limitations on the use of ASOs are their delivery, duration of action, and specificity. Delivery and duration of action can be assessed using miRNA sensors, genes engineered to place a reporter, such as green fluorescent protein (GFP) or

luciferase, under the control of the miRNA of interest (see Experimental Design and Anticipated Results). Using the protocol described below, transfection is efficient (>90%) and miRNA inhibition is long lasting (>7 days). ASOs likely do not discriminate among miRNAs that differ by a single nucleotide. This can be a limitation or an advantage. Because many miRNAs are members of highly related families, i.e., they contain identical seeds, a single ASO likely blocks the function of more than one miRNA in a family. However, a single ASO may not strongly inhibit miRNAs whose only common sequence is the seed(Ebert et al., 2007; Davis et al., 2006). For such applications, co-transfection of multiple ASOs targeting various isoforms is possible(Bommer et al., 2007). In this respect, genetic approaches are superior for studying individual miRNA family members, whereas miRNA sponges or multiple ASOs are appropriate for studying miRNA families whose members only contain a common seed sequence; single ASO studies may simplify the study of nearly identical miRNA paralogs.

Combinations of ASOs targeting unrelated miRNAs have also been used to disrupt more than one miRNA in the same transfected cells, obviating the need to make and combine multiple genetic knockouts. Because combinatorial control of targets by miRNAs may be common(Bartel and Chen, 2004), this approach may prove particularly important for uncovering networks of miRNAs that act together. Vermeulen and co-workers showed that co-transfection of a six-ASO mixture can effectively de-repress reporters for each individual miRNA(Vermeulen et al., 2007). Functional studies also suggest that co-transfection of ASOs is effective. For instance, Pedersen and colleagues asked if five interferon-β induced miRNAs with seed matches to Hepatitis C genes had anti-viral effects; indeed simultaneous cotransfection of all five ASOs, but not controls, significantly enhanced Hepatitis C RNA production(Pedersen et al., 2007).

Experimental Design

Control experiments are required to ensure that miRNAs are indeed inactivated by the transfected ASOs. All experiments should employ a miRNA-specific ASO and a mismatched or unrelated control ASO. Suitable controls include

a) Antisense sequence of a non-homologous gene from another species,

b) A randomly scrambled version the experimental ASO,

c) A sequence derived from the experimental ASO incorporating purine:purine mismatches in at least 4 evenly spaced positions spanning the sequence of the miRNA. In theory, an ideal control would be a single mismatch in the miRNA seed region, but the enhanced binding affinity of 2′-*O*-Me:RNA may compensate for a single seed mismatch. 4 mismatches spanning the miRNA sequence should be sufficient to disrupt binding.

After transfecting cells with these ASOs, miRNA inhibition can be assessed by measuring the abundance of a protein encoded by (1) a validated miRNA target, relative to a control gene or (2) a reporter protein that is regulated by one or more miRNA-binding site(s) in the 3′ UTR of its mRNA. If miRNA mediated repression is blocked by the ASO, expression of target genes will increase compared to control genes. miRNA reporter or "sensor" constructs typically place one or two perfectly complementary miRNA sites in the 3′ UTR of reporter gene. In mammalian cells, we use a dual luciferase reporter system in which *Photinus pyralis* luciferase containing a perfectly paired 3′ UTR miRNA site is cotransfected with an unregulated *Renilla Reniformis* luciferase control gene (or vice versa). The relative expression of these two enzymes can be easily quantified by measuring luminescence activity(Hutvágner et al., 2004) (Box 4).

In *Drosophila* S2 cells, we typically use stably integrated GFP sensor reporters and derive clonal cell lines(Förstemann et al., 2007). Changes in GFP expression are measured by flow cytometry (FACS). An advantage of this approach is that transfection

efficiency can be assessed by observing the fraction of cells that have increased GFP levels after ASO transfection (Fig. 4).

After miRNA inhibition is established, any number of functional assays can be performed in the absence of reporters. Examples are discussed in Anticipated Results.

Gain-of-function studies can also be conducted to complement ASO loss-of-function studies. The finding that introduction of a miRNA into cultured cells has the opposite effect of ASO inhibition on an mRNA provides strong support for a regulatory relationship between the miRNA and the mRNA target. Importantly, it also reduces the likelihood that a cellular phenotype observed with an ASO is due to a non-specific effect. miRNAs can be introduced using a pri-miRNA expression plasmid(Zeng et al., 2002; Chen et al., 2004; Voorhoeve et al., 2006; Förstemann et al., 2007), an siRNA whose sequence corresponds to a miRNA(Doench et al., 2003; Lim et al., 2005), or a synthetic pre-miRNA(Wang and Wang, 2006). For instance, we used a pri-miR-277 expression vector to augment miR-277 levels and thus increase silencing of GFP reporters(Förstemann et al., 2007). Pedersen and colleagues complemented their ASO loss-of-function studies (see above), with a gain-of-function study in which they transfected a mix of 5 miRNA-like siRNAs into cultured cells and found that Hepatitis C virus replication was reduced, even in the absence of IFN-β induction(Pedersen et al., 2007).

MATERIALS

REAGENTS

· Fetal Bovine Serum, Heat Inactivated (Invitrogen, 10082-139)

· Dharmafect 4 Transfection Reagent (Dharmacon, T-2004)

· siLentFect (Bio-Rad, 170-3360)

· Lipofectamine 2000 (Invitrogen, 11668-027)

· Dulbecco's Phosphate Buffered Saline, no Calcium or Magnesium (Invitrogen, 14190)

· Antisense oligonucleotides (Dharmacon, Sigma, or many other oligo synthesis vendors)

· Trypan Blue (Invitrogen, 15250-061)

· Sterile deionized H_2O

· *Drosophila* Schneider 2 (S2) cells (Invitrogen, R690-07)

· Schneider's *Drosophila* Medium (Invitrogen, 11720-034)

· HeLa cells (ATCC, CCL-2.2) or NTera2 cells (ATCC, CRL-1973)

· Dulbecco's Modified Eagle Media (Invitrogen, 11965)

· Trypsin-EDTA Solution (Invitrogen, 12605)

· psiCheck 2 Vector (Promega, C8021)

EQUIPMENT

· Sterile 24-well Dishes (Beckton Dickinson, 35 3047)

· Sterile 6-well Dishes (Beckton Dickinson, 35 3046)

· Sterile 10 cm Plate (Nunc, 172958)

· Laminar Flow Hood (class II)

· Stereomicroscope with 50x magnification and a bright field setting

· Hemocytometer

· Sterilized standard 100-1000 µl, 20-200 µl, 1-20 µl, and 0.1-10 µl pipette tips

· Micropipettors, P-1000, 200, 20, and 10 (Gilson)

· Serological Pipets: 5 ml, 10 ml, and 20 ml

· Pipet-aid (Becton Dickinson, 357565)

· Sterile Plasticware: 1.5 ml Eppendorf tubes (Eppendorf, 22 36-411-1), 15 ml conical tubes (Beckton Dickinson, 35 2097)

· Centrifuges for 1.5 ml and 15 ml tubes

· Tissue Culture Incubator at 25°C (without CO_2; NuAire, 8700)

· Tissue Culture Incubator at 37°C with 5% CO_2 (NuAire, 8700)

· BD FACScan Flow Cytometer (Becton Dickinson) or equivalent

· Veritas Microplate Luminometer (Tuner Biosystems, 9100-000) or equivalent

REAGENT SETUP

Antisense Oligonucleotide Stock Solution. Dilute antisense oligo to 100 μM with sterile dH_2O. To be certain the concentration is correct, we check the stock concentration by measuring its absorbance at 260 nM using a spectrophotometer. Extinction coefficients and molecular weights are usually provided with the oligo. 2′-*O*-Me oligonucleotides do not require deprotection. For pipetting accuracy it may also be necessary to make a 10 μM stock, especially when transfecting a single well or very small wells with an ASO. ASO stock solutions can be stored short term (<1 month) at -20°C and long term at -80°C.

S2 + FBS Media. Combine Schneider's media with 1/10 volume of fetal bovine serum. Warm to room temperature (~23°C) before use. Store at 4°C.

S2 Media. Schneider's *Drosophila* Medium (no serum) used for transfection mixes Warm to room temperature before use. Store at 4°C.

DMEM + FBS Media. Combine DMEM with 1/10 volume of fetal bovine serum. Warm to 37°C before use. Store media at 4°C.

DMEM. DMEM (no serum) used for transfection should be warmed to room temperature.

Trypsin-EDTA. Pre-warm Trypsin-EDTA solution to 37°C.

PBS. Pre-warm Dulbecco's Phosphate Buffered Saline solution to 37°C.

PROCEDURE

Design of Antisense Oligonucleotides to Disrupt miRNA Function: Timing — ~1 hour

1. Retrieve the sequence of the miRNA(s) of interest from miRBase (http://microrna.sanger.ac.uk/sequences/)(Griffiths-Jones et al., 2006).

2. Record the reverse complement of the miR strand sequence.
3. Add 5 arbitrary bases to both the 5′and 3′ ends of the antisense miR sequence. Our inhibitors have used the sequence 5′-UCUUA—antisense miRNA—ACCUU-3′.
4. Check the full length sequence for potential secondary structure using mFold: http://mfold.bioinfo.rpi.edu/cgi-bin/rna-form1-2.3.cgi(Zuker, 2003). We use the default settings.
5. If the flanking sequences are predicted to be involved in formation of strong secondary structure elements (ΔG> user defined cutoff value), alter the flanking sequence base composition and repeat step 4.
6. Perform a BLAST search using the full length oligonucleotide. If fortuitous stable base pairing to an mRNA is predicted involving the flanking sequences and 13 or more bases within the targeting sequence, repeat step 3-6.
7. Design a control oligo (see Experimental Design for a discussion of appropriate controls). Flanking sequences can be identical to those in the experimental ASO. All control oligos should also be checked for strong secondary structure or unintended complementarity to mRNAs as detailed in Steps 4–6. Strong secondary structure elements in any part of the sequence should be minimized by altering that part the sequence.
8. Order 2′-*O*-Me-modified oligonucleotides (Dharmacon, Sigma, or many other oligo synthesis vendors). We find that 3′ conjugation of cholesterol enhances the potency of miRNA inhibition in *Drosophila* S2 cells (Fig. S2A). We order custom cholesterol conjugated oligonucleotides from Dharmacon using the custom RNA module (www.dharmacon.com/rna/rna.aspx).

Cell culture, transfection and analysis of inhibition

9. If using Drosophila S2 cells to study miRNA function, follow option A. If using mammalian cells, follow option B; in our lab, this strategy has been used successfully to transfect both HeLa and NTera2 cells. These transfection protocols can be adapted for RNAi using siRNA and dsRNA by altering only a few steps, as outlined in Box 1.

Option A: Culture and Transfection of S2 Cells: Timing – Up to 14 days

i. Grow S2 cells in S2-FBS Media in a 25°C incubator to a density of 8–10 x 10^6 cells/ml with at least 90% viability; cell number and viability should be checked using Trypan blue and a hemocytometer (see Box 2). If starting from a frozen stock, up to two weeks of growth may be necessary to reach >90% viability. Cells can be propagated in one well of a 6 well plate with 2 ml total volume per well.

CRITICAL STEP: Having S2 cells at high density before transfection is important because at lower densities S2 cells form clumps that may limit transfection efficiency. As the cells reach high density these clumps disperse.

ii. In a laminar flow hood, dilute cells from a density of 8–10 x 10^6 cells/ml to a density of 2.75 x 10^5 cells/ml with S2 + FBS media. Cells can be removed from the 6-well plate and diluted in a 50 ml conical tube, and then dispensed into the desired dishes.

CRITICAL STEP: Diluting the cells to this density is very important. Transfection of too few cells will result in cell death. Transfection of too many cells will cause uptake of the ASO to be inefficient (see Fig. 5).

iii. For a 24-well plate add 450 µl of diluted cells per well (i.e., 90% of the 500 µl final volume per well) and place the plate in the 25°C incubator.

For other types of plates or dishes, all the transfection mixes can be scaled linearly. See Table 1.

iv. Vortex the ASO stock. In a new 1.5 ml Eppendorf tube mix 1.25 µl of a 10 µM ASO stock solution with 23.75 µl of Schneider media per well of a 24 well plate. Gently mix by tapping the side of the tube. If transfecting multiple wells with the same ASO, make 5% extra to avoid running short due to pipetting errors (1.31 µl 10 µM ASO/well X number of wells, and 25 µl S2 Media/well X number of wells).
CRITICAL STEP: Cholesterol-modified ASOs can pool near the walls of the tube. It is important to mix both the ASO stock and the S2 Media-ASO mixture.

v. In a new 1.5 ml Eppendorf tube, mix 1 µl Dharmafect 4 transfection reagent with 24 µl of S2 media per well of a 24 well plate. If transfecting multiple wells with the same ASO, add 5% extra to compensate for pipetting errors.

vi. Combine the mixtures from step iv and v by adding the Dharmafect 4 mixture to the tube containing the ASO. Gently mix by tapping the side of the tube.

vii. Incubate transfection mixture(s) at room temperature for 20 minutes.

viii. Remove cells from the incubator and add 50 uL of the ASO-Dharmafect 4 transfection mix (10% total volume) to each well of the diluted cells. Try to distribute drops evenly over the wells and mix by gentle agitation after the mix is added.
CRITICAL STEP: Move the plate back and forth in straight lines rather than circles to evenly distribute cells and transfection mix. Circular motions cause cells to pool in the middle, which may reduce transfection efficiency.

ix. Allow cells to grow for 1–8 days depending on experimental design. For example, if validating the effectiveness of miRNA inhibition with a dual luciferase miRNA sensor system (Box 4), transfect sensor/control reporters at 48 h with siLentfect (Bio-Rad); perform dual luciferase assay at 72 h. Alternatively, if checking miRNA inhibition with a stable GFP cell line, FACS can be performed at 72 h. Because S2 cells are semi-adherent, GFP reporter cells can be transferred to test tubes and assayed directly in the FACS machine according to the manufacturer's instructions. Because Dharmafect 4 is not very toxic to S2 cells, media does not need to be changed until cells reach a density of 1 x 10^7 cells/ml. The effects of miRNA inhibition on the expression of regulated mRNAs and proteins can be seen as early as 24 h and persist beyond 8 days (Fig. S2C).

Option B: Culture and Transfection of HeLa or NTera2 (NT2) Cells: Timing — 72 h

i. Grow cells to confluence in 10 ml DMEM + FBS in a 10 cm dish in a 37°C incubator with 5% CO_2.

ii. 24 h before transfection, treat cells with Trypsin-EDTA and split cells (Box 3) into a 6-well plate so that they will be 30–40% confluent at the time of transfection (~2 x 10^5 cells/well in 2 ml DMEM + FBS in one well of a 6-well plate). For other types of plates or dishes, cell and transfection mixes can be scaled linearly. See Table 2 for volumes.

iii. Check that cells are ~30-40% confluent.

CRITICAL STEP: Transfection of too few cells can be toxic. Transfection of too many cells is inefficient. Be sure your cells are at the correct density before transfection.

iv. Remove media and replace with 1.8 ml of fresh pre-warmed DMEM + FBS.

v. Vortex 10 µM ASO stock solution. For each well of a 6-well plate, to be transfected, add 5 µl of a 10 µM ASO stock solution to 95 µl of DMEM in a sterile 1.5 ml Eppendorf tube. Gently mix by tapping the side of the tube. If transfecting multiple wells with the same ASO, add 5% extra to compensate for pipetting errors.

vi. For each well of a 6-well plate, add 4 µl Dharmafect 4 to 96 µl of DMEM in a sterile 1.5 ml Eppendorf tube. If transfecting multiple wells with the same ASO, add 5% extra to compensate for pipetting errors. Gently mix by tapping the side of the tube.

vii. Combine mixtures from step v and vi by adding the Dharmafect 4 mixture to the tube containing the ASO. Gently mix by tapping the side of the tube.

viii. Incubate the transfection mixture(s) at room temperature for 20 min.

ix. Remove the cells from incubator and add 200 µl of the ASO/Dharmafect 4 mix to each well of the 6-well plate. Try to distribute drops evenly over the dish or plate and mix by gently agitating after the mix is added. CRITICAL STEP: Move the plate back and forth in straight lines rather than circles to evenly distribute cells and transfection mix.

x. Allow cells to grow for 24–48 h depending on experimental design; for example, if validating the effectiveness of miRNA inhibition with a dual luciferase miRNA sensor (Box 4), transfect the sensor/control reporters at 24 h with Lipofectamine 2000 (Invitrogen) according to the manufacturer. Perform the dual luciferase assay at 48 h. With Dharmafect 4, the media does not need to be changed until cells reach confluence (~48 h). Effects of miRNA inhibition on target mRNA and

protein levels can be seen as early as 24 h post-transfection and are still present after 48 h. We have not defined the persistence of the miRNA inhibition in mammalian cells.

TIMING

ASO Transfection of *Drosophila* S2 Cells

Step 1: 1–14 days

Steps 2–8: approximately 1 hour

Step 9: 1–8 days

Box 1: Design of Antisense Oligonucleotides

Steps 1-7: approximately 1 h

Box 2: ASO Transfection of Mammalian cells

Step 1: 1–4 days

Steps 2: approximately 30 min, then wait 24 h

Step 3-8: approximately 1 h

Step 9: 1–3 days

Box 3: siRNA or dsRNA Transfection of *Drosophila* S2 Cells or siRNA Transfection of Mammalian cells

Same as ASO Transfections above.

TROUBLESHOOTING

Troubleshooting advice can be found in Table 3.

ANTICIPATED RESULTS.

***Reporter Assays*:**

In a typical experiment, a reporter mRNA is used to detect the activity of a specific endogenous miRNA and an ASO is used to inhibit that miRNA. In our experience, inhibiting a miRNA with an ASO typically produces a 3-5 fold increase in reporter protein expression when the reporter mRNA contains perfect target sites that can be cleaved by RISC (Fig. 4). miR-277, a miRNA that is expressed in *Drosophila* S2 cells, does not regulate a GFP reporter lacking target sites. Control and miR-277 ASOs did not change the levels of the non-targeted reporter, ruling out any non-specific effects of the ASOs on the reporter. When two miR-277-binding sites were placed in the 3′ UTR of the reporter mRNA, the miR-277-complementary ASO inhibited miR-277 regulation, increasing expression of the GFP reporter 4–5-fold ; the control ASO had no effect. miR-277 directs repression of a reporter with two, fully complementary sites (4–5 fold increase) to a greater extent than of a reporter bearing four, imperfectly paired miR-277-binding sites (~30% increase). For this reason, we recommend perfectly matched reporters for testing ASOs. miR-277 inhibition by our ASOs was nearly complete, because the degree of derepression was similar to that observed when Ago2 and Ago1, the core RISC proteins that guide miRNA silencing, were depleted by dsRNA-triggered RNAi (Förstemann et al., 2007).

Using our optimized protocol we see a uniform shift in the FACS curve when miR-277 is inhibited indicating that transfection was very efficient (>90%) (Fig. 4 and 5). If transfection is incomplete, two peaks will be observed: one corresponding to cells that received the ASO and the other from those that did not. This is seen if cells are transfected at too high a density (Fig. 5). Unlike stable GFP cell lines in which fluorescence is measured in every cell, it is more difficult to assess transfection efficiency using the luciferase assay, in which an average from all cells is obtained. In the sequential transfection procedure detailed in Box 4, if ASO treatment derepresses the Renilla

Figure AI-4. A Sensitive Reporter System For miR-277 Silencing. Clonal *Drosophila* S2 cell lines bearing stably integrated GFP transgenes containing no sites, two perfect or four bulged miR-277-complementary sites in the 3′ UTR were transfected with control or miR-277-complementary ASOs (33 nt 2′-*O*-Me bearing a 3′ cholesterol modification). Five days after transfection, GFP was measured by FACS.

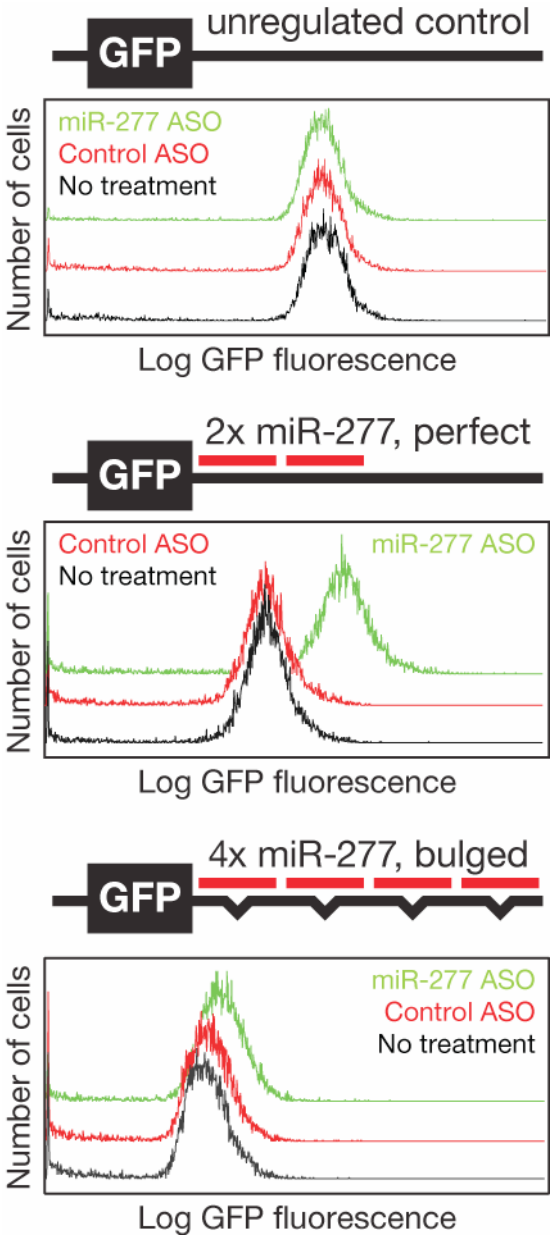

Figure AI-5. Efficient Transfection Requires Optimal Cell Density. S2 cells were transfected at 20 nM with 33 nt 2′-*O*-Me 3′-cholesterol modified miR-277 ASO, using Dharmafect 4 at the indicated cell density.

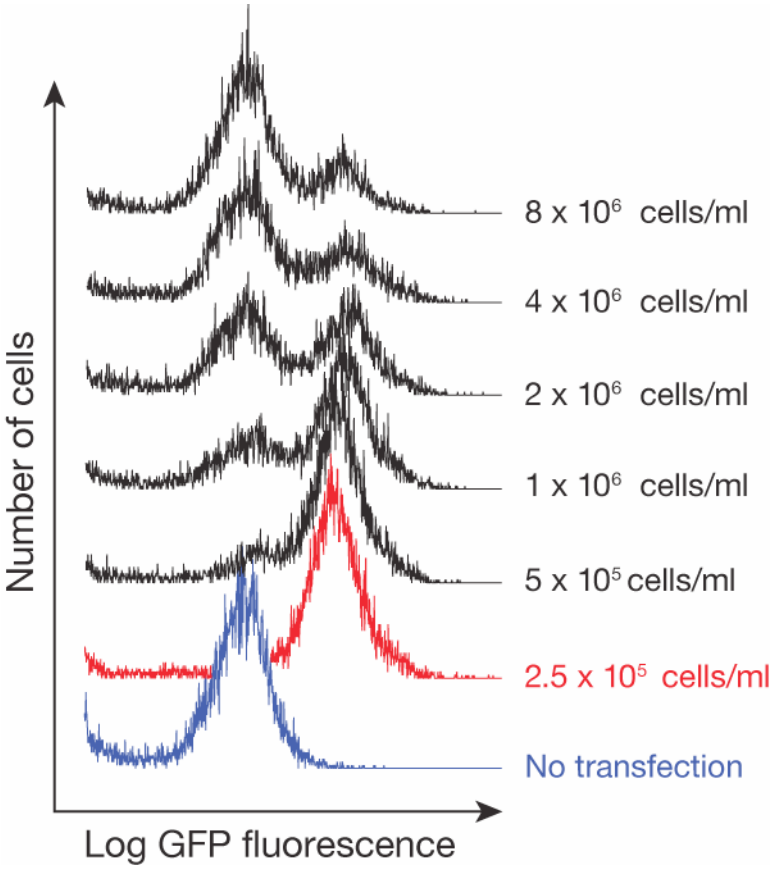

luciferase reporter to a level near that of the non-targeted reporter, ASO transfection must have been efficient (i.e., miRNA was inhibited by ASO in all cells that received the reporter). However, if miRNA repression cannot be inhibited by an ASO, low transfection efficiency may be an explanation. Low potency may also be an explanation. This can be tested by co-transfecting the ASO with the reporter instead of sequential transfection; all transfected cells should receive both the reporter and the ASO. If incomplete derepression is still seen, potency may be the problem rather than transfection efficiency. A dose response curve can be performed to ensure that maximal derepression is being achieved (sample dose response curve, Fig. S2A).

Endogenous Target Validation

Having established that an ASO disrupts the function of an endogenous miRNA, it is now possible to study the cellular consequences of miRNA loss of function. One common application of ASOs is miRNA target validation—testing if computationally predicted target mRNAs(Rajewsky, 2006) are, in fact, regulated by a given miRNA in cultured cells. For instance, the Bartel and Dutta groups studied the oncogene HMGA2, which contains seven predicted target sites for the miRNA *let-7*(Lee and Dutta, 2007; Mayr et al., 2007). HMGA2 protein and mRNA increase 4–6 fold in HeLa cells treated with a *let-7* ASO, but not a control. Conversely, transfected *let-7* siRNAs cause a ~3 fold reduction in HMGA2 protein. With so many sites, HMGA2 probably represents an extreme case for regulation by a single miRNA (Lee and coworkers note that the HMGA2 mRNA changed more than any other mRNA following Dicer or Drosha depletion by RNAi).

Regulation of targets by miRNAs can be quite modest, depending on miRNA and target abundance; two-fold regulation or less is not uncommon. While mRNA abundance is often affected by miRNA regulation, some targets appear to be regulated solely by translational repression(Aleman et al., 2007; Naguibneva et al., 2006; Zhao et al., 2005).

Thus the absence of a change in mRNA abundance of a putative target is not always meaningful, especially if regulation at the mRNA level has not been previously demonstrated. When possible, measurements of the protein regulated is preferred, as changes in mRNA stability or translation should both affect protein levels. When direct measurement of target protein levels is not feasible, protein level regulation by a miRNA can be assessed using luciferase (Box 4) or GFP reporter assays in which the putative target 3′ UTR is cloned into the reporter mRNA. In this case, ASO treatment is predicted to increase reporter levels; conversely, increasing miRNA levels should reduce reporter levels.

When specific target seed sequences are suspected, analysis of 3′ UTRs with mutant seeds can reveal the importance of a specific site for regulation. Such mutational analysis is especially convincing, as it shows miRNA:target complementarity is required for regulation in the context of a potentially quite large 3′UTR. However, the approach assumes that 1) the reporter target expression level is physiologically relevant, and 2) the target and the miRNA are in fact expressed in the same cells. Whenever possible it is preferable to examine endogenous target mRNA and/or protein levels. Reporter assays are best used to augment analysis and allow more focused studies of 3′ UTR sequence motifs.

Proving that a miRNA regulates a given target may implicate it in a particular biological pathway, giving a hint at its function. However, with each miRNA having hundreds of putative targets, proving a biological function for any one interaction may be difficult – individual miRNAs' critical function may be modest regulation of hundreds of genes, or more substantial regulation of just a few.

Cellular Assays

Functional analysis of loss of miRNA function in cultured cells can be performed using any number of cellular assays. Because a growing body of evidence implicates

miRNAs in cancer development, maintenance, and metastasis, several studies have now employed standard assays for proliferation, apoptosis, and metastasis. Using MTT assays and propidium iodide staining coupled with FACS analysis, Matsubara and colleagues found that blocking miR-20a and miR-17-5p with ASOs reduced cell viability and increased the proportion of sub G1 cells. They also used a TUNEL assay to show increased apoptosis when these same miRNAs are inhibited with ASOs(Matsubara et al., 2007). Similarly, Bommer and colleagues used propidium iodide staining and FACS to show that miR-34 inhibition results in increased viability of colon cancer cells. In parallel, these authors demonstrated that ES cells genetically deleted of all three miR-34 isoforms had essentially the same phenotype as pooled ASO inhibition of miR-34: increased cell viability and increased concentration of anti-apoptotic Bcl2 protein(Bommer et al., 2007).

Ma and colleagues found that miR-10b expression enhances metastasis; invasive breast cancer cells failed to migrate as far when treated with miR-10b ASO(Ma et al., 2007). ASOs have also been used in xenograft cancer models to demonstrate that some miRNAs affect metastatic potential and in vivo growth of tumors. While Tavazoie and colleagues found that miR-335 limits breast cancer metastasis (ASO inhibition increases metastasis of xenografted cell lines)(Tavazoie et al., 2008), Corsten and colleagues saw that transplanted gliomas treated with miR-21-specific ASO were sensitized to a chemotherapeutic agent(Corsten et al., 2007).

Several studies use ASOs in conjunction with in vitro differentiation systems to show the importance of individual miRNAs in cellular differentiation. Esau and colleagues showed that miR-143 expression increases during cultured adipocyte differentiation and that this differentiation is inhibited by a miR-143 ASO(Esau et al., 2004). Similarly, Naguibneva and colleagues showed that miR-181 expression is induced upon myoblast terminal differentiation and that an ASO prevents this differentiation by blocking repression of the miR-181 target mRNA, Hox-A11(Naguibneva et al., 2006).

Finally, multiple studies using ASOs suggest roles for endogenous miRNAs in viral defense or replication. Lecellier and colleagues found that ASO inhibition of miR-32, a miRNA with potential target sites in primate foamy cell virus genes, permits enhanced production of viral RNA in human tissue culture cells(Lecellier et al., 2005). Similarly, inhibition of IFN-β induced miRNAs permits Hepatitis C viral production(Pedersen et al., 2007). However, ASO inhibition of liver specific miR-122 in cultured hepatocytes cripples Hepatitis C replication, suggesting its requirement in the Hepatitis C viral life cycle(Jopling et al., 2005; Pedersen et al., 2007). These ASO studies suggest that combinatorial expression of pro- or anti-viral miRNAs may affect tissue tropism of some viruses.

In sum, miRNA function can be efficiently disrupted in cultured mammalian and *Drosophila* S2 cells. The approaches detailed here should be readily adaptable to study miRNA function in any cell line.

BOX 1: Transfection of siRNA and dsRNA for RNAi

The same protocol can be adapted for RNAi using siRNA and dsRNA with just a few alterations, as detailed below. In our experience, transfection of dsRNA into *Drosophila* S2 cells is far more effective than soaking(Clemens et al., 2000) and dsRNA transfection is more effective than siRNA transfection in S2 cells (MDH unpublished).

For Drosophila S2 cells:

Step 8A(iv): Instead of ASO, use 10 pmol siRNA or 1 μg dsRNA per well of a 24 well plate (scaled linearly for other volumes).

Step 8A(ix): Allow S2 cells to grow for 5 days, and then check protein or mRNA abundance. In our experience the best knock-down is achieved if a second transfection is performed at day 5. The cells are analyzed on day 10.

For mammalian cells:

Step 8B(v): Instead of ASO, use 10 pmol siRNA per well of a 24 well plate (scaled linearly for other volumes).

Step 8B(x): For mammalian cells, reduction of protein from the gene targeted by the siRNA can usually be achieved after 3–4 days. A second transfection can be performed if knockdown is insufficient, e.g. if the protein half-life is long.

BOX 2: Analysis of cell number and viability

i. To dislodge S2 cells, pipette media across the bottom of the well or plate several times. S2 cells are semi-adherent and form loose clumps at low density. As the cells approach the correct density they become less adherent and the clumps disperse.

ii. Remove 50 µl of freshly dislodged cells and mix with 50 µl Trypan blue solution in a 1.5 ml Eppendorf tube. Wait 3 min.

iii. Add ~20 µl of the cell suspension to the hemocytometer slide.

iv. Count the number of live cells (clear) and dead cells (blue) contained in the largest box in the field. Count two other complete fields and calculate the average.

v. Multiply by 2×10^4 to determine cells/ml. If the cell number is too great to count (>200 cells in the field), dilute the cells 1:5 in PBS, then proceed from step ii, and multiply by 1×10^5 to determine cells/ml.

vi. When propagating S2 cultures, cells can be diluted to ~2.5×10^5 cells/ml and split each time they reach 8–10 x 10^6 cells/ml. Growth between these densities typically takes ~5 days.

BOX 3: Splitting Adherent Mammalian Cells

i. To split cells using Trypsin-EDTA, pre-warm Trypsin-EDTA solution, PBS, and DMEM-FBS media to 37°C (45min).

ii. Remove media and rinse cells twice with 10 ml pre-warmed PBS.

iii. Add 1 ml Trypsin-EDTA solution evenly cover the cells and place cells in the 37°C , 5% CO_2 incubator for ~5 min.

iv. Briefly check to see that cells have been liberated from the dish and each other using a 50x bright field microscope. If not, place cells back in the 37°C, 5% CO_2 incubator for several additional minutes and re-check them.

v. Add 9 ml pre-warmed DMEM-FBS to cells to inactivate the Trypsin.

vi. Count cells using a hemocytometer and dilute to a density of 1 x 10^5 cells/ml with pre-warmed DMEM-FBS in a 15 ml conical.

vii. Add 2 ml of cells for each well of a 6-well plate.

BOX 4: Assessing miRNA Inhibition with the Dual Luciferase Assay

The dual luciferase system offers a relatively simple approach to assess miRNA inhibition. The psiCheck2 vector system from Promega is a commercially available vector which encodes both *Photinus pyralis* and *Renilla Reniformis* luciferase genes on a single plasmid with a multiple cloning site in the 3′ UTR of *Renilla* luciferase for insertion of synthetic oligonucleotides encoding the miRNA target sites (or other cloned regulatory sequences, such as target 3′UTRs). We have not tested this system in S2 cells, but it has been previously reported(Okamura et al., 2007). Here we briefly list the steps necessary to adapt this reporter system for miRNA sensing and assessment of miRNA inhibition in cultured cells. Additional information is available from the manufacturer (Dual luciferase Assay Manual: www.promega.com/tbs/tm040/tm040.pdf):

i. **Design a miRNA Target Site Insert**. Design a set of two oligonucleotides corresponding to two tandem copies of the miRNA of interest and its reverse complement. Add appropriate overhanging bases corresponding to the restriction enzyme(s) used to digest the psiCheck vector such that the mature miRNA's reverse complement is in the 5′ to 3′ orientation (See manufacturer's information for restriction map; www.promega.com/tbs/tb329/tb329.pdf). XhoI and NotI sites are convenient for directional cloning of inserts. For instance:

miR-277
3′acagcauggucuaucacguaaau5′

5′ggccgc **tgtcgtaccagatagtgcattta** **tgtcgtaccagatagtgcattta** c 3′

3′ cg **acagcatggtctatcacgtaaat** **acagcatggtctatcacgtaaat** gagct **5′**

NotI **miR-277 site** **miR-277 site**

XhoI

ii. **Clone the miRNA Site Insert Into psiCheck 2 Vector.** Digest psiCheck 2 vector, ligate miRNA site insert, transform into *E. coli*, and sequence the insert using a custom sequencing primer to confirm correct orientation of insert (Vector sequence is available in GenBank, accession number AY535007).

iii. **Transfect Mammalian or S2 Cells with ASO.** Prepare mammalian or S2 cells for 6 triplicate transfections (18 wells in a 24 well plate). Transfect 6 wells of cells with miRNA directed ASO and 6 wells with control ASO as described in procedure option A (S2 cells) or option B (mammalian cells). The remaining 6 wells will be used as a no transfection control.

iv. **Transfect Mammalian or S2 Cells with psiCheck 2 Vector.** 24 hours later (mammalian cells) or 48 hour later (S2 cells) perform a second transfection with psiCheck2 (control) or psiCheck2+miR (miRNA sensor). Each vector should be transfected into 3 wells of miRNA ASO treated cells, 3 wells of control ASO treated cells, and 3 wells of untreated cells. Lipofectamine 2000 (Invitrogen) can be used for mammalian cell transfection according to the manufacturers instructions (Promega recommends using 0.1 μg vector/ well of a 24 well plate). siLentFect can be used for transfection of psiCheck2 and psiCheck2+miR vectors into S2 cells as described above, with the following alterations: step iv - DNA mix: 0.1 μg vector + Schneider media to 25 μl final volume , step v - Lipid Mix: 2 μl siLentFect + 23 μl Schneider media.

v. **Perform Luciferase Assay.** 24 hours (mammalian cells) or 48 hours (S2 cells) after transfection of psiCheck vectors, cells can be assayed for luciferase activity. Briefly, cells are washed with PBS, lysed in passive lysis buffer, luciferin reagents are added, and samples are read in a luminometer. Note: Adherent cells can be grown, washed, and lysed in the same plate. S2 cells must be pelleted in Eppendorf tubes (1000 x g for 2 min) each time the media is changed. Details for the dual luciferase assay reagents and protocol are provided by Promega (see above).

vi. **Assessing miRNA Inhibition.** The relative levels of R*enilla* luciferase should reveal first, whether the vector was regulated by the endogenous miRNA, and second, whether the ASO blocked this regulation. In control ASO treated cells, the endogenous miRNA should only regulate psiCheck2+miR, giving it lower *Renilla* luciferase levels than psiCheck2. However, when the miRNA is inhibited in miRNA ASO treated cells, *Renilla* luciferase levels should be similar in all samples. If they are not, miRNA silencing was not fully blocked. Potential problems are described below (see Troubleshooting).

Supplementary Material

Optimization and Comparison of 3' Cholesterol-Modified ASOs

To obtain the maximum possible transfection efficiency, we tested a panel of transfection reagents to find those that were most effective in S2 cells for either 3´-cholesterol-conjugated or unconjugated ASOs. The two perfect-site reporter cell line was transfected with miR-277 or control ASOs, and then FACS analysis was performed three days later. For all seven reagents tested, the 3´ cholesterol-conjugated ASO derepressed the reporter more than the ASO without cholesterol (Fig. S1). Dharmafect 4 performed best. Addition of 1 μM or 5 μM cholesterol-conjugated ASO without a transfection reagent also inhibited miR-277 silencing. Although soaking may be useful in cell lines that cannot be easily transfected, the 80-fold higher concentration required makes soaking less cost effective.

Cell density is critical to the efficient transfection of S2 cells. Because Dharmafect 4 worked well in our survey of transfection reagents, we performed a cell density titration with the two perfect site reporter cell line, using the 3´-cholesterol-conjugated ASO and Dharmafect 4 (Fig. 5). The fraction of transfected cells increased at lower cell density. Optimal transfection was achieved at 2.5 x 10^5 cells/ml.

Figure AI-S1. **Optimization of ASO Transfectio**n. S2 cells expressing a GFP reporter bearing two perfect miR-277-complementary sites were transfected with 20 nM 33 nt 2′-*O*-Me miR-277-specific ASO or a control ASO. Both 3′-Chl and unmodified ASOs were tested for several different transfection reagents. Cells were transfected at 1 x 10^6 cells/ml. GFP fluorescence was measured by FACS. For each transfection reagent, the mean GFP fluorescence of three separate transfections was normalized to the unmodified control ASO transfection. Error bars represent standard deviation of three transfections. Soaking experiments were done in single wells; ASOs were mixed as for transfections, but the transfection reagents were omitted.

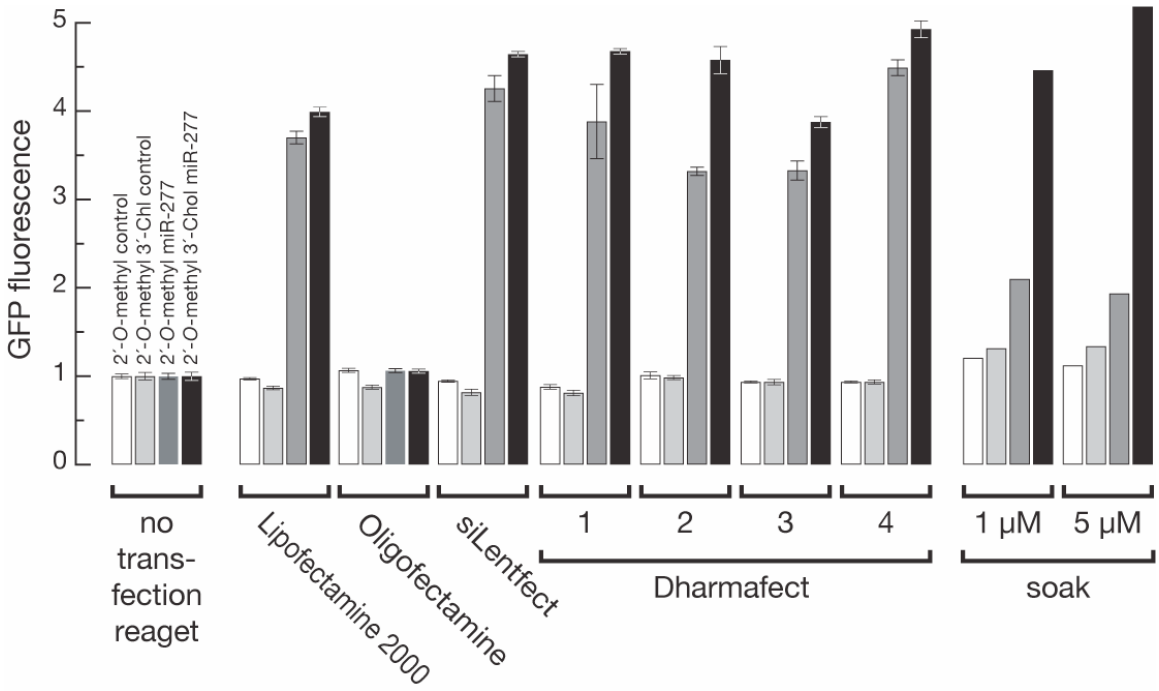

Figure AI-S2. Enhanced miRNA Inhibition with 3′-Cholesterol Modified ASO. (A) Dose response of 3′-cholesterol modified and unmodified ASO. S2 cells expressing a GFP reporter bearing two perfect miR-277-complementary sites were transfected with an increasing concentration of the indicated ASO, and GFP was measured by FACS for three replicate wells. Percent repression was calculated by dividing the mean GFP levels for miR-277 ASOs at the indicated concentration by the GFP level in a control transfection. Error bars represent standard deviation of three separate transfections. IC_{50} values were estimated by fitting to a sigmoidal curve (Hill coefficient = 1). (B) Indicated combinations of free cholesterol, 3′-cholesterol conjugated and unconjugated miR-277 and control ASOs were mixed and transfected into S2 cells. After four days GFP fluorescence was measured by FACS. Percent repression was calculated by dividing the mean GFP levels for miR-277-specific ASO transfection by the GFP levels from a control transfection. IC_{50} values were estimated by fitting to a sigmoidal curve (Hill coefficient = 1). (C) Percent repression was calculated as described above. miR-277 reporter cells were transfected with 10 nM ASOs. The structure of the miR-277 "antagomir" is shown in Fig. 2,(Krutzfeldt et al., 2007).

Figure AI-S2

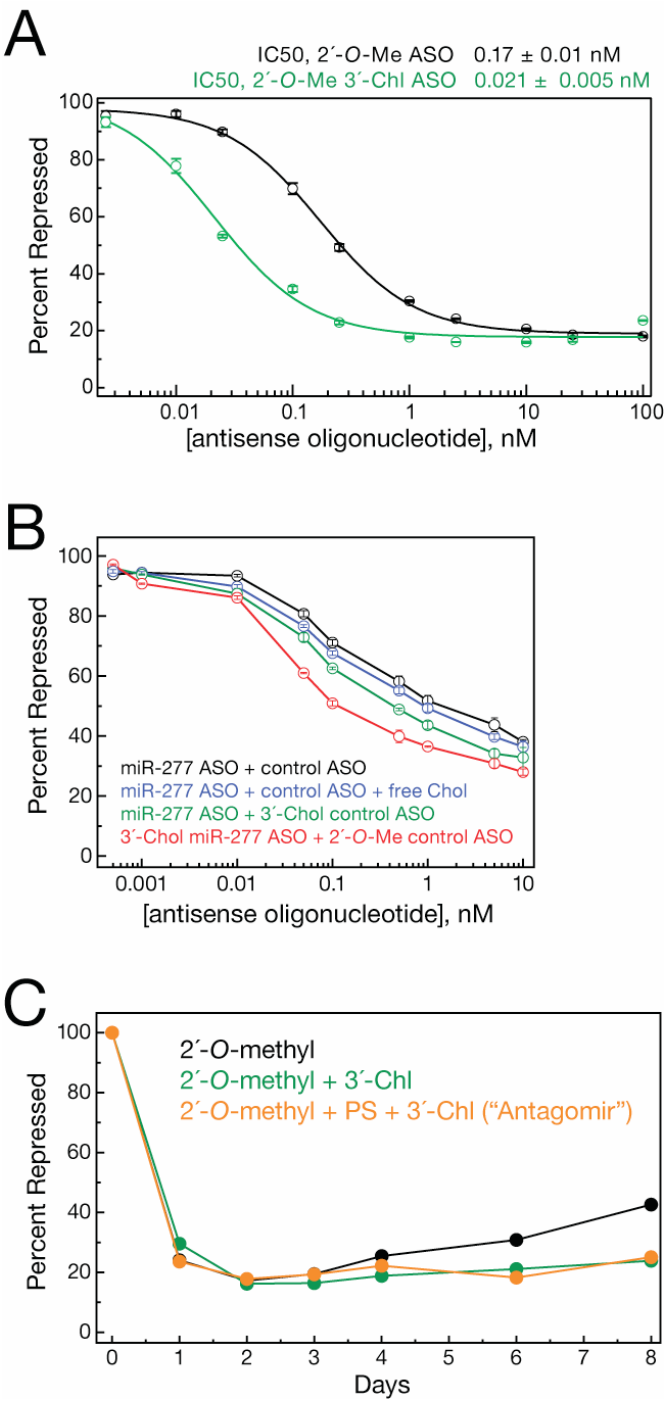
A
IC50, 2′-O-Me ASO 0.17 ± 0.01 nM
IC50, 2′-O-Me 3′-Chl ASO 0.021 ± 0.005 nM
Percent Repressed
[antisense oligonucleotide], nM
B
Percent Repressed
miR-277 ASO + control ASO
miR-277 ASO + control ASO + free Chol
miR-277 ASO + 3′-Chol control ASO
3′-Chol miR-277 ASO + 2′-O-Me control ASO
[antisense oligonucleotide], nM
C
2′-O-methyl
2′-O-methyl + 3′-Chl
2′-O-methyl + PS + 3′-Chl ("Antagomir")
Percent Repressed
Days

Next, we determined the optimal concentration of ASO for cholesterol-conjugated and unconjugated miR-277 ASO (Fig. S2A). Cholesterol-conjugated ASO maximally derepressed the reporter at 2.5 nM, while the ASO without cholesterol required 25 nM ASO for the same extent of derepression.

How does cholesterol conjugation improve ASO-mediated inhibition of miRNAs? We can imagine that conjugation with cholesterol might enhance incorporation of the ASO into liposomes, improve liposome fusion with cells, or potentiate an intracellular step in ASO function, such as delivery of the ASO to the correct intracellular compartment. To assess how cholesterol enhances ASO function, we compared transfection of the cholesterol-conjugated ASO to transfection of an equal amount of a mixture of cholesterol-conjugated and unconjugated ASO and to unconjugated ASOs supplemented with free cholesterol. For each, we determined the IC_{50}. We maintained a constant concentration of cholesterol conjugated and unconjugated ASO (10 nM each), but varied which oligo, miR-277 or control ASO, carried the cholesterol modification. To keep total modified and unmodified ASO constant in the ASO dilution series, miR-277 ASO was mixed with control ASO with the same chemistry.

We found that the IC_{50} for a mixture of 3´-chl miR-277 ASO with unmodified control mixture was ~5 fold lower than that of an unmodified miR-277 ASO mixed with a 3´-cholesterol-conjugated control ASO. These data demonstrate that the enhancement by cholesterol is greatest when it is linked to the miRNA-complementary ASO, suggesting that the cholesterol does not primarily improve ASO function by altering a property of the liposome. Supporting this view, free cholesterol only modestly enhanced the potency of an unmodified ASO, although the addition of a cholesterol-conjugated control ASO enhanced the potency of an unconjugated miRNA-specific ASO (Fig. S2B). We cannot currently distinguish between an effect of the 3´-cholesterol on the assembly of the ASO into the liposome and improved intracellular ASO function. Regardless of the mechanism, 3′-cholesterol-conjugated miR-277 ASO was ~8-fold more potent than

unconjugated ASO (Fig. S2A). This enhanced potency may allow inhibition of multiple miRNAs simultaneously by permitting concurrent transfection of many 3′-cholesterol-conjugated ASOs.

We also tested if cholesterol enhanced the duration of miR-277 inhibition (Fig. S2C). After reaching similar maximal inhibitions at 48 hrs, ~60% of the maximal miRNA inhibition persisted 8 days after transfection of the 3′-cholesterol-conjugated ASO, whereas <30% of the maximal inhibition remained for unmodified ASO. A miR-277 "antagomir" performed similarly to the 3′-cholesterol-conjugated 31-mer, suggesting that it was the cholesterol moiety, not the phosphorothioate modifications that enhanced the persistence of inhibition.

Table AI-1. Cell, ASO, and Lipid Volumes for Transfection of Cultured *Drosophila* Cells

	Volume of cells (2.75×10^5 / ml)	ASO mix		Lipid mix	
		ASO (10 µM)	Schneider media	Dharmafect 4	Schneider media
24 well plate	450 µl / well	1.25 µl	23.75 µl	1 µl	24 µl
6 well plate	1.8 ml / well	5 µl	95 µl	4 µl	94 µl
10 cm Dish	9 ml / dish	25 µl	475 µl	20 µl	480 µl

Table AI-2. Cell, ASO, and Lipid Volumes for Transfection of Cultured Mammalian Cells

	Volume fresh DMEM+10% FBS	ASO mix		Lipid mix	
		ASO (10 µM)	DMEM	Dharmafect 4	DMEM
24 well plate	450 µl / well	1.25 µl	23.75 µl	1 µl	24 µl
6 well plate	1.8 ml / well	5 µl	95 µl	4 µl	94 µl
10 cm Dish	9 ml / dish	25 µl	475 µl	20 µl	480 µl

Table AI-3. TROUBLESHOOTING:

PROBLEM	POSSIBLE REASONS	SOLUTION
ASO does not derepress reporter.	ASO forms strong secondary structure.	Redesign flanking sequences.
	ASO transfection was not efficient.	Co-transfect plasmid and ASO. If derepression is now observed, ASO transfection was inefficient. Repeat ASO transfection or optimize transfection.
	Endogenous miRNA is not abundant enough to repress the reporter.	Check miRNA level by northern blot. Try co-transfection with a frayed siRNA corresponding to the miRNA strand(Schwarz et al., 2003) to be sure it is not a problem with the reporter. A pri-miRNA expression vector could also be used.
	Incorrect reporter target site.	If the reporter cannot be repressed, check the miRNA target site in reporter sequence.
	Cholesterol modified ASO was not mixed.	Vortex ASO stock before use and mix ASO-S2 cell mix by tapping the tube.
Cells die after ASO transfection.	Too much transfection reagent or ASO used.	Possible if cell death is seen in miRNA-specific ASO and control ASO transfected samples. Repeat with correct amount of transfection reagent or ASO or replace media after 12–24 h.
	Cell density was too low.	Repeat with correct cell density.
		Possible if miRNA ASO kills

	miRNA inhibited is required for cell survival.	cells, but control ASO does not. Determine mechanism of cell death. Perhaps the miRNA is anti-apoptotic. Gain of function studies may also be informative (e.g. does overexpression protect cells from apoptosis?).

Appendix II:

Feedback Control by the Human microRNA, *let-7*, Regulates Expression of the microRNA Processing Enzyme, Dicer

Hervé Seitz[1], Michael Horwich[1], Benjamin Haley[1], Bradford Stadler[2], Benjamin Lewis[3], Sanchita Bhattacharya[4], Jan Krützfeldt[5], Markus Stoffel[5], Phillip D. Zamore[1*], and György Hutvágner[6*]

[1]Department of Biochemistry and Molecular Pharmacology and [2]Department of Molecular Genetics and Microbiology, University of Massachusetts Medical School, Worcester 01605, USA; [3]Department of Biology and The Whitehead Institute for Biomedical Research and [4]BioMicro Center, Massachusetts Institute of Technology, Cambridge, MA 02139, USA; [5]Laboratory of Metabolic Diseases, The Rockefeller University, 1230 York Avenue, New York, New York 10021, USA; [6]University of Dundee School of Life Sciences, Department of Gene Regulation and Expression, Dundee, UK DDE 5EH.

Contributions: This is a submitted manuscript that is in revision. The author conducted experiments for figures 9, 10, and S2. Jan Krützfeldt injected mice and collected tissues. Ben Haley did target cleavage experiments (fig 8). Gyorgy Hutvagner did experiments in figures 1, 2, 3, and 6. Ben Lewis provided data for figures 4 and 5. Herve Seitz did everything else.

Summary

microRNAs (miRNAs) are small, ~21 nucleotide long RNAs that repress gene expression via the RNA silencing pathway. *let-7* was the first human miRNA identified, but few of its regulatory target genes are known. Using microarray analysis of human cell lines in which *let-7* miRNA function was either blocked or ectopically introduced, we identified Dicer, the ribonuclease that generates miRNAs, and HMGA2, an architectural transcription factor implicated in oncogenesis, as *let-7* regulatory targets. The mRNAs of both genes contain multiple predicted *let-7*-responsive elements. Although none of the target sites have sufficient complementarity to support *let-7*-directed endonucleolytic cleavage, *let-7* nonetheless represses the steady-state levels of both the mRNA and proteins encoded by these two target genes. Our human cultured cell data and experiments in vivo in adult mice indicate that feedback regulation by *let-7* controls expression of Dicer, suggesting that *let-7* is a global regulator of the small RNA biogenesis pathway.

Introduction

miRNAs are an abundant class of 21-22 nucleotide long RNAs. They constitute more than 1% of human genes and are thought to repress gene expression of target genes to which they are complementary (Bartel, 2004); one-third of all human protein coding genes have been proposed to be evolutionarily conserved regulatory targets of miRNAs (Bartel, 2004; Krek et al., 2005; Lewis et al., 2005). When miRNAs pair extensively with their mRNA targets, they direct target RNA cleavage at the phosphodiester bond across from miRNA nucleotides ten and eleven (Hutvágner and Zamore, 2002), much as small interfering RNAs (siRNAs) do in the RNA interference (RNAi) pathway (Elbashir et al., 2001b). At least six animal miRNAs and most if not all plant miRNAs guide the cleavage of their targets in vivo (Davis et al., 2005; Llave et al., 2002; Reinhart et al., 2002;

Rhoades et al., 2002; Tang et al., 2003; Yekta et al., 2004). However, most animal miRNAs pair only imperfectly to sites within their mRNA targets. Consequently, they repress the expression of their target genes without directing mRNA endonucleolytic cleavage (Doench et al., 2003; Doench and Sharp, 2004; Olsen and Ambros, 1999; Pillai et al., 2005). Originally, such translational regulation was thought to occur without altering target mRNA stability, but recent evidence suggests that miRNAs can destabilize the mRNAs to which they bind, even when they cannot direct mRNA cleavage (Bagga et al., 2005; Jing et al., 2005; Lim et al., 2005; Wu et al., 2006; Giraldez et al., 2006; Wu et al., 2006).

First discovered in *C. elegans* (Reinhart et al., 2000), the *let-7* miRNA family is conserved throughout bilaterally symmetric animals and was the first identified in humans (Pasquinelli et al., 2000). *let-7* regulates developmental timing in *C. elegans* (Reinhart et al., 2000), its expression is dramatically increased at metamorphosis in flies (Bashirullah et al., 2003; Hutvágner and Zamore, 2002; Sempere et al., 2002), and has been proposed to repress expression of Ras proto-oncogenes in human cells (Johnson et al., 2005). Here, we report that Dicer, the ribonuclease that generates miRNAs, and HMGA2, an architectural transcription factor implicated in oncogenesis, are regulated in vertebrates by *let-7*. The mRNAs of both genes contain multiple, evolutionarily conserved *let-7*-responsive elements. Although none of the target sites has sufficient complementarity to support *let-7*-directed endonucleolytic cleavage, *let-7* nonetheless represses the steady-state levels of both the mRNAs and proteins encoded by these two target genes. In adult mice, inhibition of *let-7* function increases the steady-state concentration of Dicer mRNA. Our data indicate that *let-7* controls expression of Dicer in vivo, suggesting that optimal Dicer mRNA levels are maintained by miRNA-directed negative feedback regulation. In plants, miR-162 directs a similar negative feedback loop to regulate expression of DICER-LIKE1, the plant Dicer protein that produces miRNAs

(Xie et al., 2003). Because the miRNA pathways in plants and animals evolved separately—no miRNA species are shared by the two kingdoms—negative feedback control of Dicer expression by miRNAs in plants and animals appears to have evolved at least twice, an example of the convergent evolution of a common strategy for regulating a key enzyme in the production of miRNAs.

Results

Identifying let-7-Regulated mRNAs by Expression Profiling

We sought to identify experimentally human genes regulated by *let-7*. First, we compared the steady-state mRNA profile of cultured human HeLa cells, which express about 13,000 molecules of *let-7* per cell (GH and PDZ unpublished), with that of HeLa cells in which *let-7* function was experimentally inhibited. Then, we compared the mRNA profile of human embryonic carcinoma NT2 cells, which do not detectably express *let-7* (Figure 1) and which do not repress expression of a *let-7*-responsive reporter plasmid (Figure S1A), with that of NT2 cells into which *let-7a* was introduced. For those genes expressed in both cell lines, we anticipated that expression of authentic *let-7* target genes would be increased by blocking *let-7* function in HeLa cells and decreased by introducing *let-7a* into NT2 cells.

2′-*O*-methyl antisense oligonucleotides containing a central region complementary to the sequence of a miRNA are potent inhibitors of miRNA function in vitro and in vivo (Hutvágner et al., 2004; Meister et al., 2004a). To block *let-7* function, we used a 31-nucleotide long, 2′-*O*-methyl oligonucleotide that had been shown previously to inhibit *let-7* function in HeLa cell cytoplasmic extracts and in *C. elegans* larvae (Hutvágner et al., 2004). The *let-7*-specific 2′-*O*-methyl oligonucleotide effectively inhibited *let-7*-mediated repression of a reporter gene containing a single *let-7*-responsive sequence element (LRE) (Kiriakidou et al., 2004), but had no effect on expression of a reporter bearing a non-functional, mutant LRE (Figure S1B).

Figure AII-1

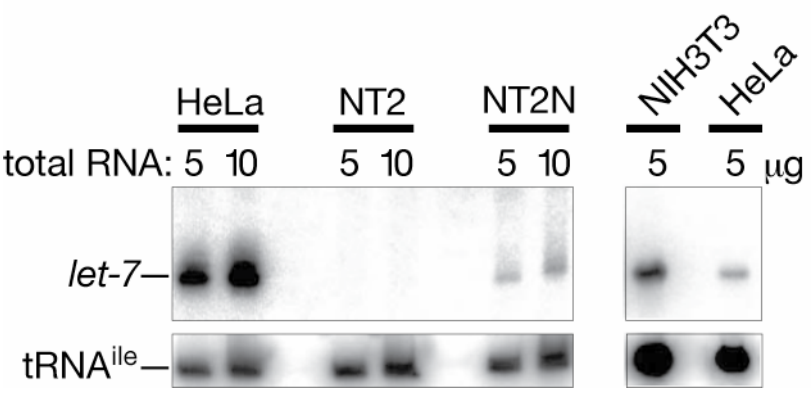

Figure AII-1. *let-7* expression was determined by Northern analysis for human HeLa cervical carcinoma, NT2 embryonic carcinoma, retinoic acid-treated NT2N cells, and mouse NIH3T3 fibroblasts. $tRNA^{ile}$ was used as a loading control. The *let-7* probe was designed to detect *let-7a*, but cannot distinguish among the most closely related *let-7* paralogs.

We used the *let-7*-specific 2′-*O*-methyl oligonucleotide to inhibit *let-7* function in human HeLa cells and profiled mRNA expression levels by microarray analysis. A 2′-*O*-methyl oligonucleotide with no complementarity to any known human miRNA or gene served as a control. mRNA expression was detected for 6,294 unique human genes, out of a possible 13,110 genes detectable by the array. Microarray analysis was performed on three independently prepared samples for both the experiment and the control. In parallel, we introduced into NT2 cells an siRNA in which the guide strand corresponded to *let-7a* or, as a control, an siRNA targeting the luciferase mRNA. The *let-7a* siRNA, but not the control siRNA, repressed expression of a *let-7*-responsive reporter in NT2 cells (Figure S1C). The transcriptional profiles of the cells treated with the *let-7a* siRNA and the cells treated with the control siRNA were determined by microarray analysis for three independent experiments. For NT2 cells, mRNA expression was detected for 6,458 unique human genes. Eighty-six percent of the mRNAs whose expression was detected in NT2 cells were also expressed in HeLa cells. Of the 5,537 genes whose expression was detected in both HeLa and NT2 cells, we detected only two genes, Dicer and HMGA2, whose mRNA level was significantly increased when *let-7* function was inhibited in HeLa cells (Dicer, 2.6-fold, $p < 0.05$, and HMGA2, 3.4-fold, $p < 1.6 \times 10^{-7}$) and whose mRNA level also showed a corresponding, statistically significant decrease in the NT2 cells when the *let-7a* siRNA was introduced (Dicer, 2.5-fold, $p < 1.1 \times 10^{-8}$, and HMGA2 3.4-fold, $p < 6 \times 10^{-17}$) (Figure 2A, Tables S1 and S2).

let-7 reduces Dicer and HMGA2 mRNA and Protein Accumulation

Quantitative reverse transcription/polymerase chain reaction (qRT-PCR) experiments confirmed our microarray results for Dicer and HMGA2 mRNAs (Figure 2B). When *let-7* function was blocked in HeLa cells, Dicer mRNA increased by a factor of 2.0 ± 0.9 (average of three trials ± standard deviation) and HMGA2 mRNA increased by a factor of 3.9 ± 1.7 in this assay. Conversely, when *let-7a* was introduced into NT2

Figure AII-2. *let-7* regulates Dicer and HMGA2 mRNA stability in cells that express this miRNA. (A) Microarray analysis of steady-state mRNA levels when *let-7* function was blocked in HeLa cells or when *let-7a* was introduced as an siRNA into NT2 cells. The average (n = 3) change in abundance, relative to the control, is reported for each mRNA versus the statistical significance of the change (adjusted p-value). (B) Quantitative PCR analysis of Dicer and HMGA2 mRNA levels after *let-7* function was predicted to be a target of any miRNA known to be expressed in HeLa cells.

Figure AII-2

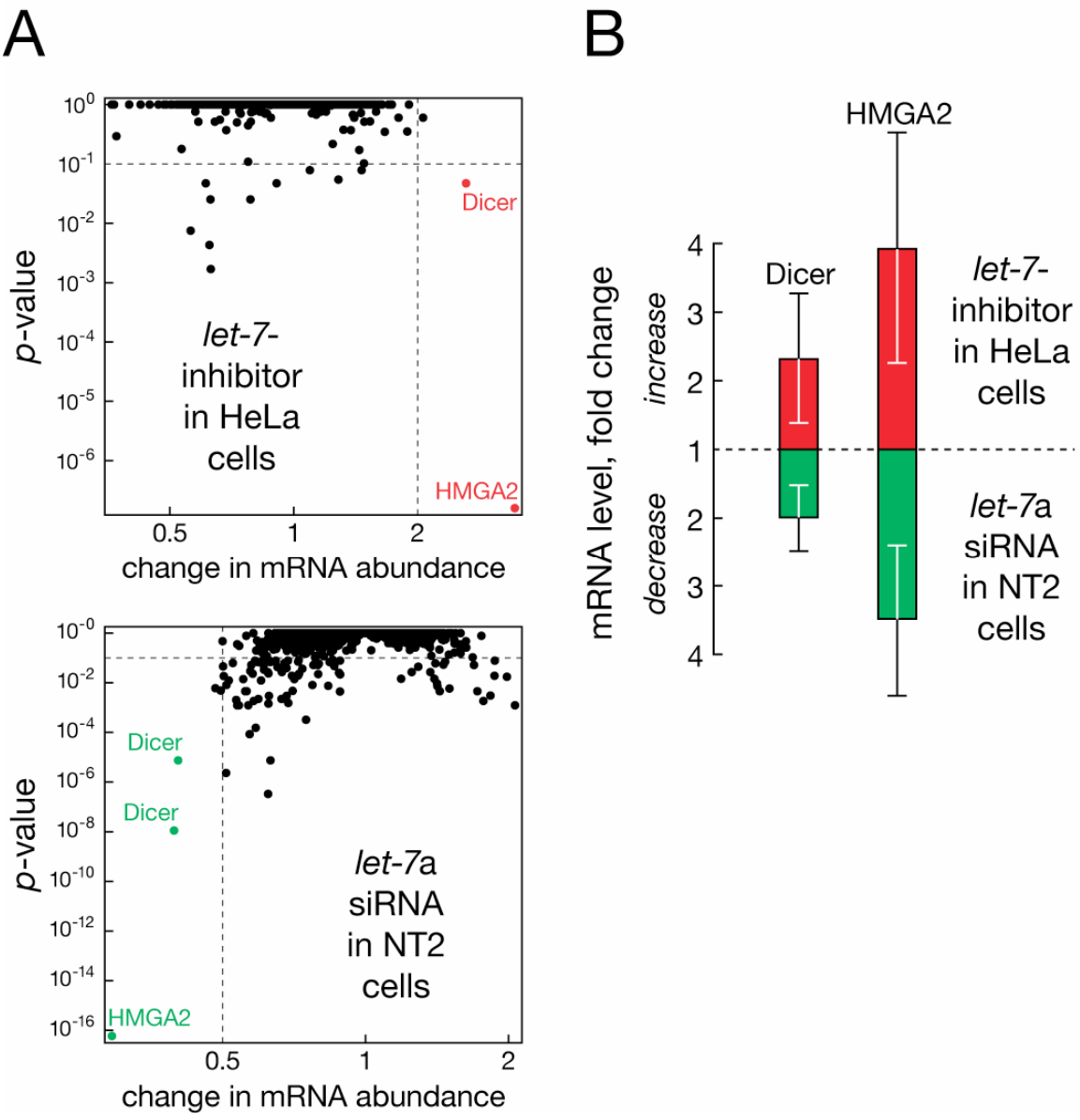
A
p-value
Dicer
HMGA2
let-7-
inhibitor
in HeLa
cells
change in mRNA abundance
Dicer
Dicer
HMGA2
let-7a
siRNA
in NT2
cells
change in mRNA abundance
B
mRNA level, fold change
increase
decrease
Dicer
HMGA2
let-7-
inhibitor
in HeLa
cells
let-7a
siRNA
in NT2
cells

cells, Dicer mRNA decreased by a factor of 2.0 ± 0.5 and HMGA2 mRNA decreased by a factor of 3.5 ± 1.1. Like Dicer mRNA, Dicer protein increased when *let-7* function was blocked in HeLa cells and decreased when *let-7a* was introduced into NT2 cells (Figure 3). Inhibition of *let-7* in HeLa cells using the *let-7*-specific 2´-*O*-methyl oligonucleotide nearly doubled Dicer protein levels (Figure 3A). Conversely, transfection of the *let-7a* siRNA into NT2 cells reduced Dicer expression (Figure 3B). In fact, the effect of the *let-7a* siRNA was comparable to that of a perfectly matched siRNA targeting the Dicer mRNA for cleavage (Figure 3B). HMGA2 protein also decreased when the *let-7a* siRNA was introduced into NT2 cells (Figure 3C). The *let-7a* siRNA reduced HMGA2 protein expression more than 3-fold, comparable to the reduction caused by transfection of an siRNA with perfect complementarity to the HMGA2 mRNA (Figures 2B and 3C). Unlike HMGA2 mRNA, HMGA2 protein was not detectable in HeLa cells before (Figure 3D) or after increasing its steady-state transcript level by inhibiting *let-7* (data not shown), suggesting that some other mechanism—perhaps miRNAs other than *let-7*—still represses its translation in the absence of *let-7* function. To confirm that translation of the HMGA2 mRNA is regulated by *let-7*, at least in part, we examined HMGA2 in NIH3T3 mouse fibroblast cells, where the HMGA2 protein was readily detected (Figure 3D). These cells express both *let-7* (Figure 1A) and HMGA2 protein (Figure 3D). Inhibition of *let-7* function in NIH3T3 cells more than doubled HMGA2 protein (Figure 3E). Conversely, transfection of *let-7a* siRNA into these cells, to increase the amount of *let-7a*, reduced expression of HMGA2 protein. HMGA2 expression also paralleled the developmental expression of *let-7*. *let-7* expression is induced when NT2 cell differentiate along a neuronal pathway following treatment with retinoic acid (Sempere et al., 2002) (Figure 1A), and HMGA2 protein significantly decreased upon retinoic acid-induced neuronal differentiation of NT2 to NT2N cells (Figure 3D). HMGA2 is an architectural transcription factor that binds the minor groove of AT-rich DNA (Tessari et al., 2003) and is a component of the enhancesome (Reeves, 2000). Overexpression of

HMGA2 in mice leads to pituitary adenomas and natural killer cell lymphomas (Fedele et al., 2002). HMGA2 expression is increased in a wide range of tumors including pulmonary cancer (Wisniewski and Schwanbeck, 2000). Tantalizingly, the most aggressive lung cancers are those that have lost *let-7* expression (Takamizawa et al., 2004).

Dicer and HMGA2 mRNAs Contain Conserved let-7-Responsive Elements

Small RNAs, such as miRNAs and siRNAs, bind their target RNAs primarily by sequence complementarity between the target and six or seven nucleotides in the 5′ end of the small RNA (Brennecke et al., 2005; Doench and Sharp, 2004; Haley and Zamore, 2004; Krek et al., 2005; Lai, 2002; Lewis et al., 2005; Lewis et al., 2003; Mallory et al., 2004). This specialized small RNA domain, the 'seed' sequence, is thought to reflect how small RNAs are bound to members of the Argonaute family of proteins, the core components of the ribonucleoprotein complexes called RISC (RNA-induced silencing complex), which mediate silencing by both miRNAs and siRNAs. Computational prediction of miRNA targets begins with the premise that pairing of the miRNA seed—nucleotides 2–7 of the small RNA—recruits a miRNA-programmed RISC to a target RNA. In fact, both Dicer and HMGA2 were previously predicted to contain multiple *let-7*-responsive elements (LRE) (Krek et al., 2005; Lewis et al., 2005). The Dicer mRNA contains four evolutionarily conserved, *let-7* seed matches in its coding region (Figure 4). The HMGA2 mRNA contains seven evolutionarily conserved, *let-7* seed matches in its 3′ untranslated region (UTR) (Figure 5), consistent with earlier findings that HMGA2 mRNA translation is negatively regulated by elements in its 3′ UTR (Borrmann et al., 2001). Historically, miRNA-binding sites were thought to reside mainly in 3′ UTRs, but

Figure AII-3. Dicer and HMGA2 protein expression are repressed by *let-7*. (A) Antisense inhibition of *let-7* in HeLa cells increased Dicer protein expression, relative to an unrelated, luciferase-specific 2′-*O*-methyl antisense oligonucleotide. (B) Introduction of *let-7a* as an siRNA into NT2 cells, which do not normally contain detectable *let-7*, decreased Dicer protein expression, relative to the expression of tubulin. A GFP siRNA provided a negative control, and a Dicer-specific siRNA (targeting LRE 2, see Supplementary Table 3) provided a positive control. (C) Transfection of *let-7a* siRNA decreased HMGA2 protein level in NT2 cells. A GFP siRNA served as a negative control; an HMGA2-specific siRNA served as a positive control. (D) HMGA2 protein expression decreased when NT2 cells were differentiated by treatment with retinoic acid into NT2N cells. Retinoic acid-treatment induces *let-7* expression in NT2 cells. (E) Inhibiting *let-7* function in NIH3T3 cells using a 2′-*O*-methyl oligonucleotide increased HMGA2 protein levels >2-fold. Conversely, adding additional *let-7* by transfecting a *let-7a* siRNA decreased the expression of HMGA2 protein >3-fold. Above each lane, the fold-change in Dicer or HMGA2 protein levels, normalized to tubulin, are reported elative to the control treatment.

Figure AII-3

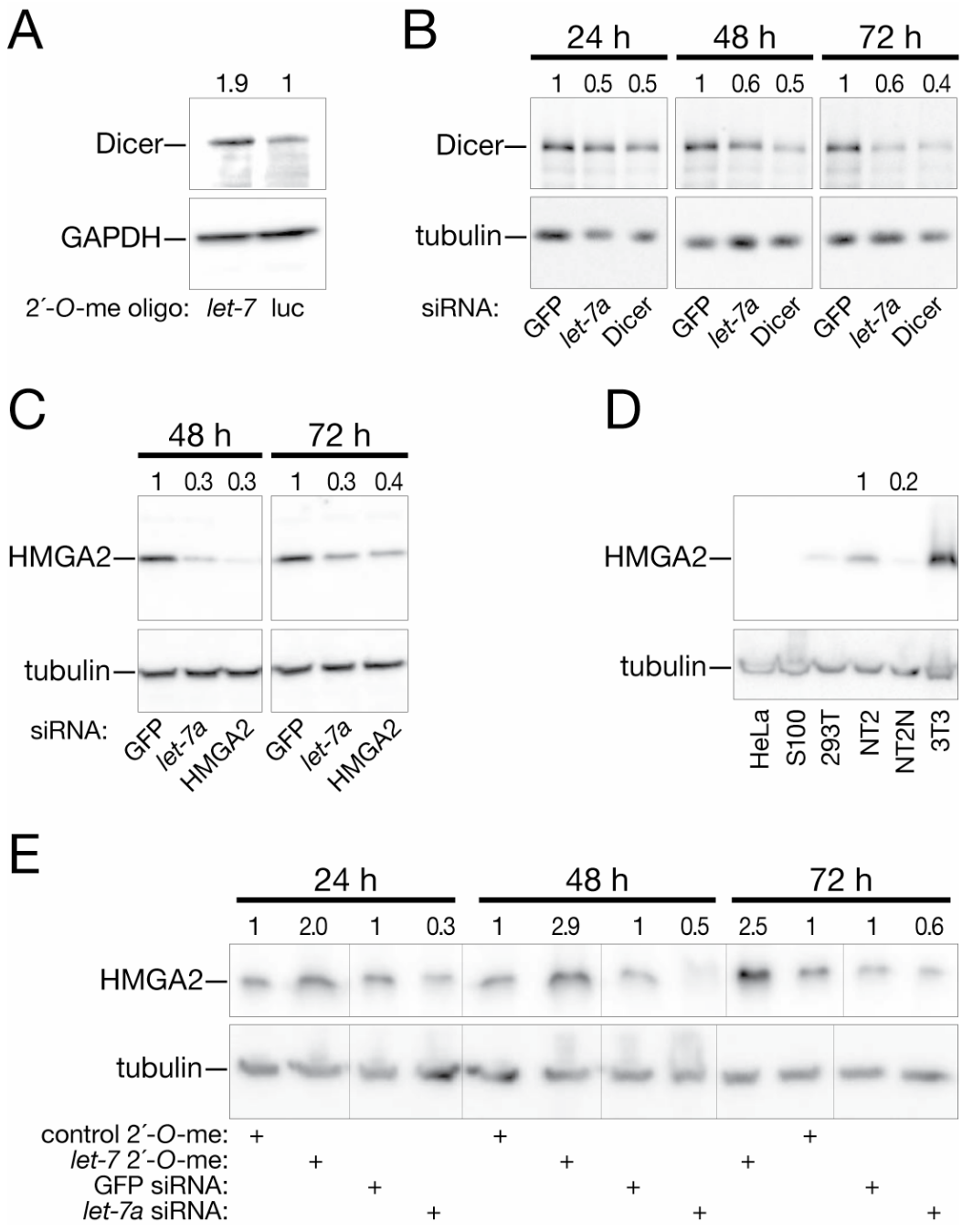
A
1.9 1
Dicer—
GAPDH—
2´-O-me oligo: let-7 luc
B
24 h
48 h
72 h
1 0.5 0.5 1 0.6 0.5 1 0.6 0.4
Dicer—
tubulin—
siRNA: GFP let-7a Dicer GFP let-7a Dicer GFP let-7a Dicer
C
48 h
72 h
1 0.3 0.3 1 0.3 0.4
HMGA2—
tubulin—
siRNA: GFP let-7a HMGA2 GFP let-7a HMGA2
D
1 0.2
HMGA2—
tubulin—
HeLa S100 293T NT2 NT2N 3T3
E
24 h
48 h
72 h
1 2.0 1 0.3 1 2.9 1 0.5 2.5 1 1 0.6
HMGA2—
tubulin—
control 2´-O-me: + + +
let-7 2´-O-me: + + +
GFP siRNA: + + +
let-7a siRNA: + + +

small RNAs can also repress expression of their target genes when they pair imperfectly to as few as one or two sites in the target mRNA coding region (Kloosterman et al., 2004; Saxena et al., 2003). The Dicer and HMGA2 LREs are conserved among at least nine and five vertebrates, respectively.

let-7 Represses Dicer and HMGA2 mRNA Expression, but Does Not Direct mRNA Cleavage

Studies in *C. elegans* and in cultured human cells suggest that animal miRNAs repress translation of their target mRNAs without altering their steady-state levels (Doench et al., 2003; Olsen and Ambros, 1999). However, recent data suggest that miRNAs can alter mRNA target stability (Bagga et al., 2005; Jing et al., 2005; Lim et al., 2005), even when they lack sufficient complementarity to direct Argonaute2-catalyzed, endonucleolytic cleavage of their mRNA targets. Since *let-7* reduces the steady-state RNA level of Dicer and HMGA2, we asked if this decrease is the consequence of endonucleolytic cleavage of the target RNA or rather results from recruitment of the mRNA into a more general pathway for RNA destruction. Of the ten predicted LREs in Dicer and HMGA2, HMGA2 LRE 6 is most complementary to *let-7* (Figure 5) and is thus the best candidate to direct Argonaute2-catalyzed mRNA cleavage (Chiu and Rana, 2002; Haley and Zamore, 2004; Hutvágner and Zamore, 2002). We used 5´ RACE to identify stable cleavage products deriving from *let-7*-directed cleavage of the HMGA2 mRNA within LRE 6. Such cleavage products are diagnostic of Argonaute2-catalyzed, small RNA-directed endonucleolytic cleavage (Llave et al., 2002; Yekta et al., 2004), and are prima facie evidence that an mRNA is destroyed by the RNAi pathway

Figure AII-4. Conservation of the four predicted Dicer LREs among vertebrate species. (A) *Hs*, *Homo sapiens*; *Mm*, *Mus musculus*, house mouse; *Rn*, *Rattus norvegicus*, rat; *Cf*, *Canis familiaris*, dog; *Bt*, *Bos taurus*, cow; *Gg*, *Gallus gallus*, chicken; *Xt*, *Xenopus tropicalis*, frog; *Dr, Danio rerio*, zebrafish; *Fr*, *Fugu rubripes*, Pufferfish. Dark blue denotes bases conserved in all vertebrates analyzed; the bar indicates the region matching the *let-7* augmented seed region[3]. The corresponding amino acid is indicated for each Dicer codon. (B) Putative LREs in the Dicer mRNA coding region and their complementarity to *let-7a*.

Figure AII-4

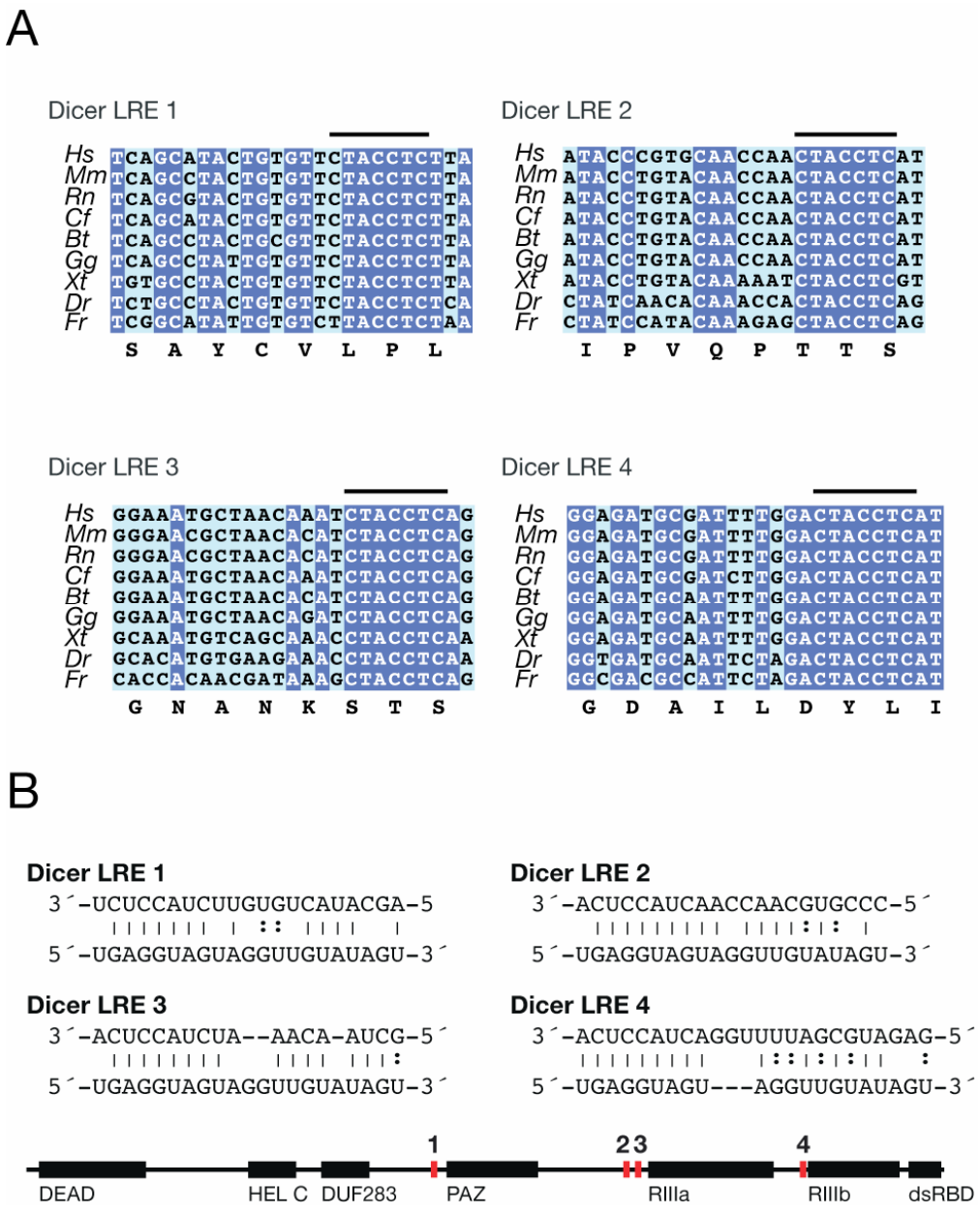
A
Dicer LRE 1
Hs TCAGCATACTGTGTTCTACCTCTTA
Mm TCAGCCTACTGTGTTCTACCTCTTA
Rn TCAGCGTACTGTGTTCTACCTCTTA
Cf TCAGCATACTGTGTTCTACCTCTTA
Bt TCAGCCTACTGCGTTCTACCTCTTA
Gg TCAGCCTATTGTGTTCTACCTCTTA
Xt TGTGCCTACTGTGTTCTACCTCTTA
Dr TCTGCCTACTGTGTTCTACCTCTCA
Fr TCGGCATATTGTGTCTTACCTCTAA
S A Y C V L P L
Dicer LRE 2
Hs ATACCCGTGCAACCAACTACCTCAT
Mm ATACCTGTACAACCAACTACCTCAT
Rn ATACCTGTACAACCAACTACCTCAT
Cf ATACCTGTACAACCAACTACCTCAT
Bt ATACCTGTACAACCAACTACCTCAT
Gg ATACCTGTACAACCAACTACCTCAT
Xt ATACCTGTACAAAATCTACCTCGT
Dr CTATCAACACAAACCACTACCTCAG
Fr CTATCCATACAAAGAGCTACCTCAG
I P V Q P T T S
Dicer LRE 3
Hs GGAAATGCTAACAAATCTACCTCAG
Mm GGGAACGCTAACACATCTACCTCAG
Rn GGGAACGCTAACACATCTACCTCAG
Cf GGAAATGCTAACAAATCTACCTCAG
Bt GGAAATGCTAACACATCTACCTCAG
Gg GGAAATGCTAACAGATCTACCTCAG
Xt GCAAATGTCAGCAAACCTACCTCAA
Dr GCACATGTGAAGAAACCTACCTCAA
Fr CACCACAACGATAAAGCTACCTCAG
G N A N K S T S
Dicer LRE 4
Hs GGAGATGCGATTTTGGACTACCTCAT
Mm GGAGATGCGATTTTGGACTACCTCAT
Rn GGAGATGCGATTTTGGACTACCTCAT
Cf GGAGATGCGATCTTGGACTACCTCAT
Bt GGAGATGCAATTTTGGACTACCTCAT
Gg GGAGATGCAATTTTGGACTACCTCAT
Xt GGAGATGCAATTTTGGACTACCTCAT
Dr GGTGATGCAATTCTAGACTACCTCAT
Fr GGCGACGCCATTCTAGACTACCTCAT
G D A I L D Y L I
B
Dicer LRE 1
3´-UCUCCAUCUUGUGUCAUACGA-5
5´-UGAGGUAGUAGGUUGUAUAGU-3´
Dicer LRE 2
3´-ACUCCAUCAACCAACGUGCCC-5´
5´-UGAGGUAGUAGGUUGUAUAGU-3´
Dicer LRE 3
3´-ACUCCAUCUA--AACA-AUCG-5´
5´-UGAGGUAGUAGGUUGUAUAGU-3´
Dicer LRE 4
3´-ACUCCAUCAGGUUUUAGCGUAGAG-5´
5´-UGAGGUAGU---AGGUUGUAUAGU-3´
1
2 3
4
DEAD
HEL C
DUF283
PAZ
RIIIa
RIIIb
dsRBD

Figure AII-5. Predicted *let-7* target sites in human HMGA2 mRNA. (A) HMGA2 LREs and their complementarity to *let-7a*. (B) Location of the seven LREs in the 3′ untranslated region of *Homo sapiens* (*Hs*), mouse (*Mm*), rat (*Rn*), dog (*Cf*), and chicken (*Gg*) HMGA2 mRNAs. (C) Conservation of bases in the HMGA2 3′ untranslated region among the five vertebrate species analyzed. The position of the seven LREs is indicated.

Figure AII-5

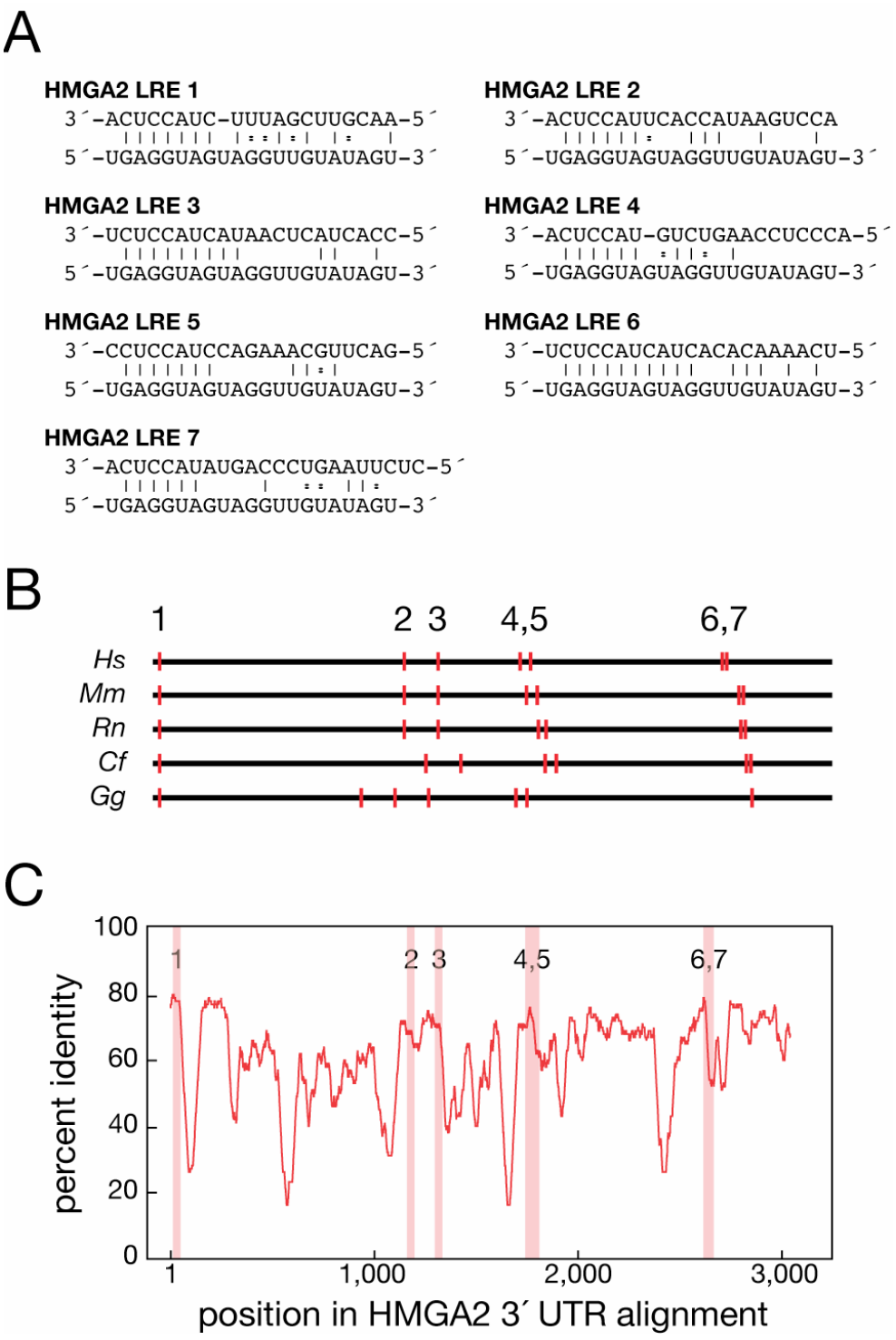
A
HMGA2 LRE 1
3´-ACUCCAUC-UUUAGCUUGCAA-5´
5´-UGAGGUAGUAGGUUGUAUAGU-3´
HMGA2 LRE 2
3´-ACUCCAUUCACCAUAAGUCCA
5´-UGAGGUAGUAGGUUGUAUAGU-3´
HMGA2 LRE 3
3´-UCUCCAUCAUAACUCAUCACC-5´
5´-UGAGGUAGUAGGUUGUAUAGU-3´
HMGA2 LRE 4
3´-ACUCCAU-GUCUGAACCUCCCA-5´
5´-UGAGGUAGUAGGUUGUAUAGU-3´
HMGA2 LRE 5
3´-CCUCCAUCCAGAAACGUUCAG-5´
5´-UGAGGUAGUAGGUUGUAUAGU-3´
HMGA2 LRE 6
3´-UCUCCAUCAUCACACAAAACU-5´
5´-UGAGGUAGUAGGUUGUAUAGU-3´
HMGA2 LRE 7
3´-ACUCCAUAUGACCCUGAAUUCUC-5´
5´-UGAGGUAGUAGGUUGUAUAGU-3´
B
1
2 3
4,5
6,7
Hs
Mm
Rn
Cf
Gg
C
100
80
60
40
20
0
percent identity
1
2 3
4,5
6,7
1
1,000
2,000
3,000
position in HMGA2 3´ UTR alignment

(Soutschek et al., 2004). Although HMGA2 LRE 6 can mediate *let-7*–repression of reporter gene expression, we could not detect any stable 3′ cleavage product for this region of the HMGA2 mRNA in HeLa cells (Figure 8). In contrast, a stable 3′ cleavage product for the LRE 6 region of HMGA2 mRNA was readily detected when a control siRNA with complete complementarity to LRE 6 was introduced into the HeLa cells (Figure 8A). For the control siRNA, the cDNAs of these cleavage products were cloned and sequenced; the 5′ ends of 14 of 18 clones corresponded precisely to the scissile phosphate predicted for the siRNA with perfect complementarity to the HMGA2 LRE 6 (Figure 8A).

Our data demonstrate that *let-7* regulates both Dicer and HMGA2 expression in cultured human cells. To assess if *let-7* controls these target mRNAs through the predicted Dicer and HMGA2 LREs, we constructed reporter vectors containing Dicer LRE 2 and 3, HMGA2 LRE 2, 3, 4, and 5, or HMGA2 LRE 6 and 7 inserted into the 3′ UTR of the *Renilla reniformis* (*Rr*) luciferase mRNA . Each reporter was tested for its ability to respond to *let-7* in HeLa, NT2 and NIH3T3 cells. The expression of each of the three reporter constructs increased when the function of the endogenous *let-7* RISC was inhibited in HeLa cells and NIH3T3 cells (Figure 6A). Conversely, introduction of the *let-7a* siRNA into NT2 cells repressed each of the three LRE-containing reporter plasmids (Figure 6B). Reporter regulation by *let-7* was lost when mutations were introduced into the seed region of the Dicer and HMGA2 LREs (Figure 7).

In vitro RNAi provides a more sensitive method for detecting small RNA activity than cultured cell experiments (Haley and Zamore, 2004). Cleavage products are stable and continue to accumulate in RNAi reactions derived from *Drosophila* embryos for at

Figure AII-6. *let-7*-responsive elements (LREs) mediate Dicer and HMGA2 repression by *let-7*. (A) LRE-containing Renilla luciferase reporter expression was increased in *let-7*-containing human HeLa or mouse NIH 3T3 cells when *let-7* function was blocked with a *let-7*-specific, but not a control, 2′-*O*-methyl oligonucleotide. (B) In NT2 cells, LRE-containing reporter expression decreased upon introduction of *let-7a* as an siRNA, relative to introduction of a GFP-specific siRNA. Reporter expression was unaltered by the *let-7*-specific 2′-*O*-methyl oligonucleotide or the *let-7a* siRNA when the reporter lacked LREs (Figure S1).

Figure AII-6

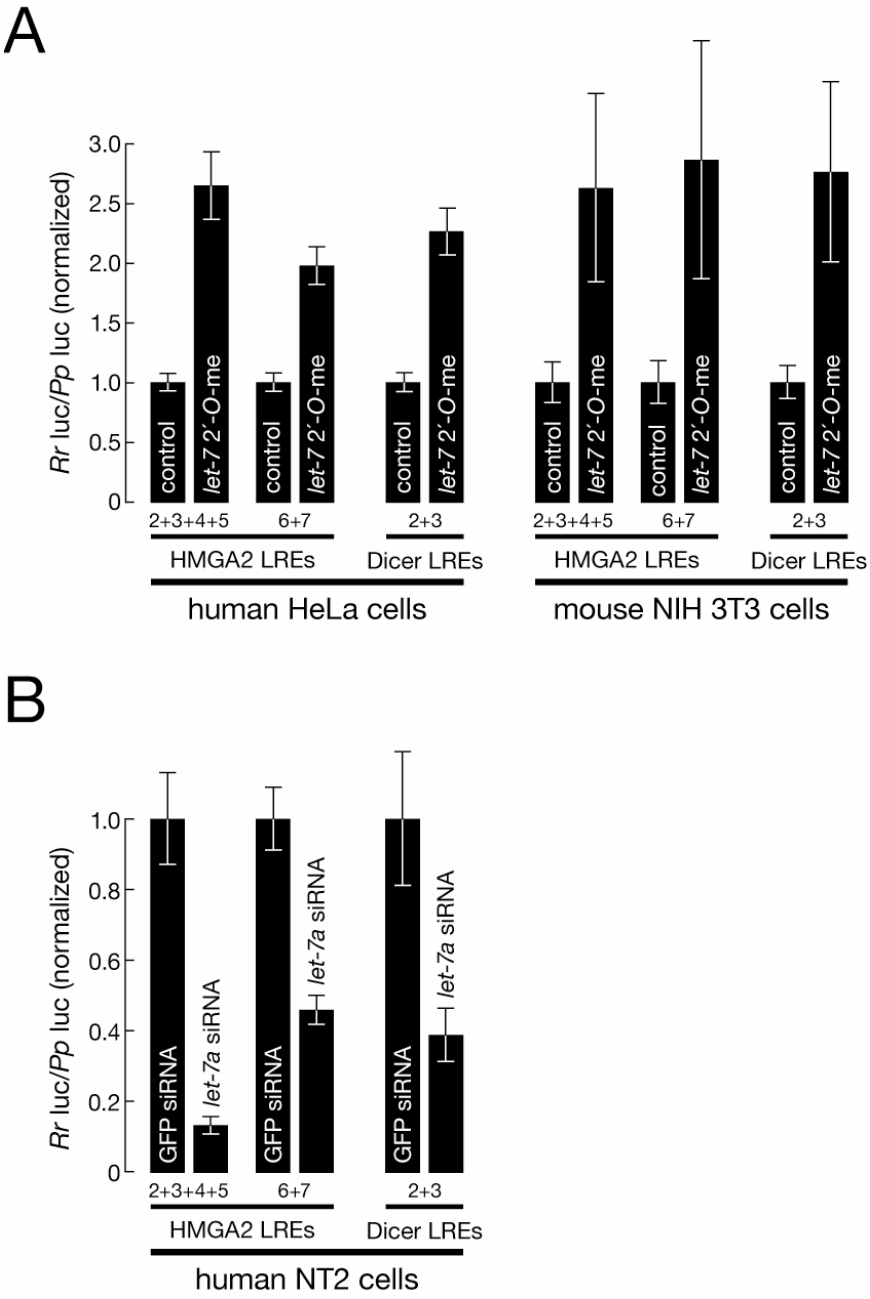
A
Rr luc/Pp luc (normalized)
3.0
2.5
2.0
1.5
1.0
0.5
0
control
let-7 2´-O-me
2+3+4+5
6+7
2+3
HMGA2 LREs
Dicer LREs
human HeLa cells
mouse NIH 3T3 cells
B
GFP siRNA
let-7a siRNA
1.0
0.8
0.6
0.4
0.2
human NT2 cells

Figure AII-7

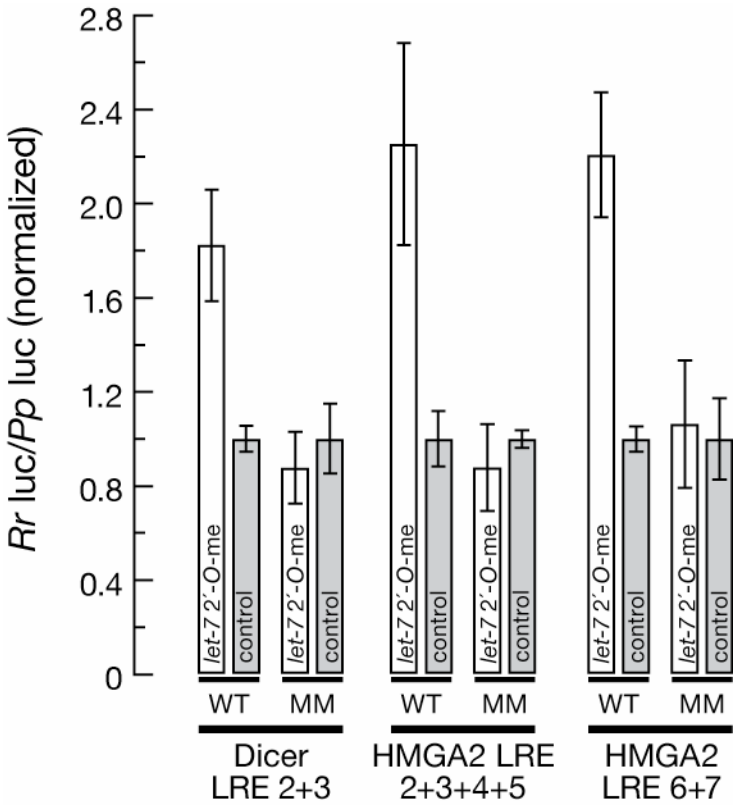

Figure AII-7. Mutations in the seed sequence abrogate *let-7*-directed repression of reporter constructs containing the Dicer or HMGA2 LREs. For each LRE, nucleotides 2–4 (CUC) were changed to GUG to reduce complementarity to the *let-7* seed and therefore to disrupt *let-7* binding.

Figure AII-8. *let-7* alters Dicer and HMGA2 mRNA steady-state levels without directing target mRNA cleavage. (A) 5′ RACE analysis of RNA harvested 72 h after NT2 cells were transfected with either a *let-7a* siRNA or an siRNA with perfect complementarity to HMGA2 LRE 6. The nested 5′ RACE PCR products were resolved on a 1.5% agarose gel. No product could be detected for the *let-7a* siRNA, although a discrete 3′ cleavage product was readily detected for the siRNA corresponding to LRE 6. The lower panel shows a digital over-exposure. Fourteen of 18 cloned 5′ RACE products corresponded precisely to the cleavage site predicted for the LRE 6 siRNA, diagnostic of siRNA-directed RNAi. (B) The ability of the *let-7a* siRNA to direct target cleavage was assessed in an in vitro reaction using *Drosophila* embryo lysate. Eight target RNAs were examined: a target containing a sequence fully complementary to *let-7a*, four targets corresponding to the four predicted Dicer LREs, and three targets corresponding to HMGA2 LRE1, 4, and 6. For each LRE-containing target RNA, a perfectly matched siRNA was used as a control demonstrating that the site can be targeted for cleavage by the RNAi pathway. None of the seven LRE-containing target RNAs were detectably cleaved in the presence of *let-7a*, after 24 h incubation. (C) The seven target RNAs were also analyzed in RNAi reactions using human HeLa cell S10 cytoplasmic extract. This extract contains functional, endogenous *let-7*-programmed RISC, as evidenced by the cleavage of the *let-7*-complementary target RNA in the absence of any exogenous siRNA. In contrast, the four Dicer and three HMGA2 LRE-containing target RNAs were only detectably cleaved in this assay when an siRNA with perfect complementarity to the LRE was included in the reaction.

Figure AII-8

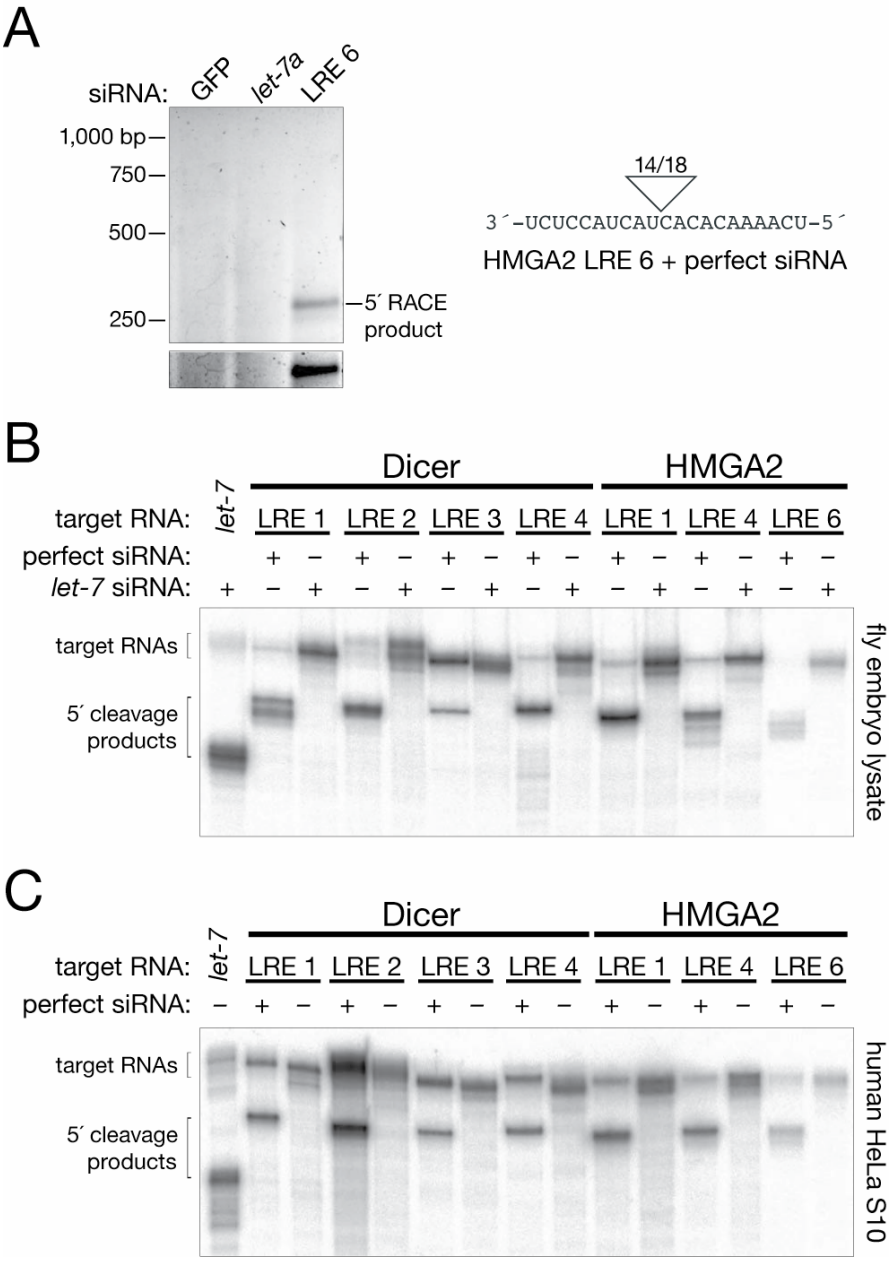
A
siRNA:
GFP
let-7a
LRE 6
1,000 bp
750
500
250
5′ RACE product
14/18
3′–UCUCCAUCAUCACACAAAACU–5′
HMGA2 LRE 6 + perfect siRNA
B
Dicer
HMGA2
let-7
target RNA:
LRE 1
LRE 2
LRE 3
LRE 4
LRE 1
LRE 4
LRE 6
perfect siRNA:
let-7 siRNA:
target RNAs
5′ cleavage products
fly embryo lysate
C
Dicer
HMGA2
let-7
target RNA:
LRE 1
LRE 2
LRE 3
LRE 4
LRE 1
LRE 4
LRE 6
perfect siRNA:
target RNAs
5′ cleavage products
human HeLa S10

least 24 h, allowing detection of target cleavage even for siRNAs complementary to as few as eleven target bases (Haley and Zamore, 2004). When tested in this assay, a *let-7a* siRNA failed to direct cleavage of target RNAs containing any of the four Dicer LREs or HMGA2 LREs 1, 4, or 6, although fully complementary siRNAs readily directed cleavage of the target RNAs at each of the seven tested LRE sites (Figure 8B). Similarly, S10 extract from cultured human HeLa cells, which contains endogenous *let-7*-programmed RISC, did not direct cleavage at any of the seven tested LRE sites, although fully complementary siRNAs readily directed cleavage at the corresponding sites (Figure 8C). Moreover, the endogenous *let-7*-programmed RISC present in the S10 extract cleaved a target RNA with complete complementarity to *let-7* (Figure 8C). We conclude that *let-7*-directed repression of the Dicer and HMGA2 mRNAs occurs by a mechanism distinct from Argonaute2-catalyzed endonucleolytic cleavage.

In human cells, miRNAs bound to Ago2 can relocalize their mRNA targets from the cytosol to subcellular structures called P-bodies (Liu et al., 2005; Sen and Blau, 2005). P-bodies contain both Dcp1 and Dcp2, enzymes that remove the characteristic 5′ cap of eukaryotic mRNA, and Xrn1, a 5′-to-3′ exonuclease that degrades uncapped mRNA. *let-7*-directed destruction of Dicer and HMGA2 mRNAs may reflect the active relocalization of these mRNAs by *let-7* to the P-body. Alternatively, destabilization of Dicer and HMGA2 may be an indirect consequence of a block to translational initiation(Pillai et al., 2004; Pillai et al., 2005) or miRNA-promoted removal of the mRNA poly(A) tail (Giraldez et al., 2006; Wu et al., 2006).

mRNAs Down-Regulated by let-7 are Enriched in Conserved 3′ UTR Seed Matches

Does *let-7* generally regulate the stability of human mRNAs predicted to be its regulatory targets (Krek et al., 2005; Lewis et al., 2005), because they contain evolutionarily conserved complementarity between the *let-7* seed and the mRNA? We compared the proportion of predicted *let-7* targets among the set of mRNAs whose steady-state concentration was significantly reduced (*p-value* < 0.1) upon the introduction of the *let-7a* siRNA into NT2 cells to those mRNAs that were not. Of the mRNAs whose concentration declined significantly in the presence of *let-7a*, one-quarter (13 of 51) contain *let-7* seed matches in the 3′ UTR that are conserved among four mammals (Lewis et al., 2005) (Supplementary Table 2). In contrast, less than four percent (221 of 6429) of mRNAs whose concentration was not significantly reduced contain such conserved seed matches. Thus, the set of mRNAs whose stability is reduced by *let-7* is enriched more than seven-fold for conserved 7-nt *let-7* seed complementarity. A similar enrichment was observed when we used either seed matches conserved among five vertebrates, which include both 8-nt open-reading frame matches and 6-nt 3′ UTR matches (> 6-fold enrichment) (Lewis et al., 2005) or when we used the 3′ UTR predictions of Krek et al. (Krek et al., 2005) (> 9-fold enrichment for conservation among 6 vertebrates or > 5-fold enrichment for conservation among 5 mammals). We conclude that a sizeable proportion of mRNAs proposed to contain evolutionarily conserved *let-7*-binding sites can, in fact, be regulated at the level of mRNA stability by *let-7*. However, not all proposed *let-7* targets were regulated at the mRNA level in our experiments. Expression of three members of the Ras proto-oncogene family were recently reported to be regulated by *let-7* (Johnson et al., 2005). In our experiments, the concentration of the mRNAs of each of these three Ras genes did not change significantly when *let-7* was inhibited in HeLa cells nor when *let-7a* was introduced into NT2 cells, although all three were readily detected by the microarray (Supplementary Table 1, Unigene ID's Hs.37003, Hs.505033, and

Hs.486502). This result suggests that stability of those three mRNAs is not regulated by *let-7*, although their translation may be *let-7*-regulated.

let-7 represses Dicer mRNA expression in vivo

Our finding that *let-7* regulates Dicer mRNA levels in cultured human cells and that the four sites proposed to mediate this regulation are conserved among the nine vertebrates examined, suggest that *let-7*-directed regulation of Dicer mRNA expression is physiologically relevant. To test this idea in vivo, we blocked *let-7* function in adult mice by intravenous administration of cholesterol-conjugated, phosphorothioate-modified 2′-*O*-methyl oligonucleotides (Krutzfeldt et al., 2005). Three mice received 40 mg/kg daily for three days of a *let-7a*-complementary 2′-*O*-methyl oligonucleotide, and three received a control oligonucleotide; liver tissue was harvested on the fourth day and Dicer mRNA, relative to Actin mRNA, measured by qRT-PCR (Figure 9A). (As HMGA2 mRNA is not detectably produced in adult mouse somatic tissues (Zhou et al., 1996), we did not measure its expression in these experiments.) Relative to the control, intravenous administration of the *let-7a*-specific 2′-*O*-methyl oligonucleotide increased the steady-state concentration of Dicer mRNA in liver tissue by a factor of 3.5 ± 0.5 (average ± standard deviation, $n = 3$; $0.001 < p < 0.004$).

In parallel, we examined the effect of the *let-7*-specific and control 2′-*O*-methyl oligonucleotides on *let-7* expression, measured by Northern hybridization using a locked-nucleic acid (LNA) probe complementary to *let-7a*. Control experiments with synthetic RNAs corresponding to the nine mouse *let-7* paralogs demonstrated that the LNA probe detected *let-7b*, *let-7c*, *let-7d*, *let-7e*, and *let-7f* in addition to detecting *let-7a*; *let-7g*, *let-7i*, or miR-98 were not efficiently detected (Figure 9B). *let-7a*, *let-7b*, and *let-7c* are all expressed in mouse liver (Lagos-Quintana et al., 2002). Intravenous administration of cholesterol-conjugated, phosphorothioate-modified 2′-*O*-methyl oligonucleotides

Figure AII-9. Intravenous administration of a *let-7*-specific, but not a control, antisense oligonucleotide increases the steady-state concentration of Dicer mRNA in liver. 2′-*O*-methyl antisense oligonucleotides contained two 5′ and four 3′ phosphorothioate modifications and were 3′ conjugated via a hydroxyprolinol linkage to cholesterol to facilitate uptake by liver cells (Krutzfeldt et al., 2005). Each of the six mice in the study received 40 mg/kg modified, conjugated 2′-*O*-methyl oligonucleotide daily on three successive days; liver tissue was harvested on the fourth day. (A) Dicer mRNA levels were measured by qRT-PCR in liver tissue. (B) The concentration of *let-7*, miR-16, $tRNA^{ile}$, and pre-*let-7* (Figure S2B) were measured in the same tissue by quantitative Northern blotting. (C) Quantitation of the data in (B).

Figure AII-9

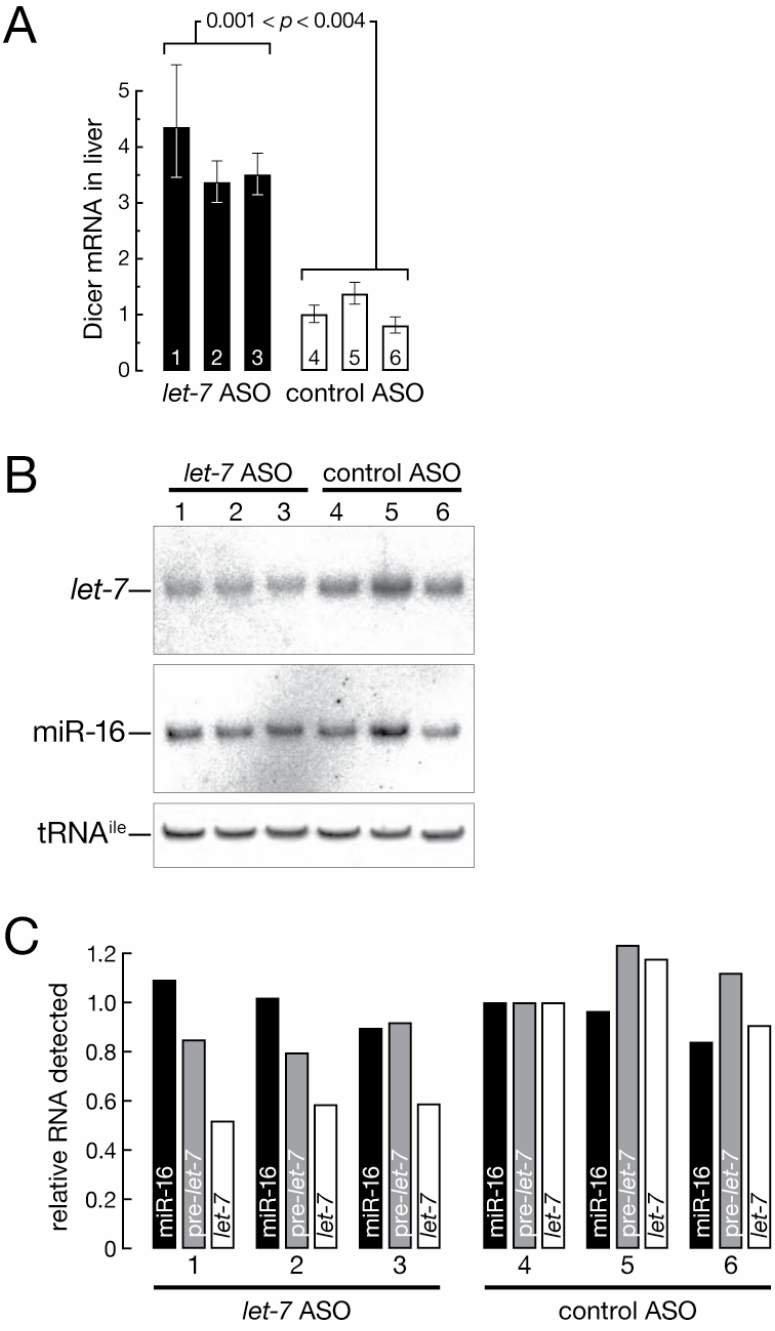
A
0.001 < p < 0.004
Dicer mRNA in liver
0
1
2
3
4
5
1
2
3
4
5
6
let-7 ASO
control ASO
B
let-7 ASO
control ASO
1 2 3 4 5 6
let-7—
miR-16—
tRNAile—
C
relative RNA detected
0
0.2
0.4
0.6
0.8
1.0
1.2
miR-16
pre-let-7
let-7
1
2
3
4
5
6
let-7 ASO
control ASO

Figure AII-10. pre-miRNAs Accumulate in *Let-7* Treated Cells. NT2 cells were transfected with *Let-7* siRNA or a GFP control siRNA at 72 hr interval for nine days. RNA was extracted and 20μg was analyzed by Northern blot using LNA probes for miRNAs as indicated. Relative abundances of pre-miRNAs and miRNAs were normalized to isoleucine tRNA as a loading control. Error bars represent standard deviation for three separate trials.

Figure AII-10

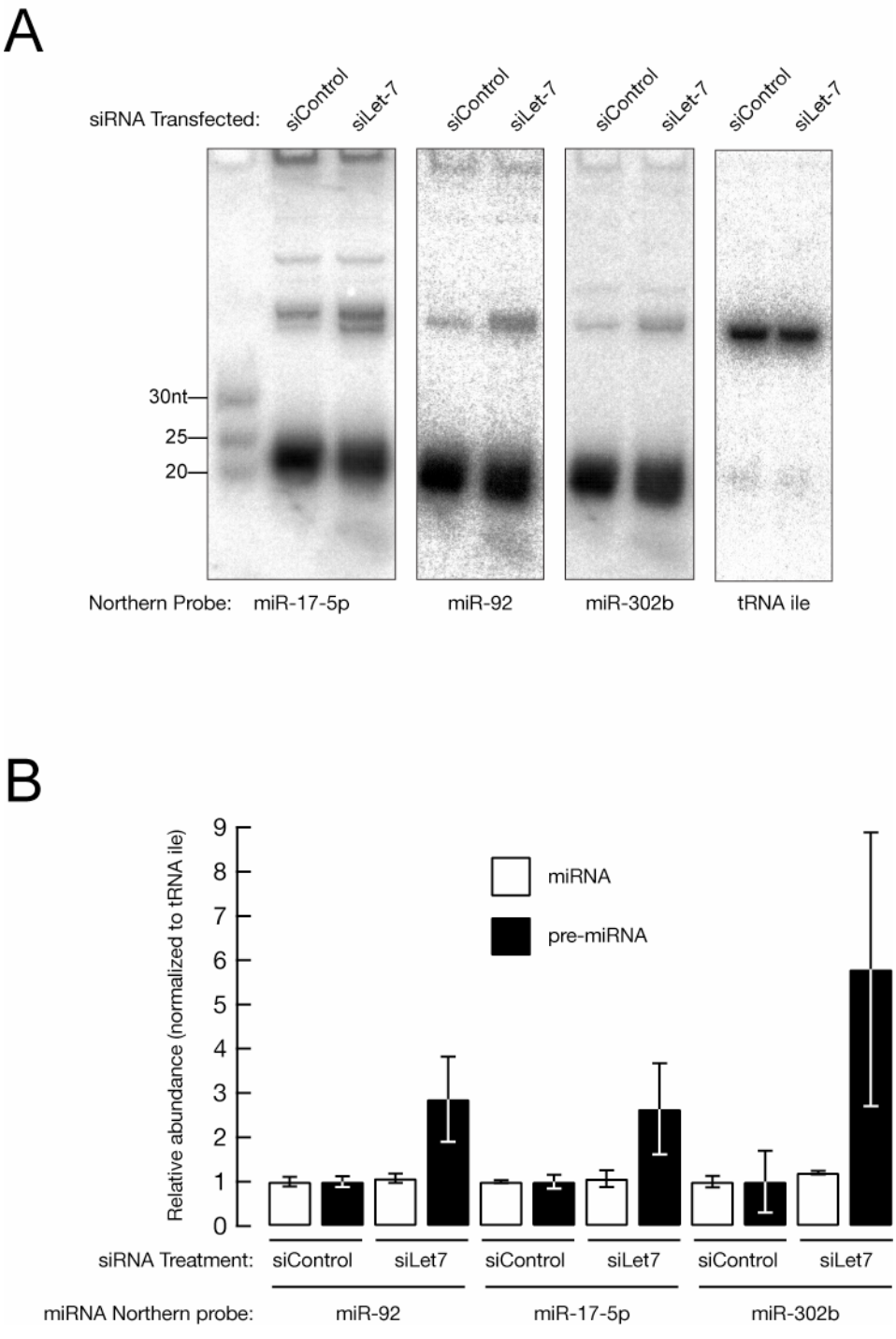

(Krutzfeldt et al., 2005) or 2′-*O*-methoxyethyl phosphorothioate oligonucleotides (Esau et al., 2006) has been reported to reduce accumulation of the complementary miRNA. We found that *let-7* was partially depleted (~45% reduction) in the three mice that received the *let-7*-specific oligonucleotide, but not in the controls (Figure 9C), suggesting that the oligonucleotide inhibited *let-7* function in part by reducing the steady-state concentration of *let-7* and in part by binding *let-7*-programmed Argonaute-protein complexes and competing with binding to target mRNAs such as Dicer.

let-7 can regulate miRNA biogenesis

We detected no change in the level of an endogenous miRNA, miR-16, in our *let-7* loss of function experiments in mice. Perhaps Dicer is abundant in many cell types and thus not rate limiting for miRNA production under normal circumstances. To test if *let-7* is capable of regulating miRNA biogenesis we sequentially transfected NT2 cells with *let-7a* or a control every 3 days for a total of 9 days. We then assessed miRNA and pre-miRNA levels by northern blot. Although miRNA levels did not significantly change, pre-miRNAs increased 3-6 fold for each miRNA examined (miR-17-5p, miR-92, and miR-302b) suggesting that Dicer levels were reduced to a level that globally inhibits pre-miRNA processing (Figure 10). Despite our prolonged treatment regimen miRNAs in RISC may be very stable, which may explain why we did not see a corresponding reduction in mature miRNAs.

Discussion

The finding that Dicer is regulated in human cells by *let-7* reveals a feedback circuit controlling the RNA silencing pathway in vertebrates. The intracellular

concentration of Dicer, the RNase III enzyme that converts pre-miRNAs to mature miRNAs and long double-stranded RNA into siRNAs (Bernstein et al., 2001; Grishok et al., 2001; Hutvágner et al., 2001; Ketting et al., 2001), limits the production of *let-7* (Hutvágner et al., 2001) and likely miRNAs generally. We hypothesize that when *let-7* levels are high, Dicer levels fall, reducing the overall production of mature miRNAs. Conversely, when *let-7* levels are low, Dicer levels would rise, leading to increased processing of pre-miRNA to mature miRNA.

Feedback control of components of the RNA silencing pathway by miRNAs is not without precedent: in plants, both DCL1, the Dicer enzyme that excises miRNA from pre-miRNA, and the Argonaute protein AGO1 are regulated by miRNAs that target their mRNAs for cleavage (Vaucheret et al., 2004; Xie et al., 2003). As plant and animal miRNA genes are believed to have evolved separately (Allen et al., 2004; Bartel, 2004), it is remarkable that Dicer is the target of miRNA-mediated, feedback control in both kingdoms and underscores the importance of maintaining Dicer homeostasis in higher organisms.

Materials and methods

General methods

Drosophila embryo lysate, *in vitro* RNAi reactions, and cap-labeling of target RNAs were as described (Haley et al., 2003). HeLa S10 was prepared as described (Dignam et al., 1983). For both *Drosophila* and HeLa reactions, the siRNA was incubated for 1 h at 25˚C (*Drosophila*) or 37˚C (HeLa) to assemble RISC, RISC assembly inactivated with 10 mM *N*-ethylmaleimide for 10 min on ice followed by 11 mM DTT for 5 min on ice. Next, 0.02 □g/□l (f.c.) creatine kinase was added to restore the ATP-regenerating system, and then 0.25 nM, ^{32}P-cap-radiolabeled target RNA was added and the incubation continued for 24 h. Cleavage products of RNAi reactions were

analyzed by electrophoresis on 8% denaturing acrylamide gels. Gels were dried, exposed to image plates, and then scanned with a FLA-5000 phosphorimager (Fuji, Tokyo, Japan). Images were analyzed using Image Gauge version 3.45 (Fuji). Data analysis was performed using Excel (Microsoft) and IgorPro 5.0 (Wavemetrics, Lake Oswego, OR).

RNA, 2′-*O*-methyl, and DNA oligonucleotides

Synthetic siRNA (Dharmacon, Lafayette, CO) were deprotected according to the manufacturer, annealed and used at 20 nM final concentration unless otherwise noted. siRNA sequences appear in Table S3. 2′-*O*-methyl oligonucleotides (IDT, Coralville, IA, or Dharmacon) were: 5′-Bio-CAU CAC GUA CGC GGA AUA CUU CGA AAU GUC C-3′ (complementary to the *Pp*-luc siRNA sense strand), 5′-Bio-UCU UCA CUA UAC AAC CUA CUA CCU CAA CCU U-3′ (complementary to *let-7*); 5′ Biotin was attached via a six-carbon spacer arm. For intravenous injection into mice, fully 2′-*O*-methyl-modified oligonucleotides (Dharmacon) were: 5′-ApsApsC UAU ACA ACC UAC UAC psCpsUpsC psA-hydroxyprolinol-cholesterol-3′ (*let-7*-specific) and 5′-CpsGpsU ACG CGG AAU ACU UCG psApsApsA psU-hydroxypolinol-cholesterol-3′ (control), where 'ps' indicates a phosphorothioate linkage.

DNA oligonucleotides for synthesizing *in vitro* RNA targets containing individual Dicer or HMGA2 LRES were from IDT (Table S4). DNA oligonucleotides (Table S4) were used to PCR amplify templates for target RNA transcription using plasmid pGL-2 (Promega) as a PCR template. RNA was transcribed from the PCR products using T7 RNA polymerase as described (Haley et al., 2003). To generate reporter constructs to test the putative *let-7*-responsive elements from Dicer and HMGA2, DNA oligonucleotides were used for PCR with either Dicer or HMGA2 cDNA as template: HMGA2 LREs 2-5, 5′-ATT CTA GAC TCT CCC TCT CTC TTT TCA TGT G-3′ and 5′-ATT CTA GAA CAA ATG AAT GCT GCA AGT AAC AAG-3′; HMGA2 LREs 6-7, 5′-ATT CTA GAG GAA GCA ATT GCT CAT GTT GGC-3′ and 5′-ATT CTA GAG TCT TAT GTA

GCT GCG ACC AAC-3′; Dicer LREs 2-3, 5′-ATT CTA GAC TCC TCT CTA GAA AAT CAT GAC C-3′ and 5′-ATT CTA GAC AAT AGA AGG GCT CTG CTC AG-3′. The PCR fragments were digested with Xba I, cloned into plasmid pRL-TK, and sequenced to confirm their identity.

Construction of mutant *let-7* responsive elements

The seed sequence of each Dicer or HMGA2 LRE was altered by substituting GAG for nucleotides 2–4 of the wild-type *let-7* seed sequence (CTC) using the Quick-Change site-directed mutagenesis method (Stratagene, La Jolla, CA) using KOD polymerase (Novagen, San Diego, CA). All mutant sites were verified by sequencing. The primers used for mutagenesis were: Dicer LRE2, cgt gca acc aac tac gag ata ttc cat tca gaa and ttct gaa tgg aat atc tcg tag ttg gtt gca cg; Dicer LRE3, tgc taa caa atc tac gag aga tgg aag tcc tgt and aca gga ctt cca tct ctc gta gat ttg tta gca; HMGA2 LRE2, ctg aat acc act tac gag aaa tta agc ata tgt and aca tat gct taa ttt ctc gta agt ggt att cag; HMGA2 LRE3, act act caa tac tac gag tga atg tta caa cga and tcg ttg taa cat tca ctc gta gta ttg agt agt; HMGA2 LRE4, cct cca agt ctg tac gag aaa tga att ctt taa and tta aag aat tca ttt ctc gta cag act tgg agg; HMGA2 LRE5, ctt gca aag acc tac gag cag act tca aaa gga and tcc ttt tga agt ctg ctc gta ggt ctt tgc aag; HMGA2 LRE6, aaa aca cac tac tac gag tta agt ccc agt ata and tat act ggg act taa ctc gta gta gtg tgt ttt; HMGA2 LRE7, taa gtc cca gta tac gag att ttt cat act gaa and ttc agt atg aaa aat ctc gta tac tgg gac tta.

Cell culture and transfection

HeLa, NT2, and NT2N cells (ATTC) were co-transfected with siRNA (Table S3), 2′-*O*-methyl oligonucleotides, or plasmid DNA using Lipofectamine 2000 (Invitrogen, Carlsbad, CA) following the manufacturer's instructions. NT2 cells were differentiated to NT2N cells by supplementing the culture medium with 0.01 nM retinoic acid for at least two weeks. pRL-TK-LIN28 and pRL-TK-M1 (Kiriakidou et al., 2004) Renilla luciferase

plasmids were used to monitor *let-7* expression, and pGL-2 (Promega, Madison, WI) firefly luciferase plasmid was used as an internal control in transfection experiments. For figure 10 NT2 were split and transfected every third day at ~30% confluence using 20nM *Let-7* or GFP siRNA and Dharmafect 4, according to the manufacturer's instructions.

Microarray analysis

Microarray analysis was performed in triplicate using Affymetrix Human Genome Array U133A (Affymetrix, Santa Clara, CA). RNA from HeLa and NT2 cells was isolated with TRIZOL (Invitrogen). 5 □g total RNA was used for cDNA synthesis using the GeneChip Expression 3´-Amplification One-Cycle cDNA synthesis kit (Affymetrix). cRNA was synthesized and labeled with the GeneChip Expression 3´-Amplification IVT labeling kit (Affymetrix), then purified and fragmented with the GeneChip Sample Cleanup Module (Affymetrix). Raw data were extracted using Affymetrix GCOS software. The .cel files were imported into the S-plus Array Analyzer module (version 2.0) and the data normalized using the RMA (Robust Multichip Average) method based on quantiles . Differential expression testing was performed using the Local Pooled Error Test (LPE) (Jain et al., 2003). Genes which were differentially expressed were filtered based on the Benjamini Hochberg method (Benjamini and Hochberg, 1995) of testing significance (FDR ≤ 0.05) and empirical fold-change (≥ 2-fold). The complete set of gene expression data can be viewed on the NCBI gene expression omnibus web site (http://www.ncbi.nlm.nih.gob/geo/, accession number GSE 2918).

Quantitative PCR analysis

0.5-1 □g RNA was primed with oligo(dT) and reverse transcribed with Superscript II (Invitrogen). Quantitative PCR reactions were performed in triplicate with 0.5 □M gene specific primers using the Quantitect SYBR Green PCR reaction mix

(Qiagen) in a DNA Engine Opticon2 (MJ Research). Analysis was performed using Opticon Monitor (MJ Research), Excel (Microsoft), and IgorPro 5.0 (Wavemetrics). Relative steady-state mRNA levels were determined from the threshold cycle for amplification by the $2^{-\Delta\Delta CT}$ method (Livak and Schmittgen, 2001). PCR primers for human cells were: GAPDH, 5′-GAA GGT GAA GGT CGG AGT-3′ and 5′-GAA GAT GGT GAT GGG ATT TC-3′; Dicer , 5′-CAG AAC GTT GCT CAG CGA GTC-3′ and 5′-GGT TGC ACG GGT ATT TCC TG-3′; HMGA2, 5′-GAA GAC CCA AAG GCA GCA AA-3′ and 5′-CGG CAG ACT CTT GTG AGG ATG-3′. For mouse mRNA, PCR primers were: Actin, 5′-ATG CCA ACA CAG TGC TGT CTG G-3′ and 5′-TGC TTG CTG ATC CAC ATC TGC T-3′; Dicer , 5′-GCA GGC TTT TTA CAC ACG CCT-3′ and 5′-GGG TCT TCA TAA AGG TGC TT-3′ (Sago et al., 2004).

3′ cleavage product analysis by RACE

5′ RACE was carried out as described (Llave et al., 2002) for HMGA2 LRE 6 using the HMGA2 reverse transcriptase primer (above) and a reverse PCR primer, 5′-CAA GCA AGC GAT TCA AAG TAC AAT C-3′, and a nested 3′ PCR primer, 5′-GTT AGA AGA CAC TCA AAG GAA CAG-3′.

Western blot analysis

Proteins were separated on 4-20% gradient SDS-PAGE gels, blotted to Immobilon-P membrane (Millipore) using semi-dry electro-blot (Bio-Rad), and probed with antibodies: α-Dicer rabbit polyclonal antibody (Billy et al., 2001) (Figure 3A) diluted 1:1000 followed by HRP-conjugated mouse anti-rabbit secondary antibody (Pierce) or α -Dicer monoclonal antibody (Clonegene, Hartford, CT) (Figure 3B) diluted 1:500 followed by HRP-conjugated sheep anti-mouse secondary antibody (GE Healthcare, Piscataway, NJ); α -HMGA2 antibody (Tessari et al., 2003) diluted 1:1000

followed by HRP-conjugated rabbit secondary antibody (Cell Signaling Technology, Danvers, MA) and visualized with SuperSignal West Dura kit (Pierce, Rockford, IL) using an LAS 5000 imager (Fuji).

Acknowledgements

We thank Witold Filipowicz for anti-human Dicer antibody, Guidalberto Manfioletti for anti-human HMGA2 antibody, Zissimos Mourelatos for the pRL-TK-LIN28 and pRL-TK-M1 plasmids, members of the Zamore lab for advice, suggestions, and comments on the manuscript, and Dianne Schwarz for providing S10 extract. PDZ is a W.M. Keck Foundation Young Scholar in Medical Research; G.H. is a Wellcome Trust CD Fellow. This work was supported in part by grants from the National Institutes of Health to PDZ (GM62862 and GM65236) and from the Wellcome Trust to GH (076624/Z/05/Z), a Charles A. King Trust fellowship to GH, an EMBO long-term fellowship (ALTF 910-2004) to HS, and a DOE fellowship to BL.

Supporting Information

Figure AII-S1. Validation of the *let-7*-responsive reporter, the *let-7*-specific 2′-*O*-methyl antisense oligonucleotide, and the *let-7a* siRNA. (A) A *Renilla* luciferase reporter bearing a single *let-7*-responsive element (LRE) from human Lin-28 mRNA (Kiriakidou et al., 2004) was repressed in human HeLa cells and in differentiated NT2N cells, demonstrating that the *let-7* expressed in these two cell lines functions in RNA silencing. In contrast, the LRE-containing reporter was not repressed in NT2 cells, which lack detectable *let-7*. A reporter bearing a mutated LRE (mLRE) (Kiriakidou et al., 2004) was not repressed in any of the cell lines. (B) In HeLa cells, a *let-7*-specific 2′-*O*-methyl antisense oligonucleotide blocked repression of the LRE-containing reporter, increasing its expression relative to both the expression of the mutant LRE-containing reporter (mLRE) and the control 2′-*O*-methyl oligonucleotide specific for a firefly luciferase siRNA. (C) In NT2 cells, a *let-7a* siRNA repressed expression of the LRE-containing reporter, but not the mutant LRE-containing reporter (mLRE); an siRNA specific for firefly luciferase had no detectable effect on reporter expression. In (A) the level of normalized *Renilla* luciferase expression of the mLRE reporter in NT2 cells was set to 1; in (B) and (C) the level of expression of the mLRE reporter in the presence of the control 2′-*O*-methyl oligonucleotide or siRNA was set to 1.

Figure AII-S1

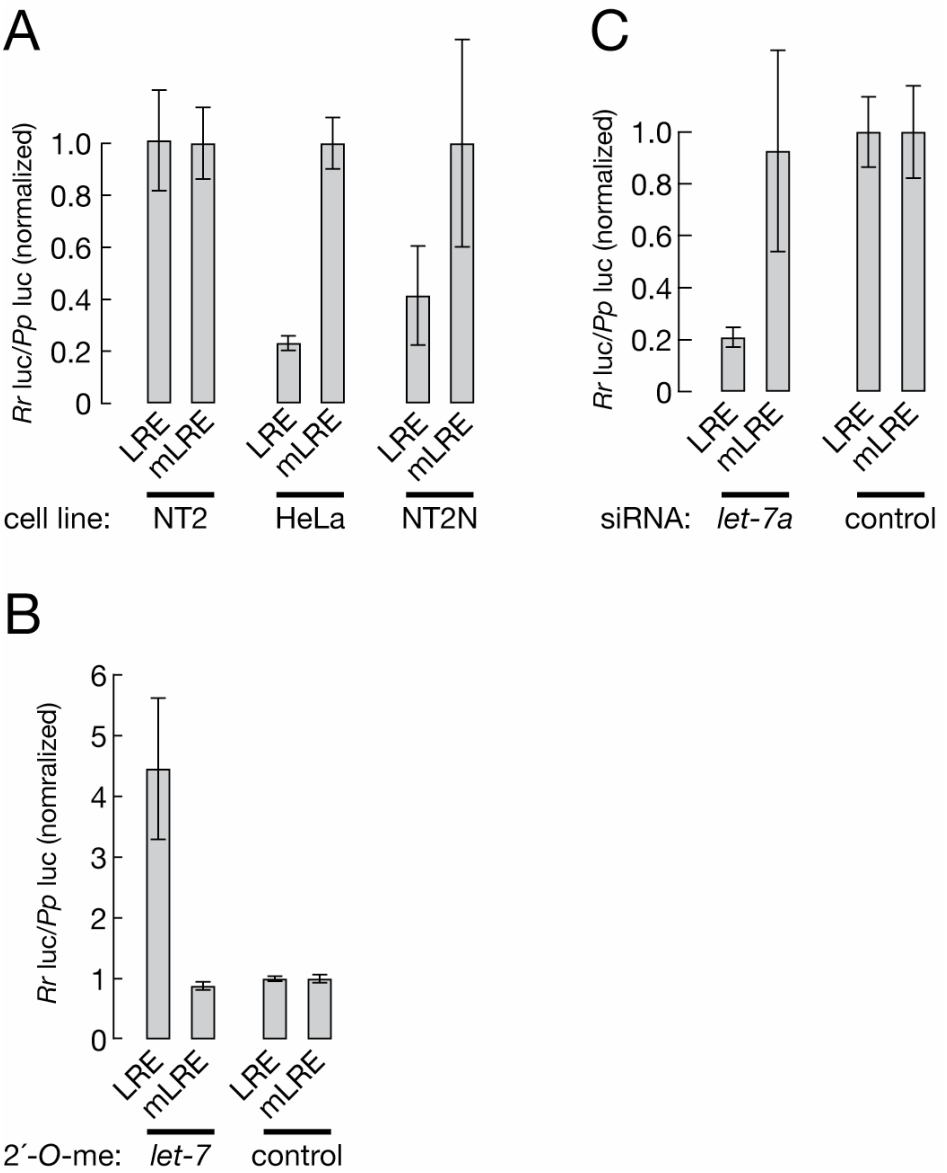

Figure AII-S2

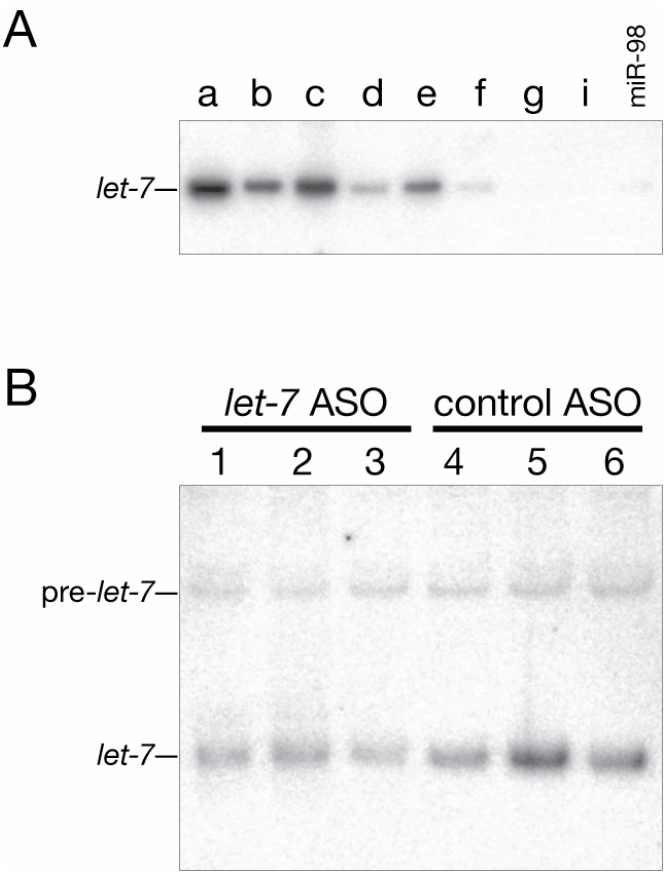

Figure AII-S2. (A) A lock-nucleic acid (LNA) oligonucleotide probe can distinguish among some, but not all, of the vertebrate *let-7* paralogs. Synthetic RNA corresponding to each of the nine *let-7* paralogs was detected by Northern analysis using a 5′-^{32}P-radiolabeled LNA probe corresponding to the perfect reverse complement of *let-7a*. (B) The same LNA probe was used to detect pre-*let-7* in liver tissue from the experiment in Figure 9.

Table AII-S1. Microarray data and analysis. (A) 'Inhibition of *let-7* in HeLa' and (B) '*let-7* siRNA in NT2' report raw data for gene expression with a control 2′-*O*-methyl antisense oligonucleotide ('control') versus a *let-7*-specific 2′-*O*-methyl oligonucleotide ('experimental') and with a control siRNA ('control') or a *let-7a* siRNA ('experimental'), respectively. Each worksheet gives the value for the three independent replicates, the average value for all trials, , as well as identifying information and functional annotation for each gene. *P*-values for the change in expression between experiment and control ('Adj. *p*-value') were adjusted using the local-pooled-error test (Jain et al., 2003). (C) 'NT2 experiment vs. miRNA predictions' summarizes the predicted regulatory relationships between each gene on the microarray and human miRNAs, as previously reported (Lewis et al., 2005). miRNA predictions are from either Lewis et al. Supplemental Table 2 (columns F, G, H, I, J and K) for microRNA binding sites conserved among five vertebrates (5 v) and from Lewis et al. Supplemental Table 3 (columns L, M, N, O, P and Q) for microRNA binding sites conserved among four mammals (4 m) (Lewis et al., 2005). Columns J and P indicate whether the corresponding gene is a predicted microRNA target, according to Lewis et al.'s supplemental tables 2 and 3, respectively; an asterisk indicates that the mRNA for this gene contains at least one predicted microRNA binding site, either in its ORF or in its 3′UTR. Columns K and Q indicate whether *let-7* is predicted to regulate the corresponding gene; 'Y' indicates that at least one *let-7* binding site was predicted for the mRNA of the gene, and 'N' means that no *let-7* binding site was predicted. (D) 'Up-reg. non-*let-7* targets (5 v)' and 'Up-reg. non-*let-7* targets (4)' summarize the predictions of Lewis et al. (Lewis et al., 2005) for genes which were significantly (adj. *p*-value < 0.1) up-regulated following *let-7* siRNA transfection into NT2 cells. Only genes not predicted to be regulated by *let-7* are included. **(Too large to include)**

Table AII-S2. Comparison of mRNAs down-regulated upon the introduction of a *let-7a* siRNA into NT2 cells with previously published predictions of *let-7* target mRNAs based on the presence of evolutionarily conserved complementarity between the mRNA and the *let-7* seed sequence. **(Too large to include)**

Table AII-S3. siRNAs used in this study.

Table AII-S4. DNA oligonucleotides used for PCR to produce templates for transcription of the eight target RNAs used in Figure 4.

Table S4. DNA oligonucleotides used in PCR to generate templates for RNA target transcription. Green: pGL-2 sequence; red, LRE site.

Forward primer for pGL-2 5′-gcgtaatacgactcactatagTCACATCTCATCTACCTCC-3′ (T7 promoter in lowercase)

Reverse primers

Completely complementary to *let-7a*

5′-CCCATTTAGGTGACACTATAGATTTACATCGCGTTGAGTGTAGAACGGTTGTATAAAAGGTTGAGGTAGTAGGTTGTATAGTGAAGAGAGGAGTTCATGATCAGTG-3′

Dicer LRE 1

5′-TCCAAAGTGCTGGAGTCATTAACAACATTAAGAGGTAGAACACAGTATGCTGAATCAGCGTCTGTAGGTTTAAATTCTAGTAGAGGAGTTCATGATCAGTG-3′

Dicer LRE 2

5′-TTCTCGTAACTGTATAAATTCTGAATGGAATATGAGGTAGTTGGTTGCACGGGTATTTCCTGCTTGTAGTAATTTAGCTGATTAGAGGAGTTCATGATCAGTG-3′

Dicer LRE 3

5′-AGGCATTACGGCCATCACAGGACTTCCATCTGAGGTAGATTTGTTAGCATTTCCATCAAGGTATTTATTACTCAGGAGAGAGGAGTTCATGATCAGTG-3′

Dicer LRE 4

5′-GCCGCGGGTCTTCATAAAGGTGCTTGGTTATGAGGTAGTCCAAAATCGCATCTCCCAGGAATTCTAAGCGCTGGTAACAATCAGAGGAGTTCATGATCAGTG-3′

HMGA2 LRE 1

5′-TCTTCTCCCTTCAAAAGATCCAACTGCTGCTGAGGTAGAAATCGAACGTTGGCGCCCCCTAGTCCTCTTCGGCAGACTCTAGAGGAGTTCATGATCAGTG-3′

HMGA2 LRE 4

5′-CAATTAGTCCATCTCCTTAAAGAATTCATTTGAGGTACAGACTTGGAGGGTAATATTTAAATATTACAGTCAAATCTTGTGAGAGGAGTTCATGATCAGTG-3′

HMGA2 LRE 6

5′-AGTATGAAAAATGAGGTATACTGGGACTTAAGAGGTAGTAGTGTGTTTTGATTGTACAACATACAGGAAATAAAAGTGTAAAGAGGAGTTCATGATCAGTG-3′

Bibliography

Abbott, A. L., Alvarez-Saavedra, E., Miska, E. A., Lau, N. C., Bartel, D. P., Horvitz, H. R., and Ambros, V. (2005). The *let-7* MicroRNA family members mir-48, mir-84, and mir-241 function together to regulate developmental timing in Caenorhabditis elegans. Dev Cell *9*, 403-414.

Akira S, Uematsu S, Takeuchi O. Pathogen recognition and innate immunity.Cell. 2006 Feb 24;124(4):783-801.

Aleman, L. M., Doench, J., and Sharp, P. A. (2007). Comparison of siRNA-induced off-target RNA and protein effects. RNA *13*, 385-395.

Allen, E., Xie, Z., Gustafson, A. M., Sung, G. H., Spatafora, J. W., and Carrington, J. C. (2004). Evolution of microRNA genes by inverted duplication of target gene sequences in Arabidopsis thaliana. Nat Genet *36*, 1282-1290.

Ambros, V., and Horvitz, H. R. (1984). Heterochronic mutants of the nematode Caenorhabditis elegans. Science *226*, 409-416.

Ameres, S. L., Martinez, J., and Schroeder, R. (2007). Molecular basis for target RNA recognition and cleavage by human RISC. Cell *130*, 101-112.

Andl, T., Murchison, E. P., Liu, F., Zhang, Y., Yunta-Gonzalez, M., Tobias, J. W., Andl, C. D., Seykora, J. T., Hannon, G. J., and Millar, S. E. (2006). The miRNA-processing enzyme dicer is essential for the morphogenesis and maintenance of hair follicles. Curr Biol *16*, 1041-1049.

Aoki, K., Moriguchi, H., Yoshioka, T., Okawa, K., and Tabara, H. (2007). In vitro analyses of the production and activity of secondary small interfering RNAs in C. elegans. EMBO J *26*, 5007-5019.

Arasu, P., Wightman, B., and Ruvkun, G. (1991). Temporal regulation of lin-14 by the antagonistic action of two other heterochronic genes, lin-4 and lin-28. Genes Dev *5*, 1825-1833.

Aravin, A., Gaidatzis, D., Pfeffer, S., Lagos-Quintana, M., Landgraf, P., Iovino, N., Morris, P., Brownstein, M. J., Kuramochi-Miyagawa, S., Nakano, T., Chien, M., Russo, J. J., Ju, J., Sheridan, R., Sander, C., Zavolan, M., and Tuschl, T. (2006). A novel class of small RNAs bind to MILI protein in mouse testes. Nature *442*, 203-207.

Aravin, A. A., Hannon, G. J., and Brennecke, J. (2007). The Piwi-piRNA pathway provides an adaptive defense in the transposon arms race. Science *318*, 761-764.

Aravin, A. A., Lagos-Quintana, M., Yalcin, A., Zavolan, M., Marks, D., Snyder, B., Gaasterland, T., Meyer, J., and Tuschl, T. (2003). The small RNA profile during Drosophila melanogaster development. Dev Cell *5*, 337-350.

Aravin, A. A., Naumova, N. M., Tulin, A. V., Vagin, V. V., Rozovsky, Y. M., and Gvozdev, V. A. (2001). Double-stranded RNA-mediated silencing of genomic tandem repeats and transposable elements in the D. melanogaster germline. Curr Biol *11*, 1017-1027.

Aravin, A. A., Sachidanandam, R., Girard, A., Fejes-Toth, K., and Hannon, G. J. (2007). Developmentally regulated piRNA clusters implicate MILI in transposon control. Science *316*, 744-747.

Ashraf, S. I., McLoon, A. L., Sclarsic, S. M., and Kunes, S. (2006). Synaptic protein synthesis associated with memory is regulated by the RISC pathway in Drosophila. Cell *124*, 191-205.

Aza-Blanc, P., Cooper, C. L., Wagner, K., Batalov, S., Deveraux, Q. L., and Cooke, M. P. (2003). Identification of modulators of TRAIL-induced apoptosis via RNAi-based phenotypic screening. Mol Cell *12*, 627-637.

Bagga, S., Bracht, J., Hunter, S., Massirer, K., Holtz, J., Eachus, R., and Pasquinelli, A. E. (2005). Regulation by *let-7* and lin-4 miRNAs results in target mRNA degradation. Cell *122*, 553-563.

Bartel, D. P. (2004). MicroRNAs: genomics, biogenesis, mechanism, and function. Cell *116*, 281-297.

Bartel, D. P., and Chen, C. Z. (2004). Micromanagers of gene expression: the potentially widespread influence of metazoan microRNAs. Nat Rev Genet *5*, 396-400.

Bashirullah, A., Pasquinelli, A. E., Kiger, A. A., Perrimon, N., Ruvkun, G., and Thummel, C. S. (2003). Coordinate regulation of small temporal RNAs at the onset of Drosophila metamorphosis. Dev Biol *259*, 1-8.

Baskerville, S., and Bartel, D. P. (2005). Microarray profiling of microRNAs reveals frequent coexpression with neighboring miRNAs and host genes. RNA *11*, 241-247.

Bass, B. L. (2000). Double-stranded RNA as a template for gene silencing. Cell *101*, 235-238.

Baulcombe, D. C. (1996). RNA as a target and an initiator of post-transcriptional gene silencing in transgenic plants. Plant Mol Biol *32*, 79-88.

Baumberger, N., and Baulcombe, D. C. (2005). Arabidopsis ARGONAUTE1 is an RNA Slicer that selectively recruits microRNAs and short interfering RNAs. Proc Natl Acad Sci U S A *102*, 11928-11933.

Behm-Ansmant, I., Rehwinkel, J., Doerks, T., Stark, A., Bork, P., and Izaurralde, E. (2006). mRNA degradation by miRNAs and GW182 requires both CCR4:NOT deadenylase and DCP1:DCP2 decapping complexes. Genes Dev *20*, 1885-1898.

Beitzinger, M., Peters, L., Zhu, J. Y., Kremmer, E., and Meister, G. (2007). Identification of human microRNA targets from isolated argonaute protein complexes. RNA Biol *4*, 76-84.

Benjamini, Y., and Hochberg, Y. (1995). Controlling the false discovery rate: a practical and powerful approach to multiple testing. Journal of the Royal Statistical Society *Series B 57*, 289:300.

Berezikov, E., Thuemmler, F., van Laake, L. W., Kondova, I., Bontrop, R., Cuppen, E., and Plasterk, R. H. (2006). Diversity of microRNAs in human and chimpanzee brain. Nat Genet *38*, 1375-1377.

Berger, E. M., Dubrovsky, E. B., Appleby, L., and Dubrovskaya, V. (2005). Inhibition of micro-RNA-induced RNA silencing by 2´-*O*-methyl oligonucleotides in Drosophila S2 cells. In Vitro Cell Dev Biol Anim *41*, 12-18.

Bernstein, E., Caudy, A. A., Hammond, S. M., and Hannon, G. J. (2001). Role for a bidentate ribonuclease in the initiation step of RNA interference. Nature *409*, 363-366.

Bernstein, E., Kim, S. Y., Carmell, M. A., Murchison, E. P., Alcorn, H., Li, M. Z., Mills, A. A., Elledge, S. J., Anderson, K. V., and Hannon, G. J. (2003). Dicer is essential for mouse development. Nat Genet *35*, 215-217.

Billy, E., Brondani, V., Zhang, H., Muller, U., and Filipowicz, W. (2001). Specific interference with gene expression induced by long, double-stranded RNA in mouse embryonal teratocarcinoma cell lines. Proc Natl Acad Sci U S A *98*, 14428-14433.

Blower, P. E., Verducci, J. S., Lin, S., Zhou, J., Chung, J. H., Dai, Z., Liu, C. G., Reinhold, W., Lorenzi, P. L., Kaldjian, E. P., Croce, C. M., Weinstein, J. N., and Sadee, W. (2007). MicroRNA expression profiles for the NCI-60 cancer cell panel. Mol Cancer Ther *6*, 1483-1491.

Bommer, G. T., Gerin, I., Feng, Y., Kaczorowski, A. J., Kuick, R., Love, R. E., Zhai, Y., Giordano, T. J., Qin, Z. S., Moore, B. B., MacDougald, O. A., Cho, K. R., and Fearon, E. R. (2007). p53-mediated activation of miRNA34 candidate tumor-suppressor genes. Curr Biol *17*, 1298-1307.

Borrmann, L., Wilkening, S., and Bullerdiek, J. (2001). The expression of HMGA genes is regulated by their 3'UTR. Oncogene *20*, 4537-4541.

Boutet, S., Vazquez, F., Liu, J., Beclin, C., Fagard, M., Gratias, A., Morel, J. B., Crete, P., Chen, X., and Vaucheret, H. (2003). Arabidopsis HEN1: a genetic link between endogenous miRNA controlling development and siRNA controlling transgene silencing and virus resistance. Curr Biol *13*, 843-848.

Boutla, A., Delidakis, C., and Tabler, M. (2003). Developmental defects by antisense-mediated inactivation of micro-RNAs 2 and 13 in Drosophila and the identification of putative target genes. Nucleic Acids Res *31*, 4973-4980.

Brennecke, J., Aravin, A. A., Stark, A., Dus, M., Kellis, M., Sachidanandam, R., and Hannon, G. J. (2007). Discrete small RNA-generating loci as master regulators of transposon activity in Drosophila. Cell *128*, 1089-1103.

Brennecke, J., Hipfner, D. R., Stark, A., Russell, R. B., and Cohen, S. M. (2003). bantam Encodes a Developmentally Regulated microRNA that Controls Cell Proliferation and Regulates the Proapoptotic Gene hid in Drosophila. Cell *113*, 25-36.

Brennecke, J., Stark, A., Russell, R. B., and Cohen, S. M. (2005). Principles of microRNA-target recognition. PLoS Biol *3*, e85.

Brigneti, G., Voinnet, O., Li, W. X., Ji, L. H., Ding, S. W., and Baulcombe, D. C. (1998). Viral pathogenicity determinants are suppressors of transgene silencing in Nicotiana benthamiana. EMBO J *17*, 6739-6746.

Britten, R. J., and Davidson, E. H. (1969). Gene regulation for higher cells: a theory. Science *165*, 349-357.

Buhler, M., and Moazed, D. (2007). Transcription and RNAi in heterochromatic gene silencing. Nat Struct Mol Biol *14*, 1041-1048.

Caudy, A. A., Ketting, R. F., Hammond, S. M., Denli, A. M., Bathoorn, A. M., Tops, B. B., Silva, J. M., Myers, M. M., Hannon, G. J., and Plasterk, R. H. (2003). A micrococcal nuclease homologue in RNAi effector complexes. Nature *425*, 411-414.

Caudy, A. A., Myers, M., Hannon, G. J., and Hammond, S. M. (2002). Fragile X-related protein and VIG associate with the RNA interference machinery. Genes Dev *16*, 2491-2496.

Chan, J. A., Krichevsky, A. M., and Kosik, K. S. (2005). MicroRNA-21 is an antiapoptotic factor in human glioblastoma cells. Cancer Res *65*, 6029-6033.

Chen, C. Z., Li, L., Lodish, H. F., and Bartel, D. P. (2004). MicroRNAs modulate hematopoietic lineage differentiation. Science *303*, 83-86.

Chen, J. F., Murchison, E. P., Tang, R., Callis, T. E., Tatsuguchi, M., Deng, Z., Rojas, M., Hammond, S. M., Schneider, M. D., Selzman, C. H., Meissner, G., Patterson, C., Hannon, G. J., and Wang, D. Z. (2008). Targeted deletion of Dicer in the heart leads to dilated cardiomyopathy and heart failure. Proc Natl Acad Sci U S A *105*, 2111-2116.

Chen, X., Liu, J., Cheng, Y., and Jia, D. (2002). HEN1 functions pleiotropically in Arabidopsis development and acts in C function in the flower. Development *129*, 1085-1094.

Chendrimada, T. P., Finn, K. J., Ji, X., Baillat, D., Gregory, R. I., Liebhaber, S. A., Pasquinelli, A. E., and Shiekhattar, R. (2007). MicroRNA silencing through RISC recruitment of eIF6. Nature *447*, 823-828.

Chendrimada, T. P., Gregory, R. I., Kumaraswamy, E., Norman, J., Cooch, N., Nishikura, K., and Shiekhattar, R. (2005). TRBP recruits the Dicer complex to Ago2 for microRNA processing and gene silencing. Nature *436*, 740-744.

Chiu, Y.-L., and Rana, T. M. (2002). RNAi in Human Cells: Basic Structural and Functional Features of Small Interfering RNA. Molecular Cell *10*, 549-561.

Clemens, J. C., Worby, C. A., Simonson-Leff, N., Muda, M., Maehama, T., Hemmings, B. A., and Dixon, J. E. (2000). Use of double-stranded RNA interference in Drosophila cell lines to dissect signal transduction pathways. Proc Natl Acad Sci U S A *97*, 6499-6503.

Colmenares, S. U., Buker, S. M., Buhler, M., Dlakic, M., and Moazed, D. (2007). Coupling of double-stranded RNA synthesis and siRNA generation in fission yeast RNAi. Mol Cell *27*, 449-461.

Corsten, M. F., Miranda, R., Kasmieh, R., Krichevsky, A. M., Weissleder, R., and Shah, K. (2007). MicroRNA-21 knockdown disrupts glioma growth in vivo and displays synergistic cytotoxicity with neural precursor cell delivered S-TRAIL in human gliomas. Cancer Res *67*, 8994-9000.

Cuellar, T. L., Davis, T. H., Nelson, P. T., Loeb, G. B., Harfe, B. D., Ullian, E., and McManus, M. T. (2008). Dicer loss in striatal neurons produces behavioral and neuroanatomical phenotypes in the absence of neurodegeneration. Proc Natl Acad Sci U S A *105*, 5614-5619.

Czech, B., Malone, C. D., Zhou, R., Stark, A., Schlingeheyde, C., Dus, M., Perrimon, N., Kellis, M., Wohlschlegel, J. A., Sachidanandam, R., Hannon, G. J., and Brennecke, J. (2008). An endogenous small interfering RNA pathway in Drosophila. Nature

Dalmay, T., Horsefield, R., Braunstein, T. H., and Baulcombe, D. C. (2001). SDE3 encodes an RNA helicase required for post-transcriptional gene silencing in Arabidopsis. EMBO J *20*, 2069-2078.

Danilevskaya, O. N., Slot, F., Traverse, K. L., Hogan, N. C., and Pardue, M. L. (1994). Drosophila telomere transposon HeT-A produces a transcript with tightly bound protein. Proc Natl Acad Sci U S A *91*, 6679-6682.

Davis, E., Caiment, F., Tordoir, X., Cavaille, J., Ferguson-Smith, A., Cockett, N., Georges, M., and Charlier, C. (2005). RNAi-mediated allelic trans-interaction at the imprinted Rtl1/Peg11 locus. Curr Biol *15*, 743-749.

Davis, S., Lollo, B., Freier, S., and Esau, C. (2006). Improved targeting of miRNA with antisense oligonucleotides. Nucleic Acids Res *34*, 2294-2304.

Davis, T. H., Cuellar, T. L., Koch, S. M., Barker, A. J., Harfe, B. D., McManus, M. T., and Ullian, E. M. (2008). Conditional loss of Dicer disrupts cellular and tissue morphogenesis in the cortex and hippocampus. J Neurosci *28*, 4322-4330.

Desjardins, J., Mata, J., Brown, T., Graham, D., Zon, G., and Iversen, P. (1995). Cholesteryl-conjugated phosphorothioate oligodeoxynucleotides modulate CYP2B1 expression in vivo. J Drug Target *2*, 477-485.

Dignam, J. D., Lebovitz, R. M., and Roeder, R. G. (1983). Accurate transcription initiation by RNA polymerase II in a soluble extract from isolated mammalian nuclei. Nucleic Acids Res *11*, 1475-1489.

Ding, L., Spencer, A., Morita, K., and Han, M. (2005). The developmental timing regulator AIN-1 interacts with miRISCs and may target the argonaute protein ALG-1 to cytoplasmic P bodies in C. elegans. Mol Cell *19*, 437-447.

Doench, J. G., Petersen, C. P., and Sharp, P. A. (2003). siRNAs can function as miRNAs. Genes Dev *17*, 438-442.

Doench, J. G., and Sharp, P. A. (2004). Specificity of microRNA target selection in translational repression. Genes Dev *18*, 504-511.

Doi, N., Zenno, S., Ueda, R., Ohki-Hamazaki, H., Ui-Tei, K., and Saigo, K. (2003). Short-Interfering-RNA-Mediated Gene Silencing in Mammalian Cells Requires Dicer and eIF2C Translation Initiation Factors. Curr Biol *13*, 41-46.

Du, T., and Zamore, P. D. (2005). microPrimer: the biogenesis and function of microRNA. Development *132*, 4645-4652.

Duursma, A. M., Kedde, M., Schrier, M., le Sage, C., and Agami, R. (2008). miR-148 targets human DNMT3b protein coding region. RNA *14*, 872-877.

Easow, G., Teleman, A. A., and Cohen, S. M. (2007). Isolation of microRNA targets by miRNP immunopurification. RNA *13*, 1198-1204.
Ebert, M. S., Neilson, J. R., and Sharp, P. A. (2007). MicroRNA sponges: competitive inhibitors of small RNAs in mammalian cells. Nat Methods *4*, 721-726.

Elbashir, S. M., Harborth, J., Lendeckel, W., Yalcin, A., Weber, K., and Tuschl, T. (2001a). Duplexes of 21-nucleotide RNAs mediate RNA interference in cultured mammalian cells. Nature *411*, 494-498.

Elbashir, S. M., Lendeckel, W., and Tuschl, T. (2001b). RNA interference is mediated by 21- and 22-nucleotide RNAs. Genes Dev *15*, 188-200.

Elmen, J., Lindow, M., Schutz, S., Lawrence, M., Petri, A., Obad, S., Lindholm, M., Hedtjarn, M., Hansen, H. F., Berger, U., Gullans, S., Kearney, P., Sarnow, P., Straarup, E. M., and Kauppinen, S. (2008a). LNA-mediated microRNA silencing in non-human primates. Nature *452*, 896-899.

Elmen, J., Lindow, M., Silahtaroglu, A., Bak, M., Christensen, M., Lind-Thomsen, A., Hedtjarn, M., Hansen, J. B., Hansen, H. F., Straarup, E. M., McCullagh, K., Kearney, P., and Kauppinen, S. (2008b). Antagonism of microRNA-122 in mice by systemically administered LNA-antimiR leads to up-regulation of a large set of predicted target mRNAs in the liver. Nucleic Acids Res *36*, 1153-1162.

Enright, A. J., John, B., Gaul, U., Tuschl, T., Sander, C., and Marks, D. S. (2003). MicroRNA targets in Drosophila. Genome Biol *5*, R1.

Esau, C., Davis, S., Murray, S. F., Yu, X. X., Pandey, S. K., Pear, M., Watts, L., Booten, S. L., Graham, M., McKay, R., Subramaniam, A., Propp, S., Lollo, B. A., Freier, S., Bennett, C. F., Bhanot, S., and Monia, B. P. (2006). miR-122 regulation of lipid metabolism revealed by in vivo antisense targeting. Cell Metab *3*, 87-98.

Esau, C., Kang, X., Peralta, E., Hanson, E., Marcusson, E. G., Ravichandran, L. V., Sun, Y., Koo, S., Perera, R. J., Jain, R., Dean, N. M., Freier, S. M., Bennett, C. F., Lollo, B., and Griffey, R. (2004). MicroRNA-143 regulates adipocyte differentiation. J Biol Chem *279*, 52361-52365.

Esau, C. C. (2008). Inhibition of microRNA with antisense oligonucleotides. Methods *44*, 55-60.

Eulalio, A., Behm-Ansmant, I., Schweizer, D., and Izaurralde, E. (2007). P-body formation is a consequence, not the cause, of RNA-mediated gene silencing. Mol Cell Biol *27*, 3970-3981.

Eulalio, A., Huntzinger, E., and Izaurralde, E. (2008). GW182 interaction with Argonaute is essential for miRNA-mediated translational repression and mRNA decay. Nat Struct Mol Biol *15*, 346-353.

Fabani, M. M., and Gait, M. J. (2008). miR-122 targeting with LNA/2'-O-methyl oligonucleotide mixmers, peptide nucleic acids (PNA), and PNA-peptide conjugates. RNA *14*, 336-346.

Fedele, M., Battista, S., Kenyon, L., Baldassarre, G., Fidanza, V., Klein-Szanto, A. J., Parlow, A. F., Visone, R., Pierantoni, G. M., Outwater, E., Santoro, M., Croce, C. M., and Fusco, A. (2002). Overexpression of the HMGA2 gene in transgenic mice leads to the onset of pituitary adenomas. Oncogene *21*, 3190-3198.

Filipowicz, W. (2005). RNAi: the nuts and bolts of the RISC machine. Cell *122*, 17-20.
Fire, A., Albertson, D., Harrison, S. W., and Moerman, D. G. (1991). Production of antisense RNA leads to effective and specific inhibition of gene expression in C. elegans muscle. Development *113*, 503-514.

Fire, A., Xu, S., Montgomery, M. K., Kostas, S. A., Driver, S. E., and Mello, C. C. (1998). Potent and specific genetic interference by double-stranded RNA in Caenorhabditis elegans. Nature *391*, 806-811.

Flavell, R. B., Bennett, M. D., Smith, J. B., and Smith, D. B. (1974). Genome size and the proportion of repeated nucleotide sequence DNA in plants. Biochem Genet *12*, 257-269.

Förstemann, K., Horwich, M. D., Wee, L., Tomari, Y., and Zamore, P. D. (2007). Drosophila microRNAs are sorted into functionally distinct argonaute complexes after production by dicer-1. Cell *130*, 287-297.

Förstemann, K., Tomari, Y., Du, T., Vagin, V. V., Denli, A. M., Bratu, D. P., Klattenhoff, C., Theurkauf, W. E., and Zamore, P. D. (2005). Normal microRNA maturation and germ-line stem cell maintenance requires Loquacious, a double-stranded RNA-binding domain protein. PLoS Biol *3*, e236.

Galiana-Arnoux, D., Dostert, C., Schneemann, A., Hoffmann, J. A., and Imler, J. L. (2006). Essential function in vivo for Dicer-2 in host defense against RNA viruses in drosophila. Nat Immunol *7*, 590-597.

García MA, Gil J, Ventoso I, Guerra S, Domingo E, Rivas C, Esteban M.Impact of protein kinase PKR in cell biology: from antiviral to antiproliferative action.Microbiol Mol Biol Rev. 2006 Dec;70(4):1032-60.

Gaur, A., Jewell, D. A., Liang, Y., Ridzon, D., Moore, J. H., Chen, C., Ambros, V. R., and Israel, M. A. (2007). Characterization of microRNA expression levels and their biological correlates in human cancer cell lines. Cancer Res *67*, 2456-2468.

Ghildiyal, M., Seitz, H., Horwich, M. D., Li, C., Du, T., Lee, S., Xu, J., Kittler, E. L., Zapp, M. L., Weng, Z., and Zamore, P. D. (2008). Endogenous siRNAs Derived from Transposons and mRNAs in Drosophila Somatic Cells. Science

Giraldez, A. J., Cinalli, R. M., Glasner, M. E., Enright, A. J., Thomson, J. M., Baskerville, S., Hammond, S. M., Bartel, D. P., and Schier, A. F. (2005). MicroRNAs regulate brain morphogenesis in zebrafish. Science *308*, 833-838.

Giraldez, A. J., Mishima, Y., Rihel, J., Grocock, R. J., Van Dongen, S., Inoue, K., Enright, A. J., and Schier, A. F. (2006). Zebrafish MiR-430 promotes deadenylation and clearance of maternal mRNAs. Science *312*, 75-79.

Girard, A., Sachidanandam, R., Hannon, G. J., and Carmell, M. A. (2006). A germline-specific class of small RNAs binds mammalian Piwi proteins. Nature *442*, 199-202.

Griffiths-Jones, S., Grocock, R. J., van Dongen, S., Bateman, A., and Enright, A. J. (2006). miRBase: microRNA sequences, targets and gene nomenclature. Nucleic Acids Res *34*, D140-4.

Grimson, A., Farh, K. K., Johnston, W. K., Garrett-Engele, P., Lim, L. P., and Bartel, D. P. (2007). MicroRNA targeting specificity in mammals: determinants beyond seed pairing. Mol Cell *27*, 91-105.

Grishok, A., Pasquinelli, A. E., Conte, D., Li, N., Parrish, S., Ha, I., Baillie, D. L., Fire, A., Ruvkun, G., and Mello, C. C. (2001). Genes and Mechanisms Related to RNA Interference Regulate Expression of the Small Temporal RNAs that Control C. elegans Developmental Timing. Cell *106*, 23-34.

Grun, D., Wang, Y. L., Langenberger, D., Gunsalus, K. C., and Rajewsky, N. (2005). microRNA target predictions across seven Drosophila species and comparison to mammalian targets. PLoS Comput Biol *1*, e13.

Gunawardane, L. S., Saito, K., Nishida, K. M., Miyoshi, K., Kawamura, Y., Nagami, T., Siomi, H., and Siomi, M. C. (2007). A Slicer-Mediated Mechanism for Repeat-Associated siRNA 5' End Formation in Drosophila. Science

Guo, S., and Kemphues, K. J. (1995). par-1, a gene required for establishing polarity in C. elegans embryos, encodes a putative Ser/Thr kinase that is asymmetrically distributed. Cell *81*, 611-620.

Haley, B., Tang, G., and Zamore, P. D. (2003). In vitro analysis of RNA interference in Drosophila melanogaster. Methods *30*, 330-336.

Haley, B., and Zamore, P. D. (2004). Kinetic analysis of the RNAi enzyme complex. Nat Struct Mol Biol *11*, 599-606.

Hamilton, A. J., and Baulcombe, D. C. (1999). A species of small antisense RNA in posttranscriptional gene silencing in plants. Science *286*, 950-952.

Hammond, S. M., Bernstein, E., Beach, D., and Hannon, G. J. (2000). An RNA-directed nuclease mediates post-transcriptional gene silencing in Drosophila cells. Nature *404*, 293-296.

Hammond, S. M., Boettcher, S., Caudy, A. A., Kobayashi, R., and Hannon, G. J. (2001). Argonaute2, a link between genetic and biochemical analyses of RNAi. Science *293*, 1146-1150.

Han, J., Lee, Y., Yeom, K. H., Nam, J. W., Heo, I., Rhee, J. K., Sohn, S. Y., Cho, Y., Zhang, B. T., and Kim, V. N. (2006). Molecular basis for the recognition of primary microRNAs by the Drosha-DGCR8 complex. Cell *125*, 887-901.

Harfe, B. D., McManus, M. T., Mansfield, J. H., Hornstein, E., and Tabin, C. J. (2005). The RNaseIII enzyme Dicer is required for morphogenesis but not patterning of the vertebrate limb. Proc Natl Acad Sci U S A *102*, 10898-10903.

Harris, K. S., Zhang, Z., McManus, M. T., Harfe, B. D., and Sun, X. (2006). Dicer function is essential for lung epithelium morphogenesis. Proc Natl Acad Sci U S A *103*, 2208-2213.

Hatfield, S. D., Shcherbata, H. R., Fischer, K. A., Nakahara, K., Carthew, R. W., and Ruohola-Baker, H. (2005). Stem cell division is regulated by the microRNA pathway. Nature *435*, 974-978.

He, L., Thomson, J. M., Hemann, M. T., Hernando-Monge, E., Mu, D., Goodson, S., Powers, S., Cordon-Cardo, C., Lowe, S. W., Hannon, G. J., and Hammond, S. M. (2005). A microRNA polycistron as a potential human oncogene. Nature *435*, 828-833.

Horwich, M. D., Li, C., Matranga, C., Vagin, V., Farley, G., Wang, P., and Zamore, P. D. (2007). The Drosophila RNA methyltransferase, DmHen1, modifies germline piRNAs and single-stranded siRNAs in RISC. Curr Biol *17*, 1265-1272.

Houwing, S., Kamminga, L. M., Berezikov, E., Cronembold, D., Girard, A., van den Elst, H., Filippov, D. V., Blaser, H., Raz, E., Moens, C. B., Plasterk, R. H., Hannon, G. J., Draper, B. W., and Ketting, R. F. (2007). A role for Piwi and piRNAs in germ cell maintenance and transposon silencing in Zebrafish. Cell *129*, 69-82.

Hutvágner, G., McLachlan, J., Pasquinelli, A. E., Balint, É., Tuschl, T., and Zamore, P. D. (2001). A cellular function for the RNA-interference enzyme Dicer in the maturation of the *let-7* small temporal RNA. Science *293*, 834-838.

Hutvágner, G., Simard, M. J., Mello, C. C., and Zamore, P. D. (2004). Sequence-specific inhibition of small RNA function. PLoS Biol *2*, E98.

Hutvágner, G., and Zamore, P. D. (2002). A microRNA in a Multiple-Turnover RNAi Enzyme Complex. Science *297*, 2056-2060.

Inoue, H., Hayase, Y., Imura, A., Iwai, S., Miura, K., and Ohtsuka, E. (1987). Synthesis and hybridization studies on two complementary nona(2'-O-methyl)ribonucleotides. Nucleic Acids Res *15*, 6131-6148.

Ishizuka, A., Siomi, M. C., and Siomi, H. (2002). A Drosophila fragile X protein interacts with components of RNAi and ribosomal proteins. Genes Dev *16*, 2497-2508.

Jackson, A. L., Bartz, S. R., Schelter, J., Kobayashi, S. V., Burchard, J., Mao, M., Li, B., Cavet, G., and Linsley, P. S. (2003). Expression profiling reveals off-target gene regulation by RNAi. Nat Biotechnol *21*, 635-637.

Jackson, A. L., Burchard, J., Schelter, J., Chau, B. N., Cleary, M., Lim, L., and Linsley, P. S. (2006). Widespread siRNA "off-target" transcript silencing mediated by seed region sequence complementarity. RNA *12*, 1179-1187.

Jain, N., Thatte, J., Braciale, T., Ley, K., O'Connell, M., and Lee, J. K. (2003). Local-pooled-error test for identifying differentially expressed genes with a small number of replicated microarrays. Bioinformatics *19*, 1945-1951.

Jiang, F., Ye, X., Liu, X., Fincher, L., McKearin, D., and Liu, Q. (2005). Dicer-1 and R3D1-L catalyze microRNA maturation in Drosophila. Genes Dev *19*, 1674-1679.

Jing, Q., Huang, S., Guth, S., Zarubin, T., Motoyama, A., Chen, J., Di Padova, F., Lin, S. C., Gram, H., and Han, J. (2005). Involvement of microRNA in AU-rich element-mediated mRNA instability. Cell *120*, 623-634.

Johnson, S. M., Grosshans, H., Shingara, J., Byrom, M., Jarvis, R., Cheng, A., Labourier, E., Reinert, K. L., Brown, D., and Slack, F. J. (2005). RAS is regulated by the *let-7* microRNA family. Cell *120*, 635-647.

Jones-Rhoades, M. W., Bartel, D. P., and Bartel, B. (2006). MicroRNAS and their regulatory roles in plants. Annu Rev Plant Biol *57*, 19-53.

Jopling, C. L., Yi, M., Lancaster, A. M., MLemon, S., and Sarnow, P. (2005). Modulation of Hepatitis C Virus RNA Abundance by a Liver-Specific MicroRNA. Science *309*, 1577-1581.

Kanellopoulou, C., Muljo, S. A., Kung, A. L., Ganesan, S., Drapkin, R., Jenuwein, T., Livingston, D. M., and Rajewsky, K. (2005). Dicer-deficient mouse embryonic stem cells are defective in differentiation and centromeric silencing. Genes Dev *19*, 489-501.

Kapitonov, V. V., and Jurka, J. (2003). Molecular paleontology of transposable elements in the Drosophila melanogaster genome. Proc Natl Acad Sci U S A *100*, 6569-6574.

Karres, J. S., Hilgers, V., Carrera, I., Treisman, J., and Cohen, S. M. (2007). The conserved microRNA miR-8 tunes atrophin levels to prevent neurodegeneration in Drosophila. Cell *131*, 136-145.

Kataoka, Y., Takeichi, M., and Uemura, T. (2001). Developmental roles and molecular characterization of a Drosophila homologue of Arabidopsis Argonaute1, the founder of a novel gene superfamily. Genes Cells *6*, 313-325.

Kawamura, Y., Saito, K., Kin, T., Ono, Y., Asai, K., Sunohara, T., Okada, T. N., Siomi, M. C., and Siomi, H. (2008). Drosophila endogenous small RNAs bind to Argonaute 2 in somatic cells. Nature

Kennerdell, J. R., and Carthew, R. W. (1998). Use of dsRNA-mediated genetic interference to demonstrate that frizzled and frizzled 2 act in the wingless pathway. Cell *95*, 1017-1026.

Kertesz, M., Iovino, N., Unnerstall, U., Gaul, U., and Segal, E. (2007). The role of site accessibility in microRNA target recognition. Nat Genet *39*, 1278-1284.

Ketting, R. F., Fischer, S. E., Bernstein, E., Sijen, T., Hannon, G. J., and Plasterk, R. H. (2001). Dicer functions in RNA interference and in synthesis of small RNA involved in developmental timing in C. elegans. Genes Dev *15*, 2654-2659.

Ketting, R. F., Haverkamp, T. H., van Luenen, H. G., and Plasterk, R. H. (1999). Mut-7 of C. elegans, required for transposon silencing and RNA interference, is a homolog of Werner syndrome helicase and RNaseD. Cell *99*, 133-141.

Khvorova, A., Reynolds, A., and Jayasena, S. D. (2003). Functional siRNAs and miRNAs exhibit strand bias. Cell *115*, 209-216.

Kim, J., Inoue, K., Ishii, J., Vanti, W. B., Voronov, S. V., Murchison, E., Hannon, G., and Abeliovich, A. (2007). A MicroRNA feedback circuit in midbrain dopamine neurons. Science *317*, 1220-1224.

Kim, K., Lee, Y. S., and Carthew, R. W. (2006). Conversion of pre-RISC to holo-RISC by Ago2 during assembly of RNAi complexes. RNA *13*, 22-29.

Kim, Y. K., and Kim, V. N. (2007). Processing of intronic microRNAs. EMBO J *26*, 775-783.

Kiriakidou, M., Nelson, P. T., Kouranov, A., Fitziev, P., Bouyioukos, C., Mourelatos, Z., and Hatzigeorgiou, A. (2004). A combined computational-experimental approach predicts human microRNA targets. Genes Dev *18*, 1165-1178.

Kiriakidou, M., Tan, G. S., Lamprinaki, S., De Planell-Saguer, M., Nelson, P. T., and Mourelatos, Z. (2007). An mRNA m(7)G Cap Binding-like Motif within Human Ago2 Represses Translation. Cell *129*, 1141-1151.

Kirino, Y., and Mourelatos, Z. (2007a). Mouse Piwi-interacting RNAs are 2'-O-methylated at their 3' termini. Nat Struct Mol Biol *14*, 347-348.

Kirino, Y., and Mourelatos, Z. (2007b). The mouse homolog of HEN1 is a potential methylase for Piwi-interacting RNAs. RNA *13*, 1397-1401.

Klattenhoff, C., Bratu, D. P., McGinnis-Schultz, N., Koppetsch, B. S., Cook, H. A., and Theurkauf, W. E. (2007). Drosophila rasiRNA pathway mutations disrupt embryonic axis specification through activation of an ATR/Chk2 DNA damage response. Dev Cell *12*, 45-55.

Kleinman ME, Yamada K, Takeda A, Chandrasekaran V, Nozaki M, Baffi JZ, Albuquerque RJ, Yamasaki S, Itaya M, Pan Y, Appukuttan B, Gibbs D, Yang Z, Karikó K, Ambati BK, Wilgus TA, DiPietro LA, Sakurai E, Zhang K, Smith JR, Taylor EW, Ambati J.Sequence- and target-independent angiogenesis suppression by siRNA via TLR3.Nature. 2008 Apr 3;452(7187):591-7.

Klenov, M. S., Lavrov, S. A., Stolyarenko, A. D., Ryazansky, S. S., Aravin, A. A., Tuschl, T., and Gvozdev, V. A. (2007). Repeat-associated siRNAs cause chromatin silencing of retrotransposons in the Drosophila melanogaster germline. Nucleic Acids Res *35*, 5430-5438.

Kloosterman, W. P., Lagendijk, A. K., Ketting, R. F., Moulton, J. D., and Plasterk, R. H. (2007). Targeted inhibition of miRNA maturation with morpholinos reveals a role for miR-375 in pancreatic islet development. PLoS Biol *5*, e203.

Kloosterman, W. P., Wienholds, E., Ketting, R. F., and Plasterk, R. H. (2004). Substrate requirements for *let-7* function in the developing zebrafish embryo. Nucleic Acids Res *32*, 6284-6291.

Krek, A., Grun, D., Poy, M. N., Wolf, R., Rosenberg, L., Epstein, E. J., MacMenamin, P., da Piedade, I., Gunsalus, K. C., Stoffel, M., and Rajewsky, N. (2005). Combinatorial microRNA target predictions. Nat Genet *37*, 495-500.

Krieg, A. M., Tonkinson, J., Matson, S., Zhao, Q., Saxon, M., Zhang, L. M., Bhanja, U., Yakubov, L., and Stein, C. A. (1993). Modification of antisense phosphodiester oligodeoxynucleotides by a 5' cholesteryl moiety increases cellular association and improves efficacy. Proc Natl Acad Sci U S A *90*, 1048-1052.

Krutzfeldt, J., Kuwajima, S., Braich, R., Rajeev, K. G., Pena, J., Tuschl, T., Manoharan, M., and Stoffel, M. (2007). Specificity, duplex degradation and subcellular localization of antagomirs. Nucleic Acids Res *35*, 2885-2892.

Krutzfeldt, J., Rajewsky, N., Braich, R., Rajeev, K. G., Tuschl, T., Manoharan, M., and Stoffel, M. (2005). Silencing of microRNAs in vivo with 'antagomirs'. Nature *438*, 685-689.

Kurihara, Y., and Watanabe, Y. (2004). Arabidopsis micro-RNA biogenesis through Dicer-like 1 protein functions. Proc Natl Acad Sci U S A *101*, 12753-12758.

Kwon, C., Han, Z., Olson, E. N., and Srivastava, D. (2005). MicroRNA1 influences cardiac differentiation in Drosophila and regulates Notch signaling. Proc Natl Acad Sci U S A *102*, 18986-18991.

Lagos-Quintana, M., Rauhut, R., Lendeckel, W., and Tuschl, T. (2001). Identification of Novel Genes Coding for Small Expressed RNAs. Science *294*, 853-858.

Lagos-Quintana, M., Rauhut, R., Yalcin, A., Meyer, J., Lendeckel, W., and Tuschl, T. (2002). Identification of Tissue-Specific MicroRNAs from Mouse. Curr Biol *12*, 735-739.

Lai, E. C. (2002). Micro RNAs are complementary to 3' UTR sequence motifs that mediate negative post-transcriptional regulation. Nat Genet *30*, 363-364.

Lander, E. S., Linton, L. M., Birren, B., Nusbaum, C., Zody, M. C., Baldwin, J., Devon, K., Dewar, K., Doyle, M., FitzHugh, W., Funke, R., Gage, D., Harris, K., Heaford, A., Howland, J., Kann, L., Lehoczky, J., LeVine, R., McEwan, P., McKernan, K., Meldrim, J., Mesirov, J. P., Miranda, C., Morris, W., Naylor, J., Raymond, C., Rosetti, M., Santos, R., Sheridan, A., Sougnez, C., Stange-Thomann, N., Stojanovic, N., Subramanian, A., Wyman, D., Rogers, J., Sulston, J., Ainscough, R., Beck, S., Bentley, D., Burton, J., Clee, C., Carter, N., Coulson, A., Deadman, R., Deloukas, P., Dunham, A., Dunham, I., Durbin, R., French, L., Grafham, D., Gregory, S., Hubbard, T., Humphray, S., Hunt, A., Jones, M., Lloyd, C., McMurray, A., Matthews, L., Mercer, S., Milne, S., Mullikin, J. C., Mungall, A., Plumb, R., Ross, M., Shownkeen, R., Sims, S., Waterston, R. H., Wilson, R. K., Hillier, L. W., McPherson, J. D., Marra, M. A., Mardis, E. R.,

Fulton, L. A., Chinwalla, A. T., Pepin, K. H., Gish, W. R., Chissoe, S. L., Wendl, M. C., Delehaunty, K. D., Miner, T. L., Delehaunty, A., Kramer, J. B., Cook, L. L., Fulton, R. S., Johnson, D. L., Minx, P. J., Clifton, S. W., Hawkins, T., Branscomb, E., Predki, P., Richardson, P., Wenning, S., Slezak, T., Doggett, N., Cheng, J. F., Olsen, A., Lucas, S., Elkin, C., Uberbacher, E., Frazier, M., Gibbs, R. A., Muzny, D. M., Scherer, S. E., Bouck, J. B., Sodergren, E. J., Worley, K. C., Rives, C. M., Gorrell, J. H., Metzker, M. L., Naylor, S. L., Kucherlapati, R. S., Nelson, D. L., Weinstock, G. M., Sakaki, Y., Fujiyama, A., Hattori, M., Yada, T., Toyoda, A., Itoh, T., Kawagoe, C., Watanabe, H., Totoki, Y., Taylor, T., Weissenbach, J., Heilig, R., Saurin, W., Artiguenave, F., Brottier, P., Bruls, T., Pelletier, E., Robert, C., Wincker, P., Smith, D. R., Doucette-Stamm, L., Rubenfield, M., Weinstock, K., Lee, H. M., Dubois, J., Rosenthal, A., Platzer, M., Nyakatura, G., Taudien, S., Rump, A., Yang, H., Yu, J., Wang, J., Huang, G., Gu, J., Hood, L., Rowen, L., Madan, A., Qin, S., Davis, R. W., Federspiel, N. A., Abola, A. P., Proctor, M. J., Myers, R. M., Schmutz, J., Dickson, M., Grimwood, J., Cox, D. R., Olson, M. V., Kaul, R., Raymond, C., Shimizu, N., Kawasaki, K., Minoshima, S., Evans, G. A., Athanasiou, M., Schultz, R., Roe, B. A., Chen, F., Pan, H., Ramser, J., Lehrach, H., Reinhardt, R., McCombie, W. R., de la Bastide, M., Dedhia, N., Blocker, H., Hornischer, K., Nordsiek, G., Agarwala, R., Aravind, L., Bailey, J. A., Bateman, A., Batzoglou, S., Birney, E., Bork, P., Brown, D. G., Burge, C. B., Cerutti, L., Chen, H. C., Church, D., Clamp, M., Copley, R. R., Doerks, T., Eddy, S. R., Eichler, E. E., Furey, T. S., Galagan, J., Gilbert, J. G., Harmon, C., Hayashizaki, Y., Haussler, D., Hermjakob, H., Hokamp, K., Jang, W., Johnson, L. S., Jones, T. A., Kasif, S., Kaspryzk, A., Kennedy, S., Kent, W. J., Kitts, P., Koonin, E. V., Korf, I., Kulp, D., Lancet, D., Lowe, T. M., McLysaght, A., Mikkelsen, T., Moran, J. V., Mulder, N., Pollara, V. J., Ponting, C. P., Schuler, G., Schultz, J., Slater, G., Smit, A. F., Stupka, E., Szustakowski, J., Thierry-Mieg, D., Thierry-Mieg, J., Wagner, L., Wallis, J., Wheeler, R., Williams, A., Wolf, Y. I., Wolfe, K. H., Yang, S. P., Yeh, R. F., Collins, F., Guyer, M. S., Peterson, J., Felsenfeld, A., Wetterstrand, K. A., Patrinos, A., Morgan, M. J., de Jong, P., Catanese, J. J., Osoegawa, K., Shizuya, H., Choi, S., and Chen, Y. J. (2001). Initial sequencing and analysis of the human genome. Nature *409*, 860-921.

Landgraf, P., Rusu, M., Sheridan, R., Sewer, A., Iovino, N., Aravin, A., Pfeffer, S., Rice, A., Kamphorst, A. O., Landthaler, M., Lin, C., Socci, N. D., Hermida, L., Fulci, V., Chiaretti, S., Foa, R., Schliwka, J., Fuchs, U., Novosel, A., Muller, R. U., Schermer, B., Bissels, U., Inman, J., Phan, Q., Chien, M., Weir, D. B., Choksi, R., De Vita, G., Frezzetti, D., Trompeter, H. I., Hornung, V., Teng, G., Hartmann, G., Palkovits, M., Di Lauro, R., Wernet, P., Macino, G., Rogler, C. E., Nagle, J. W., Ju, J., Papavasiliou, F. N., Benzing, T., Lichter, P., Tam, W., Brownstein, M. J., Bosio, A., Borkhardt, A., Russo, J. J., Sander, C., Zavolan, M., and Tuschl, T. (2007). A mammalian microRNA expression atlas based on small RNA library sequencing. Cell *129*, 1401-1414.

Lau, N. C., Lim, L. P., Weinstein, E. G., and Bartel, D. P. (2001). An abundant class of tiny RNAs with probable regulatory roles in Caenorhabditis elegans. Science *294*, 858-862.

Lau, N. C., Seto, A. G., Kim, J., Kuramochi-Miyagawa, S., Nakano, T., Bartel, D. P., and Kingston, R. E. (2006). Characterization of the piRNA complex from rat testes. Science *313*, 363-367.

Leaman, D., Chen, P. Y., Fak, J., Yalcin, A., Pearce, M., Unnerstall, U., Marks, D. S., Sander, C., Tuschl, T., and Gaul, U. (2005). Antisense-mediated depletion reveals essential and specific functions of microRNAs in Drosophila development. Cell *121*, 1097-1108.

Lecellier, C. H., Dunoyer, P., Arar, K., Lehmann-Che, J., Eyquem, S., Himber, C., Saib, A., and Voinnet, O. (2005). A cellular microRNA mediates antiviral defense in human cells. Science *308*, 557-560.

Lee, R. C., and Ambros, V. (2001). An Extensive Class of Small RNAs in Caenorhabditis elegans. Science *294*, 862-864.

Lee, R. C., Feinbaum, R. L., and Ambros, V. (1993). The C. elegans heterochronic gene lin-4 encodes small RNAs with antisense complementarity to lin-14. Cell *75*, 843-854.
Lee, Y., Ahn, C., Han, J., Choi, H., Kim, J., Yim, J., Lee, J., Provost, P., Radmark, O., Kim, S., and Kim, V. N. (2003). The nuclear RNase III Drosha initiates microRNA processing. Nature *425*, 415-419.

Lee, Y., Hur, I., Park, S. Y., Kim, Y. K., Suh, M. R., and Kim, V. N. (2006). The role of PACT in the RNA silencing pathway. EMBO J *25*, 522-532.

Lee, Y. S., and Dutta, A. (2007). The tumor suppressor microRNA *let-7* represses the HMGA2 oncogene. Genes Dev

Lee, Y. S., Kim, H. K., Chung, S., Kim, K. S., and Dutta, A. (2005). Depletion of human micro-RNA miR-125b reveals that it is critical for the proliferation of differentiated cells but not for the down-regulation of putative targets during differentiation. J Biol Chem *280*, 16635-16641.

Lee, Y. S., Nakahara, K., Pham, J. W., Kim, K., He, Z., Sontheimer, E. J., and Carthew, R. W. (2004). Distinct roles for Drosophila Dicer-1 and Dicer-2 in the siRNA/miRNA silencing pathways. Cell *117*, 69-81.

Letsinger, R. L., Zhang, G. R., Sun, D. K., Ikeuchi, T., and Sarin, P. S. (1989). Cholesteryl-conjugated oligonucleotides: synthesis, properties, and activity as inhibitors of replication of human immunodeficiency virus in cell culture. Proc Natl Acad Sci U S A *86*, 6553-6556.

Leuschner, P. J., Ameres, S. L., Kueng, S., and Martinez, J. (2006). Cleavage of the siRNA passenger strand during RISC assembly in human cells. EMBO Rep *7*, 314-320.
Lewis, B. P., Burge, C. B., and Bartel, D. P. (2005). Conserved seed pairing, often flanked by adenosines, indicates that thousands of human genes are microRNA targets. Cell *120*, 15-20.

Lewis, B. P., Shih, I. H., Jones-Rhoades, M. W., Bartel, D. P., and Burge, C. B. (2003). Prediction of mammalian microRNA targets. Cell *115*, 787-798.

Li, J., Yang, Z., Yu, B., Liu, J., and Chen, X. (2005). Methylation protects miRNAs and siRNAs from a 3'-end uridylation activity in Arabidopsis. Curr Biol *15*, 1501-1507.

Li, X., and Carthew, R. W. (2005). A microRNA mediates EGF receptor signaling and promotes photoreceptor differentiation in the Drosophila eye. Cell *123*, 1267-1277.

Li, Y., Wang, F., Lee, J. A., and Gao, F. B. (2006). MicroRNA-9a ensures the precise specification of sensory organ precursors in Drosophila. Genes Dev *20*, 2793-2805.

Lim, L. P., Lau, N. C., Garrett-Engele, P., Grimson, A., Schelter, J. M., Castle, J., Bartel, D. P., Linsley, P. S., and Johnson, J. M. (2005). Microarray analysis shows that some microRNAs downregulate large numbers of target mRNAs. Nature *433*, 769-773.

Lingel, A., Simon, B., Izaurralde, E., and Sattler, M. (2003). Structure and nucleic-acid binding of the Drosophila Argonaute 2 PAZ domain. Nature *426*, 465-469.

Liu, J., Carmell, M. A., Rivas, F. V., Marsden, C. G., Thomson, J. M., Song, J. J., Hammond, S. M., Joshua-Tor, L., and Hannon, G. J. (2004). Argonaute2 is the catalytic engine of mammalian RNAi. Science *305*, 1437-1441.

Liu, J., Rivas, F. V., Wohlschlegel, J., Yates, J. R. r., Parker, R., and Hannon, G. J. (2005). A role for the P-body component GW182 in microRNA function. Nat Cell Biol *7*, 1161-1166.

Liu, Q., Rand, T. A., Kalidas, S., Du, F., Kim, H. E., Smith, D. P., and Wang, X. (2003). R2D2, a bridge between the initiation and effector steps of the Drosophila RNAi pathway. Science *301*, 1921-1925.

Liu, X., Jiang, F., Kalidas, S., Smith, D., and Liu, Q. (2006). Dicer-2 and R2D2 coordinately bind siRNA to promote assembly of the siRISC complexes. RNA *12*, 1514-1520.

Livak, K. J., and Schmittgen, T. D. (2001). Analysis of relative gene expression data using real-time quantitative PCR and the 2(-Delta Delta C(T)) Method. Methods *25*, 402-408.

Llave, C., Xie, Z., Kasschau, K. D., and Carrington, J. C. (2002). Cleavage of *Scarecrow-Like* mRNA Targets Directed by a Class of *Arabidopsis* miRNA. Science *297*, 2053-2056.

Lohmann, J. U., Endl, I., and Bosch, T. C. (1999). Silencing of Developmental Genes in Hydra. Dev Biol *214*, 211-214.

Lynn, F. C., Skewes-Cox, P., Kosaka, Y., McManus, M. T., Harfe, B. D., and German, M. S. (2007). MicroRNA expression is required for pancreatic islet cell genesis in the mouse. Diabetes *56*, 2938-2945.

Ma, J. B., Ye, K., and Patel, D. J. (2004). Structural basis for overhang-specific small interfering RNA recognition by the PAZ domain. Nature *429*, 318-322.

Ma, J. B., Yuan, Y. R., Meister, G., Pei, Y., Tuschl, T., and Patel, D. J. (2005). Structural basis for 5'-end-specific recognition of guide RNA by the *A. fulgidus* Piwi protein. Nature *434*, 666-670.

Ma, L., Teruya-Feldstein, J., and Weinberg, R. A. (2007). Tumour invasion and metastasis initiated by microRNA-10b in breast cancer. Nature *449*, 682-688.

MacRae, I. J., Ma, E., Zhou, M., Robinson, C. V., and Doudna, J. A. (2008). In vitro reconstitution of the human RISC-loading complex. Proc Natl Acad Sci U S A *105*, 512-517.

MacRae, I. J., Zhou, K., and Doudna, J. A. (2007). Structural determinants of RNA recognition and cleavage by Dicer. Nat Struct Mol Biol *14*, 934-940.

Mallory, A. C., Reinhart, B. J., Jones-Rhoades, M. W., Tang, G., Zamore, P. D., Barton, M. K., and Bartel, D. P. (2004). MicroRNA control of PHABULOSA in leaf development: importance of pairing to the microRNA 5' region. EMBO J *23*, 3356-3364.

Mansfield, J. H., Harfe, B. D., Nissen, R., Obenauer, J., Srineel, J., Chaudhuri, A., Farzan-Kashani, R., Zuker, M., Pasquinelli, A. E., Ruvkun, G., Sharp, P. A., Tabin, C. J., and McManus, M. T. (2004). MicroRNA-responsive 'sensor' transgenes uncover Hox-like and other developmentally regulated patterns of vertebrate microRNA expression. Nat Genet *36*, 1079-1083.

Maroney, P. A., Yu, Y., Fisher, J., and Nilsen, T. W. (2006). Evidence that microRNAs are associated with translating messenger RNAs in human cells. Nat Struct Mol Biol *13*, 1102-1107.

Marques JT, Devosse T, Wang D, Zamanian-Daryoush M, Serbinowski P, Hartmann R, Fujita T, Behlke MA, Williams BR.A structural basis for discriminating between self and nonself double-stranded RNAs in mammalian cells.Nat Biotechnol. 2006 May;24(5):559-65.

Martinez, J., Patkaniowska, A., Urlaub, H., Luhrmann, R., and Tuschl, T. (2002). Single-stranded antisense siRNAs guide target RNA cleavage in RNAi. Cell *110*, 563-574.

Mathonnet, G., Fabian, M. R., Svitkin, Y. V., Parsyan, A., Huck, L., Murata, T., Biffo, S., Merrick, W. C., Darzynkiewicz, E., Pillai, R. S., Filipowicz, W., Duchaine, T. F., and Sonenberg, N. (2007). MicroRNA inhibition of translation initiation in vitro by targeting the cap-binding complex eIF4F. Science *317*, 1764-1767.

Matranga, C., Tomari, Y., Shin, C., Bartel, D. P., and Zamore, P. D. (2005). Passenger-strand cleavage facilitates assembly of siRNA into Ago2-containing RNAi enzyme complexes. Cell *123*, 607-620.

Matsubara, H., Takeuchi, T., Nishikawa, E., Yanagisawa, K., Hayashita, Y., Ebi, H., Yamada, H., Suzuki, M., Nagino, M., Nimura, Y., Osada, H., and Takahashi, T. (2007). Apoptosis induction by antisense

oligonucleotides against miR-17-5p and miR-20a in lung cancers overexpressing miR-17-92. Oncogene *26*, 6099-6105.

Mayr, C., Hemann, M. T., and Bartel, D. P. (2007). Disrupting the pairing between *let-7* and Hmga2 enhances oncogenic transformation. Science *315*, 1576-1579.

McManus, M. T., Petersen, C. P., Haines, B. B., Chen, J., and Sharp, P. A. (2002). Gene silencing using micro-RNA designed hairpins. RNA *8*, 842-850.

Meister, G., Landthaler, M., Dorsett, Y., and Tuschl, T. (2004a). Sequence-specific inhibition of microRNA- and siRNA-induced RNA silencing. RNA *10*, 544-550.

Meister, G., Landthaler, M., Patkaniowska, A., Dorsett, Y., Teng, G., and Tuschl, T. (2004b). Human Argonaute2 mediates RNA cleavage targeted by miRNAs and siRNAs. Mol Cell *15*, 185-197.

Meister, G., Landthaler, M., Peters, L., Chen, P. Y., Urlaub, H., Luhrmann, R., and Tuschl, T. (2005). Identification of novel argonaute-associated proteins. Curr Biol *15*, 2149-2155.

Meister, G., and Tuschl, T. (2004). Mechanisms of gene silencing by double-stranded RNA. Nature *431*, 343-349.

Meyer, W. J., Schreiber, S., Guo, Y., Volkmann, T., Welte, M. A., and Muller, H. A. (2006). Overlapping functions of argonaute proteins in patterning and morphogenesis of Drosophila embryos. PLoS Genet *2*, e134.

Mi, S., Cai, T., Hu, Y., Chen, Y., Hodges, E., Ni, F., Wu, L., Li, S., Zhou, H., Long, C., Chen, S., Hannon, G. J., and Qi, Y. (2008). Sorting of small RNAs into Arabidopsis argonaute complexes is directed by the 5' terminal nucleotide. Cell *133*, 116-127.

Miska, E. A., Alvarez-Saavedra, E., Abbott, A. L., Lau, N. C., Hellman, A. B., McGonagle, S. M., Bartel, D. P., Ambros, V. R., and Horvitz, H. R. (2007). Most Caenorhabditis elegans microRNAs Are Individually Not Essential for Development or Viability. PLoS Genet *3*, e215.

Miyoshi, K., Tsukumo, H., Nagami, T., Siomi, H., and Siomi, M. C. (2005). Slicer function of Drosophila Argonautes and its involvement in RISC formation. Genes Dev *19*, 2837-2848.

Montgomery, T. A., Howell, M. D., Cuperus, J. T., Li, D., Hansen, J. E., Alexander, A. L., Chapman, E. J., Fahlgren, N., Allen, E., and Carrington, J. C. (2008). Specificity of ARGONAUTE7-miR390 interaction and dual functionality in TAS3 trans-acting siRNA formation. Cell *133*, 128-141.

Mortensen, R. M., Conner, D. A., Chao, S., Geisterfer-Lowrance, A. A., and Seidman, J. G. (1992). Production of homozygous mutant ES cells with a single targeting construct. Mol Cell Biol *12*, 2391-2395.

Mourelatos, Z., Dostie, J., Paushkin, S., Sharma, A. K., Charroux, B., Abel, L., Rappsilber, J., Mann, M., and Dreyfuss, G. (2002). miRNPs: a novel class of Ribonucleoproteins containing numerous microRNAs. Genes Dev *16*, 720-728.

Murchison, E. P., Partridge, J. F., Tam, O. H., Cheloufi, S., and Hannon, G. J. (2005). Characterization of Dicer-deficient murine embryonic stem cells. Proc Natl Acad Sci U S A *102*, 12135-12140.

Murchison EP, Kheradpour P, Sachidanandam R, Smith C, Hodges E, Xuan Z, Kellis M, Grützner F, Stark A, Hannon GJ.Conservation of small RNA pathways in platypus.Genome Res. 2008 Jun;18(6):995-1004.

Naguibneva, I., Ameyar-Zazoua, M., Polesskaya, A., Ait-Si-Ali, S., Groisman, R., Souidi, M., Cuvellier, S., and Harel-Bellan, A. (2006). The microRNA miR-181 targets the homeobox protein Hox-A11 during mammalian myoblast differentiation. Nat Cell Biol *8*, 278-284.

Napoli, C., Lemieux, C., and Jorgensen, R. A. (1990). Introduction of a chimeric chalcone synthase gene into Petunia results in reversible co-suppression of homologous genes in trans. Plant Cell *2*, 279-289.

Ngo, H., Tschudi, C., Gull, K., and Ullu, E. (1998). Double-stranded RNA induces mRNA degradation in *Trypanosoma brucei*. Proc Natl Acad Sci U S A *95*, 14687-14692.

Nicholson, A. W. (1999). Function, mechanism and regulation of bacterial ribonucleases. FEMS Microbiol Rev *23*, 371-390.

Nykanen, A., Haley, B., and Zamore, P. D. (2001). ATP requirements and small interfering RNA structure in the RNA interference pathway. Cell *107*, 309-321.

O'Rourke, J. R., Georges, S. A., Seay, H. R., Tapscott, S. J., McManus, M. T., Goldhamer, D. J., Swanson, M. S., and Harfe, B. D. (2007). Essential role for Dicer during skeletal muscle development. Dev Biol *311*, 359-368.

Ohara, T., Sakaguchi, Y., Suzuki, T., Ueda, H., Miyauchi, K., and Suzuki, T. (2007). The 3' termini of mouse Piwi-interacting RNAs are 2'-O-methylated. Nat Struct Mol Biol *14*, 349-350.

Okamura, K., Chung, W. J., Ruby, J. G., Guo, H., Bartel, D. P., and Lai, E. C. (2008). The Drosophila hairpin RNA pathway generates endogenous short interfering RNAs. Nature

Okamura, K., Hagen, J. W., Duan, H., Tyler, D. M., and Lai, E. C. (2007). The mirtron pathway generates microRNA-class regulatory RNAs in Drosophila. Cell *130*, 89-100.
Okamura, K., Ishizuka, A., Siomi, H., and Siomi, M. C. (2004). Distinct roles for Argonaute proteins in small RNA-directed RNA cleavage pathways. Genes Dev *18*, 1655-1666.

Olsen, P. H., and Ambros, V. (1999). The lin-4 regulatory RNA controls developmental timing in Caenorhabditis elegans by blocking LIN-14 protein synthesis after the initiation of translation. Dev Biol *216*, 671-680.

Orban, T. I., and Izaurralde, E. (2005). Decay of mRNAs targeted by RISC requires XRN1, the Ski complex, and the exosome. RNA *11*, 459-469.

Orom, U. A., Kauppinen, S., and Lund, A. H. (2006). LNA-modified oligonucleotides mediate specific inhibition of microRNA function. Gene *372*, 137-141.

Paddison, P. J., Caudy, A. A., Bernstein, E., Hannon, G. J., and Conklin, D. S. (2002). Short hairpin RNAs (shRNAs) induce sequence-specific silencing in mammalian cells. Genes Dev *16*, 948-958.

Pak, J., and Fire, A. (2007). Distinct populations of primary and secondary effectors during RNAi in C. elegans. Science *315*, 241-244.

Pal-Bhadra, M., Leibovitch, B. A., Gandhi, S. G., Rao, M., Bhadra, U., Birchler, J. A., and Elgin, S. C. (2004). Heterochromatic silencing and HP1 localization in Drosophila are dependent on the RNAi machinery. Science *303*, 669-672.

Palakodeti D, Smielewska M, Lu YC, Yeo GW, Graveley BR. The PIWI proteins SMEDWI-2 and SMEDWI-3 are required for stem cell function and piRNA expression in planarians. RNA. 2008 Jun;14(6):1174-86.

Pane, A., Wehr, K., and Schupbach, T. (2007). zucchini and squash encode two putative nucleases required for rasiRNA production in the Drosophila germline. Dev Cell *12*, 851-862.

Park, J. K., Liu, X., Strauss, T. J., McKearin, D. M., and Liu, Q. (2007). The miRNA pathway intrinsically controls self-renewal of drosophila germline stem cells. Curr Biol *17*, 533-538.

Park, M. Y., Wu, G., Gonzalez-Sulser, A., Vaucheret, H., and Poethig, R. S. (2005). Nuclear processing and export of microRNAs in Arabidopsis. Proc Natl Acad Sci U S A *102*, 3691-3696.

Park, W., Li, J., Song, R., Messing, J., and Chen, X. (2002). CARPEL FACTORY, a Dicer homolog, and HEN1, a novel protein, act in microRNA metabolism in Arabidopsis thaliana. Curr Biol *12*, 1484-1495.

Parker, J. S., Roe, S. M., and Barford, D. (2004). Crystal structure of a PIWI protein suggests mechanisms for siRNA recognition and slicer activity. EMBO J *23*, 4727-4737.

Parker, J. S., Roe, S. M., and Barford, D. (2005). Structural insights into mRNA recognition from a PIWI domain-siRNA guide complex. Nature *434*, 663-666.

Parker, R., and Sheth, U. (2007). P bodies and the control of mRNA translation and degradation. Mol Cell *25*, 635-646.

Parrish, S., Fleenor, J., Xu, S., Mello, C., and Fire, A. (2000). Functional anatomy of a dsRNA trigger. Differential requirement for the two trigger strands in RNA interference. Mol Cell *6*, 1077-1087.

Pasquinelli, A. E., Reinhart, B. J., Slack, F., Martindale, M. Q., Kuroda, M. I., Maller, B., Hayward, D. C., Ball, E. E., Degnan, B., Muller, P., Spring, J., Srinivasan, A., Fishman, M., Finnerty, J., Corbo, J., Levine, M., Leahy, P., Davidson, E., and Ruvkun, G. (2000). Conservation of the sequence and temporal expression of *let-7* heterochronic regulatory RNA. Nature *408*, 86-89.

Pedersen, I. M., Cheng, G., Wieland, S., Volinia, S., Croce, C. M., Chisari, F. V., and David, M. (2007). Interferon modulation of cellular microRNAs as an antiviral mechanism. Nature *449*, 919-922.

Pelisson, A., Sarot, E., Payen-Groschene, G., and Bucheton, A. (2007). A novel repeat-associated small interfering RNA-mediated silencing pathway downregulates complementary sense gypsy transcripts in somatic cells of the Drosophila ovary. J Virol *81*, 1951-1960.

Pelisson, A., Song, S. U., Prud'homme, N., Smith, P. A., Bucheton, A., and Corces, V. G. (1994). Gypsy transposition correlates with the production of a retroviral envelope-like protein under the tissue-specific control of the Drosophila flamenco gene. EMBO J *13*, 4401-4411.

Petersen, C. P., Bordeleau, M.-E., Pelletier, J., and Sharp, P. A. (2006). Short RNAs Repress Translation after Initiation in Mammalian Cells. Molecular Cell *21*, 533–542.

Pham, J. W., Pellino, J. L., Lee, Y. S., Carthew, R. W., and Sontheimer, E. J. (2004). A Dicer-2-dependent 80s complex cleaves targeted mRNAs during RNAi in Drosophila. Cell *117*, 83-94.

Pillai, R. S., Bhattacharyya, S. N., Artus, C. G., Zoller, T., Cougot, N., Basyuk, E., Bertrand, E., and Filipowicz, W. (2005). Inhibition of translational initiation by *let-7* microRNA in human cells. Science *309*, 1573-1576.

Pillai, R. S., Artus, C. G., and Filipowicz, W. (2004). Tethering of human Ago proteins to mRNA mimics the miRNA-mediated repression of protein synthesis. RNA *10*, 1518-1525.

Poy, M. N., Eliasson, L., Krutzfeldt, J., Kuwajima, S., Ma, X., Macdonald, P. E., Pfeffer, S., Tuschl, T., Rajewsky, N., Rorsman, P., and Stoffel, M. (2004). A pancreatic islet-specific microRNA regulates insulin secretion. Nature *432*, 226-230.

Preall, J. B., He, Z., Gorra, J. M., and Sontheimer, E. J. (2006). Short interfering RNA strand selection is independent of dsRNA processing polarity during RNAi in Drosophila. Curr Biol *16*, 530-535.

Prud'homme, N., Gans, M., Masson, M., Terzian, C., and Bucheton, A. (1995). Flamenco, a gene controlling the gypsy retrovirus of Drosophila melanogaster. Genetics *139*, 697-711.

Qi, Y., Denli, A. M., and Hannon, G. J. (2005). Biochemical Specialization within Arabidopsis RNA Silencing Pathways. Mol Cell *19*, 421-428.

Rajewsky, N. (2006). microRNA target predictions in animals. Nat Genet *38 Suppl*, S8-13.

Rajewsky, N., and Socci, N. D. (2004). Computational identification of microRNA targets. Dev Biol *267*, 529-535.

Ramachandran, V., and Chen, X. (2008). Small RNA metabolism in Arabidopsis. Trends Plant Sci

Rand, T. A., Ginalski, K., Grishin, N. V., and Wang, X. (2004). Biochemical identification of Argonaute 2 as the sole protein required for RNA-induced silencing complex activity. Proc Natl Acad Sci U S A *101*, 14385-14389.

Rand, T. A., Petersen, S., Du, F., and Wang, X. (2005). Argonaute2 Cleaves the Anti-Guide Strand of siRNA during RISC Activation. Cell *123*, 621-629.

Ratcliff, F. G., Harrison, B. D., and Baulcombe, D. C. (1997). A Similarity Between Viral Defense and Gene Silencing in Plants. Science *276*, 1558-1560.

Reeves, R. (2000). Structure and function of the HMGI(Y) family of architectural transcription factors. Environ Health Perspect *108 Suppl 5*, 803-809.

Reinhart, B. J., Slack, F. J., Basson, M., Pasquinelli, A. E., Bettinger, J. C., Rougvie, A. E., Horvitz, H. R., and Ruvkun, G. (2000). The 21-nucleotide *let-7* RNA regulates developmental timing in Caenorhabditis elegans. Nature *403*, 901-906.

Reinhart, B. J., Weinstein, E. G., Rhoades, M. W., Bartel, B., and Bartel, D. P. (2002). MicroRNAs in plants. Genes Dev *16*, 1616-1626.

Rhoades, M. W., Reinhart, B. J., Lim, L. P., Burge, C. B., Bartel, B., and Bartel, D. P. (2002). Prediction of plant microRNA targets. Cell *110*, 513-520.

Rivas, F. V., Tolia, N. H., Song, J. J., Aragon, J. P., Liu, J., Hannon, G. J., and Joshua-Tor, L. (2005). Purified Argonaute2 and an siRNA form recombinant human RISC. Nat Struct Mol Biol *12*, 340-349.

Robb, G. B., and Rana, T. M. (2007). RNA helicase A interacts with RISC in human cells and functions in RISC loading. Mol Cell *26*, 523-537.

Rodriguez, A., Vigorito, E., Clare, S., Warren, M. V., Couttet, P., Soond, D. R., van Dongen, S., Grocock, R. J., Das, P. P., Miska, E. A., Vetrie, D., Okkenhaug, K., Enright, A. J., Dougan, G., Turner, M., and Bradley, A. (2007). Requirement of bic/microRNA-155 for normal immune function. Science *316*, 608-611.

Rong, Y. S., and Golic, K. G. (2000). Gene targeting by homologous recombination in Drosophila. Science *288*, 2013-2018.

Rubin, G. M., and Spradling, A. C. (1982). Genetic transformation of Drosophila with transposable element vectors. Science S *218*, 348-353.

Ruby, J. G., Jan, C., Player, C., Axtell, M. J., Lee, W., Nusbaum, C., Ge, H., and Bartel, D. P. (2006). Large-scale sequencing reveals 21U-RNAs and additional microRNAs and endogenous siRNAs in C. elegans. Cell *127*, 1193-1207.

Ruby, J. G., Jan, C. H., and Bartel, D. P. (2007). Intronic microRNA precursors that bypass Drosha processing. Nature *448*, 83-86.

Ruvkun, G., Ambros, V., Coulson, A., Waterston, R., Sulston, J., and Horvitz, H. R. (1989). Molecular genetics of the Caenorhabditis elegans heterochronic gene lin- 14. Genetics *121*, 501-516.

Sago, N., Omi, K., Tamura, Y., Kunugi, H., Toyo-oka, T., Tokunaga, K., and Hohjoh, H. (2004). RNAi induction and activation in mammalian muscle cells where Dicer and eIF2C translation initiation factors are barely expressed. Biochem Biophys Res Commun *319*, 50-57.

Saito, K., Ishizuka, A., Siomi, H., and Siomi, M. C. (2005). Processing of pre-microRNAs by the Dicer-1-Loquacious complex in Drosophila cells. PLoS Biol *3*, e235.

Saito, K., Nishida, K. M., Mori, T., Kawamura, Y., Miyoshi, K., Nagami, T., Siomi, H., and Siomi, M. C. (2006). Specific association of Piwi with rasiRNAs derived from retrotransposon and heterochromatic regions in the Drosophila genome. Genes Dev *20*, 2214-2222.

Saito, K., Sakaguchi, Y., Suzuki, T., Suzuki, T., Siomi, H., and Siomi, M. C. (2007). Pimet, the Drosophila homolog of HEN1, mediates 2'-O-methylation of Piwi- interacting RNAs at their 3' ends. Genes Dev *21*, 1603-1608.

Sánchez-Alvarado, A., and Newmark, P. A. (1999). Double-stranded RNA specifically disrupts gene expression during planarian regeneration. Proc Natl Acad Sci U S A *96*, 5049-5054.

Savitsky, M., Kwon, D., Georgiev, P., Kalmykova, A., and Gvozdev, V. (2006). Telomere elongation is under the control of the RNAi-based mechanism in the Drosophila germline. Genes Dev *20*, 345-354.

Saxena, S., Jonsson, Z. O., and Dutta, A. (2003). Small RNAs with imperfect match to endogenous mRNA repress translation: implications for off-target activity of siRNA in mammalian cells. J Biol Chem *278*, 44312-44319.

Schmidt, A., Palumbo, G., Bozzetti, M. P., Tritto, P., Pimpinelli, S., and Schafer, U. (1999). Genetic and molecular characterization of sting, a gene involved in crystal formation and meiotic drive in the male germ line of Drosophila melanogaster. Genetics *151*, 749-760.

Schratt, G. M., Tuebing, F., Nigh, E. A., Kane, C. G., Sabatini, M. E., Kiebler, M., and Greenberg, M. E. (2006). A brain-specific microRNA regulates dendritic spine development. Nature *439*, 283-289.

Schwarz, D. S., Hutvágner, G., Du, T., Xu, Z., Aronin, N., and Zamore, P. D. (2003). Asymmetry in the assembly of the RNAi enzyme complex. Cell *115*, 199-208.

Schwarz, D. S., Hutvagner, G., Haley, B., and Zamore, P. D. (2002). Evidence that siRNAs function as guides, not primers, in the Drosophila and human RNAi pathways. Mol Cell *10*, 537-548.

Seitz, H., Ghildiyal, M., and Zamore, P. D. (2008). Argonaute loading improves the 5' precision of both MicroRNAs and their miRNA strands in flies. Curr Biol *18*, 147-151.

Sempere, L. F., Dubrovsky, E. B., Dubrovskaya, V. A., Berger, E. M., and Ambros, V. (2002). The Expression of the *let-7* Small Regulatory RNA Is Controlled by Ecdysone during Metamorphosis in Drosophila melanogaster. Developmental Biology *244*, 170–179.

Sen, G. L., and Blau, H. M. (2005). Argonaute 2/RISC resides in sites of mammalian mRNA decay known as cytoplasmic bodies. Nat Cell Biol *7*, 633-636.
Shen, B., and Goodman, H. M. (2004). Uridine addition after microRNA-directed cleavage. Science *306*, 997.

Sijen, T., Steiner, F. A., Thijssen, K. L., and Plasterk, R. H. (2007). Secondary siRNAs result from unprimed RNA synthesis and form a distinct class. Science *315*, 244-247.

Sokol, N. S., and Ambros, V. (2005). Mesodermally expressed Drosophila microRNA-1 is regulated by Twist and is required in muscles during larval growth. Genes Dev *19*, 2343-2354.

Song, J. J., Liu, J., Tolia, N. H., Schneiderman, J., Smith, S. K., Martienssen, R. A., Hannon, G. J., and Joshua-Tor, L. (2003). The crystal structure of the Argonaute2 PAZ domain reveals an RNA binding motif in RNAi effector complexes. Nat Struct Biol *10*, 1026-1032.

Song, J. J., Smith, S. K., Hannon, G. J., and Joshua-Tor, L. (2004). Crystal structure of Argonaute and its implications for RISC slicer activity. Science *305*, 1434-1437.

Soutschek, J., Akinc, A., Bramlage, B., Charisse, K., Constien, R., Donoghue, M., Elbashir, S., Geick, A., Hadwiger, P., Harborth, J., John, M., Kesavan, V., Lavine, G., Pandey, R. K., Racie, T., Rajeev, K. G., Rohl, I., Toudjarska, I., Wang, G., Wuschko, S., Bumcrot, D., Koteliansky, V., Limmer, S., Manoharan, M., and Vornlocher, H. P. (2004). Therapeutic silencing of an endogenous gene by systemic administration of modified siRNAs. Nature *432*, 173-178.

Stark, A., Brennecke, J., Russell, R. B., and Cohen, S. M. (2003). Identification of Drosophila MicroRNA targets. PLoS Biol *1*, E60.

Steiner, F. A., Hoogstrate, S. W., Okihara, K. L., Thijssen, K. L., Ketting, R. F., Plasterk, R. H., and Sijen, T. (2007). Structural features of small RNA precursors determine Argonaute loading in Caenorhabditis elegans. Nat Struct Mol Biol *14*, 927-933.

Steller, H., and Pirrotta, V. (1985). A transposable P vector that confers selectable G418 resistance to Drosophila larvae. EMBO J *4*, 167-171.

Svoboda, P., Stein, P., Hayashi, H., and Schultz, R. M. (2000). Selective reduction of dormant maternal mRNAs in mouse oocytes by RNA interference. Development *127*, 4147-4156.

Tabara, H., Sarkissian, M., Kelly, W. G., Fleenor, J., Grishok, A., Timmons, L., Fire, A., and Mello, C. C. (1999). The rde-1 gene, RNA interference, and transposon silencing in C. elegans. Cell *99*, 123-132.

Tabara, H., Yigit, E., Siomi, H., and Mello, C. C. (2002). The dsRNA Binding Protein RDE-4 Interacts with RDE-1, DCR-1, and a DexH-Box Helicase to Direct RNAi in C. elegans. Cell *109*, 861-871.

Takamizawa, J., Konishi, H., Yanagisawa, K., Tomida, S., Osada, H., Endoh, H., Harano, T., Yatabe, Y., Nagino, M., Nimura, Y., Mitsudomi, T., and Takahashi, T. (2004). Reduced expression of the *let-7* microRNAs in human lung cancers in association with shortened postoperative survival. Cancer Res *64*, 3753-3756.

Tam, O. H., Aravin, A. A., Stein, P., Girard, A., Murchison, E. P., Cheloufi, S., Hodges, E., Anger, M., Sachidanandam, R., Schultz, R. M., and Hannon, G. J. (2008). Pseudogene-derived small interfering RNAs regulate gene expression in mouse oocytes. Nature

Tang, G., Reinhart, B. J., Bartel, D. P., and Zamore, P. D. (2003). A biochemical framework for RNA silencing in plants. Genes Dev *17*, 49-63.

Tavazoie, S. F., Alarcon, C., Oskarsson, T., Padua, D., Wang, Q., Bos, P. D., Gerald, W. L., and Massague, J. (2008). Endogenous human microRNAs that suppress breast cancer metastasis. Nature *451*, 147-152.

Teleman, A. A., Maitra, S., and Cohen, S. M. (2006). Drosophila lacking microRNA miR-278 are defective in energy homeostasis. Genes Dev *20*, 417-422.

Tessari, M. A., Gostissa, M., Altamura, S., Sgarra, R., Rustighi, A., Salvagno, C., Caretti, G., Imbriano, C., Mantovani, R., Del Sal, G., Giancotti, V., and Manfioletti, G. (2003). Transcriptional activation of the cyclin A gene by the architectural transcription factor HMGA2. Mol Cell Biol *23*, 9104-9116.

Thermann, R., and Hentze, M. W. (2007). Drosophila miR2 induces pseudo-polysomes and inhibits translation initiation. Nature *447*, 875-878.

Thomas, K. R., and Capecchi, M. R. (1986). Introduction of homologous DNA sequences into mammalian cells induces mutations in the cognate gene. Nature *324*, 34-38.

Thomson, J. M., Newman, M., Parker, J. S., Morin-Kensicki, E. M., Wright, T., and Hammond, S. M. (2006). Extensive post-transcriptional regulation of microRNAs and its implications for cancer. Genes Dev *20*, 2202-2207.

Tkaczuk, K. L., Obarska, A., and Bujnicki, J. M. (2006). Molecular phylogenetics and comparative modeling of HEN1, a methyltransferase involved in plant microRNA biogenesis. BMC Evol Biol *6*, 6.

Tolia, N. H., and Joshua-Tor, L. (2007). Slicer and the argonautes. Nat Chem Biol *3*, 36-43.

Tomari, Y., Du, T., Haley, B., Schwarz, D. S., Bennett, R., Cook, H. A., Koppetsch, B. S., Theurkauf, W. E., and Zamore, P. D. (2004). RISC assembly defects in the Drosophila RNAi mutant armitage. Cell *116*, 831-841.

Tomari, Y., Du, T., and Zamore, P. D. (2007). Sorting of Drosophila small silencing RNAs. Cell *130*, 299–308.

Tomari, Y., Matranga, C., Haley, B., Martinez, N., and Zamore, P. D. (2004). A protein sensor for siRNA asymmetry. Science *306*, 1377-1380.

Tomari, Y., and Zamore, P. D. (2005). Perspective: machines for RNAi. Genes Dev *19*, 517-529.

Tsourkas, A., Behlke, M. A., and Bao, G. (2002). Hybridization of 2'-O-methyl and 2'-deoxy molecular beacons to RNA and DNA targets. Nucleic Acids Res *30*, 5168-5174.

Tuschl, T., Zamore, P. D., Lehmann, R., Bartel, D. P., and Sharp, P. A. (1999). Targeted mRNA degradation by double-stranded RNA in vitro. Genes Dev *13*, 3191-3197.

Vagin, V. V., Klenov, M. S., Kalmykova, A. I., Stolyarenko, A. D., Kotelnikov, R. N., and Gvozdev, V. A. (2004). The RNA Interference Proteins and Vasa Locus are Involved in the Silencing of Retrotransposons in the Female Germline of *Drosophila melanogaster*. RNA Biology *1*, 54-58.

Vagin, V. V., Sigova, A., Li, C., Seitz, H., Gvozdev, V., and Zamore, P. D. (2006). A distinct small RNA pathway silences selfish genetic elements in the germline. Science *313*, 320-324.

Valoczi, A., Hornyik, C., Varga, N., Burgyan, J., Kauppinen, S., and Havelda, Z. (2004). Sensitive and specific detection of microRNAs by northern blot analysis using LNA-modified oligonucleotide probes. Nucleic Acids Res *32*, e175.

van der Krol, A. R., Mur, L. A., Beld, M., Mol, J. N. M., and Stuitji, A. R. (1990). Flavonoid genes in petunia: Addition of a limited number of gene copies may lead to a suppression of gene expression. Plant Cell *2*, 291-299.

van Rij, R. P., Saleh, M. C., Berry, B., Foo, C., Houk, A., Antoniewski, C., and Andino, R. (2006). The RNA silencing endonuclease Argonaute 2 mediates specific antiviral immunity in Drosophila melanogaster. Genes Dev *20*, 2985-2995.

Vasudevan, S., Tong, Y., and Steitz, J. A. (2007). Switching from repression to activation: microRNAs can up-regulate translation. Science *318*, 1931-1934.

Vaucheret, H., Vazquez, F., Crete, P., and Bartel, D. P. (2004). The action of ARGONAUTE1 in the miRNA pathway and its regulation by the miRNA pathway are crucial for plant development. Genes Dev *18*, 1187-1197.

Ventura, A., Young, A. G., Winslow, M. M., Lintault, L., Meissner, A., Erkeland, S. J., Newman, J., Bronson, R. T., Crowley, D., Stone, J. R., Jaenisch, R., Sharp, P. A., and Jacks, T. (2008). Targeted deletion reveals essential and overlapping functions of the miR-17 through 92 family of miRNA clusters. Cell *132*, 875-886.

Vermeulen, A., Robertson, B., Dalby, A. B., Marshall, W. S., Karpilow, J., Leake, D., Khvorova, A., and Baskerville, S. (2007). Double-stranded regions are essential design components of potent inhibitors of RISC function. RNA *13*, 723-730.

Viswanathan, S. R., Daley, G. Q., and Gregory, R. I. (2008). Selective blockade of microRNA processing by Lin28. Science *320*, 97-100.

Voinnet, O., and Baulcombe, D. C. (1997). Systemic signalling in gene silencing. Nature *389(6651)*, 553.

Voorhoeve, P. M., le Sage, C., Schrier, M., Gillis, A. J., Stoop, H., Nagel, R., Liu, Y. P., van Duijse, J., Drost, J., Griekspoor, A., Zlotorynski, E., Yabuta, N., De Vita, G., Nojima, H., Looijenga, L. H., and Agami, R. (2006). A genetic screen implicates miRNA-372 and miRNA-373 as oncogenes in testicular germ cell tumors. Cell *124*, 1169-1181.

Walter, A. E., Turner, D. H., Kim, J., Lyttle, M. H., Muller, P., Mathews, D. H., and Zuker, M. (1994). Coaxial stacking of helixes enhances binding of oligoribonucleotides and improves predictions of RNA folding. Proc Natl Acad Sci U S A *91*, 9218-9222.

Wang, X., and Wang, X. (2006). Systematic identification of microRNA functions by combining target prediction and expression profiling. Nucleic Acids Res *34*, 1646-1652.

Wang, X. H., Aliyari, R., Li, W. X., Li, H. W., Kim, K., Carthew, R., Atkinson, P., and Ding, S. W. (2006). RNA Interference Directs Innate Immunity Against Viruses in Adult Drosophila. Science *312*, 452-454.

Wargelius, A., Ellingsen, S., and Fjose, A. (1999). Double-Stranded RNA Induces Specific Developmental Defects in Zebrafish Embryos. Biochem. Biophys. Res. Commun. *263*, 156-161.

Waterhouse, P. M., Graham, M. W., and Wang, M. B. (1998). Virus resistance and gene silencing in plants can be induced by simultaneous expression of sense and antisense RNA. Proc Natl Acad Sci U S A *95*, 13959-13964.

Wianny, F., and Zernicka-Goetz, M. (2000). Specific interference with gene function by double-stranded RNA in early mouse development. Nat Cell Biol *2*, 70-75.

Wickens, M., and Takayama, K. (1994). RNA. Deviants--or emissaries. Nature *367*, 17-18.

Wightman, B., Burglin, T. R., Gatto, J., Arasu, P., and Ruvkun, G. (1991). Negative regulatory sequences in the lin-14 3'-untranslated region are necessary to generate a temporal switch during Caenorhabditis elegans development. Genes Dev *5*, 1813-1824.

Wightman, B., Ha, I., and Ruvkun, G. (1993). Posttranscriptional regulation of the heterochronic gene lin-14 by lin- 4 mediates temporal pattern formation in C. elegans. Cell *75*, 855-862.

Williams, R. W., and Rubin, G. M. (2002). ARGONAUTE1 is required for efficient RNA interference in Drosophila embryos. Proc Natl Acad Sci U S A *99*, 6889-6894.

Wisniewski, J. R., and Schwanbeck, R. (2000). High mobility group I/Y: multifunctional chromosomal proteins causally involved in tumor progression and malignant transformation (review). Int J Mol Med *6*, 409-419.

Wu, L., Fan, J., and Belasco, J. G. (2006). MicroRNAs direct rapid deadenylation of mRNA. Proc Natl Acad Sci U S A *103*, 4034-4039.

Xie, Z., Kasschau, K. D., and Carrington, J. C. (2003). Negative Feedback Regulation of Dicer-Like1 in Arabidopsis by microRNA-Guided mRNA Degradation. Curr Biol *13*, 784-789.

Xu, P., Vernooy, S. Y., Guo, M., and Hay, B. A. (2003). The Drosophila MicroRNA Mir-14 Suppresses Cell Death and Is Required for Normal Fat Metabolism. Curr Biol *13*, 790-795.

Yan, K. S., Yan, S., Farooq, A., Han, A., Zeng, L., and Zhou, M. M. (2003). Structure and conserved RNA binding of the PAZ domain. Nature *426*, 468-474.

Yang, B., Lin, H., Xiao, J., Lu, Y., Luo, X., Li, B., Zhang, Y., Xu, C., Bai, Y., Wang, H., Chen, G., and Wang, Z. (2007). The muscle-specific microRNA miR-1 regulates cardiac arrhythmogenic potential by targeting GJA1 and KCNJ2. Nat Med *13*, 486-491.

Yang, Z., Ebright, Y. W., Yu, B., and Chen, X. (2006). HEN1 recognizes 21-24 nt small RNA duplexes and deposits a methyl group onto the 2' OH of the 3' terminal nucleotide. Nucleic Acids Res *34*, 667-675.

Yekta, S., Shih, I. H., and Bartel, D. P. (2004). MicroRNA-directed cleavage of HOXB8 mRNA. Science *304*, 594-596.

Yigit, E., Batista, P. J., Bei, Y., Pang, K. M., Chen, C. C., Tolia, N. H., Joshua-Tor, L., Mitani, S., Simard, M. J., and Mello, C. C. (2006). Analysis of the C. elegans Argonaute family reveals that distinct Argonautes act sequentially during RNAi. Cell *127*, 747-757.

Yu, B., Yang, Z., Li, J., Minakhina, S., Yang, M., Padgett, R. W., Steward, R., and Chen, X. (2005). Methylation as a crucial step in plant microRNA biogenesis. Science *307*, 932-935.

Yuan, Y. R., Pei, Y., Ma, J. B., Kuryavyi, V., Zhadina, M., Meister, G., Chen, H. Y., Dauter, Z., Tuschl, T., and Patel, D. J. (2005). Crystal structure of A. aeolicus argonaute, a site-specific DNA-guided endoribonuclease, provides insights into RISC-mediated mRNA cleavage. Mol Cell *19*, 405-419.

Zambon, R. A., Vakharia, V. N., and Wu, L. P. (2006). RNAi is an antiviral immune response against a dsRNA virus in Drosophila melanogaster. Cell Microbiol *8*, 880-889.

Zamore, P. D., and Haley, B. (2005). Ribo-gnome: the big world of small RNAs. Science *309*, 1519-1524.

Zamore, P. D., Tuschl, T., Sharp, P. A., and Bartel, D. P. (2000). RNAi: double-stranded RNA directs the ATP-dependent cleavage of mRNA at 21 to 23 nucleotide intervals. Cell *101*, 25-33.

Zeng, Y., Wagner, E. J., and Cullen, B. R. (2002). Both natural and designed micro RNAs can inhibit the expression of cognate mRNAs when expressed in human cells. Mol Cell *9*, 1327-1333.

Zhao, Y., Ransom, J. F., Li, A., Vedantham, V., von Drehle, M., Muth, A. N., Tsuchihashi, T., McManus, M. T., Schwartz, R. J., and Srivastava, D. (2007). Dysregulation of cardiogenesis, cardiac conduction, and cell cycle in mice lacking miRNA-1-2. Cell *129*, 303-317.

Zhao, Y., Samal, E., and Srivastava, D. (2005). Serum response factor regulates a muscle-specific microRNA that targets Hand2 during cardiogenesis. Nature *436*, 214-220.

Zhou, X., Benson, K. F., Przybysz, K., Liu, J., Hou, Y., Cherath, L., and Chada, K. (1996). Genomic structure and expression of the murine Hmgi-c gene. Nucleic Acids Res *24*, 4071-4077.

Zuker, M. (2003). Mfold web server for nucleic acid folding and hybridization prediction. Nucleic Acids Res *31*, 3406-3415.

Appendix III:

Endogenous siRNAs Derived from Transposons and mRNAs in *Drosophila* Somatic Cells

Contribution: This published manuscript is appended below. The author performed all experiments in Figure 3.

LMA and T_b were placed into a food-restriction paradigm under DD conditions, we found that they maintained the rhythm that had been entrained by light (high-amplitude, free-running period of ~23.7 hours) and never showed an increase in LMA or T_b in anticipation of the food presentation (fig. S3). Hence, although a BMAL1-based clock is necessary to support food entrainment, restoration of clock function in the SCN alone is not able to rescue this behavior.

To test the hypothesis that the BMAL1-based clock induced in the DMH during restricted feeding might drive circadian entrainment, we performed stereotaxic bilateral delivery of AAV-BMAL1 (the same construct and vector as used in the SCN) into the DMH of *Bmal1*$^{-/-}$ mice. Mice who sustained bilateral DMH injections of the AAV-BMAL1 did not demonstrate entrainment to a 12:12 LD cycle or free-running rhythms of T_b or LMA in DD (Fig. 3A). By contrast, under conditions of food restriction in DD, they exhibited a clear anticipatory increase in T_b and LMA before food presentation (Fig. 2C and Fig. 3B). Each individual mouse showed very little day-to-day variation in the timing of the increase in T_b and LMA under DD (i.e., the phase angle of entrainment was stable). Finally, the increase in T_b and LMA before the predicted period of food presentation persisted during a 24-hour fast at the end of restricted feeding (arrow in Fig. 3B), demonstrating the circadian nature of the response.

In both our study and the study by Mieda *et al.* (*8*), clock gene expression in the DMH was largely restricted to cells in the compact part of the nucleus, which consists of small, closely packed neurons that are highly reminiscent of the SCN itself. These neurons appear mainly to have local connections with the adjacent output zones of the DMH (*23*), suggesting that the timing signal from the compact part of the DMH may impinge upon the same output neurons in the remainder of the DMH as are used to control light-entrained rhythms directed by the SCN. This relationship may explain how the DMH clock is able to override the SCN clock input during conditions of food entrainment in an intact animal. It is unlikely that feedback from the DMH alters activity in the SCN in any major way, because the SCN remains phase-locked to the LD cycle for many weeks during food entrainment (as long as the animals are not also hypocaloric). These observations also raise the interesting possibility that the DMH may form the neuroanatomic basis of the so-called methamphetamine-sensitive circadian oscillator (MASCO), which also operates independent of the SCN and does not entrain to light [for a review, see (*24*)].

Our data indicate that there is an inducible clock in the DMH that can override the SCN and drive circadian rhythms when the animal is faced with limited food availability. Thus, under restricted feeding conditions, the DMH clock can assume an executive role in the temporal regulation of behavioral state. For a small mammal, finding food on a daily basis is a critical mission. Even a few days of starvation, a common threat in natural environments, may result in death. Hence, it is adaptive for animals to have a secondary "master clock" that can allow the animal to switch its behavioral patterns rapidly after a period of starvation to maximize the opportunity of finding food sources at the same time on following days.

In an intact animal, peripheral oscillators in many tissues in the body, including the stomach and liver, as well as elsewhere in the brain, may contribute to food entrainment of circadian rhythms (*25*, *26*). Consequently, it has been difficult to dissect this system by using lesions of individual components of the pathway (*3*, *9*, *10*). However, by starting with a genetically arrhythmic mouse and using focal genetic rescue in the brain, we have identified the SCN molecular clock as sufficient for light but not food entrainment of T_b and LMA rhythms in mice, and the DMH as sufficient for food but not light entrainment of circadian rhythms of T_b and LMA. These results demonstrate the power of viral-based gene replacement in the central nervous system to dissect complex neural functions.

References and Notes

1. M. H. Hastings, A. B. Reddy, E. S. Maywood, *Nat. Rev. Neurosci.* **4**, 649 (2003).
2. C. B. Saper, J. Lu, T. C. Chou, J. Gooley, *Trends Neurosci.* **28**, 152 (2005).
3. J. J. Gooley, A. Schomer, C. B. Saper, *Nat. Neurosci.* **9**, 398 (2006).
4. F. K. Stephan, J. M. Swann, C. L. Sisk, *Behav. Neural Biol.* **25**, 346 (1979).
5. P. L. Lowrey, J. S. Takahashi, *Annu. Rev. Genomics Hum. Genet.* **5**, 407 (2004).
6. A. Kramer *et al.*, *Science* **294**, 2511 (2001).
7. F. K. Stephan, *Physiol. Behav.* **46**, 489 (1989).
8. M. Mieda *et al.*, *Proc. Natl. Acad. Sci. U.S.A.* **103**, 12150 (2006).
9. G. J. Landry, M. M. Simons, I. C. Webb, R. E. Mistlberger, *Am. J. Physiol.* **290**, 6 (2006).
10. J. J. Gooley, C. B. Saper, *J. Biol. Rhythms* **22**, 479 (2008).
11. N. Gekakis *et al.*, *Science* **280**, 1564 (1998).
12. B. Zheng *et al.*, *Cell* **105**, 683 (2001).
13. M. K. Bunger *et al.*, *Cell* **103**, 1009 (2000).
14. E. L. McDearmon *et al.*, *Science* **314**, 1304 (2006).
15. M. K. Bunger *et al.*, *Genesis* **41**, 122 (2005).
16. A. Laposky *et al.*, *Sleep* **28**, 395 (2005).
17. S. Shimba *et al.*, *Proc. Natl. Acad. Sci. U.S.A.* **102**, 12071 (2005).
18. R. D. Rudic *et al.*, *PLoS Biol.* **2**, e377 (2004).
19. Materials and methods are available as supporting material on *Science* Online.
20. T. C. Chou *et al.*, *J. Neuroscience* **23**, 1069 (2003).
21. C. A. Fuller *et al.*, *Am. J. Physiol.* **241**, 5 (1981).
22. D. T. Krieger, H. Hauser, L. C. Krey, *Science* **197**, 398 (1977).
23. R. H. Thompson, N. S. Canteras, L. W. Swanson, *Brain Res. Brain Res. Rev.* **27**, 89 (1998).
24. T. Hiroshige, K. Honma, S. Honma, *Brain Res. Bull.* **27**, 441 (1991).
25. K. A. Stokkan *et al.*, *Science* **291**, 490 (2001).
26. F. Damiola *et al.*, *Genes Dev.* **14**, 2950 (2000).

27. We thank Q. Ha and M. Ha for technical work. Support was provided by U.S. Public Health Service grants HL60292, NS33987, NS051609, NS057119, and HL07901-08.

Supporting Online Material

www.sciencemag.org/cgi/content/full/320/5879/1074/DC1
Materials and Methods
Figs. S1 to S4
References

26 November 2007; accepted 14 April 2008
10.1126/science.1153277

Endogenous siRNAs Derived from Transposons and mRNAs in *Drosophila* Somatic Cells

Megha Ghildiyal,[1]* Hervé Seitz,[1]* Michael D. Horwich,[1] Chengjian Li,[1] Tingting Du,[1] Soohyun Lee,[2] Jia Xu,[3] Ellen L.W. Kittler,[4] Maria L. Zapp,[4] Zhiping Weng,[5] Phillip D. Zamore[1]†

Small interfering RNAs (siRNAs) direct RNA interference (RNAi) in eukaryotes. In flies, somatic cells produce siRNAs from exogenous double-stranded RNA (dsRNA) as a defense against viral infection. We identified endogenous siRNAs (endo-siRNAs), 21 nucleotides in length, that correspond to transposons and heterochromatic sequences in the somatic cells of *Drosophila melanogaster*. We also detected endo-siRNAs complementary to messenger RNAs (mRNAs); these siRNAs disproportionately mapped to the complementary regions of overlapping mRNAs predicted to form double-stranded RNA in vivo. Normal accumulation of somatic endo-siRNAs requires the siRNA-generating ribonuclease Dicer-2 and the RNAi effector protein Argonaute2 (Ago2). We propose that endo-siRNAs generated by the fly RNAi pathway silence selfish genetic elements in the soma, much as Piwi-interacting RNAs do in the germ line.

Three RNA-silencing pathways have been identified in flies and mammals: RNA interference (RNAi), guided by small interfering RNAs (siRNAs) derived from exogenous double-stranded RNA (dsRNA); the microRNA (miRNA) pathway, in which endogenous small RNAs repress partially complementary mRNAs; and the Piwi-interacting RNA (piRNA) pathway, whose small RNAs repress transposons in the germ line (*1*–*3*) and can activate transcription in heterochromatin (*4*).

Endogenous siRNAs (endo-siRNAs) silence retrotransposons in plants (*5*, *6*), and siRNAs corresponding to the L1 retrotransposon have

[1]Department of Biochemistry and Molecular Pharmacology, University of Massachusetts Medical School, Worcester, MA 01605, USA. [2]Program in Bioinformatics, Boston University, Boston, MA 02215, USA. [3]Department of Biomedical Engineering, Boston University, Boston, MA 02215, USA. [4]Program in Molecular Medicine and Center for AIDS Research, University of Massachusetts Medical School, Worcester, MA 01605, USA. [5]Program in Bioinformatics and Integrative Biology, University of Massachusetts Medical School, Worcester, MA 01605, USA.

*These authors contributed equally to this work.
†To whom correspondence should be addressed. E-mail: phillip.zamore@umassmed.edu

been detected in cultured mammalian cells (*7*). Genetic and molecular evidence suggests that in addition to suppressing viral infection, the RNAi pathway silences selfish genetic elements in the fly soma: Mutations in the RNAi gene *rm62* (*8*) suppress mutations caused by retroelement insertion (*9*); depletion of the Argonaute proteins Ago1 or Ago2 increases transposon expression in cultured *Drosophila* Schneider 2 (S2) cells (*10*); small RNAs have been detected in *Drosophila* Kc cells for the *1360* transposon (*11*) and are produced during transgene silencing in flies (*12*); and siRNAs have been proposed to repress germline expression of *suffix*, a short interspersed nuclear element (SINE) (*13*).

The defining properties of *Drosophila* siRNAs are their production from long dsRNA by Dicer-2 (Dcr-2), which generates 5′-monophosphate termini; their loading into Argonaute2 (Ago2); and their Ago2-dependent, 3′-terminal, 2′-*O*-methylation by the methyltransferase Hen1 (*14*–*16*), unlike most miRNAs (*17*). In vivo (Fig. 1A, rightmost

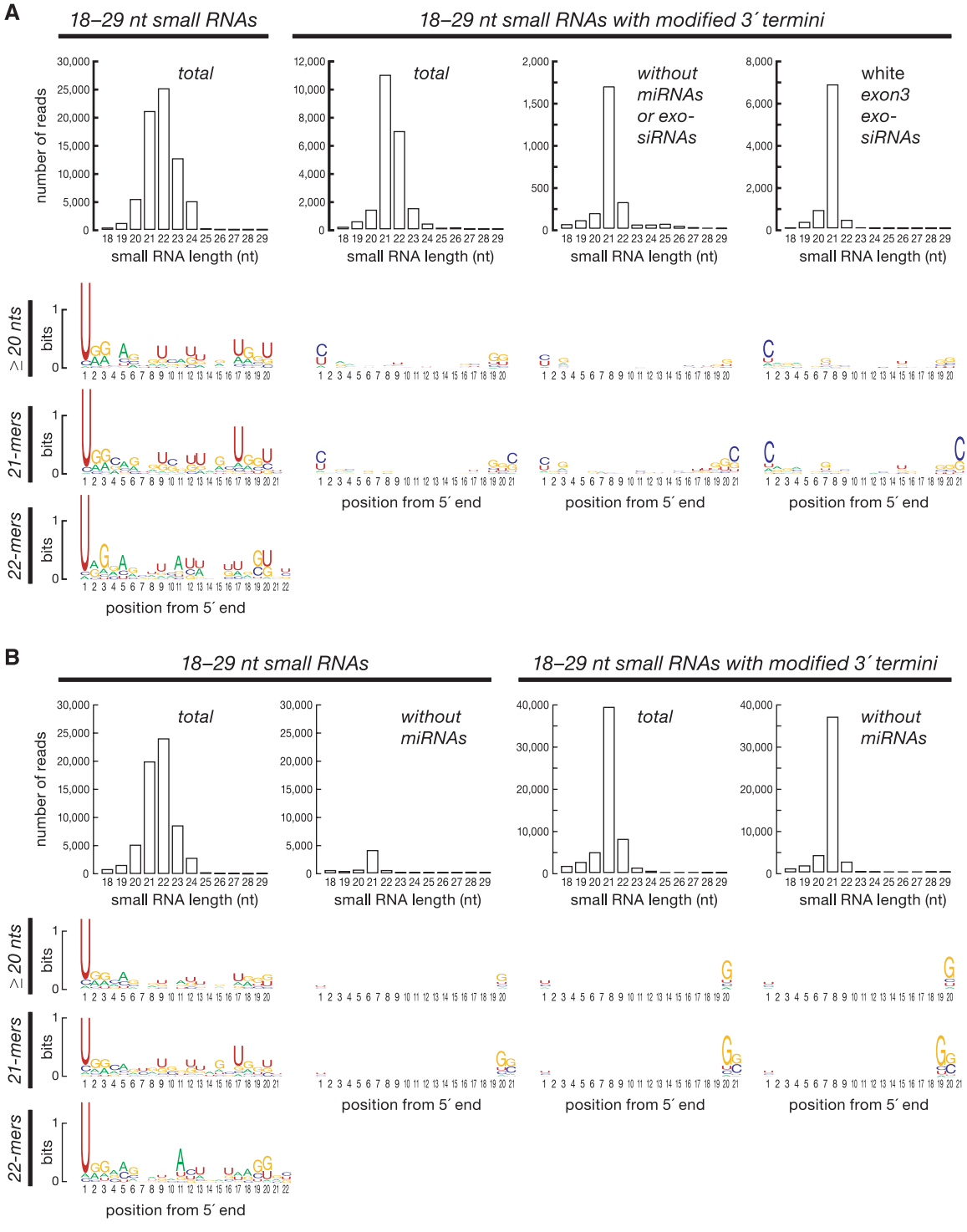

Fig. 1. High-throughput pyrosequencing revealed 3′-terminally modified 21-nt RNAs in the fly soma. (**A**) Length and sequence composition of the small RNA sequences from a library of total small RNA from the heads of flies expressing an inverted repeat (IR) silencing the *white* gene and for a parallel library enriched for RNAs modified at their 3′ ends. (**B**) Similar analysis for small RNA sequences from *Drosophila* S2 cells. For data labeled "without miRNAs," pre-miRNA–matching sequences were removed computationally.

panel) and in vitro (*18*), nearly all siRNAs produced by Dcr-2 from exogenous dsRNA are 21 nucleotides (nt) in length.

We characterized the somatic small RNA content of S2 cells (*19*) and of heads expressing an RNA hairpin silencing the *white* gene by RNAi (*20*). To identify endo-siRNA candidates, we analyzed two types of RNA libraries. For total 18- to 29-nt RNA libraries, 89% (S2 cells) and 96% (heads) mapped to annotated miRNA loci. In contrast, libraries enriched for small RNAs bearing a 3′-terminal, 2′-*O*-methyl modification (*21*) were depleted of miRNAs: Only 19% (S2 cells) and 49% (heads) of reads and 2.4% (S2 cells; 58,681 reads; 12,036 sequences) and 12% (heads; 22,685 reads; 2929 sequences) of unique sequences mapped to miRNA loci.

Table 1. Endo-siRNAs preferentially map to overlapping, complementary mRNAs.

Sample	Enrichment	Enrichment after randomization		*Z* score	*P*
		Mean	SD		
Fly heads	10.9	1.0	0.38	26.1	7.9×10^{-151}
S2 cells	12.3	1.1	0.42	27.0	5.2×10^{-161}

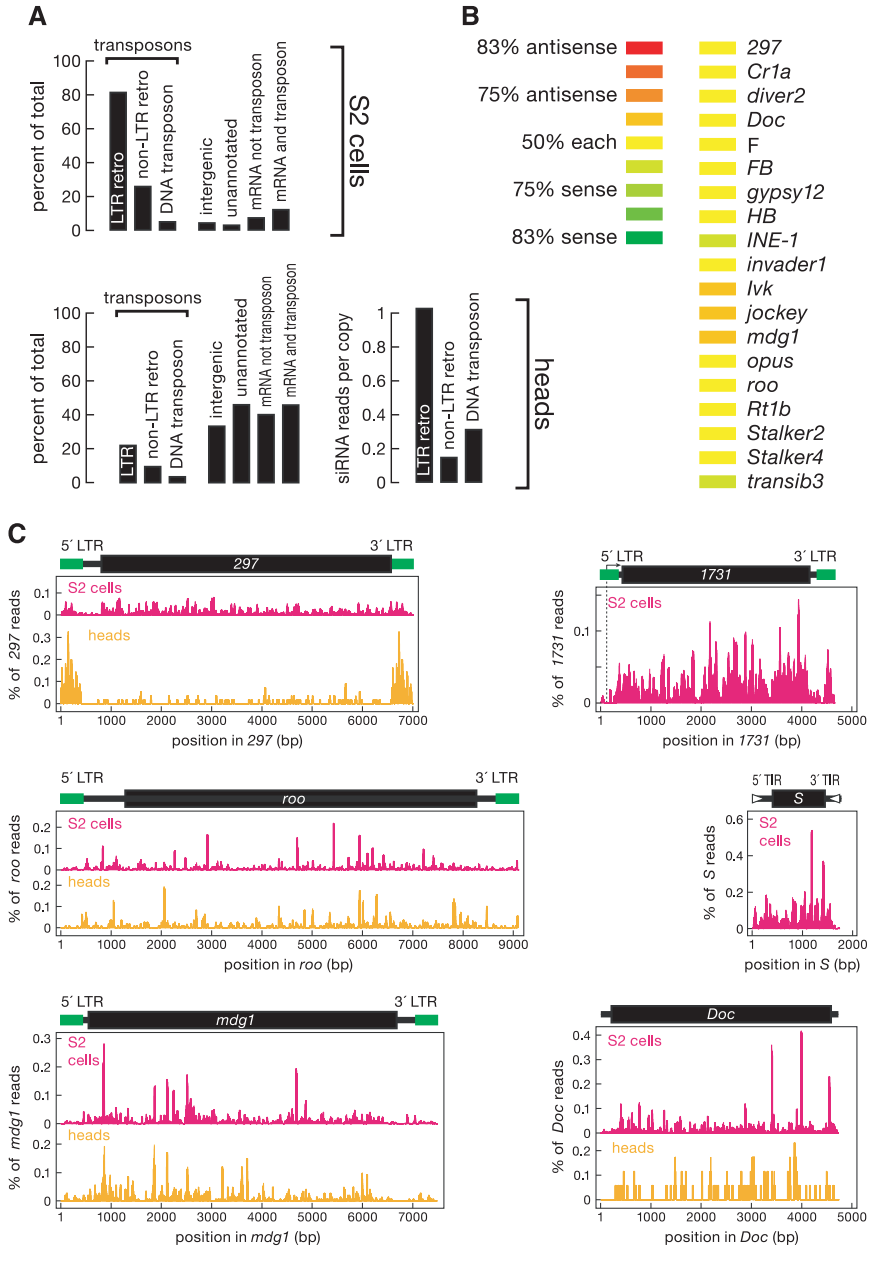

Fig. 2. Endo-siRNAs correspond to transposons. (**A**) Distribution of annotations for the genomic matches of endo-siRNA sequences. Bars total more than 100% because some siRNAs match both LTR and non-LTR retrotransposons or match both mRNA and transposons. (**B**) Transposon-derived siRNAs with more than 50 21-nt reads mapped about equally to sense and antisense orientations. (**C**) Alignment of endo-siRNA sequences to *Drosophila* transposons. The abundance of each sequence is shown as a percentage of all transposon-matching siRNA sequences. LTR, long terminal repeat; TIR, terminal inverted repeat. Here and in subsequent figures, data from high-throughput pyrosequencing and sequencing-by-synthesis were pooled for wild-type heads.

Figure 1 shows the length distribution and sequence composition of the four libraries. The total RNA samples were predominantly miRNAs, a bias reflected in their modal length (22 nt) and pronounced tendency to begin with uracil. Exclusion of miRNAs revealed a class of small RNAs with a narrow length distribution and no tendency to begin with uracil. Except for an unusual cluster of X-chromosome small RNAs (fig. S1) and a miRNA-like sequence with an unusual putative precursor on chromosome 2 (fig. S2), few of these small RNAs are likely to correspond to novel miRNAs: None lie in the arms of hairpins predicted to be as thermodynamically stable as most pre-miRNAs (i.e., < -15 kcal/mol).

After excluding known miRNAs, 64% (heads) (Fig. 1A) and 78% (S2 cells) (Fig. 1B) of sequences in the libraries enriched for 3′-terminally modified small RNAs—that is, those likely to be Ago2-associated—were 21 nt long. For fly heads, 37% (8404 reads) derived from the *white* dsRNA hairpin. The abundance of these exo-siRNAs can be estimated by comparing them to the number of reads for individual miRNAs in the total small RNA library, where 1.6% (660 antisense and 491 sense reads) were 21-nt oligomers (21-mers) and matched the *white* sequences in the dsRNA-expressing transgene. The collective abundance of all *white* exo-siRNAs was less than the individual abundance of the 10 most abundant miRNAs in this sample; the median abundance of any one exo-siRNA species was two reads. The *white*–inverted repeat (IR) transgene phenocopies a nearly null mutation in *white*, yet the sequence of the most abundant exo-siRNA was read just 37 times.

In heads, the sequence composition of the 21-nt, 3′-terminally modified small RNAs closely resembled that of exo-siRNAs, which tended to begin and end with cytosine. In heads and S2 cells, the 21-mers lacked the sequence features of piRNAs, which either begin with uracil (Aub- and Piwi-bound) or contain an adenine at position 10 (Ago3-bound) and are 23 to 29 nt long (*1*, *2*). These data suggest that the 21-nt small RNAs are somatic endo-siRNAs.

In S2 cells, endo-siRNAs mapped largely to transposons (86%); in fly heads, they mapped about equally to transposons, intergenic and unannotated sequences, and mRNAs. The finding that 41% of endo-siRNAs mapped to mRNAs without mapping to transposons suggests that endo-siRNAs may regulate mRNA

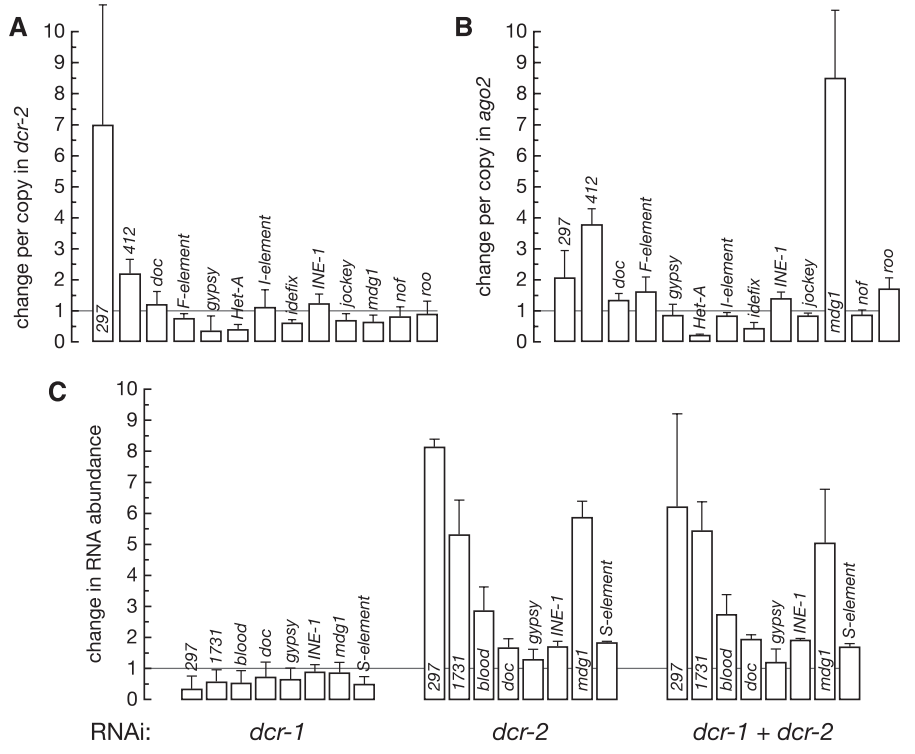

Fig. 3. Transposon silencing requires Dcr-2 and Ago2, but not Dcr-1. (**A** and **B**) The change in mRNA expression (mean ± SD, N = 3) for each transposon between *dcr-2*^{L811fsX} (A) or *ago2*^{414} (B) heterozygous and homozygous heads was measured by quantitative reverse transcription polymerase chain reaction. The data were corrected for differences in transposon copy number between the paired genotypes. (**C**) The change in transposon expression (mean ± SD, N = 3) in S2 cells was measured for the indicated RNAi depletion relative to a control dsRNA.

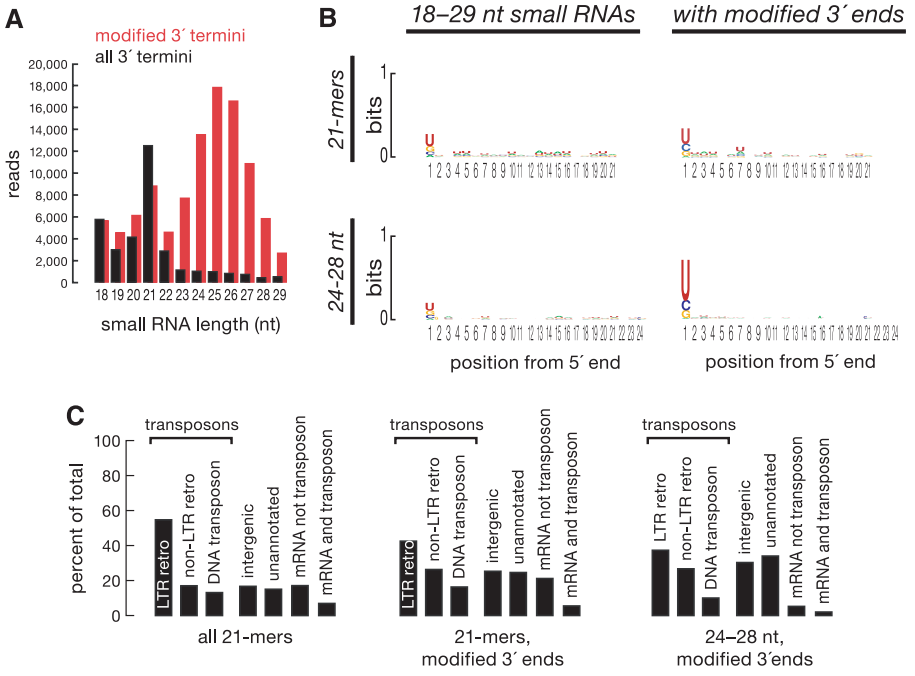

Fig. 4. The composition of somatic small RNAs is altered in the absence of Ago2. (**A** and **B**) Size distribution (A) and sequence composition (B) of sequences from a library of total 18- to 29-nt RNA from the heads of *ago2* null mutant flies or a library enriched for 3′-terminally modified RNAs. Reads matching pre-miRNA sequences were removed. (**C**) Distribution of annotations for the genomic matches of small RNA sequences from the two *ago2* libraries.

expression. Endo-siRNAs mapping to mRNAs were likelier by a factor of >10 than expected by chance ($5.22 \times 10^{-161} < P < 8 \times 10^{-151}$) to derive from genomic regions annotated to produce overlapping, complementary transcripts (Table 1 and table S1). These data suggest that such overlapping, complementary transcripts anneal in vivo to form dsRNA that is diced into endo-siRNAs. We note that among the mRNAs for which we detected complementary 21-mers was *ago2* itself.

Endo-siRNAs mapped to all three large chromosomes (figs. S3 to S5). siRNAs corresponding to the three transposon types in *Drosophila* were detected, but long terminal repeat (LTR) retrotransposons, the dominant class of selfish genetic elements in flies, were overrepresented even after accounting for their abundance in the genome (Fig. 2A and table S2). Unlike piRNAs, which are disproportionately antisense to transposons, but like siRNAs derived from exogenous dsRNA, about equal numbers of sense and antisense transposon-matching endo-siRNAs were detected (Fig. 2B and fig. S6) (*1*–*3*, *22*). Like piRNAs, endo-siRNAs map to large genomic clusters (table S3). Of 172 endo-siRNA clusters in S2 cells, four coincided with previously identified piRNA clusters (cluster 1, at 42A of chromosome 2R; clusters 7 and 10 in unassembled genomic sequence; and cluster 15 in the chromosome 3L heterochromatin). In heads, we detected 17 clusters; five corresponded to clusters found in S2 cells, but only one was shared with the germline piRNAs: the *flamenco* locus, consistent with recent genetic evidence that a Piwi-independent but *flamenco*-dependent pathway represses the *Idefix* and *ZAM* transposons in the soma (*23*). That both endo-siRNAs and piRNAs can arise from the same region suggests either that a single transcript can be a substrate for both piRNA and siRNA production or that distinct classes of transcripts arise from a single locus. The abundance and distribution of endo-siRNAs across the sequences of individual transposon species reflected the natural history of when the elements entered the fly genome, but not their mechanism of transposition (Fig. 2C) (*24*).

Statistically significant reductions in siRNA abundance were observed in *dcr-2*^{L811fsX} null mutant heads relative to heads from heterozygous siblings for 38 transposons (fig. S7 and table S4). Normalized for sequencing depth, sequencing results from homozygous *dcr-2* mutant heads yielded fewer 21-mers overall (by a factor of 3.1) and fewer 21-mers corresponding to transposons (by a factor of 6.3) than did their heterozygous siblings ($P < 2.2 \times 10^{-16}$; χ^2 test). In contrast, overall miRNA abundance—normalized to sequencing depth—was essentially unchanged between *dcr-2* heterozygotes and homozygotes (fig. S7 and table S5). These data suggest that endo-siRNAs are produced by Dcr-2, but we do not yet know why some endo-siRNAs persist in *dcr-2*^{L811fsX} mutants.

Transposon expression in the soma reflects both the silencing of transposons—potentially by either or both posttranscriptional and transcriptional mechanisms—and the tissue specificity of transposon promoters. *Drosophila* somatic cells may contain siRNAs targeting transposons that would not be highly expressed even in the absence of those siRNAs, because the promoters of those transposons are not active in some or all somatic tissues or because they are repressed by additional mechanisms. We analyzed the expression of a panel of transposons in heads from *ago2* and *dcr-2* mutants and in S2 cells depleted of Dcr-1, Dcr-2, or Ago2 by RNAi (Fig. 3 and fig. S8). We found that the steady-state abundance of RNA from the LTR retrotransposons *297* and *412* increased in heads from *dcr-2*^{L811fsX} null mutants (Fig. 3A). Similarly, the steady-state abundance of RNA from the LTR retrotransposons *297*, *412*, *mdg1*, and *roo*, the non-LTR retrotransposon *F-element*, and the SINE-like element *INE-1* increased in *ago2*^{414} mutant heads (Fig. 3B).

In S2 cells, RNA expression from the LTR retrotransposons *297*, *1731*, *mdg1*, *blood*, and *gypsy* and from the DNA transposon *S-element* all increased significantly ($0.00001 < P < 0.002$) when Dcr-2 was depleted or when both Dcr-2 and Dcr-1 were depleted, but not when Dcr-1 alone was depleted (Fig. 3C). Similarly, *ago2(RNAi)* in S2 cells desilenced transposons, including nine LTR and non-LTR retrotransposons and the DNA transposon *S-element* (fig. S8).

Is Ago2 required for the production or accumulation of endo-siRNAs? We sequenced 18- to 29-nt small RNAs from *ago2*^{414} homozygous fly heads and from the same small RNA sample treated to enrich for 3′-terminally modified RNAs. After computationally removing miRNAs, the sequences from the untreated library contained a prominent 21-nt peak (Fig. 4A) that predominantly began with uracil (Fig. 4B), much like miRNAs and unlike siRNAs in wild-type heads, which often began with cytosine (Fig. 1A). Perhaps in the absence of Ago2, only a subpopulation of endo-siRNAs that can bind Ago1 accumulates. The small RNAs from the *ago2*^{414} library enriched for 3′-terminally modified sequences were predominantly 24 to 27 nt long and often began with uracil—a length distribution and sequence bias characteristic of piRNAs, which, like siRNAs, are 2′-*O*-methylated at their 3′ ends. Both the 21-nt small RNAs and the piRNA-like RNAs in the *ago2* mutant heads mapped to transposons, unannotated heterochromatic and unassembled sequences, but the piRNA-like sequences mapped to mRNAs far less frequently than did either the 21-mers or wild-type endo-siRNAs (Fig. 4C). How these piRNA-like small RNAs are generated and whether they contribute to transposon silencing in the fly soma remain unknown.

Note added in proof: The loci described here in figs. S1 and S2 correspond to endo-siRNA–generating hairpins recently identified in (*25*–*27*).

References and Notes

1. L. S. Gunawardane *et al.*, *Science* **315**, 1587 (2007); published online 21 February 2007 (10.1126/science.1140494).
2. J. Brennecke *et al.*, *Cell* **128**, 1089 (2007).
3. V. V. Vagin *et al.*, *Science* **313**, 320 (2006); published online 28 June 2006 (10.1126/science.1129333).
4. H. Yin, H. Lin, *Nature* **450**, 304 (2007).
5. A. Hamilton, O. Voinnet, L. Chappell, D. Baulcombe, *EMBO J.* **21**, 4671 (2002).
6. R. Sunkar, T. Girke, J. K. Zhu, *Nucleic Acids Res.* **33**, 4443 (2005).
7. N. Yang, H. H. J. Kazazian, *Nat. Struct. Mol. Biol.* **13**, 763 (2006).
8. A. Ishizuka, M. C. Siomi, H. Siomi, *Genes Dev.* **16**, 2497 (2002).
9. A. K. Csink, R. Linsk, J. A. Birchler, *Genetics* **138**, 153 (1994).
10. J. Rehwinkel *et al.*, *Mol. Cell. Biol.* **26**, 2965 (2006).
11. K. A. Haynes, A. A. Caudy, L. Collins, S. C. Elgin, *Curr. Biol.* **16**, 2222 (2006).
12. M. Pal-Bhadra, U. Bhadra, J. A. Birchler, *Mol. Cell* **9**, 315 (2002).
13. N. A. Tchurikov, O. V. Kretova, *PLoS ONE* **2**, e476 (2007).
14. M. D. Horwich *et al.*, *Curr. Biol.* **17**, 1265 (2007).
15. A. Pelisson, E. Sarot, G. Payen-Groschene, A. Bucheton, *J. Virol.* **81**, 1951 (2007).
16. K. Saito *et al.*, *Genes Dev.* **21**, 1603 (2007).
17. K. Okamura, A. Ishizuka, H. Siomi, M. C. Siomi, *Genes Dev.* **18**, 1655 (2004).
18. A. Nykanen, B. Haley, P. D. Zamore, *Cell* **107**, 309 (2001).
19. *Drosophila* RNAi Screening Center at Harvard Medical School (http://flyrnai.org/cgi-bin/RNAi_FAQ_lines.pl).
20. Y. S. Lee, R. W. Carthew, *Methods* **30**, 322 (2003).
21. H. Seitz, M. Ghildiyal, P. D. Zamore, *Curr. Biol.* **18**, 147 (2008).
22. P. D. Zamore, T. Tuschl, P. A. Sharp, D. P. Bartel, *Cell* **101**, 25 (2000).
23. S. Desset, N. Buchon, C. Meignin, M. Coiffet, C. Vaury, *PLoS ONE* **3**, e1526 (2008).
24. See supporting material on *Science* Online.
25. B. Czech *et al.*, *Nature* 10.1038/nature07007 (2008).
26. Y. Kawamura *et al.*, *Nature* 10.1038/nature06938 (2008).
27. K. Okamura *et al.*, *Nature* 10.1038/nature07015 (2008).

28. We thank A. Boucher and S. Ma for technical assistance; G. Farley for encouragement, support, and technical assistance; and Roche Applied Science for high-throughput sequencing. P.D.Z. is a W. M. Keck Foundation Young Scholar in Medical Research. Supported by NIH grants GM62862 and GM65236 (P.D.Z.), GM080625 (J.X. and Z.W.), and HG003367 (S.L.); EMBO long-term (ALTF 910-2004) and Human Frontier Science Program (LT00575/2005-L) fellowships (H.S.); and a National Research Service Award predoctoral MD/PhD fellowship from the National Institute on Aging (F30AG030283) (M.D.H.). NCBI Gene Expression Omnibus accession numbers for sequence and abundance data are GSE9389 and GSE11019, respectively.

Supporting Online Material

www.sciencemag.org/cgi/content/full/1157396/DC1
Materials and Methods
Figs. S1 to S8
Tables S1 to S7
References

5 March 2008; accepted 31 March 2008
Published online 10 April 2008;
10.1126/science.1157396
Include this information when citing this paper.

Resource Partitioning and Sympatric Differentiation Among Closely Related Bacterioplankton

Dana E. Hunt,[1]* Lawrence A. David,[2]* Dirk Gevers,[1,3,4] Sarah P. Preheim,[1] Eric J. Alm,[1,5]† Martin F. Polz[1]†

Identifying ecologically differentiated populations within complex microbial communities remains challenging, yet is critical for interpreting the evolution and ecology of microbes in the wild. Here we describe spatial and temporal resource partitioning among *Vibrionaceae* strains coexisting in coastal bacterioplankton. A quantitative model (AdaptML) establishes the evolutionary history of ecological differentiation, thus revealing populations specific for seasons and life-styles (combinations of free-living, particle, or zooplankton associations). These ecological population boundaries frequently occur at deep phylogenetic levels (consistent with named species); however, recent and perhaps ongoing adaptive radiation is evident in *Vibrio splendidus*, which comprises numerous ecologically distinct populations at different levels of phylogenetic differentiation. Thus, environmental specialization may be an important correlate or even trigger of speciation among sympatric microbes.

Microbes dominate biomass and control biogeochemical cycling in the ocean, but we know little about the mechanisms and dynamics of their functional differentiation in the environment. Culture-independent analysis typically reveals vast microbial diversity, and although some taxa and gene families are differentially distributed among environments (*1*, *2*), it is not clear to what extent coexisting genotypic diversity can be divided into functionally cohesive populations (*1*, *3*). First, we lack broad surveys of nonpathogenic free-living bacteria that establish robust associations of individual strains with spatiotemporal conditions (*4*, *5*); second, it remains controversial what level of genetic diversification reflects ecological differentiation. Phylogenetic clusters have been proposed to correspond to ecological populations that arise by neutral diversification after niche-specific selective sweeps (*6*). Clusters are indeed observed among closely related isolates (e.g., when examined by multilocus sequence analysis) (*7*) and in culture-independent analyses of coastal bacterioplankton (*8*). Yet recent theoretical studies suggest